



Rossitto, Giacomo (2021) *Novel perspectives on salt and interstitium: from hypertension to heart failure*. PhD thesis.

<http://theses.gla.ac.uk/82130/>

Copyright and moral rights for this work are retained by the author

A copy can be downloaded for personal non-commercial research or study, without prior permission or charge

This work cannot be reproduced or quoted extensively from without first obtaining permission in writing from the author

The content must not be changed in any way or sold commercially in any format or medium without the formal permission of the author

When referring to this work, full bibliographic details including the author, title, awarding institution and date of the thesis must be given

Enlighten: Theses

<https://theses.gla.ac.uk/>
research-enlighten@glasgow.ac.uk

**NOVEL PERSPECTIVES
ON SALT AND INTERSTITIUM:
FROM HYPERTENSION TO
HEART FAILURE**

Giacomo Rossitto, MD

Submitted in fulfilment of the requirements
for the Degree of Doctor of Philosophy (PhD),

Institute of Cardiovascular and Medical Sciences,
College of Medical, Veterinary and Life Sciences
University of Glasgow

© G. Rossitto

ABSTRACT

Sodium (Na^+) and water are closely linked in body fluid physiology by the concepts of osmosis and long-term balance. Our traditional understanding of fluid and electrolytes homeostasis has recently been challenged by suggestions of a systemic metabolic shift favouring water preservation when excess Na^+ intake is excreted, and of skin as a depot for Na^+ accumulation in multiple cardiovascular diseases and risk factors.

In particular, a catabolic state would produce endogenous free water and facilitate its renal reabsorption independent of Na^+ , via urea generation and recycling: in the long term this could adversely impact cardiovascular risk, but has only been shown in preclinical settings. Similarly, the proposed water-independent nature of interstitial Na^+ accumulation has the potential to induce local pathogenic changes to the surrounding structures, including the microvasculature, but lacks firm demonstration.

The aims of this Thesis were therefore to investigate: 1) the impact of high Na^+ intake on renal water-preserving mechanisms and metabolism in a real-life hypertensive population; 2) the nature, distribution and clinical correlates of tissue Na^+ accumulation; 3) microvascular function, including capillary-interstitium fluid exchange and lymphatic drainage, in relation to interstitial Na^+ accumulation.

I herein retrospectively analysed clinical and biochemical blood and 24h-urinary data from consecutive patients with essential hypertension, collected at the time of screening for secondary causes, and found that kidneys can indeed dissociate Na^+ and water handling (as estimated by their fractional excretions) when exposed to high Na^+ intake. However, this comes at the cost of higher glomerular filtration rate, increased tubular energy expenditure, and protein catabolism at metabolomics signatures.

By conducting a chemical analysis of multiple tissues from rodent models of salt sensitivity/salt loading and of skin from patients with hypertension or heart failure with preserved ejection fraction (HFpEF), I showed that tissue Na^+ excess upon high Na^+ intake is a systemic, rather than skin-specific, water-paralleled phenomenon reflecting the expansion of the extracellular compartment, and subclinical oedema in most cases.

Despite the lack of any hypertonic interstitial Na^+ accumulation to osmotically drag water out of vessels and facilitate the typical “congestion”, I also identified structural and molecular alterations in the skin blood and lymphatic microvasculature of patients with

HFpEF, along with evidence of impaired lymphatic drainage of interstitial fluids upon pressure challenge.

In summary, I confirmed the previous suggestions of a Na⁺-driven metabolic shift in a real-life population of hypertensive patients and largely expanded on the novel concepts of tissue Na⁺ accumulation. In particular, I disproved its water-independence in both experimental models and human subjects and suggested systemic isotonic Na⁺ excess as an important and likely prevalent determinant in the pathogenesis of hypertension and other cardiovascular diseases. The biophysical and molecular impact of this subclinical or clinically overt oedema on organ function, as well as the mechanisms of function and dysfunction of lymphatic vessels in the control of interstitial fluid in cardiovascular disease, need further exploration.

TABLE OF CONTENTS

ABSTRACT	2
LIST OF TABLES	9
LIST OF FIGURES	10
ACKNOWLEDGEMENTS	13
AUTHOR'S DECLARATION	15
1 INTRODUCTION	16
1.1 THE CLINICAL CONTEXT: HYPERTENSION AND HEART FAILURE.....	16
1.1.1 Hypertension.....	16
1.1.2 Heart failure.....	17
1.1.3 A common ground.....	18
1.2 SALT IN CARDIOVASCULAR DISEASE – A “CLASSIC” ASSOCIATION	20
1.2.1 Salt, high blood pressure and cardiovascular outcomes.....	20
1.2.2 Salt-sensitivity of blood pressure	21
1.3 A NOVEL BLOOD PRESSURE-INDEPENDENT ASSOCIATION	23
1.4 NOVEL CONCEPTS ON SODIUM HOMEOSTASIS.....	25
1.4.1 Disproof of a constant sodium balance.....	26
1.4.2 Water-independent tissue sodium accumulation.....	26
1.5 THE LYMPHATIC SYSTEM	28
1.5.1 Lymphatic role in microvascular haemodynamics	28
1.5.2 Anatomy and function.....	30
1.6 TRADITIONAL VS NOVEL VIEWS: OPEN QUESTIONS.....	31
1.7 RESEARCH AIMS.....	33
2 GENERAL METHODS	34
2.1 ASSESSMENT OF THE METABOLIC IMPACT OF HIGH SODIUM INTAKE.....	34
2.2 ASSESSMENT OF TISSUE SODIUM ACCUMULATION	35
2.2.1 Modelling (Chapter 4).....	35
2.2.2 Animal models (Chapter 5).....	35
2.2.3 Human subjects (Chapters 6-7).....	37
2.2.4 Skin biopsy.....	39
2.2.5 Chemical analysis of tissues.....	40

2.3	ASSESSMENT OF VASCULAR AND MICROVASCULAR FUNCTION	42
2.3.1	<i>Ex-vivo study of arterial function on wire myography</i>	42
2.3.2	<i>Non-invasive study of arterial function (humans)</i>	45
2.3.3	<i>In-vivo study of fluid microvascular dynamics (humans)</i>	50
3	METABOLIC IMPACT OF HIGH SODIUM INTAKE.....	56
3.1	BACKGROUND AND STUDY AIM	56
3.2	STUDY-SPECIFIC METHODS	56
3.2.1	<i>Screening protocol and patient selection</i>	56
3.2.2	<i>Biochemistry</i>	59
3.2.3	<i>Renal function and energetics</i>	61
3.2.4	<i>Metabolomics</i>	63
3.2.5	<i>Statistics</i>	63
3.3	RESULTS.....	64
3.3.1	<i>Cohort characteristics</i>	64
3.3.2	<i>Na⁺ and Water renal handling</i>	66
3.3.3	<i>Excess Na⁺ excretion is paralleled by glomerular hyperfiltration</i>	67
3.3.4	<i>High Na⁺ increases tubular reabsorption and renal energy expenditure</i>	68
3.3.5	<i>Sympathetic nervous system activation</i>	69
3.3.6	<i>Re-setting of nitrogen balance and metabolic signatures</i>	70
3.3.7	<i>Excess cortisol upon high Na⁺ intake</i>	71
3.4	DISCUSSION.....	72
3.4.1	<i>Main findings</i>	72
3.4.2	<i>Limitations, conclusions and perspectives</i>	75
4	TISSUE SODIUM ACCUMULATION: MODELLING	78
4.1	INTRODUCTION AND RATIONALE	78
4.2	METHODS: CALCULATIONS.....	80
4.2.1	<i>Expected total concentration of Na⁺ and K⁺ in a tissue</i>	80
4.2.2	<i>Expected total concentration of Na⁺ and K⁺ in oedematous tissues</i>	81
4.2.3	<i>Changes in total tissue Na⁺, K⁺ and water due to oedema</i>	82
4.2.4	<i>Biological assumptions</i>	82
4.3	RESULTS.....	82
4.4	DISCUSSION AND IMPLICATIONS.....	84

5	TISSUE SODIUM ACCUMULATION: PRECLINICAL DATA	86
5.1	BACKGROUND AND STUDY AIMS	86
5.2	METHODS	88
5.2.1	<i>Animal protocols</i>	88
5.2.2	<i>Harvesting and chemical analysis of rat tissues</i>	88
5.2.3	<i>Histology: extracellular matrix</i>	89
5.2.4	<i>Gene expression analysis</i>	91
5.2.5	<i>Ex-vivo study of arterial function on wire myography</i>	91
5.2.6	<i>Statistical analysis</i>	92
5.3	RESULTS.....	93
5.3.1	<i>Salt-loading: experimental groups</i>	93
5.3.2	<i>Histochemical effects of salt-loading</i>	93
5.3.3	<i>Ageing model</i>	102
5.3.4	<i>Impact of salt on arterial function</i>	105
5.4	DISCUSSION.....	109
6	TISSUE SODIUM ACCUMULATION: HYPERTENSIVE PATIENTS	114
6.1	BACKGROUND AND STUDY AIMS	114
6.2	STUDY-SPECIFIC METHODS	115
6.2.1	<i>Study protocols</i>	115
6.2.2	<i>Skin punch biopsy and chemical analysis</i>	117
6.2.3	<i>Sodium intake questionnaire</i>	118
6.2.4	<i>Transepidermal water loss</i>	119
6.2.5	<i>Pilocarpine-induced sweat test</i>	119
6.2.6	<i>Statistics</i>	120
6.3	RESULTS.....	120
6.3.1	<i>Histochemical analysis</i>	122
6.3.2	<i>Clinical correlates in hypertensive patients</i>	126
6.3.3	<i>Skin-specific mechanisms of Na⁺/water exchange</i>	128
6.4	DISCUSSION.....	129
7	INTERSTITIUM AND MICROVASCULAR FUNCTION	134
7.1	BACKGROUND AND STUDY AIMS	134
7.2	STUDY- SPECIFIC METHODS	135

7.2.1	<i>Protocol and subjects</i>	135
7.2.2	<i>Blood pressure measurement</i>	136
7.2.3	<i>Echocardiography</i>	137
7.2.4	<i>Traditional non-invasive assessment of arterial function</i>	137
7.2.5	<i>Plethysmography and microvascular fluid dynamics</i>	138
7.2.6	<i>Surgical skin samples</i>	139
7.2.7	<i>Ex vivo assessment of vascular function</i>	140
7.2.8	<i>Skin histochemical analysis</i>	140
7.2.9	<i>Skin microvascular immunofluorescence and image analysis</i>	140
7.2.10	<i>Skin gene expression analysis</i>	143
7.2.11	<i>Statistical analysis</i>	143
7.3	RESULTS	144
7.3.1	<i>Subject characteristics</i>	144
7.3.2	<i>Arterial function</i>	146
7.3.3	<i>Skin salt</i>	149
7.3.4	<i>Rarefaction of skin microvessels and gene expression</i>	152
7.3.5	<i>Microvascular fluid dynamics</i>	153
7.4	DISCUSSION	156
7.4.1	<i>Rarefaction of microvessels</i>	156
7.4.2	<i>Interstitial, microvasculature and congestion in HFpEF</i>	157
7.4.3	<i>The lymphatic system in HFpEF</i>	159
7.4.4	<i>Limitations</i>	161
7.5	CONCLUSIONS	161
8	DISCUSSION	163
8.1	THE ENERGETIC IMPLICATIONS OF SALT EXCESS	163
8.2	THE NATURE OF SALT EXCESS	166
8.2.1	<i>An isotonic systemic phenomenon</i>	166
8.2.2	<i>A new speculative theoretical framework</i>	167
8.3	NEGLECTED REGULATORS OF INTERSTITIAL SALT EXCESS	170
8.4	CONCLUSIONS	173
	APPENDICES	175
	APPENDIX 1 - S ₂ ALT PROTOCOL	175
	APPENDIX 2 - S ₂ ALT PARTICIPANT INFORMATION LEAFLET	181

APPENDIX 3 - S ₂ ALT SALT INTAKE QUESTIONNAIRE	185
APPENDIX 4 - HAPPIFY PROTOCOL	187
APPENDIX 5 - HAPPIFY ADVERTISEMENT FOR HEALTHY VOLUNTEERS.....	200
APPENDIX 6 - HAPPIFY PARTICIPANT INFORMATION LEAFLET	201
APPENDIX 7 – SYCAMORE: METABOLOMIC PEAKS, > IN HIGH-NA ⁺ VS LOW-NA ⁺	208
APPENDIX 8 – SYCAMORE: METABOLOMIC PEAKS, > IN LOW-NA ⁺ VS HIGH-NA ⁺	212
APPENDIX 9 – IMAGEJ MACRO FOR ALCIAN BLUE ⁺ AREA QUANTIFICATION.	213
REFERENCES	214

LIST OF TABLES

Chapter 3

Table 3-1 Clinical and biochemical characteristics of patients by Na⁺ intake group

Table 3-2 Renal function by Na⁺ intake group.

Chapter 5

Table 5-1 Rat SKIN histochemical analysis.

Table 5-2 Rat LIVER histochemical analysis.

Table 5-3 Rat LUNG histochemical analysis.

Table 5-4 Rat SKELETAL MUSCLE histochemical analysis.

Table 5-5 Rat LEFT VENTRICULAR MYOCARDIUM histochemical analysis.

Table 5-6 Impact of in-vivo and ex-vivo Na⁺ excess on arterial function.

Chapter 6

Table 6-1 Characteristics of S₂ALT patients.

Table 6-2 Skin histochemical differences between hypertensive males and females.

Table 6-3 Characteristics of young healthy volunteers.

Chapter 7

Table 7-1 HAPPIFY: group characteristics.

Table 7-2 HAPPIFY: echocardiographic characteristics.

Table 7-3 HAPPIFY: macrovascular function.

Table 7-4 Characteristics of young healthy subjects, for contrast.

Table 7-5 Skin chemical analysis, contrasted with young healthy subjects.

Table 7-6 Microvascular dynamics.

LIST OF FIGURES

Chapter 1

- Figure 1-1 Natriuretic-ureotelic water-preserving mechanisms upon high salt intake.
Figure 1-2 Starling-Landis equilibrium and the lymphatic system.
Figure 1-3 Lymphangion contraction cycle.

Chapter 2

- Figure 2-1 WKY and SHRSP phenotype.
Figure 2-2 Skin biopsy protocol.
Figure 2-3 Reproducibility of tissue chemical analysis.
Figure 2-4 Wire myography ex-vivo experimental protocol to assess arterial function.
Figure 2-5 Central Aortic waveform and key parameters of PWA.
Figure 2-6 Flow-mediated dilatation.
Figure 2-7 Representative FMD tracings.
Figure 2-8 Application of a limb gauge and rapid inflation cuff.
Figure 2-9 Plethysmography protocol for the assessment of microvascular filtration parameters and interstitial fluid accumulation.
Figure 2-10 Extended protocol with deflation steps

Chapter 3

- Figure 3-1 SYCAMORE study flowchart.
Figure 3-2 Validation of the expanded dataset (Passing and Bablok regression).
Figure 3-3 Renal Na⁺ and Water handling upon differential Na⁺ intake.
Figure 3-4 Absolute Na⁺ excretion and reabsorption and energy cost.
Figure 3-5 Metabolomics signature.
Figure 3-6 Metabolic impact of high Na⁺ intake - summary figure.

Chapter 4

- Figure 4-1 Histochemical impact of tissue architecture.
Figure 4-2 Histochemical modelling.

Chapter 5

- Figure 5-1 Histological sulphated glycosaminoglycans myocardial quantification.
- Figure 5-2 Collagen and glycosaminoglycan deposition with ageing.
- Figure 5-3 Blood pressure in the experimental groups.
- Figure 5-4 Nature and distribution of tissue Na⁺ excess upon salt loading.
- Figure 5-5 Fat content in skin and liver.
- Figure 5-6 Regression lines for tissue Na⁺ and water content in different tissues.
- Figure 5-7 Predicted and experimental results.
- Figure 5-8 Tissue-specific TonEBP expression upon salt loading.
- Figure 5-9 Rat phenotypes in the ageing experiment.
- Figure 5-10 Myocardial Na⁺ excess and TonEBP expression in hypertensive ageing.
- Figure 5-11 Myocardial glycosaminoglycans in hypertensive ageing.
- Figure 5-12 Impact of in vivo Na⁺ excess on agonist-independent contractile function.
- Figure 5-13 Impact of in-vivo and ex-vivo Na⁺ excess on arterial function.
- Figure 5-14 Impact of prolonged tissue handling and evaporation on histochemical analysis.

Chapter 6

- Figure 6-1 Human skin samples and anatomical strategy of analysis.
- Figure 6-2 Na⁺ and K⁺ concentrations and water content by skin layer.
- Figure 6-3 Histochemical correlations.
- Figure 6-4 Histochemical sex-differences in the skin of young healthy volunteers and impact of fat.
- Figure 6-5 Histochemical parameters and ageing.
- Figure 6-6 Histochemical parameters and other relevant clinical correlates.
- Figure 6-7 Sweat Na⁺ concentration in relation to ESD Na⁺ concentration and age.
- Figure 6-8 Sweat and blood pressure.

Chapter 7

- Figure 7-1 Immunofluorescence imaging analysis.
- Figure 7-2 Peripheral arterial function assessed in vivo.
- Figure 7-3 Peripheral arterial function assessed ex vivo.
- Figure 7-4 Chemical analysis of the skin.

- Figure 7-5 Skin microvascular anatomy.
- Figure 7-6 Skin microvascular gene expression.
- Figure 7-7 Microvascular fluid dynamics.
- Figure 7-8 Microvascular fluid dynamics and reduced lymphatic reserve in HFpEF.

Chapter 8

- Figure 8-1 Secondary analysis of the DASH-Sodium trial.
- Figure 8-2 The “sieve” hypothesis.
- Figure 8-3 Human lymphnode with afferent and efferent lymphatic vessels.

ACKNOWLEDGEMENTS

I would like to express here the most profound gratitude to all those who contributed to the work in this thesis and to my professional and personal growth during my years in Glasgow.

Firstly, thanks to my supervisors Prof. Christian Delles, Prof. Mark Petrie and Prof. Rhian Touyz for providing the richest, most comprehensive and multifaceted guidance I could ever expect. Thanks also to Prof. Mike Davis, who provided the warmest welcome and the most passionate supervision when I visited his lab in Columbia, Missouri.

Thanks to the British Heart Foundation, for funding my studies, my salary and – most importantly - the BHF Centre of Research Excellence in Glasgow at the Institute of Cardiovascular and Medical Sciences (ICAMS), which truly represented a centre of continuous interdisciplinary interaction which enriched and lifted the bar of my idea of cardiovascular research.

I am also indebted to all my study participants, who made my research possible, and to the “Bearsden and Milngavie” and “Glasgow West End” University of the Third Age for the active contribution to volunteers recruitment.

In brief, but truly in depth, thanks also to:

all the colleagues who provided any input to my research in ICAMS, including Prof J. Titze when he visited Glasgow and spent time to discuss my very first experimental results;

Mrs Christine McAllister, Mrs Ammani Brown and the Clinical Research Facility team, as well as Sister Karen Campbell and the other Glasgow Blood Pressure Clinic nurses, for their support;

Dr Augusto Montezano, Dr Rheure Alves-Lopes, Dr Karla Neves, Dr Francisco Rios, Dr Adam Harvey, Mrs Jackie Thomson, Mrs Laura Haddow, Mr John McAbney, Dr Aikaterini Anagnostopoulou, Dr Livia De Lucca Camargo, Mrs Wendy Beattie, Mrs Linda Hood, Ms Margaret Kinninmont, Mrs Carol Jenkins, Mr Andrew Carswell, Mr Arun Flynn as the Touyz lab core and/or ICAMS staff, for teaching and helping me;

Mr Micheal Beglan, from the chemistry department, for providing the technical expertise and tools necessary to implement the chemical analysis of tissues.

A special 'lab' thank you goes to Dr Sheon Mary Samji, a tireless, passionate and inspirational scientist, for guiding me step-by-step in understanding and performing all the basic science I was not used to.

Much more, I'm grateful to her, to Dr Angela Lucas-Herald and to Ms Daniele Kerr for their true friendship over these years; my English still falls short in expressing all my gratitude.

Similarly, thanks to Dr Eilidh McGinnigle, Dr Sharon Mackin and Dr Jennifer Lees for sharing the joys and frustrations of this journey. A big thank you goes also to Dr Katriona Brooksbank, for her help and advice with research applications, but also for taking care of us.

Finally, thanks to Alessandra Pizziol, for standing the tests of time and distance, and for loving me. Similarly, thanks to my entire family and particularly to my parents, Lucia Campaci and Giancarlo Rossitto: I would like to dedicate this thesis to them.

AUTHOR'S DECLARATION

I declare that the studies in this thesis were the work of the author, Dr Giacomo Rossitto, under the supervision of Professors Christian Delles, Mark C. Petrie and Rhian M. Touyz, unless otherwise stated.

I acknowledge support from:

- Dr Giuseppe Maiolino, Silvia Lerco, Giulio Ceolotto, Alessio Pinato, Giorgia Antonelli (University of Padua, Padua, Italy) and Mrs Elaine Butler in completing the clinical and biochemical database informing the SYCAMORE study (Chapter 3), by reviewing charts, processing or conducting the biochemistry measurements on plasma and urine samples for my later analyses.
- Dr Gavin Blackburn and Dr Ronan Daly (Glasgow Polyomics), in processing the samples I extracted for metabolomics and independently reviewing the analysis I performed on the results (Chapter 3).
- Dr Adam Harvey and Dr Sheon Mary, in taking care of all the animal work prior to the harvesting and chemical analysis of tissues (Chapter 5).
- Dr Sheon Mary, in conducting with me all the steps of the gene expression analyses (Chapter 5 and 7)
- Ms Jun Chen, in contributing to the chemical analysis of tissues (Chapters 5) and to the conduct of the S2ALT study, including the skin biopsies, TEWL and sweat tests (Chapter 6), under my supervision in fulfilment of the requirements for a BSc degree.
- Dr Karla Neves, Mrs Laura Haddow, Dr Rheure Alves-Lopes and Mr John McAbney in dissecting the resistance arteries from my subcutaneous gluteal biopsies or rat mesenteries and mounting them for myography (Chapters 5 and 7).

No part of this work has previously been submitted in support of application for another degree or qualification by this or any other university.

Dr Giacomo Rossitto,

December 2020

INTRODUCTION

1.1 The clinical context: hypertension and heart failure

The personal background to this thesis is dual: 1) a clinical and research experience in hypertension during my years of training in Internal Medicine, and 2) a vivid and long-pre-existing interest in the hydraulic mechanisms of fluid balance. The latter dates back to my years as a medical student, when I studied the concepts of “forward” and “backward” pressures in the heart chambers and cardiovascular system in general, as well as the magic of Starling forces in the most peripheral vascular branches, and I learned to extrapolate all this from pure physiology to the most obvious clinical translation, i.e. “congestion” and heart failure (HF).

1.1.1 Hypertension

Hypertension, or high blood pressure (BP), is recognised as the biggest contributor to the global burden of cardiovascular disease (CVD) and related disability. Whilst the relationship between BP and cardiovascular events is continuous (Ettihad et al., 2016), the pragmatic use of thresholds to guide unequivocally beneficial treatments defines ‘hypertension’ as office systolic BP (SBP) values ≥ 140 mmHg and/or diastolic BP (DBP) values ≥ 90 mmHg (Williams et al., 2018). Around 2015, the estimated rate of systolic BP (SBP) above 140 mmHg was $> 20\%$ of the global population (Forouzanfar et al., 2017), 30 - 45% in adults and up to $>60\%$ in those aged >60 years (Chow et al., 2013), with 14% of all global deaths linked to SBP values above that threshold. Remarkably, all these rates were increasing compared to 1990 (Forouzanfar et al., 2017, Williams et al., 2018). In 2016 a team of experts acknowledged that “*despite extensive knowledge about ways to prevent as well as to treat hypertension, the global incidence and prevalence of hypertension and, more importantly, its cardiovascular complications are not reduced—partly because of inadequacies in prevention, diagnosis, and control of the disorder in an ageing world*” (Olsen et al., 2016). Based on the above, they listed ten key actions to globally improve the management of blood pressure, including “*better identification of people at high risk to optimise treatment approaches*”: needless to stress how this ties to the quest for better pathophysiological understanding, particularly in relation to an individual’s risk of cardiovascular events.

In the recent past, such risk was traditionally identified with ischaemic heart disease (4.9 million SBP-related deaths per year), haemorrhagic stroke (2.0 million), and ischaemic stroke (1.5 million)(Forouzanfar et al., 2017). However, hypertension is independently associated also with other common and prognostically relevant complications, such as peripheral artery disease, end-stage renal disease, atrial fibrillation, cognitive decline and heart failure (HF). In fact, most longstanding hypertension ultimately leads to HF unless the sequence of events is interrupted by other outcomes and patients with HF very commonly have a history of hypertension (Messerli et al., 2017). When HF deaths and hospitalisations were properly assessed in hypertension trials, they comprised up to 50% of primary endpoints (Wright et al., 2015) and were significantly prevented by antihypertensive treatment (ALLHAT collaborative research group 2002, Rodeheffer, 2011, Wright et al., 2015), even to a point of leading to early study termination in specific populations (64% reduction of events in the Hypertension in the Very Elderly Trial; Beckett et al., 2008).

1.1.2 Heart failure

Heart failure (HF) is defined as “*a clinical syndrome characterized by typical symptoms (e.g. breathlessness, ankle swelling and fatigue) that may be accompanied by signs (e.g. elevated jugular venous pressure, pulmonary crackles and peripheral oedema) caused by a structural and/or functional cardiac abnormality, resulting in a reduced cardiac output and/or elevated intracardiac pressures at rest or during stress*” (Ponikowski et al., 2016). These elevated intracardiac pressures and their backward transmission eventually lead to “congestion” and typical symptoms and/or signs above. Congestion, referred to as the “*core of the syndrome, regardless of the cause*” (Pfeffer et al., 2019), reflects a global disturbance in the regulation of body fluid balance and the accumulation of oedema.

According to the most recent national and international audits, HF is common (nicor.org.uk), with a prevalence of approximately 1–2% of the adult population in developed countries rising to $\geq 10\%$ among people >70 years of age (Curtis et al., 2008, Ponikowski et al., 2016), and represents a leading cause of morbidity and mortality: once a clinically determined diagnosis of HF is made, this confers a multifold higher risk for cardiovascular death as well as for subsequent repeat exacerbations of symptoms requiring hospitalizations for HF management. Mortality during a hospitalisation is approximately 4%, and 10% within 1 month after discharge (Pfeffer et al., 2019).

For the purpose of classification, HF is defined according to the fraction of the left ventricular volume ejected per beat, i.e. the Ejection Fraction (EF), with EF ranging from normal ($\geq 55\%$) or only mildly reduced (i.e. typically $\geq 50\%$ in HF with preserved EF; HFpEF) to those with markedly reduced EF (i.e. typically $< 40\%$ in HF with reduced EF; HFrEF). The grey area in between has recently been named ‘HF with mid-range EF’; its biological nature and amenability to treatment, compared to the other two extremes, is still under investigation (Ponikowski et al., 2016).

Beyond the arbitrary cut-offs of systolic function used for their definition, HFpEF and HFrEF are biologically different diseases (Lam et al., 2018): in contrast to the many therapeutic advances for HFrEF over the last decades, an effective treatment for HFpEF remains elusive. Owing to this gap and to the ageing of the population, which tends to closely cluster with HFpEF, the predicted raise in the prevalence of HF (Benjamin et al., 2018) seems driven by patients where the left ventricular ejection fraction is not markedly abnormal. Similar to the general HF prevalence, the current increases in HF hospitalizations are mostly due to HFpEF (Chang et al., 2018), carrying a 1-year prognosis almost as poor as in patients with HFrEF (Campbell et al., 2012).

The initial simplistic identification of HFpEF with diastolic HF – as opposed to the “systolic” HFrEF – evolved over the years in parallel with better appreciation and understanding of myocardial and peripheral abnormalities, as well as specific clinical fingerprints, typically associated with the syndrome. In particular, HFpEF patients are more frequently affected by multiple cardiovascular comorbidities and risk factors like hypertension (but also obesity, coronary artery disease, diabetes mellitus, atrial fibrillation and chronic kidney disease) compared to HFrEF (Pfeffer et al., 2019). This observation, along with new available data on myocardial structure, function, and signalling in HFpEF, led to the idea of a systemic microvascular disease rather than a purely cardiac phenomenon (Paulus and Tschope, 2013, Kitzman et al., 2015).

1.1.3 A common ground

Since the seminal Framingham Study, hypertension was identified as the most common risk factor for developing HF, with a hazard ratio of 2-fold in men and 3-fold in women after adjustment for age and other HF risk factors (Levy et al., 1996).

Most of the understanding from traditional pathophysiology identifies the mechanical stress on the myocardium as the initial trigger for the association (Messerli et al., 2017). In a time-dependent sequence of events, prolonged pressure overload induces concentric left ventricular hypertrophy (LVH), ventricular stiffening, diastolic dysfunction and, eventually, HFpEF (Borlaug, 2014). Indeed, more than 90% of HFpEF diagnoses are antedated by recognised or unrecognised hypertension. Whenever hypertension clusters with other conditions favouring also volume overload (e.g. obesity, chronic kidney disease, anaemia), eccentric hypertrophy with increase in both cardiac mass and chamber volume may be the prevailing phenotype. The result of longstanding pressure and volume overload is dilated end stage hypertensive cardiomyopathy, with both diastolic dysfunction and reduced ejection fraction. At this stage of LV dysfunction, patients who previously exhibited high blood pressure values may paradoxically present with “decapitated hypertension”, i.e. normal or even low BP values. Reversion of these values by improving the global performance of the ventricles, for example with cardiac resynchronization therapy (Ather et al., 2011), clearly suggests that the underlying biological derangements are still in place regardless of BP readings.

After the ‘microvascular paradigm for HFpEF’ was first put forward (Paulus and Tschope, 2013), suggesting a systemic ‘*inflammatory*’ state affecting myocardial vascularisation as the underlying cause of the disease, a large amount of clinical and preclinical data accumulated in support of the paradigm. Surprisingly, these included animal models where vascular – and ultimately ventricular – dysfunction occurred and lead to a HFpEF phenotype in the absence of arterial stiffening or elevated BP values (Waddingham and Paulus, 2017).

At variance or at least in parallel with the cause-and-consequence interpretations based on a mere pressure-overload perspective, I found the idea of a common pathophysiological ground between hypertension and HF - particularly HFpEF - of extreme speculative and potentially therapeutic interest. Emerging perspectives on the homeostasis of salt, traditionally coupled to water by the basic concepts of *osmosis* but approached as independent by these novel perspectives, gave me the stimulus to dig into this question. The research results discussed in this thesis eventually suggested that such ground is common not only to hypertension and HF, but also to many other conditions predisposing to HFpEF and herein suggested to be part of a ‘*congestion-continuum*’.

1.2 Salt in cardiovascular disease – a “classic” association

1.2.1 Salt, high blood pressure and cardiovascular outcomes

A large and diverse body of evidence supports a close association between salt (NaCl) and high BP.

On a population basis, there is general agreement that a reduction in salt (or more appropriately sodium, Na⁺) intake translates into lower BP, as shown by both observational/epidemiological (Prior et al., 1968, Intersalt, 1988) and randomised controlled interventional (Sacks et al., 2011 and other studies, reviewed in He et al., 2020). Based on the predicted benefit that would follow a population-level decrease in BP, 3 million deaths per year and 70 million disability-adjusted life-years were attributed to high salt intake (GBD 2017 diet collaborators 2019). In light of the global burden of hypertension (Murray and Lopez, 2013, Forouzanfar et al., 2017) and the relatively recent increase in Na⁺ intake due to processed food, many national and international bodies, including WHO (World Health Organization, 2012), recommended a reduction in the population’s salt consumption. To which extent, is a matter of ongoing debate.

In fact, many cohort studies have investigated the relationship between salt intake and cardiovascular events and/or mortality (He et al., 2020) beyond the above prediction. However, differences in methodologies and inclusion criteria affected the conclusions to a point that a J or U-shaped association (i.e. both low and high salt intakes being associated with an increased risk) has been suggested by some authors (O'Donnell et al., 2014, Mentz et al., 2018) and disputed by others (Cogswell et al., 2016, He et al., 2020). Therefore, a general consensus for the optimal range of salt intake is still far from reach (Messerli et al., 2018, He et al., 2019, Mentz et al., 2019, O'Donnell et al., 2020).

Conclusions from both parts have their own strengths and inherent limitations. Unfortunately, long-term randomized trials on the effect of salt reduction on cardiovascular disease, which could possibly overcome at least some of these limitations, *“are extremely scarce because they are difficult to carry out, owing to ethical concerns over subjecting participants to high salt intakes as well as to multiple methodological challenges, such as compliance with lower salt intake over many years in food environments where highly salted processed foods are widespread, cross-contamination*

between study groups, and the large sample size that would be required to achieve sufficient statistical power” (He et al., 2020).

All in all, a Cochrane review of the few studies with follow-up of at least six months reported an insufficient power to draw any firm conclusions and recommendations. Importantly, however, the estimates of the clinical benefits from dietary salt reduction were *“larger than would be predicted from the small blood pressure reductions achieved”* (Adler et al., 2014). These findings parallel previous suggestions of a link between salt-induced blood BP changes and cardiovascular events (Morimoto et al., 1997) or death (Weinberger et al., 2001) that was intriguingly independent of BP.

1.2.2 Salt-sensitivity of blood pressure

From a pathophysiological point of view, the relationship between salt and BP finds its reasons in the seminal work by Guyton and colleagues. Since the ‘70s, they proposed a mechanistic link between Na⁺ overload and the development of overt hypertension, whereby an increase in blood pressure would be a compensatory mechanism (Guyton and Hall, 2011, Guyton et al., 1980, Hall et al., 1980, Hall, 2016). In simple terms, any impairment in the multiple and intricate body systems devoted to the homeostasis of Na⁺ (Guyton et al., 1972, Elijevich et al., 2016), primarily involving the kidneys, would lead to a resetting of the steady-state blood pressure to a higher level in order to facilitate adequate Na⁺ and water excretion by pressure-natriuresis.

Over the years since the original conceptualization, Guyton’s gigantic cardiovascular physiology model of everything then known (Guyton et al., 1972) inevitably faced the advancement of knowledge, as well as criticism from those favoring a primary vascular - rather than renal - impairment in the response to a salt load as the drive for the increase in BP (Morris et al., 2016, Kurtz et al., 2016, Kurtz et al., 2018): these authors suggest that a subnormal vasodilatory response to increases in Na⁺ intake, in the absence of an abnormally large increase in renal retention of sodium, mediates the initiation of salt-induced increases in blood pressure.

A pragmatic synthesis of the opposite positions, offering a simple hydraulic but ultimately clinical point of view, indicates that derangements in either renal, or vascular, or even neural (Blaustein et al., 2012) regulations upon salt loading (or a variable mixture of these and possibly other factors) would result in a *salt-sensitive* phenotype. This concept of ‘salt-

sensitivity of blood pressure' reflects the marked heterogeneity of individuals in their BP response to salt loading (Weinberger et al., 1986). At variance with experimental animals, where the trait has been inbred since the pioneer approach by Dahl et al (Dahl et al., 1962), in humans it is normally distributed, as a result of combined genetic, environmental, physiologic (e.g. aging, gender, ethnicity) and clinical factors (Elijovich et al., 2016, Gensalt, 2007).

When these factors are clustered or dissected, as in many of the aforementioned population studies, the extent of the BP fall upon salt intake reduction appears more pronounced in old or African-American groups, in individuals with low renin hypertension (Warnock, 1999), in persons with hypertension and those consuming diets containing > 5 g Na⁺/day (Mente et al., 2014), with large variations resulting from the uneven distribution of salt-sensitivity and its determinants (He et al., 2020, Elijovich et al., 2016). When the focus is rather on a single general hypertensive patient, the unpredictable therapeutic effect of a decrease in salt intake is unraveled only by cumbersome loading tests with arbitrary diagnostic cut-offs (Weinberger et al., 1993) and a practical salt-sensitivity definition suitable for everyday clinical practice remains elusive.

Of note, the very same pathophysiological mechanisms underlying blood pressure salt-sensitivity may contribute to the risk for cardiovascular disease independent of pressure effects (Safar et al., 2000) and the role for *salt-dependent* changes in BP as the sole causal determinant of *salt-dependent* cardiovascular disease (whichever the definition is) has not been proven (Kotchen et al., 2013).

For the purpose of this thesis, the topic of salt in cardiovascular disease was not observed through the lens of what is ultimately a single, although universally accessible and adopted, biomarker, i.e. BP (Currie and Delles, 2016). Different questions, related to systemic and local sodium handling and its mechanistic implications for pathophysiology, rather emerged as the topics of interest.

1.3 A novel blood pressure-independent association

Firstly, recently work by J. Titze and co-workers suggested a BP-independent link between high Na⁺ intake and a global shift in metabolism, driven by the ultimate need to preserve water upon this dietary habit.

This conclusion came from a puzzling observation, made in the unique experimental setting of a human long-term Na⁺ balance study (Rakova et al., 2013): this unprecedented investigation took advantage of Russian spaceflight simulations. The small and tightly controlled setting of the flight program, comparable to an animal metabolic cage, allowed to circumvent the aforementioned compliance, cross-contamination and ultimately ethics issues related to the conduction of trials of salt intake modulation. The investigators modified the salt intake of 10 male cosmonauts, fixed at 12 g/day, 9 g/day or 6 g/day, each for 30-60 days, and collected 24 hr urine daily. Contrarily to previous human investigations, largely based on unphysiological short-term shifts from very low to high salt intakes, this design led to novel observations in relation to Na⁺ and water long-term homeostasis. In particular the authors reported:

- 1) Large infradian changes in total-body Na⁺ without parallel changes in body weight (Rakova et al., 2013), as discussed in the next sections;
- 2) A decrease, rather than the expected increase in water intake upon high-salt compared to low-salt diet (Rakova et al., 2017).

Notably, the latter unanticipated finding did not prevent equal (or even increased, depending on data stratification) urinary volumes upon high-salt diet. To reconcile the mismatch, the authors advocated surplus endogenous free water generation from an exaggerated catabolic state and from enhanced renal accrual, which would make any extra exogenous water intake unnecessary.

The hypothesis was tested in rodent models, where urea excess was identified as a key osmotic force to minimise free water loss (Kitada et al., 2017), via renal recycling and extrarenal generation from a salt-driven catabolic state (Figure 1-1).

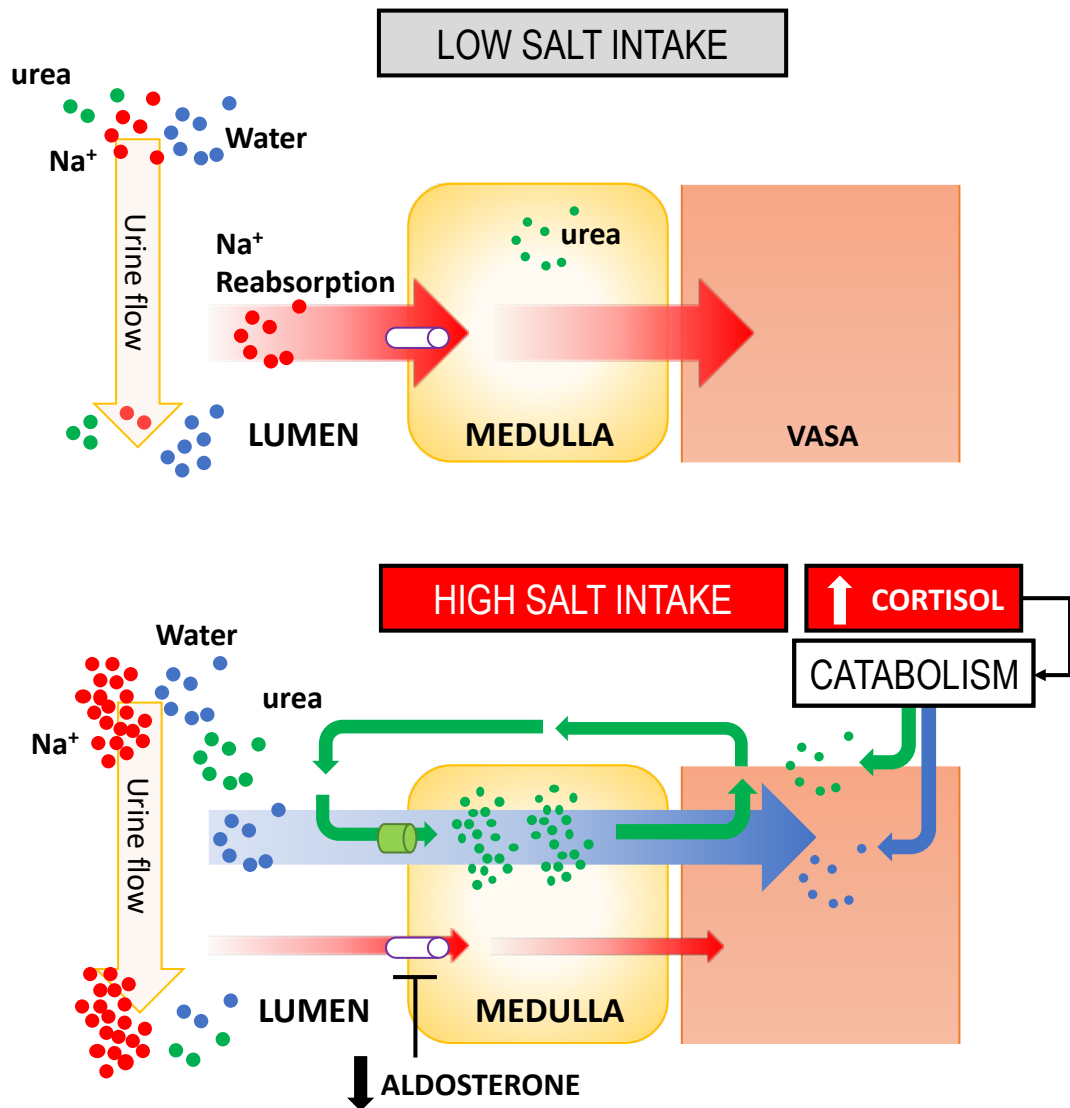


Figure 1-1. Natriuretic-ureotelic water-preserving mechanisms upon high salt intake.

Symbols: red = Na⁺, blue = water, green = urea. Upper panel: under low salt intake conditions, classic mechanisms (including the renin-angiotensin-aldosterone system) favour Na⁺ reabsorption from the urinary tubular lumen to the circulation to maintain electrolyte homeostasis. Lower panel: Rakova et al (Rakova et al., 2017) and Kitada et al (Kitada et al., 2017) suggest that upon high salt intake, renal specific and systemic mechanisms, are in place to prevent water depletion caused by passive osmotic diuresis. While Na⁺ reabsorbing mechanisms are downregulated, free water accrual is facilitated by higher reabsorptive gradients, generated by excess urea in the medulla via enhanced recycling and metabolic generation, i.e. protein catabolism. The catabolic reactions generate further endogenous water for maintenance of fluid homeostasis. Salt-driven glucocorticoid release is held to sustain the metabolic shifts and the catabolic state.

In particular, an extremely high-salt dietary regimen (4% NaCl in the chow + 0.9% saline to drink) induced a substantial weight loss upon pair-feeding with the low-salt fed controls; likewise, with ad libitum feeding, food intake was markedly increased in *high-salt + saline* mice to maintain a body weight similar to controls. Further analyses in these mice revealed muscle mass loss and protein breakdown, as a source for urea generation, as well as a global energy metabolism reprioritisation identified by metabolomics and calorimetry.

In both their human and rodent studies, the authors observed an increase in 24h urine glucocorticoids excretion upon high-salt, opposite to the trends observed for aldosterone.

While aldosterone data were in keeping with the traditional understanding of the renin-angiotensin-aldosterone axis as a sodium retentive effector in relation to salt intake, spontaneous rhythmical glucocorticoid excretion was paralleled by increased urine volume without increase in water intake, thus implying generation and excretion of surplus endogenous water. Overall, a rhythmical and/or subclinical hypercortisolism was suggested to mediate the observed metabolic shifts and lean mass loss (Figure 1-1).

With such reprioritisation of energetic and metabolic pathways, high salt intake could impact global cardiovascular health in a much broader and more complex fashion than currently appreciated. The shift of metabolic patterns observed in experimental settings upon high salt intake – representative of the current average Western diet - could significantly contribute to the highly prevalent and prognostically ominous clustering of diabetes, dyslipidaemia and obesity in the hypertensive population. Notably, a direct association between salt-intake and obesity independent of energy intake has recently been reported in the UK National Diet and Nutrition Survey (Ma et al., 2015).

1.4 Novel concepts on sodium homeostasis

Intake is just one (experimentally convenient but far from exhaustive) side of the coin for any homeostatic system. Classic physiology advocates the ultimate achievement of a balance between salt intake and excretion (Cannon, 1929), thus supporting the clinical practice of estimating Na^+ intake from 24h Na^+ urinary excretion.

Independent experimental findings by Titze and others over the last 20 years, however, challenged the assumption. Heer et al first observed that short-term (1 week) experimental increases in Na^+ consumption led to a positive Na^+ balance (i.e. Na^+ retention) without commensurate water retention or body weight changes in young healthy male subjects (Heer et al., 2000). As an explanation, they suggested the interstitial space as a site for potential sodium storage without an osmotic effect. Further work by Titze's group substantially expanded on the topic of Na^+ long-term homeostasis and tissue accumulation.

1.4.1 Disproof of a constant sodium balance

In a preliminary observational (Titze et al., 2002) and the subsequent interventional spaceflight simulation studies (Rakova et al., 2013, Lerchl et al., 2015), they identified a marked variability in daily urinary Na^+ excretion (uNaV) despite fixed intake, as well as some degree of dissociation between Na^+ and water balance. In particular, they concluded that single 24-hour urine collections at intakes ranging from 6 to 12 g salt per day did not precisely reflect individual salt intake, with repeated measurements improving this performance (Lerchl et al., 2015): this has obvious implications for use of uNaV in clinical practice. Even by accounting for this variability, periodic changes in total body Na^+ without parallel changes in body weight and extracellular water were detected and related to rhythmic hormonal control (Titze et al., 2002, Rakova et al., 2013).

Notably, in the healthy subjects taking part in these studies, steady state between sodium intake and excretion was eventually achieved (Lerchl et al., 2015), although not within few days but rather weeks or months. No such demonstration exists in the ultra-long term (lifespan) and particularly for individuals with known cardiovascular or renal disease.

1.4.2 Water-independent tissue sodium accumulation

Whether the interstitial space could offer a depot for a long-term storage of Na^+ (Heer et al., 2000), potentially preventing achievement of a steady state in individuals other than the young healthy cosmonauts involved in the spaceflight simulations, was experimentally investigated.

Preclinical rodent models of normotension, salt-resistant and salt-sensitive hypertension, showing different degrees of Na^+ -associated fluid retention upon high Na^+ intake, first suggested a role for water-independent Na^+ storage in the pathogenesis of hypertension (Titze et al., 2002a). Subsequent experiments conducted by desiccation and dry ashing of whole rat carcasses or specific compartments (e.g. bones, quadriceps muscles and skin) pointed to skin as the specific depot for excess Na^+ accumulation (Titze et al., 2003, Titze et al., 2005, Machnik et al., 2009, Wiig et al., 2013) and negatively charged glycosaminoglycans (GAGs) network was identified as the dynamically regulated substrate for putative interstitial skin Na^+ binding (Titze et al., 2004). The apparent dissociation between Na^+ and water tissue content, consistent with the results of the balance studies, led to the conceptualisation of a hypertonic phenomenon.

This was paralleled by two lines of complementary evidence: 1) the activation of pathogenic immune-inflammatory cells upon culture in supraphysiological concentrations of Na^+ and 2) the *in vivo* visualisation of Na^+ excess in the skin and skeletal muscle of patients with cardiovascular diseases or risk factors, by means of magnetic resonance imaging.

- 1) Hypertonic extracellular Na^+ was first found to boost the activation of inflammatory TH_{17} cells *in vitro* (Kleinewietfeld et al., 2013). Similar results were reported by independent investigators for macrophages (Jantsch et al., 2015, Zhang et al., 2015) and dendritic cells (Barbaro et al., 2017, Van Beusecum et al., 2019). All the above investigations assumed that the *in vitro* exposure of immune cells to a hypertonic milieu recapitulated the *in vivo* tissue conditions.
- 2) Translation of the experimental findings from rodents to humans was made possible by ^{23}Na magnetic resonance spectroscopy and high-magnetic field imaging (MRI). Spectroscopy quantification of Na^+ in skeletal muscle and skin from rats and from patients undergoing limb amputation was first validated against direct chemical analysis of tissues (Kopp et al., 2012). By using dedicated phantoms loaded with different concentrations of NaCl as calibration solution, 3-7T MR imaging quantification was thereafter implemented. This allowed to identify excess skin and/or skeletal muscle Na^+ content in patients with refractory hypertension or primary aldosteronism compared to normotensive controls (Kopp et al., 2012, Kopp et al., 2013) and in other clinical conditions such as acute heart failure (Hammon et al., 2015), systemic sclerosis (Kopp et al., 2017) and diabetes (Karg et al., 2018). Skin Na^+ was also found to correlate better than total body overhydration or blood pressure with left ventricular mass in patients with chronic kidney disease (Schneider et al., 2017), thus stimulating the quest for interventions specifically targeting tissue Na^+ to improve cardiovascular outcomes in this extremely-high-risk population.

Overall, this new notion of local Na^+ accumulation was acknowledged by independent reports as a paradigm shift (Elijovich et al., 2016, Mancia et al., 2017), closely linked to the enormous public health burden of ageing and cardiovascular disease. Other authors claimed that “*dissociation of blood pressure from fluid volumes*” could reflect “*complexities of sodium handling not accounted for by Guyton’s hypothesis*” (Coffman, 2014).

1.5 The lymphatic system

In further support of a hypertonic interstitial Na^+ accumulation was the evidence of tonicity-responsive enhancer binding protein (TonEBP) activation in the skin resident mononuclear phagocytic cells of rodents upon salt loading (Machnik et al., 2009). Downstream signalling included VEGF-C secretion, VEGF receptor 3 (VEGFR3) activation and plastic expansion of the lymphatic vascular network to provide enhanced local Na^+ excess clearance (Wiig et al., 2013). Whenever any intermediate effector of this signalling was blocked and the lymphatic expansion prevented, the resulting phenotype entailed hypertonic skin Na^+ retention and salt-sensitive hypertension.

After these first reports, enhanced cardiac lymphangiogenesis induced by VEGF-C was shown to reduce myocardial fibrosis and macrophage infiltration, decrease blood pressure and preserve myocardial function in a salt-sensitive rat model of hypertension, while VEGF-C blockade produced opposite effects (Yang et al., 2014). Similarly, an inducible genetic model of kidney-specific lymphangiogenesis proved resistant to the development of hypertension induced by high-salt diet (Lopez Gelston et al., 2018).

Overall, these studies uncovered a novel role for lymphatic vessels in the control of local Na^+ homeostasis and the pathogenesis of hypertension. In fact, the importance of this frequently neglected part of the circulation and microcirculation is currently undergoing a substantial reappraisal in the context of cardiovascular physiology as a whole (Mortimer and Rockson, 2014, Herring, 2018, Aspelund et al., 2016), as detailed below.

1.5.1 *Lymphatic role in microvascular haemodynamics*

At the level of microcirculation, where the exchange of metabolic substrates for tissues takes place, the interplay between plasma, the highly organized microvascular wall, the perivascular interstitial space and the primary force sustaining the circulation, i.e. blood pressure, generates filtration. This phenomenon is governed by the Starling-Landis principle, whereby the rate is proportional to the hydraulic pressure gradient between plasma and interstitium minus the corresponding oncotic gradient ($P_p - P_i$ and $\Pi_p - \Pi_i$, favouring and opposing filtration, respectively (Herring & Paterson, 2018)).

Contemporary evidence, based on direct measurements of the hydraulic and oncotic interstitial forces, disproved the commonly held idea of a sustained reabsorption of

interstitial fluid at the venous end of the capillary beds, where hydraulic forces drop (Figure 1.2): with few anatomical and/or disease exceptions (e.g. in intestinal mucosa or in post-haemorrhagic states), the net sum of forces along the entire length of well-perfused microvessels consistently favours filtration over absorption (Levick and Michel, 2010). Therefore, local fluid balance is achieved by other structures and mechanisms, namely the lymphatic vessels, which constantly drain the ultrafiltrate and filtered plasma protein and transport it back as lymph to the central venous blood. A substantial volume of lymph is generated and transported every day (4-8 L), even in the face of a vanishing small filtration fraction in most tissues (i.e. the fraction of plasma water that escapes during one transit through the capillary, ~0.1%-0.3%).

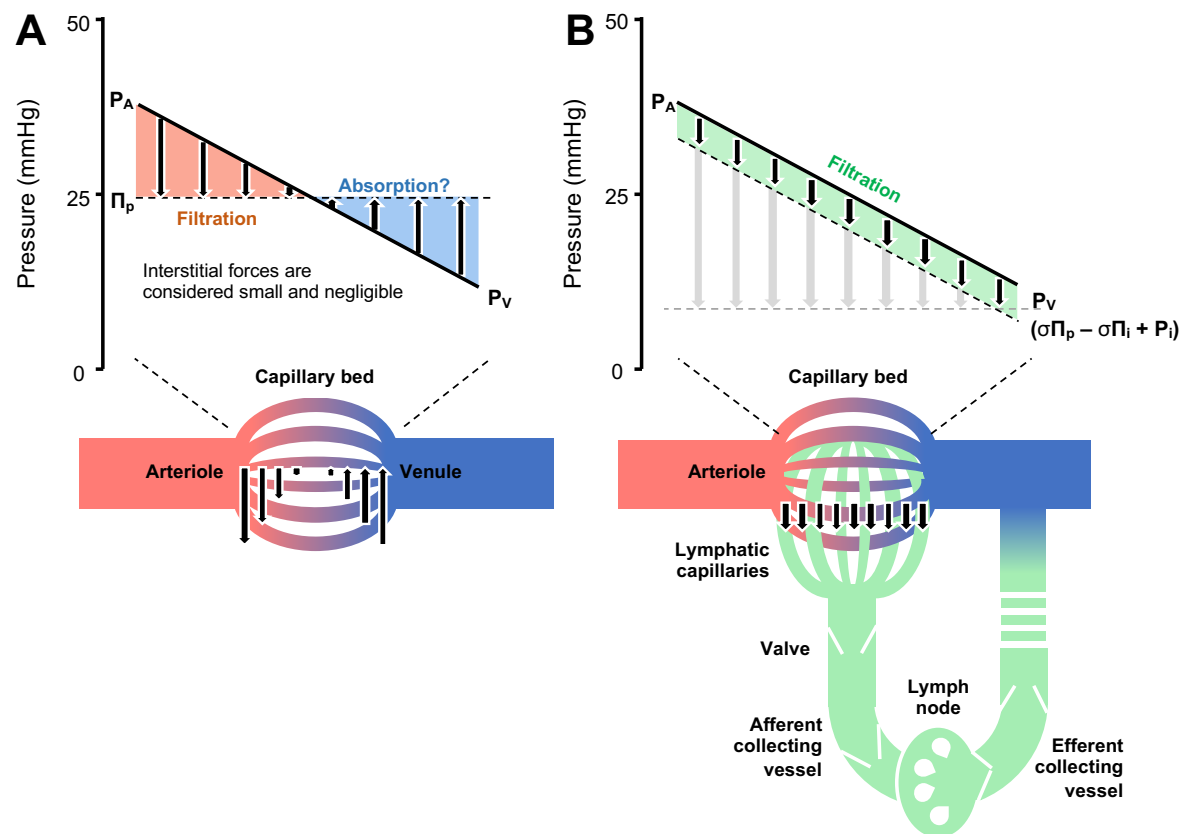


Figure 1-2. Starling-Landis equilibrium and the lymphatic system.

Panel A) traditional arteriovenocentric model assuming interstitial forces negligible and, therefore, reabsorption of fluids at the venous end of the microvascular bed. Panel B) reappraisal of the above by including direct measurement of hydrostatic (P) and oncotic (Π) pressures; calculated values (grey arrows) and actual filtration (black arrows), as vascular glycocalyx modulates Π_i across the capillary bed. Fluid filtered as a constantly positive sum of forces is drained by the lymphatic system to central venous blood via lymphatic capillaries, afferent collecting vessels, lymphnodes, efferent collecting vessels and ducts. P_A , P_V and P_i = arterial, venular and interstitial hydrostatic pressures, respectively; Π_p and Π_i = plasma and interstitial oncotic pressures, respectively; σ = reflection coefficient (adapted from Levick, Cardiovascular Research, 2010;87(2):198-210).

1.5.2 Anatomy and function

Lymphatic vessels are unidirectionally and hierarchically organized into series of blind-ended lymphatic capillaries, pre-collecting vessels and collecting vessels that, via chains of lymph nodes, ultimately drain into to the blood circulation via the thoracic or right lymphatic duct and the subclavian veins (Figure 1.2 B).

Lymphatic capillaries (diameter 20-70 μm) are composed of a single layer of lymphatic endothelial cells (LECs) with an incomplete basement membrane and characteristic “buttonlike” junctions, opened and closed by intraluminal and external pressures and suitable for the controlled entry of solutes, macromolecules and cells. The larger collecting vessels (70-500 μm) are less permeable, are covered by periendothelial lymphatic muscle cells and are organized into a series of coordinated functional units, each called “lymphangion”, separated by intraluminal one-way valves and capable of spontaneous pumping activity. In addition to the extrinsic forces resulting from intermittent compression of the lymphatics by tissue movements, like skeletal muscle contractions, intestinal peristalsis, movement of the skin or pulsation of adjacent arteries, this autonomous contractile activity generates intrinsic propulsion forces for progression of lymph through the lymphatic system.

Lymphatic muscle shares biochemical and functional aspects with both vascular and cardiac muscle. It is characterised by a pacemaker-generated action potential within each lymphangion and by a sequence of systolic (contractile) and diastolic (filling) phases which bear striking similarities with the mechanics of the cardiac pump; in particular, contractility is sensitive to preload, afterload and neuro-hormonal regulation (Figure 1-3).

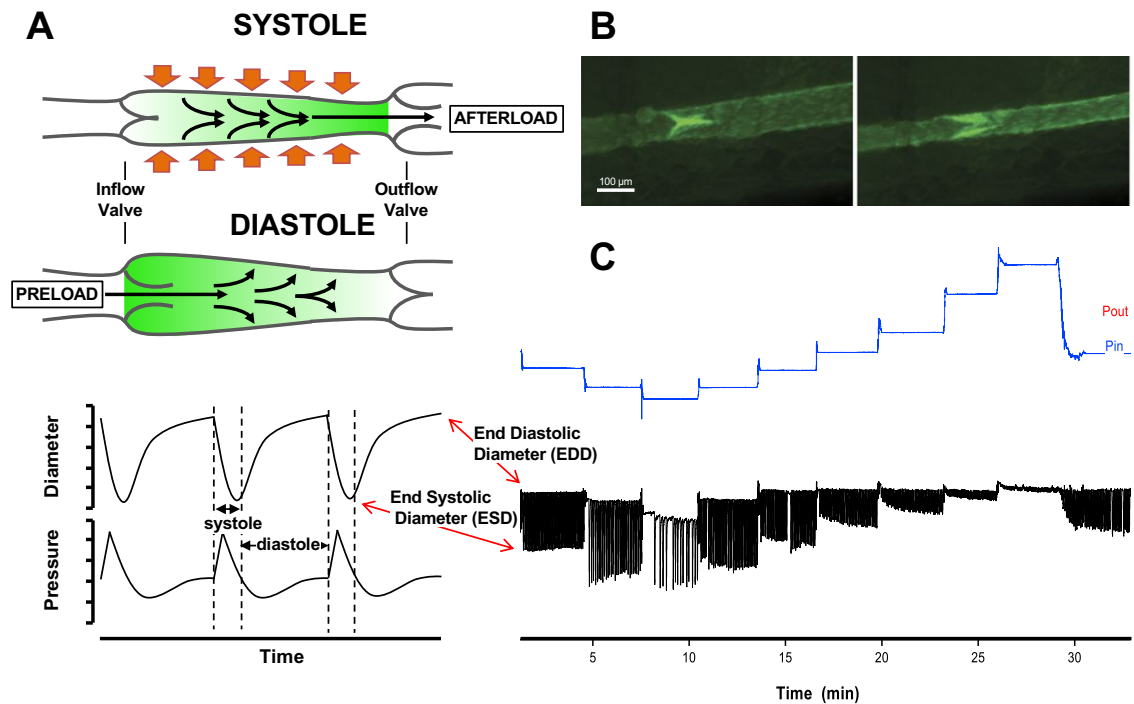


Figure 1-3. Lymphangion contraction cycle.

Panel A) scheme of the systolic-diastolic phases of lymphangion contraction, with representative pressure and diameter traces. Panel B) opening and closing of a lymphatic valve corresponding to the different phases of the contraction cycle (end-diastole for the downstream lymphangion, left; mid-systole of the upstream lymphangion, right). Panel C) contractile activity of a mouse flank lymphatic collector, isolated and mounted on a myograph system by the author of this thesis in the lab of Michael Davis (University of Missouri, Columbia, MO) and pressurised with identical input and output pressures – modulated as per blue tracing (range 0.5-8 cm H₂O). Please note the difference in systolic frequency and amplitude at different pressures; each spike corresponds to a systolic deflection, as per panel A (bottom).

Intriguingly, not only the lymphatic vascular density but also the ultimate result of this contractile activity, i.e. lymph flow, was increased in rats with evidence of skin Na⁺ accumulation after salt exposure (Karlsen et al., 2018).

1.6 Traditional vs novel views: open questions

As discussed in previous sections, all these novel perspectives on Na⁺ homeostasis and its impact on hypertension and cardiovascular disease at large, even independent of BP values, emerged as possible paradigm shifts. However, at the time my PhD studies were conceived and conducted, the concepts of a sodium-driven shift in metabolism and of water-independent accumulation in tissues had not faced the challenge of either independent confirmation or pathophysiological reappraisal, for the sake of expansion or dispute.

On the one hand, the proposed catabolic mechanisms of water preservation upon high Na^+ intake lacked demonstration in humans who were not in a dietary- and environmentally-controlled experimental setting (addressed in Chapter 3).

On the other hand, the suggestion of a water-independent hypertonic accumulation of Na^+ in tissues and its extremely high prevalence in many cardiovascular diseases and risk factors (based on chemical analysis in rodent models and ^{23}Na -MRI in humans, by syllogism) disputed, at least in the ultra-long term, the dogma of an even intake-excretion balance. While doing so, however, it raised critically important questions regarding:

- 1) differential local Na^+ handling beyond the kidney in different sexes, ages, organs and clinically relevant conditions; in other words: *“when and where – or in whom - does it happen?”* (addressed in Chapters 4-7)
- 2) differential functional impact of such hypertonic interstitium on the surrounding cells and structures other than hypertonic Na^+ -activated immune cells, such as vessels. In other words: *“is it - and if so, how is it - biologically and clinically relevant, particularly to vascular function?”* (addressed in Chapters 5 and 7)

Such key questions, addressed in this thesis by direct tissue chemical analysis and assessment of vascular function in multiple experimental settings and conditions, confronted some discrepancies in the original observations.

First, the novel phenomenon of hypertonic tissue Na^+ accumulation was initially described as skin specific (Titze et al., 2003, Titze et al., 2005) but ^{23}Na -MRI in humans identified also skeletal muscle and, more recently, myocardium (Christa et al., 2019) as a site of excess Na^+ signal, thus questioning the original specificity.

Second, it seemed difficult to unequivocally reconcile a dual osmotically-active and -inactive nature of interstitial Na^+ , driving TonEBP-mediated signalling while simultaneously eluding parallel and commensurate water accrual. Therefore, I hypothesised that a hypertonic Na^+ accumulation in the interstitium could facilitate capillary fluid extravasation and oedema, and identified patients with HF, where oedema is a typical feature, as a suitable population where to test such contention. In particular, the high prevalence and public health relevance, the established microvascular dysfunction, the overt body fluid/ Na^+ homeostasis disturbance and the typical clustering with conditions

known to exhibit excess tissue Na^+ at ^{23}Na -MRI (e.g. hypertension, diabetes and CKD) made HFpEF the ideal and clinically relevant disease for my research aims.

Additionally, based on the anatomical and functional lymphatic expansion under conditions of Na^+ excess in preclinical models, I included lymphatics in the morphological and functional assessment of the microvasculature in HFpEF (Chapter 7), under the hypothesis of a bidirectional link between microvascular dysfunction and Na^+ accumulation.

1.7 Research aims

In summary, under the overarching aim of investigating novel aspects of sodium homeostasis in cardiovascular disease, this thesis focuses on both systemic and “local” mechanisms.

Specific aims were to investigate:

- 1) the impact of high Na^+ intake on renal water-preserving mechanisms and metabolomics signatures, as well as their association with cortisol as the putative intermediate effector of the proposed BP-independent metabolic shift, in a real-life hypertensive population.
- 2) the phenomenon of tissue Na^+ accumulation in terms of:
 - isotonic (water-paralleled) or hypertonic (water-independent) nature, by theoretical modelling (Chapter 4) and experimental assessment in rodent models of salt sensitivity/salt loading (Chapter 5), in patients with hypertension (Chapter 6) and patients with HFpEF (Chapter 7);
 - tissue/organ distribution in relevant rodent models (Chapter 5);
 - clinical correlates in a hypertensive population (Chapter 6).
- 3) microvascular function, in relation to interstitial Na^+ accumulation. This was assessed:
 - ex vivo in rodent models (Chapter 5);
 - ex vivo and in-vivo in patients with HFpEF (Chapter 7), including measures of capillary-interstitium fluid exchange and lymphatic drainage.

GENERAL METHODS

This chapter is arranged as per proposed experimental aims and closely recapitulates the sequence of the chapters and sections in the thesis. The general approach and methods to address aims are presented here; additional details, particularly those specific to individual studies, are provided in the dedicated chapters.

2.1 Assessment of the metabolic impact of high sodium intake

To investigate: 1) the renal water-preserving mechanisms primarily proposed to induce a metabolic shift upon high Na⁺ intake, 2) the metabolomics signatures and 3) their association with cortisol, I took advantage of a large and carefully characterised real-life hypertensive population, as part of the *SYCAMORE study*: Sodium intake and subclinical hYper-Cortisolism: Association and MetabOlic signature.

The study analysed clinical and biochemical data from consecutive consenting patients referred to the tertiary Hypertension Center of the University of Padua, who underwent biochemical screening for secondary causes of hypertension between 2012 and 2017.

The screening protocol included blood sampling and 24h urine collection on usual diet and avoidance or washout from medications affecting the renin-angiotensin-aldosterone system. Patients with a conclusive diagnosis of essential (primary) hypertension were stratified according to classes of Na⁺ intake (Low ≤ 2.3 g/d; Medium 2.3-5g/d; High >5 g/d) defined based on urinary 24h Na⁺ excretion at the time of the screening.

Blood and 24h urine data were used to calculate creatinine clearance, as a surrogate for glomerular filtration rate (GFR), fractional excretions of Na⁺ and water, as measures of their tubular handling, and tubular energy expenditure, as estimated by measured Na⁺ reabsorption and Na⁺/ATP stoichiometry. Non-targeted liquid chromatography–mass spectrometry (LC-MS) metabolomics was conducted on plasma samples from an unselected subcohort.

Univariate and multivariate comparisons of renal measures of Na⁺/water handling, cortisol and plasma metabolomics signatures were performed across Na⁺ groups.

Please see Chapter 3 for further details.

2.2 Assessment of tissue sodium accumulation

Investigation of the nature of tissue Na⁺ accumulation, previously indicated as hypertonic by other investigators, was approached by theoretical modelling (chapter 4) and by experimental assessment in tissue samples from suitable rodent models (Chapter 5) or skin from human subjects (chapters 6 and 7). The latter entailed healthy volunteers, as controls, and patients affected by conditions where the phenomenon of tissue Na⁺ excess had been already reported (i.e. hypertension; chapter 6) or was likely to occur based on the typical clustering of comorbidities similarly associated with tissue Na⁺ accumulation (i.e. HFpEF; chapter 7).

In addition to theoretical speculations and actual conduct/interpretation of tissue chemical analyses, other relevant focuses were on: 1) the distribution of the phenomenon in organs other than skin, investigated in rodent models; 2) clinical correlates of skin Na⁺ accumulation in hypertensive patients, as well as local mechanisms of regulation as putative direct determinants.

2.2.1 Modelling (Chapter 4)

A simple mathematical model to predict the chemical composition of different tissues, which accounted for the complexity deriving from heterogeneously represented intracellular and extracellular fractions whenever a whole-tissue analysis is performed, was developed. The key underlying assumption was that Na⁺ and K⁺ are, by approximately 1.5 orders of magnitude, the most abundant cations of the extracellular and intracellular space, respectively

Specific calculations, based on physiological values of Na⁺ and K⁺ concentrations in the intracellular and extracellular fluids, are extensively reported in Chapter 4.

2.2.2 Animal models (Chapter 5)

For the purpose of this thesis, Wistar-Kyoto (WKY) and stroke-prone spontaneously hypertensive (SHRSP) rats from colonies inbred at the University of Glasgow since 1991 were used as rodent models of salt-resistance and salt-sensitivity, respectively.

SHRSP rats are a long established (Okamoto et al., 1974), sub-strain of SHR, with remarkable salt-sensitivity (Griffin et al., 2001) driven, at least in part, by a secondary aldosteronism evident since 18 weeks of age (Kim et al., 1992). Established blood pressure, body weight and RAAS phenotypes of WKY and SHRSP male rats are presented in Figure 2-1.

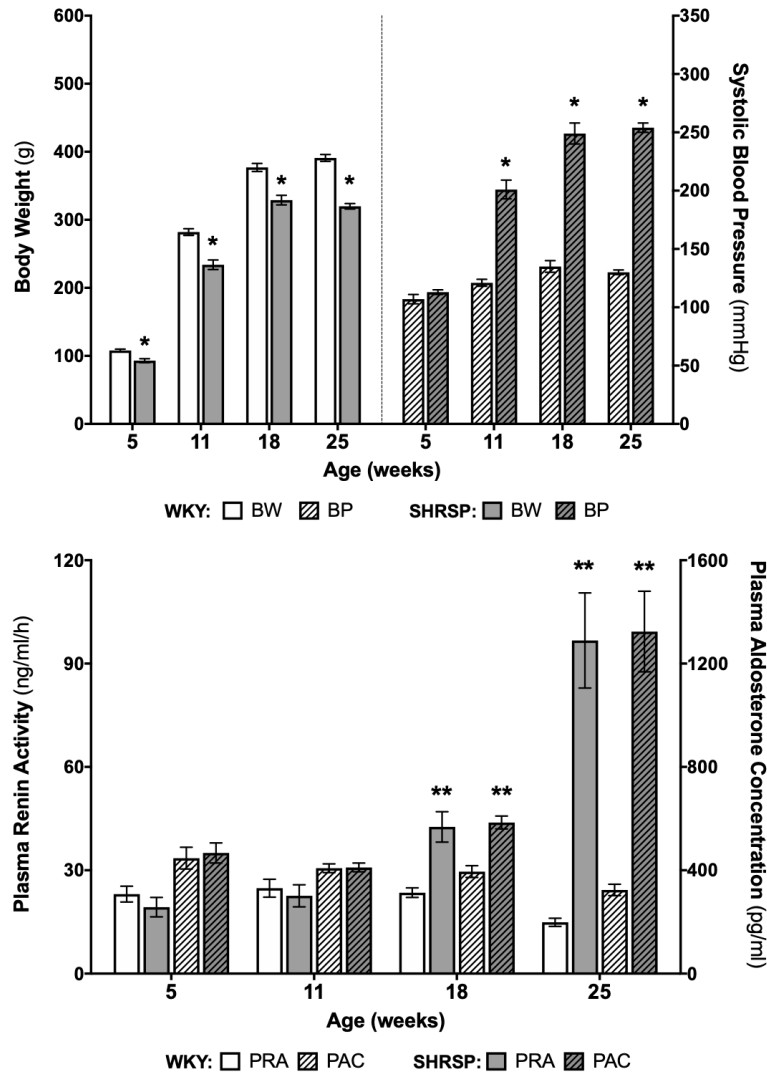


Figure 2-1: WKY and SHRSP phenotype.

BW = body weight; BP = blood pressure; PRA = plasma renin activity; PAC = plasma aldosterone concentration. Adapted and redrawn from Kim et al, *Hypertension* 1992; 20:280-291.

In two independent sets of experiments, I investigated the effect of salt-loading and ageing on Na⁺ accumulation in different tissues. Experimental details on protocols and assessment of additional outcome measures related to Na⁺ accumulation (e.g. extracellular matrix remodelling, gene expression or tissue fat content analyses) are provided in Chapter 5.

2.2.3 Human subjects (Chapters 6-7)

Na⁺ accumulation was investigated in skin samples from healthy volunteers, hypertensive patients and patients with HFpEF. Common to all these groups is the collection of a small skin punch biopsy, primarily but not solely used for the chemical analysis of the tissue.

2.2.3.1 Young healthy volunteers

A preliminary pilot study, designed to optimize of the collection and ex-vivo analysis of small human skin samples from self-defined healthy volunteers (SKILLS: SKin biopsy for Interstitium and Lymphatic vesseLS assessment), was approved by the University of Glasgow, MVLS College Ethics Committee (ref. 200160109) and conducted between May 2017 and April 2018. Due to the technical nature of the study, the sole exclusion criterion was history of potential coagulation disorders for safety reasons.

The SKILLS study allowed optimisation of the surgical procedures (2.2.4), tissue processing and chemical analysis (2.2.5), but also histology or immunohistochemical-fluorescence staining and RNA/protein isolation (please see chapters 6-7), of small human skin samples from minimally invasive punch biopsies. This was necessary to avoid jeopardizing the participation of patients or volunteers to subsequent clinical studies because of the biopsy requirement, as well as to maximize the yield of the small samples.

Eighteen subjects were involved in the study, out of a ≤ 20 initial estimate at the time of ethics application. Both ice spray and lidocaine-based topical cream were tested for local anaesthesia, in order to avoid any major impact on the chemical content of the sampled skin; upon experimental confirmation of no detectable Na⁺ or K⁺ content at flame photometry analysis (please see 2.2.5.3), the latter was confirmed as the preferred option. Both the gluteal upper quadrant and the arm were tested as suitable sites. Overall, the biopsies were well tolerated, and no adverse events were observed.

A subsequent cross-sectional study on healthy volunteers (SOWAS: SODium and WATER Skin Balance) recruited among MVLS students was approved by the University of Glasgow, MVLS College Ethics Committee (ref. 200170153) and conducted between July and December 2018. One of the study aims, relevant to this section, was to provide sex-specific skin chemical reference values from a young healthy population. Exclusion criteria entailed: lack of consent, office BP > 140/90 mmHg; obesity; previous diagnosis of

diabetes, thyroid, renal or coagulation disease; extremely low (<100 mmol/die) or high (>216 mmol/die) sodium excretion on 24h urine collection, as assessed on site by colorimetric strips (*Salinity View*, Health Mate®) at the time of the study visit. For female participants, the date of the main visit was arranged in the early follicular phase of their menstrual cycle, just after period termination; in 4 cases, due to personal logistics or continuous progesterone treatment (skin implants or vaginal coil) the main visit coincided with a luteal or luteal-like phase. Please see also section 6.2.1.2.

2.2.3.2 *Hypertensive patients*

The S₂ALT (Skin Sodium Accumulation and water balance in hyperTension) study was designed to explore the nature (iso- or hyper-tonicity) and clinical correlates of skin Na⁺ accumulation in a hypertensive population, also in relation to the mechanisms and degree of surface Na⁺/water exchange.

In brief, adult, consenting non-pregnant patients were recruited from the Blood Pressure clinic, Queen Elizabeth University Hospital, Glasgow between March and July 2019 and underwent a skin punch biopsy on the day of their scheduled clinic appointment (9:00 AM to 4:30 PM). The complete study protocol and material (Appendices 1-3), as well as assessment of correlates and additional outcome measures, including transepidermal water loss and sweat analysis, are further discussed in Chapter 6.

2.2.3.3 *Patients with HFpEF vs healthy controls of similar age and sex*

Based on the initial hypothesis of a prevalent and pathologically-relevant hypertonic skin Na⁺ accumulation in the syndrome, I designed and conducted the HAPPIFY (Heart failure with Preserved ejection fraction: Plethysmography for Interstitial Function and skin biopsY) study. Subjects with stable HFpEF (identified from outpatient HF clinics in Glasgow) and volunteers of similar age and sex, with no history or evidence at the time of the eligibility visit of cardiovascular or renal disease, hypertension or diabetes, were recruited in the study between August 2017 and December 2018.

In addition to the skin biopsies (2.2.4), participants underwent extensive vascular functional phenotyping, both in-vivo and ex-vivo (please see below, section 2.3.1 and 2.3.2), and plethysmographic assessment of microvascular dynamics and interstitial fluid accumulation in-vivo, reflecting the balance between capillary extravasation and lymphatic

drainage (please see below section 2.3.3). The complete study protocol material (Appendices 4-6), details on the histological and molecular analyses of skin samples and the approach to (micro)vascular functional assessment are further discussed in Chapter 7.

2.2.4 Skin biopsy

Approximately 40 minutes before the planned biopsy, lidocaine-based topical anaesthetic cream (LMX4) was applied: a) on the outer upper arm, approximately halfway between the elbow and shoulder, for S₂ALT study or b) on a gluteal external upper quadrant for SOWAS and HAPPIFY study. After cleaning the skin with cotton gauze pads and Na⁺/K⁺-free 70% alcohol wipes, skin punch biopsies were performed on the anaesthetised site with a disposable instrument (3-4 mm blade diameter; Kai Medical). The excised skin sample was cut on the bench into two hemicylinders, each including both epidermis and dermis: one was fixed in PFA 2% for 8-10h at room temperature, washed in PBS and stored in 70% ethanol at 4°C until paraffin inclusion for subsequent histological analyses; the second was immediately put into a pre-cooled Eppendorf tube, frozen in dry ice and stored at -80°C until tissue chemical analysis (Figure 2-2). For S₂ALT study, due to time and logistics constraints, no bench processing was feasible and the whole sample was immediately frozen in dry ice. For SOWAS, both hemicylinders were frozen and one additional biopsy was collected for whole tissue culture (please see chapter 6).

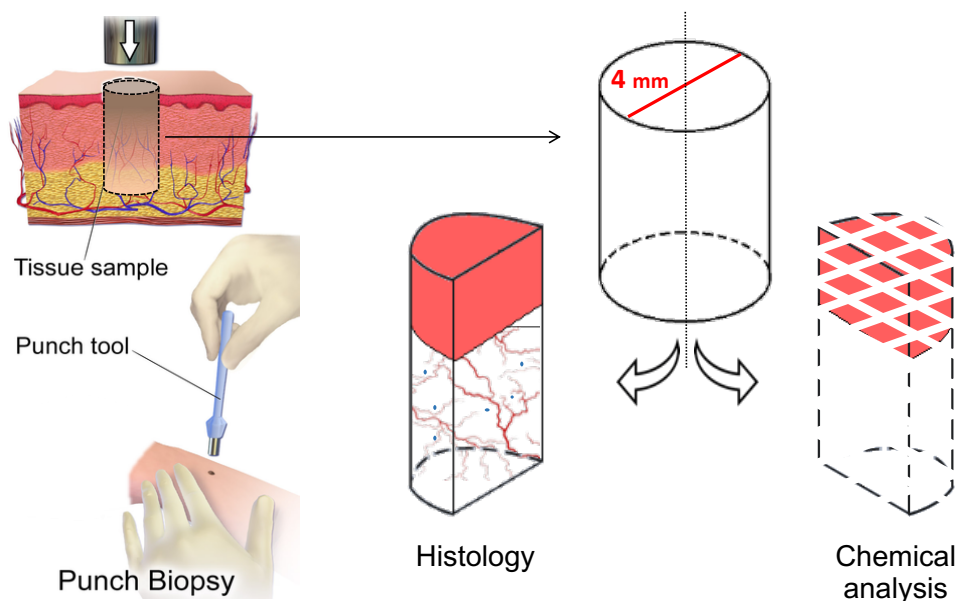


Figure 2-2. Skin biopsy protocol.

Part of this figure was modified from https://en.m.wikipedia.org/wiki/File:Skin_Punch_Biopsy.png, by BruceBlau, licensed under the Creative Commons Attribution-Share Alike 4.0 International license.

2.2.5 Chemical analysis of tissues

A chemical analysis of tissues, focused on Na⁺ but also on K⁺ and water (complementary to Na⁺ assessment and results interpretation, as per Lowry and Hastings, 1942 and Lowry et al., 1942), was conducted in all the rat tissue and human skin samples by using a consistent approach.

2.2.5.1 Gravimetric analysis of tissue water content

From frozen rat tissue samples, aliquots representative of full parenchyma were cut and their wet weights (WW) measured on a 4 decimal (0.0001 g) electronic scale (samples WW range = 15-60 micrograms).

Frozen human skin samples from punch biopsies were macroscopically transversally cut into a superficial layer, including the epidermis and the immediately adjacent superficial dermis (ESD), and deeper dermis (DD). At variance with rat tissues, a 5 decimal (0.00001 g) scale (Ohaus, DV214CD) was used for weight measurements due to the small size of the samples.

To prevent evaporation of tissue water, all the process of cutting was performed in a cold room and tissues were transported in Eppendorf tubes (Sarstedt) in dry ice. Samples were desiccated at 65°C in a ThermoMixer (Eppendorf), for > 40 hours, to a stable dry weight (DW). Water content was estimated as (WW-DW)/DW and expressed as mg water/mgDW, or as water percentage ($W\% = (WW-DW) \times 100 / WW$).

2.2.5.2 Tissue digestion

Dried samples were digested at 65°C in 20-40 µl of 70% HNO₃ (Fisher) for 3 h and, after 1:10 v/v dilution in deionised water (MilliQ), for 2 additional hours. Digestion blank controls (i.e. HNO₃ and MilliQ only) were prepared and analysed with the digested samples to confirm the lack of Na⁺/K⁺ contaminations. Digested samples and blanks were centrifuged for 1 min at 16.000 g and stored at room temperature; solubilised supernatants were used for Na⁺ and K⁺ quantification. Acid-insoluble residues from rat skin and liver samples were used for total fat quantification (please see chapter 5).

2.2.5.3 Flame photometry analysis of Na⁺/K⁺ content

After unsuccessful attempts with NMR, limited at least in part by the size of the rat tissue samples and the digestion protocol, a flame photometer (Sherwood scientific, model 410C) approach was optimised for Na⁺ and K⁺ quantification in the samples.

Na⁺ and K⁺ calibration standards of 0-5 ppm (mg/l) were prepared from 1000 ppm solutions (Fisher Chemical) using HNO₃- and milliQ- carefully washed glassware. Before photometric measurements, digested samples were further diluted to fall within the range of 0 - 5 ppm. MilliQ was used as the diluent for both standards and samples after Na⁺/K⁺ contamination of HNO₃ was excluded on blanks. Na⁺ and K⁺ concentrations in the digested sample solutions were calculated against the five-points regression line obtained from the calibration standards. At the calibration used, reported CV% for reproducibility is < 2% (i.e. < 0.005 mmol/l for both Na and K in the measured sample); in our hands CV% was 1.5 intra-sample and 3% inter-sample (from the same original tissue). Concordance correlation coefficient for replicated (technical) measurements was 0.98; random duplicate samples from the same stored tissues showed similarly good reproducibility (Figure 2-3 below).

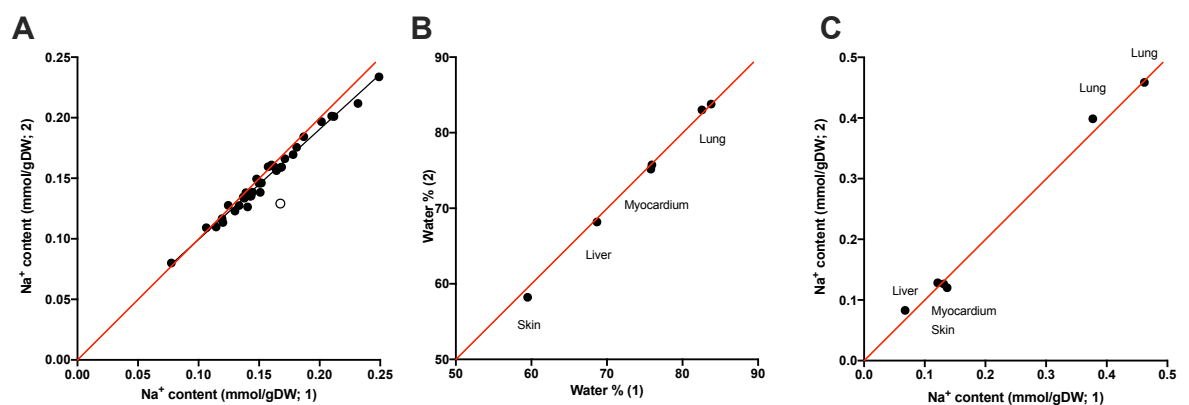


Figure 2-3. Reproducibility of tissue chemical analysis.

Panel A: replication of the flame photometer chemical analysis on the same HNO₃-digested samples (technical replicates; batch of female rat skin samples reanalyzed at time 2, months after time 1) shows excellent reproducibility ($\rho = 0.98$ [95%CI: 0.96 to 0.99]; $p < 0.0001$). The shift from the identity line (in red; slope of the regression line = 0.91 [0.87-0.95]; $p < 0.001$ vs 1.0) is likely due to unavoidable minimal differences in the progressive dilutions of calibration standards at the two different times. Panels B-C: reproducibility of results from the same tissue of the same animal; random duplicate samples from different tissues are shown for water content (gravimetric approach; panel B) and Na⁺ content (flame photometry; panel C); red= identity line.

All samples from the same type of tissue were analysed in a batch on the same day to minimise technical variability; therefore, few samples irreversibly affected by experimental issues (e.g. accidentally dropped sample, contamination, volume shortage) had to be excluded. During measurements, blank (diluent) and calibration standards were checked after every block of approximately 8 samples to control for drift. Na⁺ and K⁺ concentrations in the analysed solutions were used to back-calculate their total content in the digested samples and normalised by DW for Na⁺ and K⁺ tissue content (mmol/gDW), or by tissue water for Na⁺ and K⁺ tissue concentration (mmol/l).

The flame photometry analysis was conducted blind to group allocation of samples.

2.3 Assessment of vascular and microvascular function

The putative impact of tissue Na⁺ accumulation on vascular function was investigated in the aforementioned salt-loaded rodents (Chapter 5) and in patients with HFpEF, compared to controls of similar age and sex, in the HAPPIFY study (Chapter 7).

In rodents, the assessment of arterial function was based on ex-vivo preparations of mesenteric arteries, by using the wire myograph technique and by testing the vascular effects of dietary (in-vivo) animal exposure to high-sodium and those of ex-vivo exposure of vessels to supraphysiologic concentrations of Na⁺ in the experimental bath.

In HAPPIFY, ex-vivo assessment of subcutaneous resistance arteries was part of a comprehensive vascular phenotyping, including also in-vivo approaches, of patients with HFpEF. The primary study hypothesis was that a hypertonic interstitium would facilitate capillary fluid extravasation and accumulation of oedema. To test the above, I used a plethysmographic protocol which allowed the simultaneous evaluation of microvascular filtration and lymphatic drainage of extravasated fluid.

2.3.1 Ex-vivo study of arterial function on wire myography

Wire myography is the study of vascular muscular (and, by upstream signalling modulation, endothelial) function, applied for the purposes of this thesis to small resistance arteries. In particular, it measures capacity of the vascular wall to constrict or relax in response to different stimuli. At variance with isobaric preparations (pressure myography), where changes in vascular diameter in response to changes in intraluminal pressure are

measured, wire myography relies on the isometric set up of a vessel pre-stretched by two wires inserted through the lumen and on high-sensitivity force transducers measuring the changes in wall tension exerted on those wires. This tension is modulated by adding agonists or antagonists to the bath where the vessel is mounted, in order to induce vascular contraction (i.e. increased tension) or relaxation (i.e. decreased tension), respectively.

For this thesis, third-branch mesenteric arteries from rats (Chapter 5) and small subcutaneous arteries from HAPPIFY participants consenting also to the ‘subcutaneous fat biopsy sub-study’ (Chapter 7) were dissected. Their function was assessed on the same day for rat and on the following day, after overnight incubation at 4°C in physiological saline solution [PSS; 119.0 mM NaCl, 4.7 mM KCl, 1.2 mM MgSO₄·7H₂O, 24.9 mM NaHCO₃, 1.2 mM KH₂PO₄, 2.5 mM CaCl₂ and 11.1 mM glucose], for human vessels. 1.5-2 mm vascular ring segments were mounted on isometric wire myographs (Danish Myo Technology [DMT] Denmark) filled with 5ml of fresh PSS and continuously gassed with a mixture of 95% O₂ and 5% CO₂ while being maintained at a constant temperature of 37±0.5°C.

Following 30 minutes of equilibration, baseline tension was normalised as per DMT recommendations (www.dmt.dk/uploads/6/5/6/8/65689239/dmt_normalization_guide.pdf); this process consists of pre-stretching a vessel to an internal diameter that produces a physiologic resting transmural pressure before any experimental stimulus is applied to the vessel. This step standardises conditions across different vessels to guarantee reproducible and comparable results. Upon normalisation, the internal diameter was estimated as recommended. Vessels with an internal diameter ≥ 500 µm, traditionally identified as the maximum size of resistance arteries (Mulvany and Aalkjaer, 1990, Heagerty et al., 1993), were excluded from further analysis.

After normalization, the viability of arterial segments was assessed by the addition of KCl (62.5mmol/L), repeated after 10 minutes of washout. The contractile response of vessels to the thromboxane agonist U46619 was tested with concentration-response curves (10⁻¹⁰ - 3x10⁻⁶ M). Endothelium-dependent and -independent relaxation was assessed by a dose-response to acetylcholine (ACh; 10⁻¹⁰ - 3×10⁻⁵ M) or the nitric oxide (NO)-donor sodium nitroprusside (SNP; 10⁻¹⁰ - 10⁻⁵ M), respectively, following pre-constriction with U46619 dose that produced 75% of the maximal contractile response.

Additional vascular segments from control (non-salt loaded) normotensive and hypertensive rats were incubated for 5 hours in PSS or in NaCl-supplemented-PSS (+15 mM NaCl, hypertonic, HT) to test the impact of environmental hypertonicity on vascular function. Duration and tonicity of the incubations were based on previously reported tissue changes with high-salt diet ($\Delta(\text{treated} - \text{control})$) in Machnik et al., 2009 and Wiig et al., 2013) and effects of hypertonic culture conditions on rat vascular smooth muscle cells (VSMCs) hypertrophy (Gu et al., 1998).

After the incubation and one additional KCl stimulation, concentration-response curves for U46619 and SNP were conducted as described above (Figure 2-4).

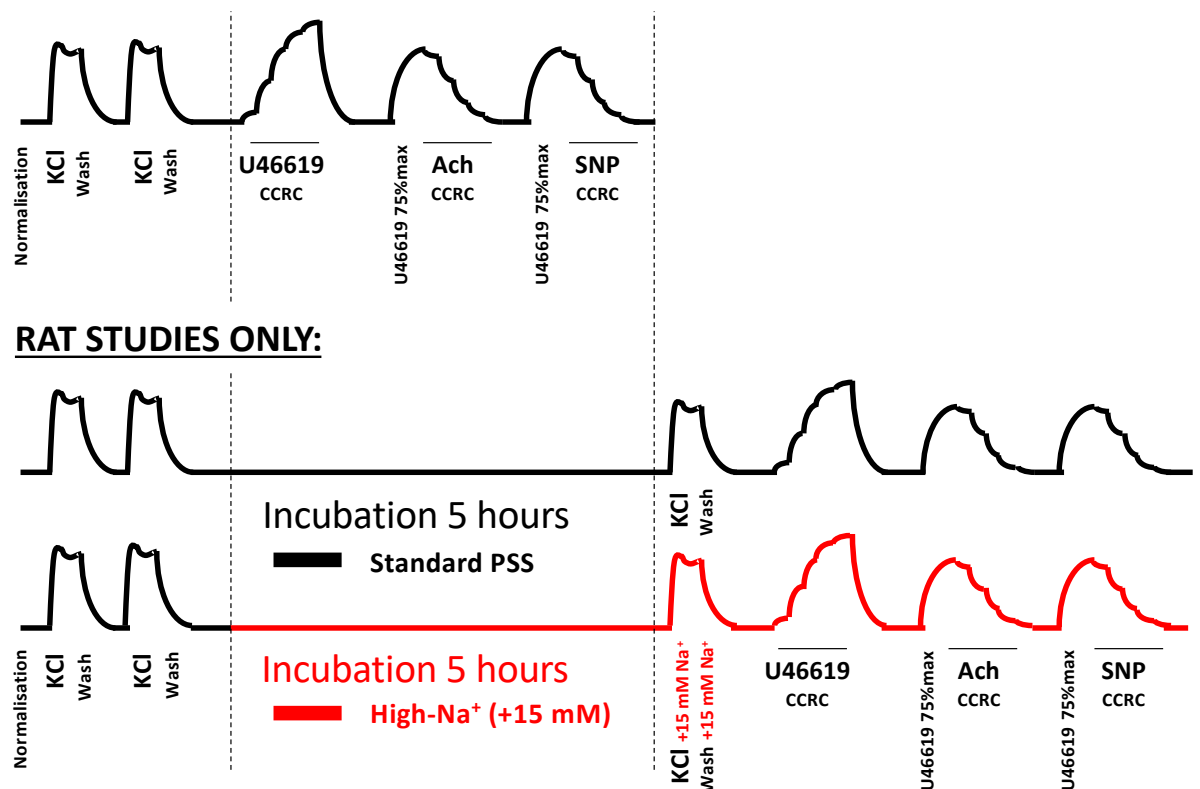


Figure 2-4. Wire myography ex-vivo experimental protocol to assess arterial function.

Top: standard protocol, used for both human and rat vessels. After normalisation, viability and agonist-independent contractility was assessed by repeated 62.5 M KCl stimulations. The magnitude of the agonist-independent contractile response to the second KCl stimulation was used as reference for the agonist-induced response. Cumulative concentration response curves (CCRC) to U46619, Acetylcholine (Ach) and sodium nitroprusside (SNP) were conducted to assess contractility, endothelium-dependent relaxation and endothelium-independent relaxation, respectively. CCRCs were conducted after 30 minutes of washout from the previous agonist/antagonist. Bottom: for rat vessels only, a similar sequence of CCRCs was conducted after vessels incubation in a hypertonic solution (+15 mM NaCl, vs 144 mmol Na⁺ in standard PSS) to test the impact of environmental hypertonicity on vascular function.

Vessels with no or trivial post-incubation response to KCl or U46619 pre-constriction were considered non-viable and their curves were excluded from the analysis.

Unfortunately, I was not able to conduct a similar incubation protocol in vessels from HAPPIFY participants due to the smaller number of viable subcutaneous arterial segments available for functional testing than originally expected.

2.3.2 Non-invasive study of arterial function (humans)

All HAPPIFY participants underwent non-invasive assessment of arterial function. In particular: Pressure Waveform Analysis (PWA) and assessment of carotid-femoral Pulse Wave Velocity (PWV) were used to estimate arterial stiffness; brachial Flow-Mediated Dilatation (bFMD) was used to estimate post-ischemic hyperaemic responses and endothelium dependent vasodilatation of large arteries.

2.3.2.1 Pressure Waveform Analysis

Arterial pressure is used in everyday clinical practice as a surrogate of arterial function. Many traditional cardiovascular risk factors, similar to the process of ageing, induce and perpetuate biological changes at the cellular level (namely chronic inflammation, oxidative stress, endothelial dysfunction and cell senescence, among others) which underpin structural changes in the vascular wall. The ultimate functional result of such changes is stiffening. This primarily affects aorta and elastic arteries and typically determines increased systolic and pulse pressure. A self-perpetuating vicious cycle ensues: the left ventricle (LV) pumping into a stiffened aorta suffers an increased afterload; the diastolic component of the aortic pulse, resulting from the sum of the forward with the backward reflected pressure wave arising from arterial branching points, undergoes anticipation to the systolic phase due to faster wave transmission in stiffened arteries and induces augmented central systolic pressure (Nichols and O'Rourke, 2011) which further increases LV stress and oxygen demand; with the loss of “cushion” properties from elastic vessels, pulsatile pressure is inappropriately transmitted into the distal microvasculature of target organs, thus maintaining and worsening endothelial damage and the biological dysfunctional changes listed above (Currie and Nilsson, 2019).

The prominent pathogenic role of central blood pressure and wave form can be investigated by non-invasive methods, which provide estimates of central parameters from

peripherally assessed pulses, by applying general transfer functions previously validated against invasive measures.

In the HAPPIFY study, I used a SphygmoCor XCEL (AtCor Medical) to perform this Pulse Wave Analysis (PWA) (Laurent et al., 2006). Briefly, multiple sequential artery pressure waveforms are acquired from a dedicated brachial cuff and averaged into an ensemble, used by the software to derive and synthesize the central aortic pressure waveform. Key derived parameters, summarised in Figure 2-5, are: systolic and diastolic central blood pressure values, resulting from the predicted sum of forward and backward waves; central pulse pressure (PP); augmentation pressure (AP), i.e. the difference between the systolic inflection point (denoting the initial upstroke of the reflected pressure wave) and the systolic peak; augmentation index (AIx), as the proportional ratio between AP and PP, traditionally normalised to a heart rate of 75 bpm (AIx@75) to correct for the confounding effect of chronotropy. More sophisticated discussion on the technique is beyond the scope of this thesis; in general, the stiffer the peripheral arteries, the faster the reflected wave returns towards the heart, merges with the forward wave and hence increases AP and AIx.

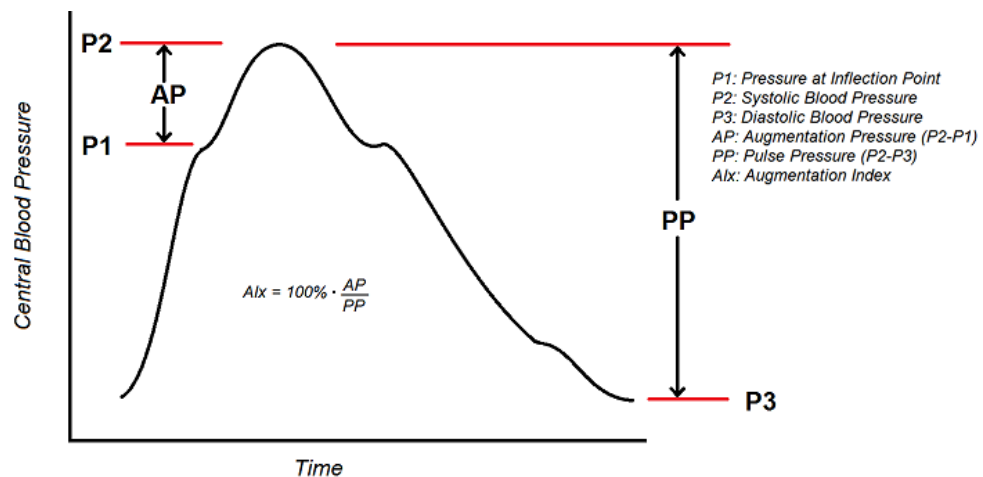


Figure 2-5. Central Aortic waveform and key parameters of PWA.

This figure is from <https://commons.wikimedia.org/wiki/File:Augmentation-index.PNG>, by Icternol, licensed under the Creative Commons Attribution-Share Alike 4.0 International license.

In HAPPIFY, AP and AIx@75 were measured as surrogates of arterial stiffness. Specific protocol details, including timing and conditions of testing, are provided in Chapter 7.

2.3.2.2 *Pulse Wave Velocity*

A more direct approach to measure arterial stiffness relies on the actual measurement of the pulse wave transit time over a certain vascular segment, i.e. velocity (PWV). In particular, the technique used in HAPPIFY, with the SphygmoCor XCEL (AtCor Medical) device, measures the speed of the pulse as it travels between the heart, carotid and femoral vessels (cfPWV): reduced vascular compliance and wall stiffening result in shorter pulse wave transit time and higher PWV (Laurent et al., 2006, Van Bortel et al., 2012). By reflecting the speed of pressure waves propagation (both forward and backward), increased PWV as a result of stiffening is a direct determinant of AP and AIx. PWV is universally accepted simple and robust measure of arterial stiffness, with independent predictive value for cardiovascular mortality and events across a variety of populations and conditions (The reference values for arterial stiffness' collaboration 2010, Townsend et al., 2015, Currie and Nilsson, 2019).

Specific protocol details for the application of cfPWV, including timing and conditions of testing, are provided in Chapter 7.

2.3.2.3 *Brachial Flow-Mediated Dilatation*

In addition to the process of stiffening, which predominantly (but not solely) involves the medial and adventitial layers of the vascular wall, the endothelium is another central determinant of vascular function. It is typically responsible for the release of nitric oxide (NO) and other vasodilatory substances. Flow-mediated dilation (FMD) is a widely used non-invasive tool for examining peripheral artery endothelium-dependent dilation (Thijssen et al., 2019). At variance with invasive approaches, which rely on the infusion of a variety of vasoactive substances in specific vascular territories, FMD relies on a phase of induced reactive hyperaemia as the stimulus for shear stress on the endothelial layer of large arteries, resulting in vasodilatation.

The technique measures the change in vessel diameter from baseline to the peak observed during the hyperaemic phase as indicative of endothelial function; simultaneous acquisition of blood flow velocity signals allows also quantification of the shear stress generated by the procedure (Figure 2-6).

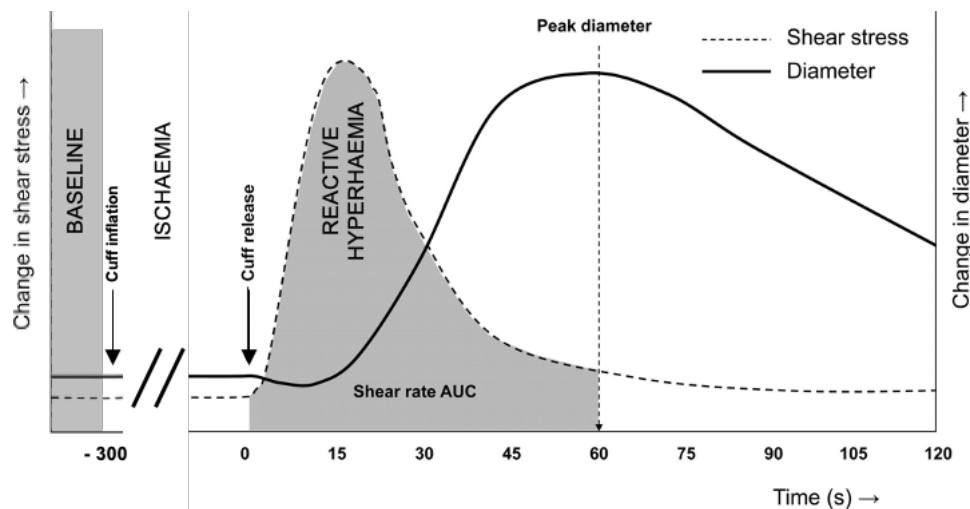


Figure 2-6. Flow-mediated dilatation.

Schematic presentation of vessel diameter and shear stress responses before and after a 5-min ischaemic stimulus. Adapted and simplified from *Thijssen DHJ et al, Eur Heart J 2019; 40, 2534–2547*.

Substantial methodological variation in performing FMD is present in the literature (Thijssen et al., 2019). However, the most widely adopted and guidelines-based approach is based on brachial artery imaging with high-resolution ultrasound, before and after distal (forearm or hand) ischaemia is induced through interruption of arterial flow using a blood pressure cuff inflated to supra-systolic pressure for 5 min. Cuff release results in dilation of the distal microvasculature via multiple mechanisms (Pyke and Tschakovsky, 2005), reactive hyperaemia is induced and arterial vasodilation follows.

In HAPPIFY, brachial FMD measurements and analysis were performed according to guidelines (Thijssen et al., 2011), using with a semi-automated device and a proprietary software (UNEX EF, Japan; <https://unex.co.jp/ENG/unexef.htm>).

The device is equipped with an automated edge-detection software and a vessel tracking system which facilitates and continuously micro-correct probe positioning for steady images at the beginning and during the test. The H-shaped probe, generating one long-axis and two short-axis B-mode images, operates at ultrasound wave frequency of 8MHz. Blood velocity is simultaneously measured by the same probe, with an automatically adapted flow sampling rate (7.1kHz, 5.9kHz, 5.0kHz, 4.0 kHz) and a sample volume adjusted to the internal vessel diameter. Intensity weighted mean velocity assuming a circular cross-section of the vessel and its time-average during the cardiac cycle are automatically calculated. Due to the dependence of velocity assessment on the angle of Doppler insonation and its fixed value in the UNEX EF device (75°), preventing absolute

comparisons with different machines, averaged blood velocity (V) and the derived flow ($V \times \pi (\text{vessel diameter}/2)^2 \times 60$) and shear rate ($8 \times V/\text{diameter}$) changes are analysed as relative to baseline.

After BP measurement and 10 additional minutes of quiet supine rest, an occlusion cuff was placed around the right forearm, the ultrasound probe 5-10 cm proximal to the elbow and ECG leads on the wrists. Following measurement of the rest diameter (intima-intima) and blood velocity for at least 30 s, the cuff was inflated 50mmHg above systolic BP to induce forearm ischaemia for 5 minutes. One minute before cuff release the tracking system automatically tracked the artery and adjusted the probe position to correct for small involuntary arm displacements; after deflation the vessel diameter was measured for 2 minutes, for a total of 3 minutes of ECG-triggered images.

All the images and automated outputs were manually reviewed and analysed with UNEX software off-line at the end of the study (Dobbie et al., 2020); the best position for edge-to-edge diameter measurement was identified on the vessel and dynamically tracked by the automatic software throughout the course of the exam. FMD was calculated as $[(\text{Max Diameter} - \text{Rest Diameter})/\text{Rest Diameter}] \times 100$.

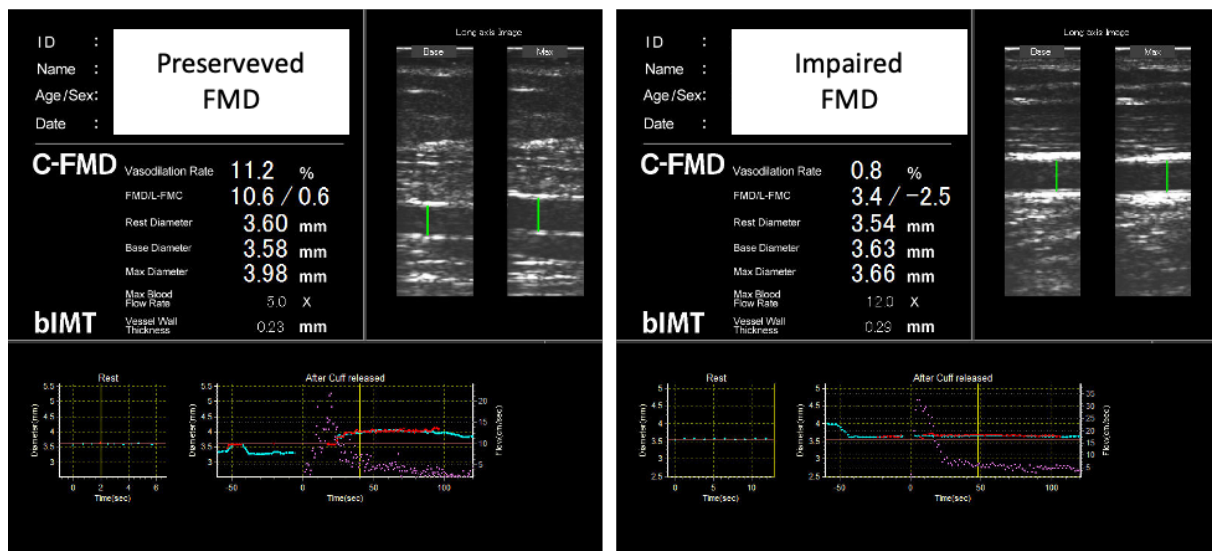


Figure 2-7. Representative FMD tracings.

Left: patient with preserved FMD (11%) in response to reactive hyperaemia. Right: patient with almost null vasodilatory response (0.8%), despite good hyperaemic response (12 x baseline flow values). In the graphs at the bottom: light blue = results of live diameter tracking during the performance of the exam; red = off-line manual review of rest and post-ischaemic diameters; purple = flow velocity signals, assessed by pulsed Doppler.

There is extensive literature on the rationale, technical aspects and clinical/research value and application of FMD; further discussion of this enormous amount of information is beyond the scope of this thesis. Literature relevant to this thesis and additional protocol details for HAPPIFY patients are discussed in the appropriate sections of Chapter 7.

2.3.3 *In-vivo study of fluid microvascular dynamics (humans)*

The exchange of fluids and solutes between the arteriovenous capillary beds and the interstitium is governed by the net result of forces summarised in the Starling equation (Herring & Paterson, 2018):

$$J_v = K_f ([P_p - P_i] - \sigma [\pi_p - \pi_i])$$

where:

- J_v is the rate (volume filtered per unit time) of fluid moving from the vascular lumen to the interstitium (extravasation)
- π_p and π_i are plasma and interstitial osmotic pressures generated by proteins in the respective compartments; notably, albumin contributes to more than two thirds of the osmotic pressure exerted by proteins (i.e. oncotic; (Herring & Paterson, 2018));
- σ is the osmotic reflection coefficient and quantifies “imperfect” semipermeability of the endothelium to proteins (or, in other words, slight leakiness, so that the potential osmotic pressure of proteins is not exerted fully but reduced by factor σ).
- K_f is the constant of filtration (or microvascular filtration coefficient), i.e. the proportionality factor between J_v and the net result of the forces above; it is index of microvascular permeability to water and equals the sum of the capillary area (A) x wall permeability per unit surface area (L_p) in a given volume of tissue.

Transcapillary fluid movement in an individual capillary was first measured by E. Landis in 1926, hence the “*Starling-Landis*” name to the principle (Krogh et al., 1932, Michel, 1980). When interstitial fluid accumulation is measured in vivo, however, the simultaneous drainage fluids guaranteed by the other arm of microcirculation (i.e. lymphatic vessels) contributes to net volumes, as already discussed in Chapter 1 (section 1.5.1). In particular, the rate of lymphatic drainage opposes the rate of microvascular filtration.

Changes in at least some of the above parameters were non-invasively investigated using an established plethysmography protocol (Gamble et al., 1993), which allowed also the evaluation of local arterial blood flow (Φ) and peripheral venous pressure (P_V), both relevant for the interpretation of microvascular dynamics data. The general rationale and conduct of the plethysmography protocol are presented here. Additional practical details, functional to the overall HAPPIFY study protocol, are provided in Chapter 7.

Strain gauge plethysmography (EC6, Hokanson), a versatile measuring device which can accurately determine volume changes in limbs and digits, was applied to the upper and lower limbs (forearm and calf, respectively) of HAPPIFY participants. Indium-Gallium strain gauges are designed so that the active portion of the gauge is the same as the circumference of the limb or digit being measured; this allows the plethysmograph to relate resistance changes induced by stretch/distention to relative volume changes, expressed as % (i.e. ml/100ml of tissue). The plethysmograph was connected to a *PowerLab* data acquisition device (ADInstruments) and measured limb volume changes were recorded and later analysed by *LabChart* software (ADInstruments).

Patients were positioned almost supine, except for an approximately 10° tilt of the back, with their forearm and calf maintained at the height of the right atrium by in-house made supports. Inflatable cuffs for venous occlusion were placed on the limbs, proximal to the strain gauges as shown in Figure 2-8.

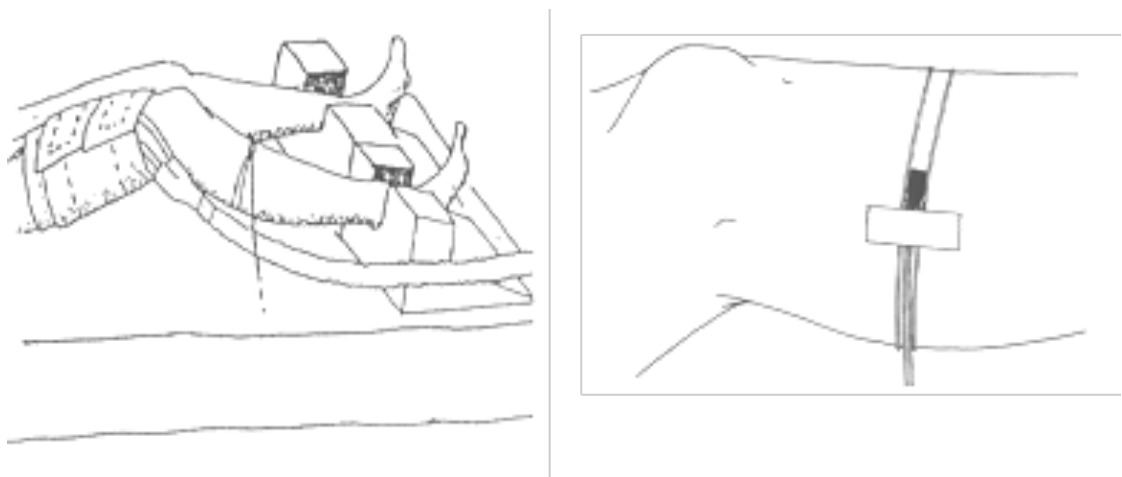


Figure 2-8. Application of a limb gauge and rapid inflation cuff.

Lower limb set-up, with dedicated supports (left) and detail of the gauge, with a double loop of indium-gallium filled rubber that hooks over the end of the gauge. The gauge is gently taped in place, so that small movements of the cable do not perturb measurements, and the two sides of the loop run in parallel around the limb in close contact with the skin (*Hokanson* material, EC6 plethysmograph manual).

After an adequate resting interval and limb volume tracing stabilization, P_V was determined by gradually increasing the occlusion pressure in the cuff until any limb volume change was detected (Christ et al., 1997, Stewart, 2003).

Limb Φ can be determined by the application of cuff pressures (P_{cuff}) great enough to occlude venous outflow, but not impede arterial inflow, and by measurement of the initial rate of swelling during the first few seconds, before vasoconstrictor axon reflex mechanisms kick in (Henriksen, 1977)). Occlusion pressures of 40 mmHg or more for ≤ 10 seconds are adequate (Wilkinson and Webb, 2001, Gamble et al., 1998). HAPPIFY Φ measurements were performed in at least quintuplicate after consecutive cycles of sudden venous occlusion to 45 mmHg (E20 Rapid Cuff Inflator, Hokanson) for 7 s of every 28 seconds. The first 1.5 seconds were excluded from calculation of the slope (rate of volume change) in *LabChart* due to limb motion artifacts induced by sudden cuff inflation.

For the assessment of microvascular filtration parameters and interstitial fluid accumulation, we used a protocol with small (8-mmHg) cumulative pressure steps, lasting 3.5 minutes each and starting at the first multiple exceeding P_V up to a maximum of 56 mmHg or less, if diastolic BP was lower. With such protocol, use of P_{cuff} values as great as arterial diastolic blood pressure was previously validated (Gamble et al., 1993) and shown not to invoke the local vasoconstrictor mechanism also known as “veno-arteriolar reflex” (Henriksen, 1977). Once applied to the cuffs, pressure is transmitted to the veins and capillaries and, when exceeding P_V , it induces a volume change due to venous distension until equalisation; at lower steps, after a curvilinear initial phase lasting approximately 1 minute, it reaches a plateau (Figure 2-9, A). However, above a certain equilibrium pressure up to which any fluid filtering across the microvascular interface due to Starling-Landis transcapillary forces is being removed at an equivalent rate by lymphatic drainage (Stewart, 2003, Michel, 1989, Bauer et al., 2004) the limb volume continues to increase linearly over time after completion of the venous filling (Figure 2-9, B). This equilibrium pressure, above which lymphatics cannot compensate for filtration and the interstitium enlarges at a rate proportionate to P_{cuff} (Stewart, 2003) is called isovolumetric pressure (P_i).

At high P_{cuff} steps, the time needed to and the proportion of limb volume change due to further venous distention decreases, with an increase in net fluid extravasation accumulating in the interstitium. The time courses (slopes) of this fluid accumulation at each pressure step was calculated off-line (*LabChart*) as the averaged first derivative from

portions of tracing devoid of motion artifacts (Gamble et al., 1993), excluding the initial curvilinear phase of venous filling (fixed for all at: 90s at 8 mmHg, 80s at 16, 70s at 24, 60s at 32, 50s at 40, 40s at 48 and 30s at 56).

These slopes were plotted against P_{cuff} to determine the relationship between interstitial fluid accumulation and experimental increases in hydraulic pressure. Least-square fitting (*Prism*, GraphPad) of at least 3 valid pressure points was used to identify these linear associations for each limb/participant, in order to determine the slope (microvascular filtration coefficient, K_f) and the intercept with the pressure axis (i.e. P_i ; Figure 2-9, C).

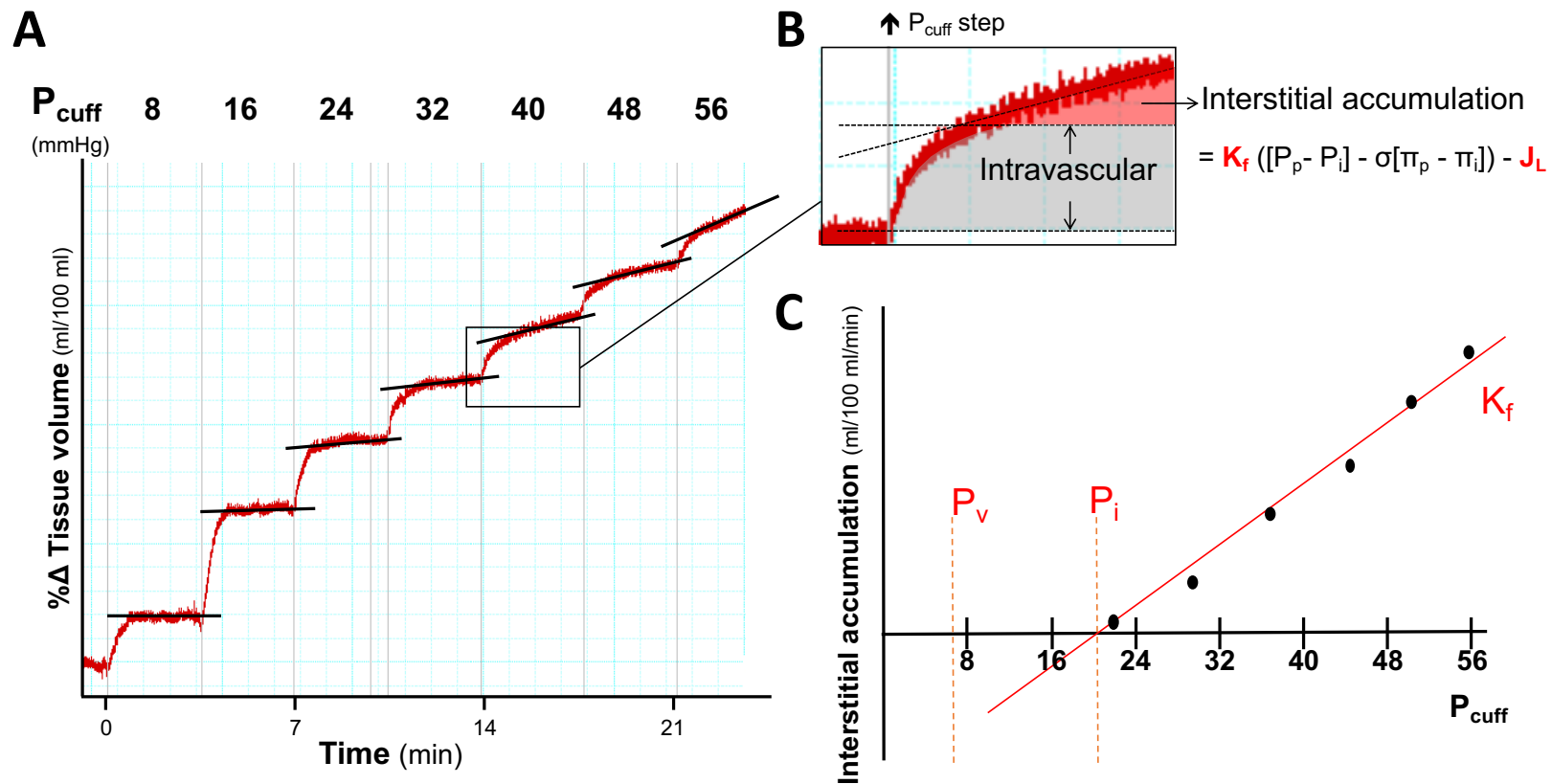


Figure 2-9. Plethysmography protocol for the assessment of microvascular filtration parameters and interstitial fluid accumulation.

Panel A: Black lines showing increasingly steep changes in limb volume during the cumulative 8-mmHg pressure steps protocol are superimposed to a representative limb plethysmographic tracing (red). *Panel B:* inset from panel A, showing the intravascular (venous filling) and the interstitial component of limb volume changes after an increase in the cuff pressure (P_{cuff}), opposing venous drainage and backward increasing the hydraulic pressure at a capillary level. In our *in vivo* set up, net interstitial accumulation equals the difference between microvascular filtration (governed by Starling-Landis forces between capillary plasma [p] and interstitium [i]) and lymphatic drainage (J_L). *Panel C:* interstitial fluid accumulation rates plotted against occluding (hydraulic) pressures. P_v = peripheral venous pressure; P_i = isovolumetric pressure, above which lymphatics cannot compensate for filtration and oedema develops; K_f = slope of the regression line, representing the microvascular coefficient of filtration.

In single capillary studies, the pressure that needs to be exceeded to induce net fluid filtration is equivalent to the value $\sigma\Pi$ (Michel, 1980). In-vivo, however, P_i is predominantly modulated by lymphatics, which provide fluid drainage equivalent to the rate of fluid extravasation up to this critical pressure point.

One may guess why, with our venous occlusion protocol, lymphatic drainage is not similarly impeded by increasingly high P_{cuff} . In fact, pumping pressures of lymphatic vessels composed of multiple contractile lymphangions in series have been reported to overcome pressures as high as 60 mmHg (Mohanakumar et al., 2019), 85 mmHg (Belgrado et al., 2016) or even above 120 mmHg (Belgrado JP, *personal communication*).

In addition, lymphatics offer plastic responses to increased demand for drainage (i.e. modulation of contractility by preload and afterload; please see section 1.5.2). A “mirror image” plethysmography protocol, in which after a standard cumulative P_{cuff} sequence the pressures were decreased in the same order and over the same time course, demonstrated that the net accumulation of interstitial fluid at each successive pressure reduction was less than that observed during the corresponding pressure increase (Bauer et al., 2004). In other words, P_i was shifted to the right without changes in K_f , thus suggesting inducible potential in lymphatic drainage (Figure 2-10). Unfortunately, such extended protocol was not routinely feasible in our HAPPIFY cohort, due to poor tolerance of most participants over extended time, resulting in frequent motion artifacts and poor quality of the tracing.

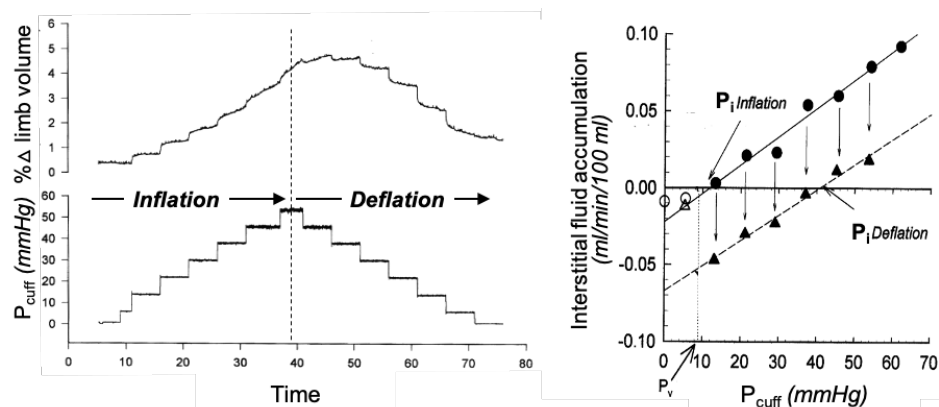


Figure 2-10. Extended protocol with deflation steps

After interstitial fluid accumulation upon inflation, slopes of $\% \Delta$ limb volume at each P_{cuff} steps during deflation were lower compared to the corresponding pressure increase (*left panel*). This corresponds to a right shift of the regression line in the right panel, with similar K_f and higher P_i , indicating increased lymphatic drainage. Adapted from Bauer A, *Clin Sci*, 106, 627-33.

METABOLIC IMPACT OF HIGH SODIUM INTAKE

3.1 Background and study aim

As discussed in Chapter 1, an independent link between high Na⁺ intake and a shift in metabolism has recently been suggested, whereby a catabolic state induced by Na⁺ would ultimately serve preservation of body water (Rakova et al., 2017, Kitada et al., 2017). A previously unrecognised, subclinical hypercortisolism associated with high Na⁺ intake was proposed to drive this catabolic state.

These mechanisms, which may have obvious implications for a cardiovascular risk independent of or disproportionate to the classic association between Na⁺ and blood pressure, lacked demonstration in humans out of a dietary- and environmentally-controlled experimental setting.

Therefore, the aim of the SYCAMORE (*Sodium intake and subclinical hYper-Cortisolism: Association and MetabOlic signature*) study was to investigate the impact of high Na⁺ intake on renal water preserving mechanisms, plasma metabolomics signatures and their association with cortisol in a real-life population of patients undergoing systematic biochemical screening for secondary causes of hypertension.

3.2 Study-specific methods

3.2.1 Screening protocol and patient selection

The study retrospectively analysed clinical and biochemical data from consecutive patients, referred to the tertiary Hypertension Center of the University of Padua between 2012 and December 2017, who provided written informed consent for data and samples use as part of a local biobank for diagnosis of adrenal disease (Prot.1925P/2009), later implemented for the ongoing multi-centre ENSAT-HT study (<http://www.ensat-ht.eu/>; Padua ethics approval protocol 3998/AO/16), in which both institutions (University of Padua, University of Glasgow) participate.

The biochemical screening entailed assessment of plasma electrolytes, aldosterone, renin and cortisol and 24h urinary Na⁺ and K⁺ excretion; additional biochemical data, including renal function, albuminuria, 24h creatinine excretion, 24h urinary

catecholamines/metanephrines and urinary free cortisol were measured as indicated by guidelines (Mancia et al., 2013, Funder et al., 2016, Nieman et al., 2008, Lenders et al., 2014) and/or at the discretion of the requesting physician. Patients were not instructed to change their usual dietary habits before the screening. They were asked to complete a 24h urine collection, reporting start and stop times: collections were used for both clinical and study purposes when sampling time was ≥ 22 hours and volume ≥ 500 ml, with no significant loss during collection reported. On the morning of completion, blood sampling was performed after one hour in semi-supine position, between 8 and 10 am. A sample from the 24h urine container and an additional blood sample in EDTA were collected depending on availability of the technician in charge on the day; the EDTA sample was centrifuged at room temperature for separation of plasma and frozen with the urine for long term storage in the local biobank. If requested, an additional sample from the 24h urine container was acidified with HCl and used for the measurement of urinary norepinephrine, epinephrine, normetanephrine, and metanephrine excretion. Attended office blood pressure values were determined at the time of the screening from 2 or 3 consecutive brachial blood pressure readings with an automated calibrated sphygmomanometer, as per guidelines (Mancia et al., 2013). Diabetes status was defined by diagnosis by a clinician or use of a diabetes medication; chronic kidney disease was defined by an estimated glomerular filtration rate <60 mL/min/1.73 m² with CKD-EPI formula (Levey et al., 2009).

The biochemical screening was systematically performed while off antihypertensive treatment or, if patients were already treated, after appropriate washout from confounding agents and switch to calcium channels blockers and/or doxazosin, as per guidelines (Funder et al., 2016); in patients on a mineralocorticoid receptor antagonist (spironolactone, canrenone or potassium canreonate), or on agents affecting the renin-angiotensin-aldosterone system (diuretics, beta-blockers, angiotensin-converting enzyme inhibitors and angiotensin II type 1 receptor antagonists) at least six-weeks or two-weeks wash-out period was required, respectively. To minimise the confounding effect of medications, individuals who could not tolerate this change or for whom it was judged unsafe/impractical in the opinion of the physician in charge were excluded from this analysis. Similarly, individuals with reported/biochemical evidence of intramuscular or intravenous steroid use or abuse and those with a final diagnosis of secondary hypertension after appropriate work-up (biochemistry, anatomical/functional imaging, adrenal/renal vein sampling) and follow-up at the time of data-lock (1st

January 2019) were excluded. Upon database scrutiny, diagnoses of essential hypertension were confirmed with the physicians in charge.

Patients with a conclusive diagnosis of essential hypertension were grouped according to classes of Na⁺ intake. Intake estimates were based on 24h urine excretion, which has limitations when applied to a single subject (Lerchl et al., 2015) but is only minimally affected by within-individual day-to-day variability when applied to groups with sufficient numbers of participants included (Cogswell et al., 2018). Intakes were defined as low ≤ 2.3 g/d (100 mmol/d); medium 2.3-5g/d; high >5 g/d (216 mmol/d; Figure 3-1), according to commonly used cut-offs (Institute of Medicine, 2005, Institute of Medicine Committee on Strategies to Reduce Sodium, 2010).

Additionally, sub-cohorts of patients from the low and the high Na⁺ intake groups and available EDTA-plasma samples stored in Padua biobank from the time of screening were compared for plasma metabolomics signatures (Figure 3-1).

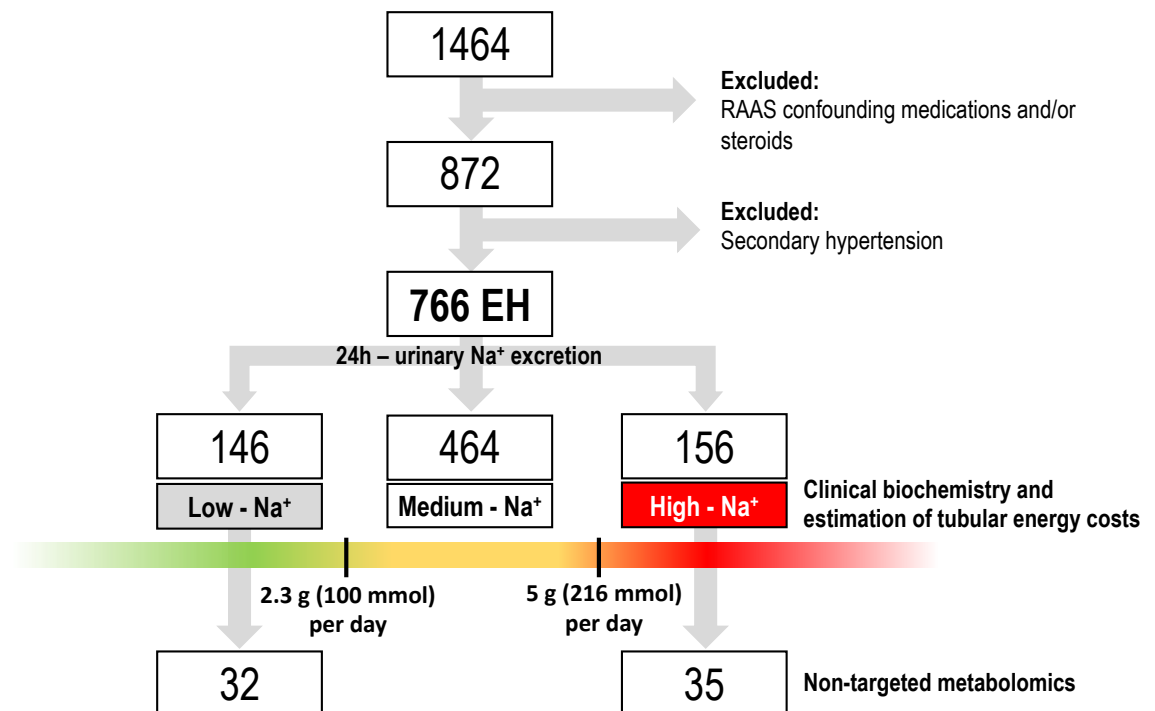


Figure 3-1. SYCAMORE study flowchart

Flowchart identifying the final study cohort, the distribution into classes of Na⁺ intake according to 24h-uNa⁺ excretion and the subcohort of patients for non-targeted metabolomics comparison (vide infra). RAAS = Renin Angiotensin Aldosterone System; EH = essential hypertension.

3.2.2 Biochemistry

Serum and urinary electrolytes, plasma renin, aldosterone and cortisol, as well as additional routine biochemistry as appropriate and detailed above, were all measured at the time of the secondary hypertension screening in an International Standard Organisation (ISO) 15189 accredited clinical laboratory (University of Padua).

Serum and urinary electrolytes were measured using ion-selective electrodes (ISE indirect Na-K-Cl Cobas, Roche Diagnostics GmbH, Mannheim). Renin was measured as plasma renin activity (PRA) until April 2015 and direct renin concentration thereafter (DRC). PRA was measured using a competitive radioimmunoassay kit (RIA, Beckman Coulter kit) based on in vitro generation of Ang I per hour, as reported (Rossi et al., 2016). DRC was measured by chemiluminescence (LIAISON[®] Direct Renin kit, DiaSorin, Saluggia, Italy); the normal range of DRC values in a multi-ethnic cohort of healthy normotensive subjects was 2.8-39.9 mIU·L⁻¹ (5th-95th percentile) in the supine position (DiaSorin, Instruction for use). Renin data for the two cohorts are reported separately in the manuscript and/or the supplemental material. Plasma aldosterone concentration (PAC) was measured by a chemiluminescence competitive immunoassay (LIAISON[®], Aldosterone kit, DiaSorin, Saluggia, Italy). Aldosterone-to-renin ratio (ARR) criteria for primary aldosteronism and further diagnostic work-up were previously reported (Maiolino et al., 2017).

Plasma cortisol concentration (PCC) was measured by a chemiluminescence competitive immunoassay (Immulite 2000 cortisol, Siemens Healthcare Diagnostics Products Ltd., Gwynedd, UK). Urinary 24h free cortisol (UFC) was measured by a home-made LC-MS/MS, validated according to ISO15189:2012. The analytical measurement range was 5-6325 nmol/L, with a lower limit of quantification of 5 nmol/L. Imprecision was less than 10% for both intra- and inter- assay coefficients of variation (Antonelli et al., 2014). Cases with cortisol values below the lower quantification limits (5,5 nmol/l for PCC and 5 nmol/l for UFC) or with 24h UFC > 197 nmol/d, which suggest exogenous steroid use/abuse and diagnostic for Cushing syndrome with 100% specificity and sensitivity (Ceccato et al., 2014), respectively, were excluded from the analysis.

Urinary catecholamines and metanephrines were measured by HPLC with electrochemical detection with a CE-IVD kit (Chromsystems[®], Chromsystems Instruments & Chemicals GmbH, Gräfelfing, Germany).

Plasma and 24h urinary urea and creatinine were not routinely determined in all screened patients; the available biochemical dataset was expanded by analysing in Glasgow urine samples stored in the Padua biobank since the time of the screening. In particular: a) urea in plasma and urine was measured by a kinetic test with urease and glutamate dehydrogenase (UREAL Cobas, Roche Diagnostics GmbH, Mannheim); b) creatinine in plasma and urine was measured by an enzymatic method (CREP Cobas, Roche Diagnostics GmbH, Mannheim). Results available from the time of the screening served for comparison and validation of the entire *de novo* measured batches, according to the Passing & Bablok method (Passing and Bablok, 1983). Briefly, this is a linear regression procedure with no special assumptions regarding the distribution of the samples, estimating systematic, proportional and random differences and controlling for linear model validity (Cusum test).

Representative results for plasma and urinary creatinine for the validation of the plasma and urine batches, respectively, are reported in Figure 3-2; no urinary values for urea were available from the time of the screening. Estimated regression equations were used for correction of results.

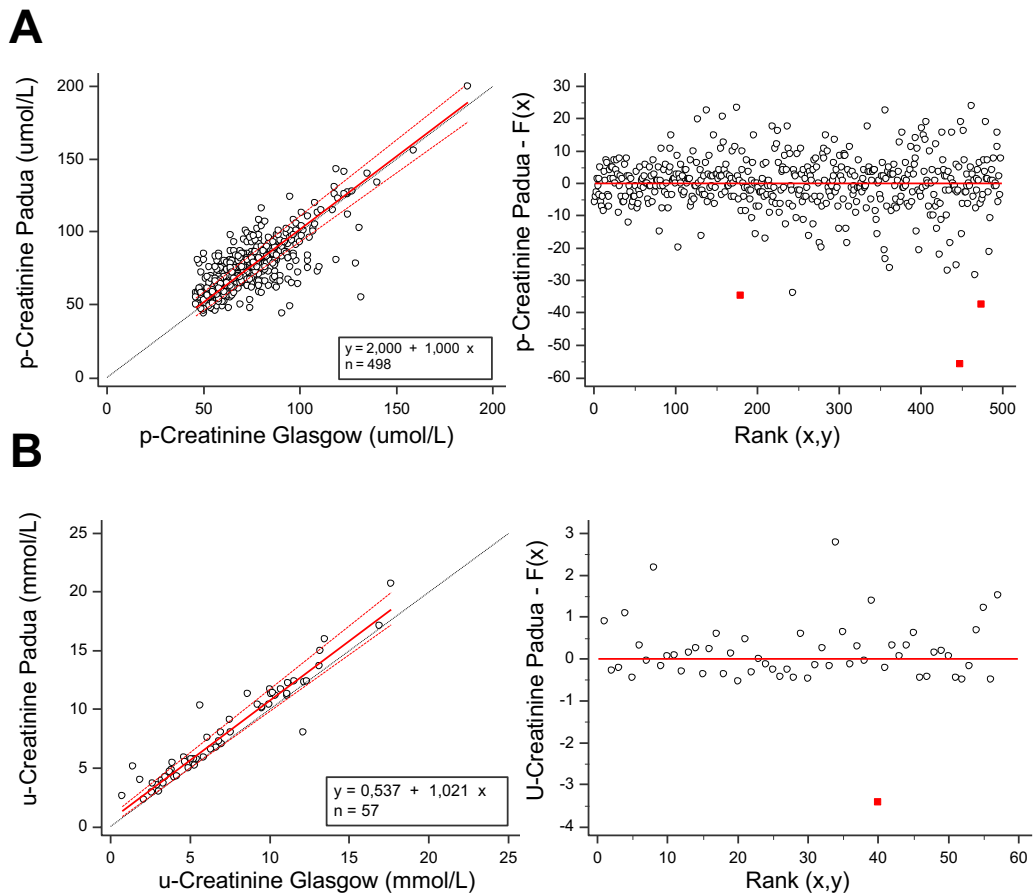


Figure 3-2. Validation of the expanded dataset (Passing and Bablok regression)

Panel A, plasma creatinine; Spearman rank $\rho=0.722$ (95% CI: 0.677 to 0.761), $p<0.0001$. Panel B, urinary creatinine; Spearman rank $\rho=0.962$ (95% CI: 0.936 to 0.977), $p<0.0001$. For both panels: left, scatter diagram and regression line; Y axis = measurements at the time of screening; X axis = new measurements on stocked samples; red solid line = regression line with confidence interval (red dashed lines), black dotted line = identity line. Right, residual plot for goodness of fit, showing a linear relationship with no artificial pattern; red dots = outliers (Passing-Bablok regression is a non-parametric procedure, not influenced by the presence of one or relative few outliers).

3.2.3 Renal function and energetics

Urine samples collected over the 24h immediately before plasma standardised sampling were used for estimation of glomerular and tubular function, according to standard equations. In particular, glomerular filtration rate (GFR) was estimated by creatinine clearance:

$$C_{Cr} = \frac{uCreatinine \times 24h \text{ urinary Volume}}{pCreatinine \times 24 \times 60 \text{ min}}$$

Body surface area (BSA)-corrected creatinine clearance was calculated as:

$$C_{Cr-BSA\ corrected} = \frac{C_{Cr} \times 1.73}{\sqrt{(Height \times Weight)/3600}}$$

GFR was also estimated according to CKD-EPI formula (eGFR),^(Levey et al., 2009) for comparison with values routinely used in clinical practice.

Tubular handling of Na⁺, K⁺ and water were assessed by their respective fractional excretions (FE), i.e. the ratio between the excreted and the filtered amount. In particular, for Na⁺ and K⁺, they were calculated as:

$$FE_{Na} = \frac{Na\ excreted}{Na\ filtered} = \frac{(pCreatinine \times uNa)}{(pNa \times uCreatinine)}$$

$$FE_K = \frac{K\ excreted}{K\ filtered} = \frac{(pCreatinine \times uK)}{(pK \times uCreatinine)}$$

later multiplied by 100 to express them as percentages; *p* and *u* prefixes indicate plasma and urinary concentrations, respectively. Fractional excretion of water is the volume of water that appears as urine compared to the filtered amount, thus:

$$FE_{Water} = \frac{urine\ flow\ rate\ (V)}{GFR} = \frac{V}{uCreatinine \times V / pCreatinine} = \frac{pCreatinine}{uCreatinine}$$

similarly multiplied by 100 for data presentation as percentages.

GFR estimation by creatinine clearance (ml/min) and FE_{Na} allowed calculation of the absolute amount (mmol/d) of filtered [GFR x pNa x 24h x 60 min], reabsorbed [1 – (filtered x FE_{Na})] and excreted Na⁺ [filtered x FE_{Na}]. Based on known stoichiometry of renal transepithelial Na⁺ transport to ATP (4.6 Na⁺/ATP) and assuming 7.3 kcal/mol for the free energy equivalent of ATP (Klahr et al., 2011), I calculated the estimated energy expenditure for the tubular reabsorptive activity [(reabsorbed Na⁺/d x 7.3 kcal/mol ATP)/4.6 Na⁺/ATP; kcal/d].

3.2.4 *Metabolomics*

Samples were extracted with HPLC grade chloroform/methanol/water (1:3:1 v/v; Merck, Sigma-Aldrich). A pooled sample was prepared by combining an aliquot from each individual sample into a single sample and they were then stored at -80°C until analysis by liquid chromatography – mass spectrometry (LC-MS). Detailed methods for the LC-MS analysis of the extracted samples, performed for the author of this thesis by others (*Glasgow Polyomics*), are reported elsewhere (Rossitto et al., 2020); importantly, before experimental sample analysis 3 mixes of authentic standards were analysed and later used to confirm the identity of metabolites where applicable based upon accurate mass and retention time. After the experimental sample analysis, fragmentation data was collected in both positive and negative ionisation mode for the pooled sample; this data was again used to confirm the identities of metabolites where applicable. The raw mass spectrometry data was converted and processed using dedicated software and eventually through PiMP (<http://polyomics.mvls.gla.ac.uk/>; Gloaguen et al., 2017), accessed by the author of this thesis.

3.2.5 *Statistics*

Categorical variables are presented as absolute numbers and percentages and compared by χ^2 test. Quantitative variables were tested for normal distribution in the whole cohort and in individual groups by graphical plot and Kolmogorov–Smirnov test; they are presented as mean \pm SD, or median and interquartile range in case of a skewed distribution. Parametric and nonparametric statistics were used for normally and non-normally distributed variables, respectively. In particular, one-way analysis of variance (ANOVA) or Kruskal-Wallis test was used to compare anthropometric, clinical, and biochemical data across study groups, with Tukey or Dunn’s as post-hoc tests, as appropriate; crude correlations were ascertained by Pearson or Spearman tests.

Multivariable-adjusted comparisons (ANCOVA) and linear regression models included significant covariates identified at comparison of Na-intake groups, i.e. age, sex, BMI, aldosterone and systolic blood pressure, upon appropriate transformation to attain normal distribution. Little’s Missing Completely At Random (MCAR) test was used beforehand to test the assumption that variables were missing completely at random, including the above covariates and urinary Na⁺ excretion in the analysis; no imputation

methods were adopted and missing data were excluded, with valid numbers for each analysis reported in the manuscript.

Slopes of the regression lines for fractional excretions, assessing tubular Na⁺ and water handling, were compared between high and low Na⁺ intake groups using the extra-sum-of-squares F test, with automatic outliers exclusion (conservative Q for ROUT approach set at 0.5%) and normality of residuals confirmed with Kolmogorov–Smirnov test.

For metabolomics, the intensity of peaks with a matching database formula (Wishart et al., 2018) was log transformed and t-test comparisons were conducted between high and low Na⁺ intake groups, using a moderated linear model. The p-values for the targeted and non-targeted analysis were corrected to control the false discovery rate (Storey et al., 2019, Benjamini et al., 2006).

The α level was set at 0.05 and all statistical tests were 2-tailed. SPSS (version 25, IBM) and Prism (version 8.02, GraphPad Software) were used for the analysis.

3.3 Results

3.3.1 Cohort characteristics

Out of 1464 patients, 592 in whom washout of confounding medications was not possible and 106 who received a final diagnosis of secondary hypertension were excluded. The final study cohort therefore included data from 766 patients, almost exclusively of Caucasian ethnicity (Figure 3-1).

Their clinical and biochemical general characteristics by Na⁺ intake groups are reported in Table 3-1. Of note, pre-defined 24 u-Na⁺ cut-off values for group allocation (low \leq 100 mmol/d; medium 100-216 mmol/d, high $>$ 216 mmol/d) closely approximated the extreme quintiles of the distribution (102 and 219 mmol/day for 20th and 80th percentile, respectively).

Table 3-1. Clinical and biochemical characteristics of patients by Na⁺ intake group

	n _{valid}	ALL	Low-Na ⁺ (n=146)	Med-Na ⁺ (n=464)	High-Na ⁺ (n=156)	P
Age (years)	766	47 ± 13	47 ± 13	47 ± 13	44 ± 13 *†	0.015
Sex (M; n/%)	766	428 / 55.9%	49 / 33.6%	248 / 53.4%*	132 / 84.1%*†	<0.001
BMI (Kg/m ²)	537	25.6 [23.0-29.0]	24.1 [21.0-27.4]	25.7 [23.2-29.1]*	26.7 [24.5-29.8] *†	<0.001
SBP (mmHg)	647	150 ± 18	153 ± 20	149 ± 18	149 ± 15	0.165
DBP (mmHg)	647	93 ± 10	93 ± 10	93 ± 10	94 ± 11	0.801
Medications (n/%):						
none	766	138 / 18.0%	27 / 18.5%	89 / 19.2%	22 / 14.0%	0.356
dhp CCB	766	444 / 58.0%	82 / 56.2%	261 / 56.3%	102 / 65%	0.158
non-dhp CCB	766	160 / 20.9%	30 / 20.5%	103 / 22.2%	27 / 17.2%	0.427
α-blockers	766	173 / 22.6%	24 / 16.4%	102 / 22.0%*	47 / 29.9% *†	0.016
Diabetes (n/%)	630	24 / 3.8%	4 / 3.3%	15 / 4.0%	5 / 3.6%	0.927
CKD (n/%)	645	24 / 3.7%	4 / 3.3%	18 / 4.7%	2 / 1.4%	0.222
p-Na⁺ (mmol/l)	675	141 ± 2	141 ± 2	141 ± 2	141 ± 2	0.650
p-K⁺ (mmol/l)	703	4.0 ± 0.4	4.0 ± 0.4	4.1 ± 0.4	4.0 ± 0.4	0.070
PAC (pmol/l)	766	241 [183-340]	265 [189-386]	232 [182-323]*	254 [174-344]*	0.040
PRA (ng/ml/h) 2012-15	313	0.64 [0.33-1.26]	1.00 [0.29-1.50]	0.61 [0.30-1.21]	0.62 [0.41-1.17]	0.361
DRC (mIU/L) 2015-17	452	7.9 [3.3-14.8]	9.5 [4.1-15.9]	7.7 [3.1-13.6]	7.6 [2.7-15.7]	0.155
ARR_{PRA} (ng/dl/ ng/ml/h)	313	15.9 [9.1-29.4]	14.9 [9.1-29.7]	16.5 [8.2-31.2]	15.7 [9.8-24.7]	0.823
ARR_{DRC} (ng/dl/ mIU/L)	452	1.09 [0.61-2.25]	0.99 [0.62-2.00]	1.14 [0.62-2.46]	1.03 [0.53-2.15]	0.514
24h-u-Diuresis (L/d)	766	1.8 [1.4-2.3]	1.5 [1.0-2.1]	1.8 [1.4-2.3]*	2.0 [1.6-2.4] *†	<0.001
24h-u-Na⁺ (mmol/d)	766	155 [112-205]	80 [66-92]	154 [128-183]*	252 [236-294] *†	<0.001
24h-u-K⁺ (mmol/d)	766	60 [48-77]	49 [38-65]	60 [48-74]*	73 [61-90] *†	<0.001

Qualitative data presented as n (%) and compared by χ^2 test. Quantitative data presented as mean \pm SD or median (interquartile range) and compared by ANOVA or Kruskal-Wallis test, respectively, as appropriate. n_{valid} = number of patients with available information. BMI = Body Mass Index; SBP and DBP = systolic and diastolic blood pressure, respectively; dhp = dihydropyridine; CCB = calcium channel blockers; CKD = chronic kidney disease; p- = plasma; 24h-u- = 24 h urine; PAC = plasma aldosterone concentration; PRA plasma renin activity; DRC = direct renin concentration; ARR = aldosterone-to-renin ratio. Post-hoc Tukey or Dunn's tests, as appropriate: * p < 0.05 vs Low-Na⁺; † p < 0.05 vs Medium-Na⁺.

Patients on high Na⁺ intake were generally younger, had a higher BMI and similar BP values, although more frequently required doxazosin on top of a first-line calcium channel blocker, compared with other Na⁺ groups. Prevalence of diabetes and/or CKD (KDIGO stage ≥ 3) in the cohort was low (<4% for both) and did not differ across study groups.

While plasma Na⁺ and K⁺ did not differ, plasma aldosterone was higher with low Na⁺ intake ($p=0.040$). Renin showed a similar trend, which reached statistical significance upon correction for age and sex, significant predictors at multivariate regression analysis (*not shown*). Overall, the aldosterone-to-renin ratio did not differ across study groups. In the 24h urine, higher Na⁺ excretion was paralleled by a higher K⁺ excretion and total urinary volume ($p<0.001$ for both).

3.3.2 Na⁺ and Water renal handling

The association between the fractional excretions (FE) of Na⁺ (available in $n=282$) and water ($n=303$), as expression of the traditional osmotic natriuresis mechanism challenged by the findings from the long-term balance space-flight simulation study (Rakova et al., 2017), was first investigated. The Little's MCAR test excluded a systematic bias deriving from selection of the cases with available FE data (sig.=0.185 for FE_{Na} and sig.=0.163 for FE_{water}).

In the context of an expected positive correlation (Spearman $\rho=0.402$, $p<0.001$), the slope of the regression line was steeper at low compared to high salt intake ($p=0.005$; Figure 3-3, panel A). In fact, the FE of Na⁺ increased with increasing Na⁺ intake ($p<0.001$ across groups; post-hoc low vs. high: 0.39% [0.30-0.47] vs. 0.81% [0.73-0.98], $p<0.001$) while FE of water decreased ($p=0.016$ across groups; post-hoc low vs. high: 1.13% [0.73-1.72] vs. 0.89% [0.69-1.12], $p=0.015$; Figure 1, panel B). No such difference was observed for K⁺ FE ($p=0.892$).

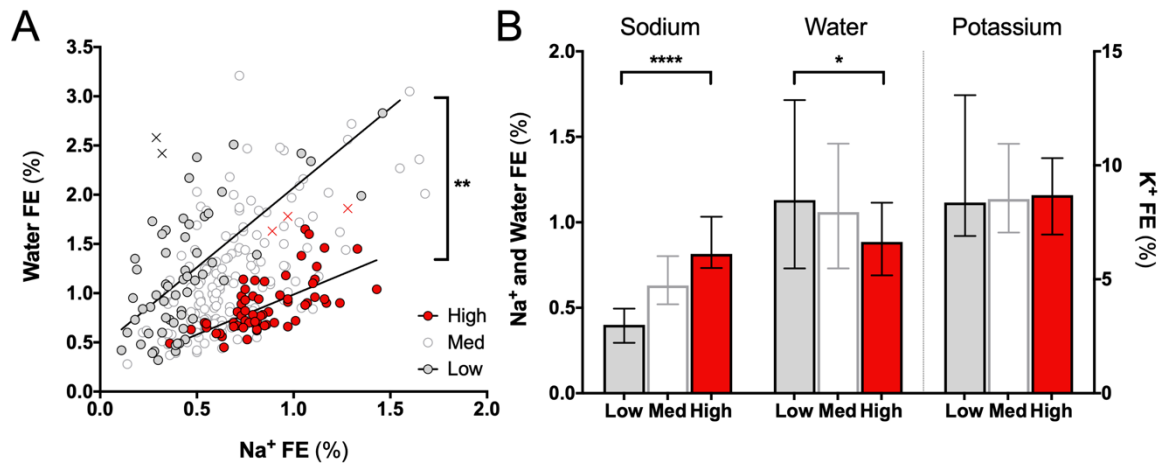


Figure 3-3. Renal Na and Water handling upon differential Na⁺ intake.

Panel A) the positive association between Water and Na⁺ fractional excretions reflects the osmotic effect of Na⁺, driving a parallel excretion of accompanying water; however, the slope of this association is steeper at low (white dots; n=61) compared to high (red dots; n=63) Na⁺ intake (1.62 [95%CI: 1.14-2.09] vs 0.81 [95%CI: 0.56-1.06], respectively; p=0.005, extra-sum-of-squares F test; X indicate automatically-excluded outliers [ROUT approach, Q=0.5%] from High and Low Na⁺ intake groups). Panel B) with increasing Na⁺ intake, Na⁺ FE increases while water FE decreases (Kruskall-Wallis test: p<0.001 and p=0.017, respectively; Dunn's post-hoc test results on top of bars); no significant difference across groups was noted for K⁺. Data are shown as median and IQR; * p<0.05, ** p<0.01; **** p<0.0001.

3.3.3 Excess Na⁺ excretion is paralleled by glomerular hyperfiltration

In keeping with evidence of a higher excretion of creatinine in the 24 h, BSA-corrected (and uncorrected) creatinine clearance was greater in high than in medium- and low-Na⁺ intake (p<0.001 across groups; n=249; Little's MCAR test Sig.=0.221; Table 3-2). In the High Na⁺ group 36.7% of the patients met the definition of “glomerular hyperfiltration” according to a commonly used cut-off (135 ml/min/1.73m²) (Tonneijck et al., 2017, Reboldi et al., 2018), compared to 16.4 and 8.2% in the Medium and Low Na⁺ intake group, respectively (χ^2 , p<0.001). Similar trends were confirmed with use of CKD-EPI formula, although with lower estimates of eGFR and of glomerular hyperfiltration prevalence, accordingly (Table 3-2).

An independent association between 24h urinary Na⁺ excretion and creatinine clearance was confirmed at multivariate regression analysis, after correction for age, sex, systolic blood pressure, BMI, and aldosterone (p<0.001). In a regression model including also 24h urinary K⁺, as an independent surrogate marker for global food intake based on the above demonstration of a constant tubule handling, both variables remained significant predictors (p=0.003 and p<0.001, respectively).

Table 3-2. Renal function by Na⁺ intake group

	n _{valid}	ALL	Low-Na ⁺	Med-Na ⁺	High-Na ⁺	p	p _{adj}
p-Creatinine (μmol/l)	664	73 [63-84]	69 [59-78]	73* [63-84]	75* [68-85]	0.002	0.027
u-Creatinine (mmol/l)	325	7.0 [5.0-10.4]	5.7 [4.1-9.4]	6.7 [4.6-10.3]	9.1*† [6.3-10.5]	0.001	<0.001
24h u-Creatinine excretion (mmol/d)	325	12.0 [8.8-15.6]	8.8 [7.1-11.9]	11.7* [8.9-15.3]	16.0*† [13.9-19.7]	<0.001	<0.001
Estimated GFR:							
Creatinine Cl (ml/min)	303	119.2 [93.0-151.1]	100.5 [75.1-117.8]	116.6* [91.7-142.4]	150.3*† [125.6-178.1]	<0.001	<0.001
Creatinine Cl/BSA (ml/min/1.73m ²)	249	108.6 [86.7-128.8]	94.1 [69.9-118.8]	103.8* [86.9-126.0]	127.5*† [108.3-147.8]	<0.001	<0.001
Glomerular HF n/tot (%)		48/249 (19.3%)	5/61 (8.2%)	21/128 (16.4%)	22/60 (36.7%)*†	<0.001	
eGFR – CKD-EPI (ml/min/1.73m ²)	664	98.4 [86.6-107.6]	98.8 [86.8-106.0]	97.0 [85.4-106.3]	100.8*† [91.4-111.7]	0.001	0.02
Glomerular HF n/tot (%)		8/664 (1.2%)	0/122 (0%)	3/405 (0.7%)	5/137 (3.6%)*	0.011	
p-Urea (mmol/l)	498	4.8 [4.0-5.7]	4.7 [4.0-5.6]	4.7 [3.9-5.6]	5.1† [4.2-6.1]	0.026	0.724
u-Urea (mmol/l)	173	196.6 [127.2-271.3]	145.5 [100.3-237.4]	177.4 [125.9-257.8]	260.2*† [177.9-314.1]	0.001	0.015
24h-u-Urea excretion (mmol/d)	173	337.5 [239.6-499.0]	242.9 [178.3-343.0]	332.1* [244.8-453.9]	496.8*† [373.0-610.6]	<0.001	<0.001

Qualitative data presented as n (%). Quantitative data presented as median (interquartile range). p- = plasma; u- = urine. GFR = Glomerular filtration rate. Cl = clearance; BSA = body surface area; HF = hyperfiltration. p_{adj} = analysis of variance adjusted for age, sex, systolic blood pressure, BMI and aldosterone. Post-hoc tests: * p < 0.05 vs Low-Na⁺; † p < 0.05 vs Medium-Na⁺. p_{adj} = sig. corrected for age, sex, systolic blood pressure, BMI, and aldosterone.

3.3.4 High Na⁺ intake increases tubular reabsorption and renal energy expenditure

Although the FE of Na⁺ was higher with high Na⁺ intake, the total amount of Na⁺ filtered by the glomerulus and reabsorbed by the tubules per day was far larger compared to medium and low Na⁺ intake (p<0.001, regardless of adjustment for the above covariates, including stratification by sex; Figure 3-4). The estimated energy cost for this excess reabsorptive tubular activity is shown in Figure 3-4, panel B (Δ high vs. low Na⁺ intake groups=18 [12-24] kcal/day; p<0.001).

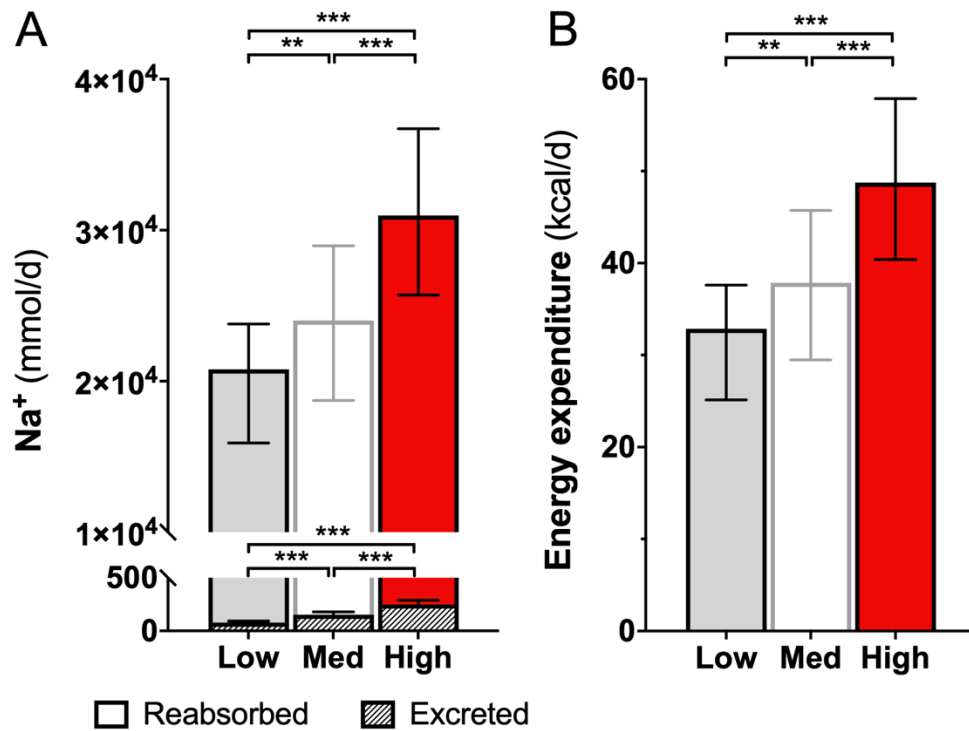


Figure 3-4. Absolute Na⁺ excretion and reabsorption and energy cost.

Panel A) The total excreted Na⁺ (shaded bars) is a trivial proportion of the reabsorbed amount; the latter is much higher upon high Na⁺ intake and resulted in 18 kcal of estimated excess energy expenditure per day (Panel B). Data are shown as median and IQR; $n_{\text{tot}}=282$, $n_{\text{low Na}}=61$, $n_{\text{high Na}}=63$. Kruskal-Wallis and Dunn's post-hoc tests: ** $p<0.01$; *** $p<0.001$.

3.3.5 Sympathetic nervous system activation

Renal sympathetic nervous system activity (RSNA) plays a key role in renal haemodynamics and tubular Na⁺ reabsorption (Kopp, 2011). 24h urinary excretion of catecholamines and their more stable catabolites metanephrines were used in SYCAMORE as an indirect measure of RSNA ($n = 372$ and 628 patients, respectively).

Urinary norepinephrine and normetanephrine, but not epinephrine or metanephrines that are predominantly produced by the adrenals, increased with higher Na⁺ intake ($p < 0.001$ and $p = 0.014$, respectively). The significant association with 24h-uNa⁺ excretion persisted at multivariate analysis for norepinephrine ($p = 0.027$), but not for the less RSNA-specific normetanephrine ($p = 0.393$), after correction for age, sex, systolic blood pressure, BMI and aldosterone, and for use of calcium channel or α -receptor blockers, included in the model as known confounders (Eisenhofer et al., 2003). These findings support the evidence of a highly reabsorptive state in Na⁺ loaded tubules.

3.3.6 Re-setting of nitrogen balance and metabolic signatures

While 24h-urine excretion data suggested a higher daily loss of both creatinine and urea with high Na⁺ intake ($p \leq 0.001$ for both), plasma values increased or did not differ, respectively (Table 3-2). No difference in the FE of urea was observed across groups ($p = 0.724$). Overall, this suggested a global re-setting of the nitrogen balance.

Analysis of non-targeted metabolomics showed that the majority of metabolites significantly increased in the High Na⁺ ($n = 35$) compared to Low Na⁺ group ($n = 32$) entailed intermediates or end products of protein catabolism (i.e. dipeptides, single amino acids or their derivatives) or urea cycle (N-Acetyl-L-glutamate 5-semialdehyde: fold change (FC) = 1.52, $p_{\text{corr}} = 0.02$; Figure 3-5, panel A). In particular, plasma levels of detectable amino acids (including the branched-chain leucine, isoleucine, and valine and with the exception of few conditionally-essential or non-essential aminoacids) were increased with High Na⁺ intake (Figure 3-5, panel B).

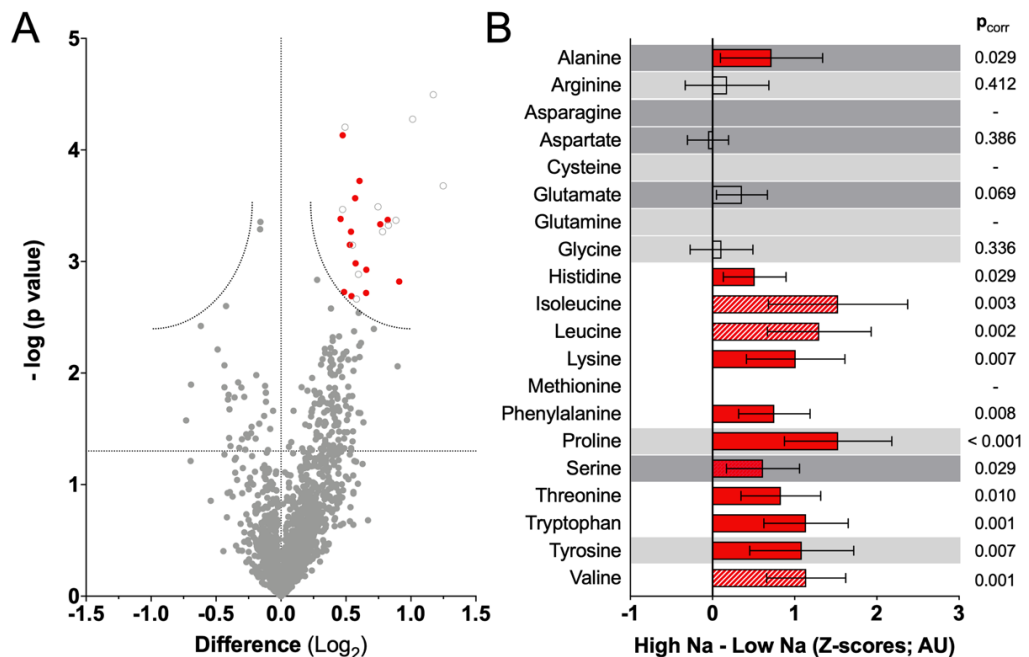


Figure 3-5. Metabolomics signature.

Panel A) Volcano plot shows the metabolomics comparison between High and Low (reference) Na⁺ intake. Y axis: uncorrected p values; curved lines: multiple comparisons-corrected significance ($p_{\text{corr}} < 0.05$). Red dots: intermediates/end products of the urea cycle or protein catabolism; empty dots: other identified metabolites. Panel B) comparative profile of plasma aminoacids LC/MS signals (mean, 95%CI); for visualisation, the x scale was made homogeneous by Z-score transformation, based on mean and SD from the low Na⁺ group, as a reference. Background: white = essential aminoacids; light grey = conditionally essential, dark grey = dispensable aminoacids. Bars: dashed for branched-chain aminoacids; red for significance ($p_{\text{corr}} < 0.05$). Peaks for asparagine, Cysteine, Glutamine and Methionine could not be unequivocally identified.

Other significantly increased metabolites identified by the non-targeted approach included products of triglycerides and fatty acid metabolism (diacylglycerols and acylglycines), acyl-carnitines and some industrial food/tobacco-related compounds (Figure 3 panel A). A complete list of significantly different metabolites is provided as Appendices 7-8.

While no obvious shift in carbohydrate metabolism was observed at metabolomics analysis, higher Na⁺ intake was associated with higher plasma glucose (n=171; High Na⁺: 4.9 [4.6-5.4] mmol/l, Medium Na⁺: 4.7 [4.3-5.0] mmol/l, Low Na⁺: 4.5 [4.2-5.0] mmol/l; p=0.004) and insulin (n=47; High Na⁺: 7.46 [4.75-11.80] μU/ml, Medium Na⁺: 5.81 [3.79-9.24] μU/ml, Low Na⁺: 4.89 [3.72-8.04] μU/ml; p=0.001); however, these associations did not persist at multivariable analysis, where BMI stood out as the strongest common independent predictor (r=0.38, p=0.002 and r=0.48, p<0.001 respectively).

3.3.7 Excess cortisol upon high Na⁺ intake

Cortisol excess had been previously suggested to be the primary drive for muscle catabolism upon High Na⁺ intake (Kitada et al., 2017). In SYCAMORE, 24h urinary free cortisol (UFC) did increase across groups of Na⁺ intake (n=137, Little's MCAR test Sig.=0.161; Low Na⁺: 63 [36-72] nmol, Medium Na⁺: 60 [47-86] nmol, High Na⁺: 86 [75-139] nmol; p<0.001) and the positive association of UFC with 24h-uNa⁺ excretion persisted at multivariable analysis after correction for age, sex, systolic blood pressure, BMI, and aldosterone (p=0.017), and also for creatinine clearance (p=0.035). However, the latter stood out as the strongest independent predictor (p<0.001).

Morning plasma-cortisol showed an opposite trend (n=658; Low Na⁺: 246 [203-309] nmol/l, Medium Na⁺: 238 [194-294] nmol/l, High Na⁺: 217 [171-294] nmol/l; p=0.047); no independent association with 24h-uNa⁺ was observed (p=0.284 at multivariate regression).

3.4 Discussion

3.4.1 Main findings

The idea that that high Na⁺ intake could induce mechanisms of water preservation and adversely affect metabolic signatures was first proposed by Titze *et al.*, based on the diet-controlled experimental settings of a rodent study and a long-term simulated space flight of 10 healthy subjects (Kitada *et al.*, 2017, Rakova *et al.*, 2017). I herein retrospectively examined this hypothesis in a large real-life population of hypertensive patients.

SYCAMORE results, obtained under normal dietary conditions and urinary salt excretions comparable to those reported in other populations (Cogswell *et al.*, 2016), showed that the higher excretion of Na⁺ was indeed coupled with a higher excretion of water, in keeping with the classic concept of osmotic natriuresis. However, opposite trends relative to their filtered amount were identified: while the fractional excretion increased for Na⁺ upon high Na⁺ intake, it decreased for water. This was paralleled by a plasma metabolomic signature consistent with protein catabolism and with the results obtained by Titze *et al.* in rodent models. Such findings indicate that kidneys can effectively dissociate Na⁺ and water handling upon high Na⁺ intake. The associated catabolic state, likely participating in this water preservation mechanism, could independently affect body composition and, ultimately, the risk of cardiovascular disease.

Previous clinical studies identified differential body water handling, assessed as body weight change and diuretic response upon salt load and depletion, between salt-sensitive and salt-resistant (insensitive) subjects (Laffer *et al.*, 2016). In this study, albeit lacking a formal assessment of salt sensitivity, I rather focused on the renal-specific differential regulation of Na⁺/water excretion and its correlates, independently of blood pressure. Such fine regulation appears to rely upon a larger amount of processed urine and a higher GFR. A recent meta-analysis identified this association also in interventional trials (Nomura *et al.*, 2017), but was limited in its conclusions by the heterogeneity in study designs, populations and approaches to estimation of GFR. The *SYCAMORE* study made use of a standardised screening approach and a rigorous protocol, including washout of confounding medications and 24h urine collections for the assessment of both Na⁺ and creatinine excretion, as well as non-targeted

metabolomics. In its large sample size, a considerable proportion of patients had glomerular hyperfiltration upon high Na⁺ intake: although estimates differ depending on the method used for GFR assessment (Levey et al., 2009), this proportion was consistently higher compared to both medium and low Na⁺ groups. Glomerular hyperfiltration, traditionally linked to obesity and diabetes (Tonneijck et al., 2017), is a recognised marker of early kidney damage, precedes microalbuminuria and/or decline in renal function and predicts cardiovascular events (Reboldi et al., 2018). The *SYCAMORE* study suggests that Na⁺ intake, independent of blood pressure values and of a surrogate for total food consumption, is a key determinant in the pathogenesis of glomerular hyperfiltration in hypertension, thus confirming previous suggestions from a smaller study (Mallamaci et al., 1996).

While higher filtration carries the ultimate advantage of more precise distal regulation of solutes (Guyton and Hall, 2011), not only has it negative long-term prognostic implications but also comes at the cost of a much higher tubular activity at more proximal segments (Figure 3-4). The increase in Na⁺ reabsorption in response to the increased filtered Na⁺ load is known as glomerulo-tubular balance and is primarily active via Na⁺/K⁺ ATPase, with ancillary passive mechanisms facilitated by changes in tubular, interstitial and capillary physical forces. The extra Na⁺/K⁺ ATPase activity implicates a higher oxygen and energy consumption (Hansell et al., 2013). Pruijm *et al.* found that one week of high-Na⁺ diet reduced renal medullary oxygenation in both normotensive and hypertensive subjects by using blood oxygen level-dependent (BOLD) MRI (Prujm et al., 2010), thus pointing to a higher oxygen extraction by tubular cells - in keeping with my contentions.

The estimate of the excess energy cost upon high vs low Na⁺ intake in *SYCAMORE* was 18 kcal. This is a rough (potentially over- or under-) estimate, based on a stoichiometry value that averages different tubular segments with different activity and that was validated in ‘standard’ conditions (Klahr et al., 2011). Albeit imprecise, it offers an order of magnitude that corresponds approximately to 4.5 g of protein or 2 g of fat per day. These values should be considered in a lifespan or population perspective. Of note, with the due haemo- and tubule-dynamic corrections required between species, the magnitude of this energy cost well justifies the weight loss observed in high Na⁺-fed mice when their total caloric food intake was paired with low Na⁺-fed controls (Kitada et al., 2017). In that animal model, the catabolic state primarily oriented toward protein degradation and muscle loss served to generate both

endogenous water and osmotically-active urea. Overall, these mechanisms allowed water preservation against Na⁺ excess and a potentially volume-depleting osmotic diuresis (Kitada et al., 2017). A similar re-setting in nitrogen balance was observed in *SYCAMORE*: along with evidence of massive excretions of urea and creatinine upon high Na⁺ intake, we identified a catabolic signature at non-targeted metabolomics, mostly entailing intermediates or end products of the urea cycle or protein catabolism. In particular, plasma levels of all the identifiable essential aminoacids were increased, thus ruling out endogenous generation or the sole renal recycling process as sources for their excess.

Finally, *SYCAMORE* explored whether a subclinical hypercortisolism were the intermediate determinant of the above catabolic state, as suggested by Titze et al. based on the increase in 24h urinary glucocorticoid excretion upon High Na⁺ diet (Rakova et al., 2017, Kitada et al., 2017). Although the limitations of a single morning plasma cortisol should not be ignored, plasma cortisol concentration did not increase – and rather decreased – with high Na⁺ intake. UFC excretion indeed increased and was independently associated with Na⁺ excretion; however, it had GFR as its far strongest predictor and its increase was clinically trivial, inconsistent with a condition of hypercortisolism, particularly when GFR-adjusted. The findings appear more in keeping with human physiological studies assessing the renal clearance of plasma cortisol, almost exclusively dependent on GFR (Schedl et al., 1959) or measuring UFC excretion in other glomerular hyperfiltration-associated conditions, like obesity (Rask et al., 2001) or simple water load (Fenske, 2006). In fact, only subtle increases in adrenal cortisol secretion in response to Na⁺ loading, possibly due to the cross stimulation of the hypothalamic-pituitary-adrenal axis by the water-preserving vasopressin (Tanoue et al., 2004), were observed by Ehrlich *et al.* despite marked changes in urinary excretion (Ehrlich, 1966). As discussed above, I propose that glomerular hyperfiltration and the consequent glomerulo-tubular balance *per se* would suffice to induce extra energy requirements and the development of a catabolic state.

It is interesting to note that the authors of the first observations recently reported that the changes in cardiovascular energy expenditure and catabolism in rats fed high salt are dependent on renal sympathetic nerve activity (Morisawa et al., 2020), thus providing further ground to my conclusion in humans.

3.4.2 Limitations, conclusions and perspectives

Some relevant study limitations should be acknowledged.

Firstly, the analysis made use of use of a single 24-hour urine collection, which may not accurately estimate an individual's usual long-term daily sodium intake, because of the previously reported day-to-day variability of Na⁺ excretion (Lerchl et al., 2015). However, estimates of intake by 24-hour urine collections in properly sized groups are not significantly affected by random variability across individuals (Cogswell et al., 2018), particularly when they are not instructed to artificially change their dietary habits. In fact, even the fiercest proponents of multiple collections to estimate an individual's Na⁺ intake observed that, despite the variability: “*average urinary excretion of Na⁺ provided the expected valid estimate of mean salt intake*” (Lerchl et al., 2015).

In other words, the higher the number (*n*) of collections averaged, the higher the precision of the estimate; but accuracy, i.e. closeness to a true value, is unaffected (provided *n* is not trivial). Additionally, use of the same 24 urine samples for the assessment of all renal handling parameters in *SYCAMORE* provided an intra-patient control, with all fluctuations going in the same biological direction and, overall, levelling off in large numbers.

Secondly, there were some missing data that potentially reduced the power of some analyses, e.g. for UFC. However, absence of evidence of systematic bias and strong statistical significance for most of our results makes type II error or any considerable impact of missing data on the overall conclusions unlikely.

Thirdly, the ethnicity of our study participants was almost exclusively Caucasian; this obviously warrants validation in other ethnic groups.

The most important limitation, worth appropriate discussion, is that the retrospective cross-sectional nature of the study is unsuitable to prove causality. Notably, however, mechanistic evidence of a metabolic shift had already been provided in preclinical models (Kitada et al., 2017); *SYCAMORE*, at variance, offers the advantage of a real-life perspective, without fixed or restricted caloric and/or water intake. The study design indeed prevents discrimination as to how the renal energy cost (predominantly

but not exclusively in the form of protein) was paid and, although the association between Na⁺ intake and renal haemodynamics/energetics was independent of K⁺ excretion, a crude surrogate for total food intake, this could well reflect catabolism of either endogenous (muscle mass) or exogenous (dietary excess) sources. Based on the higher BMI and a larger urea clearance in the high Na⁺ group, one can speculate that both options could be exploited to different degrees in different individuals, according to multiple determinants. These would include cultural and socio-economical aspects, favouring or limiting food access. Overall, the importance of an altered caloric balance is such that the excess exploitation of exogenous protein sources would ultimately result in excess fat deposition, regardless of food relative composition (Bray et al., 2012), and eventually obesity (Ma et al., 2015). Therefore, excess food consumption and lean mass loss, alternative or complementary sources for the catabolic state observed in our study, are both likely to favour a long-term adverse insulin-resistant metabolic phenotype, universally associated to worse cardiovascular outcomes (Figure 3-6).

Notably, the sodium-specific water-preserving mechanisms presented in Figure 3-6 and their detrimental effects on cardiorenal prognosis are actionable: specific dietary strategies and/or novel pharmacological approaches like SGLT-2 inhibition, reducing both glomerular hyperfiltration and the energy-demanding tubular Na⁺ reabsorption, could favourably impact the consequences of excess Na⁺ intake and the global risk profile of hypertensive patients.

In order to address the above hypotheses in the design of future research, due consideration to the aforementioned methodological aspects should be paid.

In particular, the per-protocol controlled caloric intake in the 10 healthy male cosmonauts could account for the reduced excretion and increased recycling of urea observed in the original study (Rakova et al., 2017) but not in our real-life cohort. Similarly, it could account for the discrepancy of those preclinical data with a recent secondary analysis of the DASH (Dietary Approaches to Stop Hypertension)-Sodium trial (Sacks et al., 2001), which found increased thirst upon high Na⁺ diet when caloric intake was not fixed (Juraschek et al., 2020). Such finding is possibly in keeping with reduced need for recycling of endogenous sources and reduced endogenous water preservation or generation, accordingly.

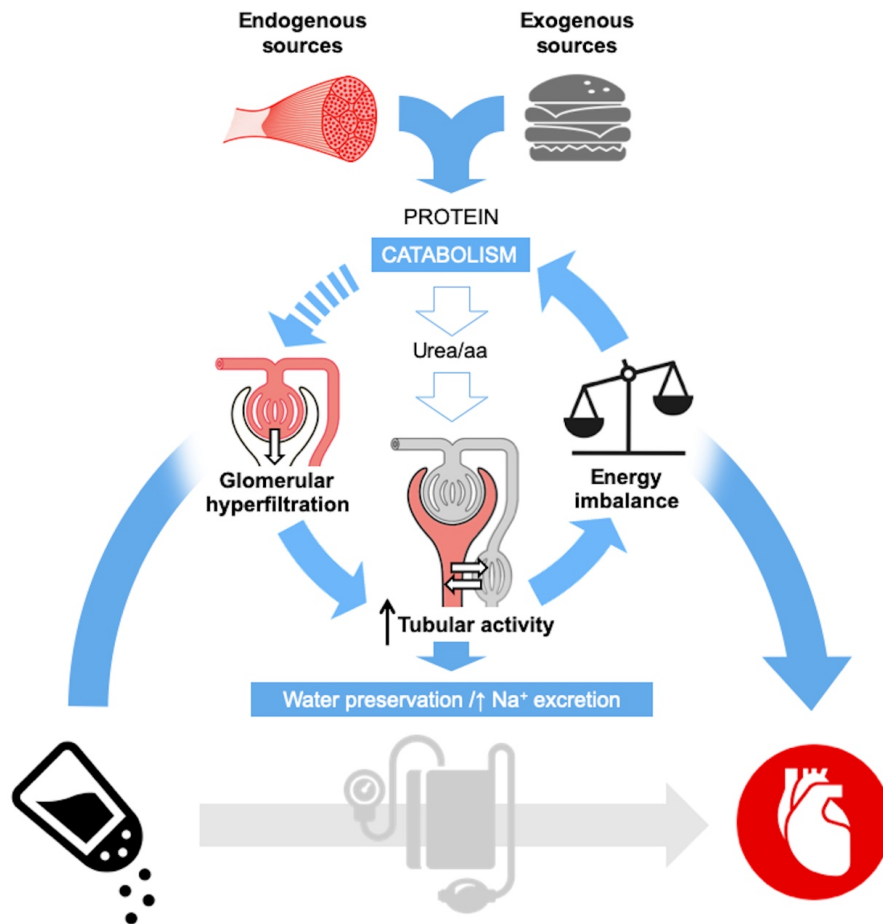


Figure 3-6. Metabolic impact of high Na⁺ intake - summary figure.

High salt intake is traditionally linked to cardiovascular risk via its effect on blood pressure (BP, in grey). Preclinical studies recently described a metabolic shift toward catabolism upon high sodium (Na⁺) diet, ultimately favouring body water preservation and possibly impacting cardiovascular risk, irrespective of BP. In a large cohort of hypertensive patients, kidneys preserve water and excrete sodium excess upon high salt intake; this was associated with glomerular hyperfiltration, higher tubular workload and a plasma metabolomic signature suggestive of protein catabolism. Muscle loss and/or excess food consumption, paralleled by adverse renal haemodynamics in a putative vicious circle, could represent a novel BP-independent link between salt intake and cardiovascular disease.

For this figure I used the file https://commons.wikimedia.org/wiki/File:Physiology_of_Nephron.png by Madhero88, licensed under the Creative Commons Attribution 3.0 Unported license.

Additional findings and conclusions from that study, apparently opposing Titze's original results, are of great interest and by-extension embrace many the topics discussed in this thesis, to a point that I requested access to DASH-Sodium data (available to researchers from the National Heart, Lung, and Blood Institute BioLINCC repository) for a complementary independent secondary analysis (University of Glasgow MVLS College Ethics Committee approval, 6th March 2020). An excursus on the findings of both analyses is provided in Chapter 8, as part of the conclusive thesis discussion.

TISSUE SODIUM ACCUMULATION: MODELLING

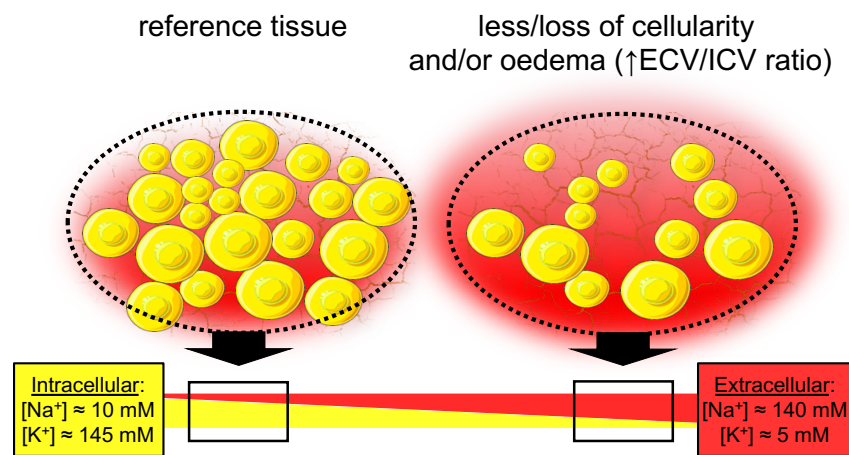
4.1 Introduction and rationale

In the last decade the traditionally nephrocentric view of Na⁺ homeostasis expanded to include the concept of tissue Na⁺ (Titze and Luft, 2017). The negatively-charged glycosaminoglycans and a TonEBP/NFAT5-VEGFc-mediated expansion of the lymphatic network were suggested to serve as a depot and draining system for Na⁺ accumulation in the interstitium, respectively (Machnik et al., 2009, Wiig et al., 2013, Karlsen et al., 2018). The proposed water-independent nature of this phenomenon (Titze et al., 2002a, Titze et al., 2003, Titze et al., 2005) marked its novelty (Elijovich et al., 2016) and its potential implications in the pathogenesis of hypertension and cardiovascular disease at large, as independent studies reported a boosted activation of pathogenic immune-inflammatory cells upon culture in supraphysiological concentrations of Na⁺ (Kleinewietfeld et al., 2013, Jantsch et al., 2015, Zhang et al., 2015, Barbaro et al., 2017, Van Beusecum et al., 2019). The translational value of this evidence relies on the presence of Na⁺-hypertonic microenvironments in tissues.

Importantly, the assessment of interstitial Na⁺ accumulation has thus far relied on whole tissue measurements. In their seminal body composition study (Titze et al., 2005) and those which followed, Titze et al used a gravimetric approach (wet weight – dry weight) to measure the water weight of the skin, the carcasses and the muscles; the dried samples were then extensively ashed and dissolved in HNO₃ for electrolyte measurement with a flame or atomic absorption. Such protocol gives a Na⁺ final readout which reflects the Na⁺ in the whole tissue “homogenate”. Therefore, all the available estimates of Na⁺ hypertonicity should more precisely refer to the tissue, rather than the extracellular compartment, i.e. interstitium. Unfortunately, more sophisticated approaches to separate the intracellular from extracellular fractions, for example by means of Nuclear Magnetic Resonance, are cumbersome and intrinsically limited by a similar relaxation time of Na⁺ in both compartments (Foy and Burstein, 1990); even use of chemical shift reagents is often unfeasible, at least in-vivo, because of their toxicity (Wimperis, 2011). Finally, new proposed methods in the field of MR imaging (Madelin et al., 2014) are limited by assumptions on aspects like constancy of extracellular Na⁺ concentration, which are the actual topic of investigation of this thesis.

Whole tissue data still retain informative value, if properly interpreted. In this regard, over the course of my PhD studies, it became clear that any estimate of Na⁺ based on a destructive measurement in the whole-tissue is exquisitely sensitive to the relative proportions of extracellular to intracellular volumes (where Na⁺ and K⁺ are the most abundant cations, respectively). By sampling a volume of tissue and averaging the signal from the whole volume, regardless of the intracellular or extracellular source, ²³Na MRI voxels can be seen as similarly “destructive” (Figure 4-1).

CHEMICAL ANALYSIS – [Na⁺] and [K⁺]



²³Na MAGNETIC RESONANCE IMAGING

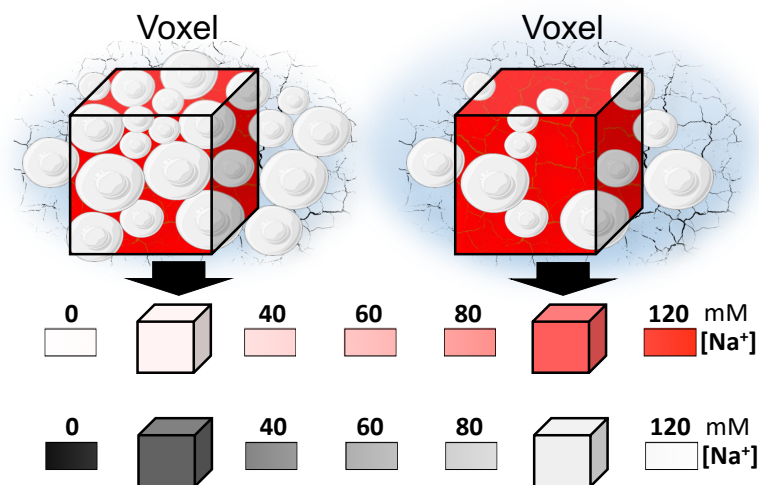


Figure 4-1. Histochemical impact of tissue architecture.

Intracellular compartments are rich in K⁺ (yellow), while extracellular compartments in Na⁺ (red); in both, the sum of K⁺ and Na⁺ concentrations ([K⁺] and [Na⁺], respectively) is similar. When intracellular and extracellular compartments are mixed, i.e. a whole tissue chemical analysis is performed, total [Na⁺] is higher in any tissue with physiologically less intracellular volume or undergoing loss of cellularity or oedema accumulation compared to a reference tissue. The concept applies to ²³Na MRI (bottom), where the average signal from a voxel is presented as a shade of colour, typically grey in the commonly used radiological black-white lookup table. ECV = extracellular volume; ICV = intracellular volume.

I only later learned that others, almost 80 years ago, conducted chemical studies on rat tissues in relation to ageing, with a similar so-called “*histochemical deductive*” approach and interpretation (Lowry and Hastings, 1942, Lowry et al., 1942, Lowry et al., 1946).

Based on the above appreciation, I first developed a simple model for prediction of total Na⁺ and K⁺ composition of any tissue, as a function of the extracellular volume fraction (ECV%). This model later served as reference for a throughout reevaluation of the nature and tissue/organ distribution of the previously reported hypertonic Na⁺ excess, in preclinical and clinical settings (Chapters 5 and 6, respectively).

4.2 Methods: calculations

For the purpose of the model calculations, the following abbreviations were used:

[Na⁺]_i, [Na⁺]_e and [Na⁺]_T = intracellular (IC), extracellular (EC) and total Na⁺ concentration (mmo/l), respectively; [K⁺]_i, [K⁺]_e and [K⁺]_T = IC, EC and total Na⁺ concentration (mmo/l), respectively; V_i, V_e, V_T = volume of IC, EC and total (EC + IC) water solution in tissue; ECV% = extracellular volume fraction (%) = 100 · V_e/V_T.

4.2.1 Expected total concentration of Na⁺ and K⁺ in a tissue

For any tissue, considered as a sum of two different water solutions (EC and IC):

Na⁺ total moles = Na⁺ extracellular moles + Na⁺ intracellular moles.

Therefore: $[\text{Na}^+]_T \cdot V_T = [\text{Na}^+]_e \cdot V_e + [\text{Na}^+]_i \cdot V_i$

or $[\text{Na}^+]_T = [\text{Na}^+]_e \cdot V_e/V_T + [\text{Na}^+]_i \cdot V_i/V_T$
 $= [\text{Na}^+]_e \cdot \text{ECV}\%/100 + [\text{Na}^+]_i \cdot (1-\text{ECV}\%/100)$

Assuming a convenient reference volume of tissue containing 1 L of total (EC + IC) water solution, absolute Na⁺ tissue content (moles) numerically coincides (≈) with [Na⁺]_T.

Similarly, for potassium: $[\text{K}^+]_T = [\text{K}^+]_e \cdot \text{ECV}\%/100 + [\text{K}^+]_i \cdot (1-\text{ECV}\%/100)$. For a similar reference volume of tissue as above, absolute K⁺ tissue content (moles) ≈ [K⁺]_T

The last two equations were used to generate the model for expected total concentration of Na⁺ and K⁺ for any tissue.

4.2.2 Expected total concentration of Na⁺ and K⁺ in oedematous tissues

The effect of a “Guytonian”, isotonic, water-paralleled extra amount of Na⁺ on the system was simulated by adding fixed and biologically plausible moieties (1%, 2.5% and 5%) of a solution equal in composition to the extracellular; this corresponds to oedema (OE% = percentage of oedema added to the tissue). The above OE% percentages were defined as v/v in relation to the “baseline” volume of the water solution in the tissue, which equals 1 L in the aforementioned convenient reference tissue.

As per first equation above, absolute Na⁺ content in the oedematous tissue (OT) is:

$$\begin{aligned} \text{Na}^+ \text{ total moles}_{OT} &= (\text{Na}^+ \text{ EC moles} + \text{Na}^+ \text{ IC moles})_T + \text{Na}^+ \text{ moles in oedema} \\ &= (\text{Na}^+ \text{ total moles})_T + \text{Na}^+ \text{ moles in oedema} \end{aligned}$$

For the reference tissue, it numerically corresponds to

$$\approx [\text{Na}^+]_e \cdot \text{ECV}\%/100 + [\text{Na}^+]_i \cdot (1-\text{ECV}\%/100) + [\text{Na}^+]_e \cdot \text{OE}\%/100$$

Total Na⁺ concentration in the oedematous tissue is:

$$\begin{aligned} [\text{Na}^+]_{OT} &= \text{Na}^+ \text{ total moles}_{OT} / \text{total Volume} \\ &= \text{Na}^+ \text{ total moles}_{OT} / (\text{Volume}_T + \text{Volume}_{\text{oedema}}) \\ &= \text{Na}^+ \text{ total moles}_{OT} / (1\text{L} + 1\text{L} \cdot \text{OE}\%/100) \\ &\approx \{[\text{Na}^+]_e \cdot \text{ECV}\%/100 + [\text{Na}^+]_i \cdot (1-\text{ECV}\%/100) + [\text{Na}^+]_e \cdot \text{OE}\%/100\} / (1\text{L} + 1\text{L} \cdot \text{OE}\%/100) \end{aligned}$$

Similarly, for potassium:

$$\text{K}^+ \text{ total moles}_{OT} \approx [\text{K}^+]_e \cdot \text{ECV}\%/100 + [\text{K}^+]_i \cdot (1-\text{ECV}\%/100) + [\text{K}^+]_e \cdot \text{OE}\%/100$$

$$[\text{K}^+]_{OT} \approx \{[\text{K}^+]_e \cdot \text{ECV}\%/100 + [\text{K}^+]_i \cdot (1-\text{ECV}\%/100) + [\text{K}^+]_e \cdot \text{OE}\%/100\} / (1\text{L} + 1\text{L} \cdot \text{OE}\%/100)$$

[Na⁺]_{OT} and [K⁺]_{OT} equations were used to generate the model for expected total concentration of Na⁺ and K⁺ in an oedematous tissue, after addition of oedema.

4.2.3 Changes in total tissue Na⁺, K⁺ and water due to oedema

Percentage changes ($\Delta\%$) for absolute Na⁺ content and concentration were defined as:

$$\Delta\% \text{ absolute Na}^+ \text{ content} = (\text{Na}^+ \text{ total moles}_{\text{OT}} - \text{Na}^+ \text{ total moles}_{\text{T}}) \cdot 100 / \text{Na}^+ \text{ total moles}_{\text{T}}$$

$$\Delta\% \text{ Na}^+ \text{ concentration} = ([\text{Na}^+]_{\text{OT}} - [\text{Na}^+]_{\text{T}}) \cdot 100 / [\text{Na}^+]_{\text{T}}$$

Percentage changes ($\Delta\%$) for absolute K⁺ content and concentration were similarly calculated. Percentage changes ($\Delta\%$) for water content was assumed as equal to OE%, which in fact corresponds to the v/v $\Delta\%$ of the solution, rather than solvent. This approximation would at most over-estimate the $\Delta\%$ for water compared to $\Delta\%$ for Na⁺ and K⁺.

4.2.4 Biological assumptions

The herein presented Figure 4-2 was generated assuming $[\text{Na}^+]_{\text{e}} = 144 \text{ mmol/l}$ and $[\text{K}^+]_{\text{e}} = 4.64 \text{ mmol/l}$ (as reported in a relevant experimental setting, for comparability (Titze et al., 2005); normal values for humans: 135-145 and 3.5-5.5 mmol/l, respectively (Herring & Paterson, 2018). $[\text{Na}^+]_{\text{i}}$ and $[\text{K}^+]_{\text{i}}$ were assumed as 10 and 140 mmol/l, respectively, as classically reported (Herring & Paterson, 2018).

4.3 Results

As one would predict based on Figure 4-1, the model revealed that the higher the ECV% (i.e. the proportion of the Na⁺-rich extracellular solution), the higher the total concentration of Na⁺ in the “final solution” from whole tissue (Figure 4-2, panel A, open circles). Vice versa, the parallel decrease in K⁺ concentration, previously described by others as a “loss” (Titze et al., 2005, Bhawe and Neilson, 2011) can be simply explained by a proportionally less represented intracellular K⁺-rich compartment (panel A, open squares), without any need for ionic exchange or “loss” mechanisms.

When the above model was challenged by simulating the effect of adding a fixed and biologically plausible amount of oedema (please see methods above), the curves shifted up for Na⁺ and down for K⁺, as expected from the equivalent of a global increase in ECV% (Figure 4-2, panel A, representative closed symbols for 5% oedema).

However, the model also revealed that the proportional increase ($\Delta\%$) in tissue Na⁺ concentration secondary to oedema is higher than the increase in water in tissues where the ECV% is low, such as skeletal muscle and myocardium which have an ECV% of 16-20% and 25-30%, respectively (Bhave and Neilson, 2011; panel B; black lines). This phenomenon is even more pronounced and holds true across all the spectrum of possible ECV% when absolute Na⁺ content, rather than concentration, is taken into account (panel B; red lines).

Percentage changes ($\Delta\%$) for absolute K⁺ content and concentration, calculated as for Na⁺, were not plotted because scarcely informative: they showed a stable decrease, numerically close to $-OE\%$, non-significantly affected by ECV% (*data not shown*).

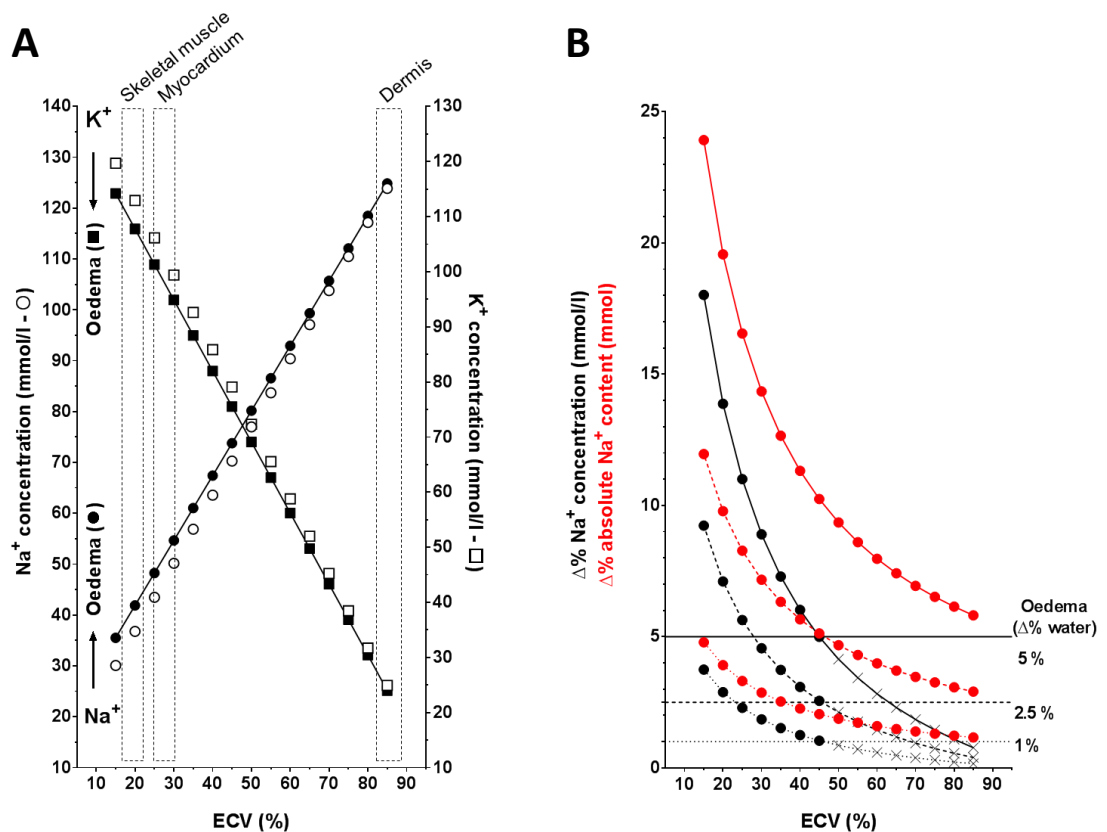


Figure 4-2. Histochemical modelling.

Panel A: Model for expected total concentration of Na⁺ (open circles) and K⁺ (open squares) in a tissue, before and after addition of 5% of oedema (closed squares and circles, respectively), as a function of the extracellular volume fraction (ECV%). Values for representative tissues with different ECV% are shown in boxes. Panel B: Percentage change of tissue Na⁺ concentration (black) or absolute content (red) after addition of 1% (dotted line), 2.5% (dashed line) or 5% (continuous line) oedema to the tissue, as a function of the extracellular volume fraction (ECV%).

4.4 Discussion and implications

The mechanisms accounting for “excess Na⁺ storage” had already been addressed in a conceptual manner by Bhave and Neilson (Bhave and Neilson, 2011). They suggested that cell rich tissues like muscle would exchange K⁺ or other intracellular osmolytes with the extracellular phase in situations with ion surplus, whereas relatively acellular connective tissues with minimal intracellular osmolytes at their disposal, like skin, may use osmotic active storage with interstitial glycosaminoglycans.

What the herein presented model adds to this “*hypothetical framework*” (Bhave and Neilson, 2011) is the additional mechanism for ‘apparent’ hypertonic excess Na⁺ storage, consistent with the aforementioned *histochemical deductive* considerations (Lowry et al., 1942, Lowry and Hastings, 1942, Lowry et al., 1946). The model provides confirmation and quantitation of how much relative differences and/or changes in the proportion of IC and EC compartments in a tissue, for example due to an isotonic phenomenon like oedema, can affect total tissue Na⁺ and K⁺ concentrations *per se*. While many metabolic studies neglected a careful K⁺ balance investigation, as pointed out by Bhave and Neilson, and chronic total-body potassium ‘loss’ can indeed occur in conditions such as primary aldosteronism, Figures 4-1 and 4-2 show how a decrease in whole-tissue K⁺ concentration in cell-rich tissues (and a parallel increase in [Na⁺]) can become apparent whenever the relative volumetric proportion of intracellular and extracellular compartments is affected, without the need for ‘exchange’ or any long-term metabolic re-setting.

This histochemical concept applies to chemical analysis of digested tissues, but also to any other technique that does not allow accurate spatial differentiation between intracellular and extracellular compartments. As alluded above, this is the case for MRI voxels in clinical practice: apart from some approaches currently limited to research (Gerhalter et al., 2017, Petracca et al., 2016), ²³Na-MRI only offers “total” ²³Na signal thus far.

Importantly, the analysis of Na⁺ can be much (up to 3.5-4 times) more sensitive than water itself to detect isotonic accumulation, i.e. oedema, particularly in highly cellular tissues. Therefore, it is not acceptable to claim solely for a “*more pronounced Na⁺-than water- accumulation*” (Nikpey et al., 2017) to support its water-free, hypertonic nature. This is key for MRI, in particular: by recording signals from single atoms in

voxels, it provides measurements closer to absolute (i.e. red lines in Figure 4-2) rather than concentrations changes. In fact, when differences or changes in human skin or muscle water content were carefully examined in parallel to those reported for tissue Na⁺, despite sometimes lacking statistical significance due to the sensitivity issue described above, they could often be found (Schneider et al., 2017, Karg et al., 2018). Recent evidence of higher sensitivity of ²³Na-based analysis over standard ¹H T₂ MRI approaches to monitor acute ischaemic extracellular compartment changes within skeletal muscle in humans (Gerhalter et al., 2017) further supports the contention of differential sensitivity rather than distinct biology.

Overall, the results of the model prompted a throughout reappraisal of the nature and tissue/organ distribution of the previously reported hypertonic Na⁺ excess in a new body composition study (Chapter 5).

TISSUE SODIUM ACCUMULATION: PRECLINICAL DATA

5.1 Background and study aims

Over the last decade, our understanding of Na⁺ homeostasis has been reshaped by the suggestion of skin as a depot for “osmotically inactive”-Na⁺ accumulation.

Based on evidence from 7-days Na⁺ balance studies in humans (Heer et al., 2000), failing to show the expected total body water storage upon salt-loading, Titze et al first conducted similar studies in rodent models of normotension, salt-resistant and salt-sensitive hypertension and observed differences in total body Na⁺, Na⁺-associated volume and BP increases across groups (Titze et al., 2002). Additional rodent studies, in which different body compartments were separated, led to the suggestion of a skin-specific and water-independent tissue Na⁺ accumulation (Titze et al., 2003, Titze et al., 2005). The depot for this local hypertonic Na⁺ accumulation was identified in the plastic and negatively charged glycosaminoglycans (GAGs) network in the extracellular matrix (Titze et al., 2004). A local self-regulatory system, driven by activation of the osmo-sensor TonEBP/NFAT5 and VEGFc/VEGFR3-mediated signalling to induce expansion/functional stimulation of the lymphatic network and provide interstitial Na⁺ clearance, was later described (Machnik et al., 2009, Wiig et al., 2013, Karlsen et al., 2018). Disruption of the system led to skin Na⁺ accumulation and salt-sensitive hypertension in the animals.

In humans, evidence of skin Na⁺ excess has been found in many cardiovascular diseases or associated risk factors (i.e. older age and hypertension, in Kopp et al., 2012 and Kopp et al., 2013; diabetes, in Karg et al., 2018; chronic kidney disease, in Schneider et al., 2017; acute heart failure, in Hammon et al., 2015), as well as in sclerodermic (Kopp et al., 2017) or infected skin (Jantsch et al., 2015), by means of ²³Na-MRI. However, in most of these studies skeletal muscle (and more recently also myocardium in patients with primary aldosteronism, a prototypic example of salt-sensitive hypertension; Christa et al., 2019) similarly showed high Na⁺ signal, thus questioning the skin-specificity of the phenomenon.

Moreover, the results of the theoretical model discussed in chapter 4 casted some doubts on the proposed water-independent nature of this tissue Na⁺ accumulation, which has experimentally-demonstrated potential to induce local pathogenic changes

(Kleinewietfeld et al., 2013, Jantsch et al., 2015, Zhang et al., 2015, Barbaro et al., 2017, Van Beusecum et al., 2019) but lacks demonstration in tissues.

On these premises, I sought to test the existence of a hypertonic, water-independent tissue Na⁺ accumulation in preclinical models of arterial hypertension by probative and disprobative approaches (i.e., by verifying and by assuming its occurrence, respectively).

In particular, I conducted a new body composition study in rats similar to those used by Titze et al in their original experiments. Wistar-Kyoto (WKY) and stroke-prone spontaneously hypertensive (SHRSP) rats, inbred at the University of Glasgow since 1991, conveniently represented the extremes of a spectrum which goes from normotension to salt-sensitive hypertension. In different sets of experiments, animals were “challenged” by salt-loading or by physiological ageing, which carries intrinsic predisposition to or worsening of salt-sensitivity (Elijovich et al., 2016). Taking into account the histochemical implications of the architectural heterogeneity of tissues discussed in chapter 4, I adapted Titze’s approach of tissue harvesting and processing to obtain robust information on multiple different organs. Additional histochemical considerations presented below and the previously developed theoretical model (chapter 4) guided the interpretation of chemical data.

The disprobative approach, independent of the chemical results above, aimed to investigate the impact of extracellular Na⁺ excess on the function of resistance arteries, based on the salt-sensitive hypertensive phenotype induced by experimental blockade of the TonEBP-VEGFC-lymphangiogenic signaling (Machnik et al., 2009, Wiig et al., 2013). If the resulting excess tissue Na⁺ were independent of water (i.e., volume), the expectation is that it would impact on the other determinant of hypertension, i.e. peripheral resistance. To test this hypothesis, the effects of in-vivo (HS) and ex-vivo Na⁺ excess on arteries were compared.

5.2 Methods

5.2.1 *Animal protocols*

All protocols were performed in accordance with the United Kingdom Animals Scientific Procedures Act 1986 (Project Licence 70/9021 held by Delyth Graham) and ARRIVE Guidelines and approved by the institutional ethics review committee (University Animal Welfare and Ethics Review Board, University of Glasgow, UK).

Rats were housed under controlled environmental temperatures (21 ± 3 °C) and lighting (12-hour light-dark cycles). In a first set of experiments testing the effects of salt-loading, male and female SHRSP and WKY were maintained on standard rat diet (rat and mouse no. 1 maintenance diet; Special Diet Services, Grangemouth, United Kingdom) and provided tap water ad libitum until 11 weeks of age. At 12 weeks, rats (littermates) were randomized to 1% NaCl (High Salt, HS) or normal drinking water (Normal Salt, NS) for three weeks (n=8 males/group and n=10 females/group, except n=9 female WKY NS). Systolic blood pressure was measured at 11 weeks of age (baseline) and then monitored weekly by tail-cuff plethysmography, in an operator-blind fashion whenever possible.

In a second set of experiments testing the effects of ageing, male SHRSP and WKY were maintained on standard diet and normal tap water ad libitum until 20 and 52 weeks of age (WKY 20w n=10; WKY 52w = 9; SHRSP 20w = 6; SHRSP 52w = 9).

5.2.2 *Harvesting and chemical analysis of rat tissues*

At the end of the 3 weeks of experimental treatment (main experiment) or at the appropriate age (additional experiment) rats were euthanized by exsanguination under general terminal isoflurane anaesthesia. Myocardium (left ventricle), lungs, liver and samples from shaved abdominal skin and skeletal muscle from the thigh, freed of fascia and tendon, were dissected and snap-frozen in liquid nitrogen. The dissection time was kept to a minimum to prevent evaporation of moisture. Any excess blood was removed by gently blotting the tissues on tissue paper; prior to blotting, the heart was cut into transverse sections. An aliquot from each tissue was cut on the surgical table and stored into tubes pre-filled with RNA-later (Qiagen Group). All tissues were stored at -80°C until use.

The protocol for water and Na⁺/K⁺ tissue content analysis has been already extensively discussed in Chapter 2 and is only briefly recollected here. Tissue aliquots representative of full parenchyma were cut from frozen rat tissue samples and weighted to determine Wet Weight (WW); sample cutting and handling was performed in a cold room to prevent evaporation of tissue water. After complete desiccation of samples at 65°C to a stable dry weight (DW), water content was estimated as (WW-DW)/DW, or as percentage (WW-DW) · 100/WW.

Dried samples underwent complete digestion in HNO₃ and the resulting solutions were used for Na⁺ and K⁺ quantification by flame photometry (Sherwood Scientific, model 410C), with calibration standards as reference. All samples from the same type of tissue were analysed in a batch. Na⁺ and K⁺ concentrations in the analysed solutions were used to back-calculate their total content in the digested samples and normalised by DW for Na⁺ and K⁺ tissue content (mmol/gDW), or by tissue water for Na⁺ and K⁺ tissue concentration (mmol/l). The flame photometry analysis was conducted blind to group allocation of samples.

Acid-insoluble residues from rat skin and liver samples were used for total fat quantification. After careful removal of the solubilised material (used for Na⁺/K⁺ quantification, as described above), 200 ul of a chloroform/methanol, 2:1 v/v mixture were added to the insoluble residues (protocol adapted from Lowry and Hastings, 1942 and Folch et al., 1957). This protocol was unfeasible with all rat tissue samples other than skin or liver because of scarcity or total absence of the insoluble residue. After overnight incubation at room temperature under agitation, solubilised extracts were transferred to pre-weighed glass tube inserts (Agilent Technologies) and solvents evaporated at 55°C to constant weight through repeated SpeedVac cycles. Total fat content in tissues was normalised by the original WW (%WW).

5.2.3 Histology: extracellular matrix

Sulphated glycosaminoglycans (sGAG) myocardial content was estimated by Alcian Blue staining of available paraffin-embedded transverse mid-ventricular 5 µm sections from the 20 or 52 weeks old WKY and SHRSP male rats (n = 4-5/group). After deparaffinization (HistoClear) and progressive rehydration to distilled water, slides were incubated in Alcian Blue solution (1% Alcian Blue 8GX, Sigma, in 3% acetic acid; pH2.5) for 20 minutes, washed in running tap water for 5 minutes, rinsed in

distilled water and counterstained in Nuclear Fast Red solution (Vector), washed again in running tap water for 1 minute and mounted following dehydration. Random, non-consecutive pictures were taken at 40x from mid-myocardium ($n \geq 25/\text{animal}$) and subepicardium ($n \geq 12/\text{animal}$; immediately below the epicardial layer) with an Olympus BX41 microscope and dedicated image capture software. sGAG were quantified as %AlcianBlue⁺ stained area after standardised thresholding across pictures, with an in-house developed macro (Appendix 9) for ImageJ (Figure 5-1).

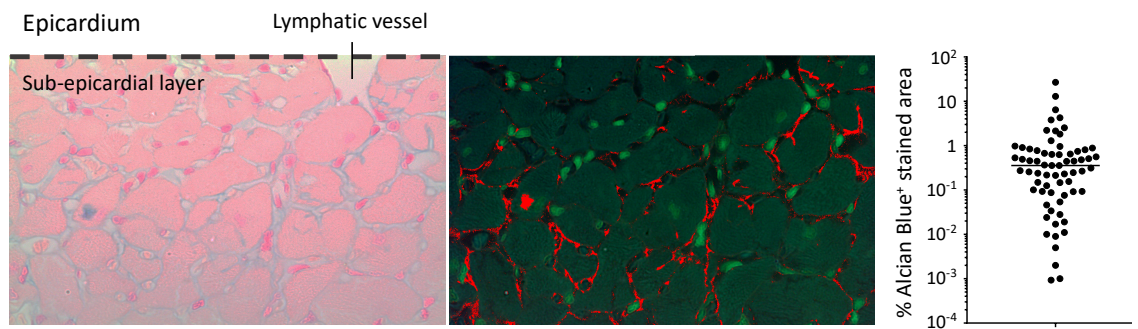
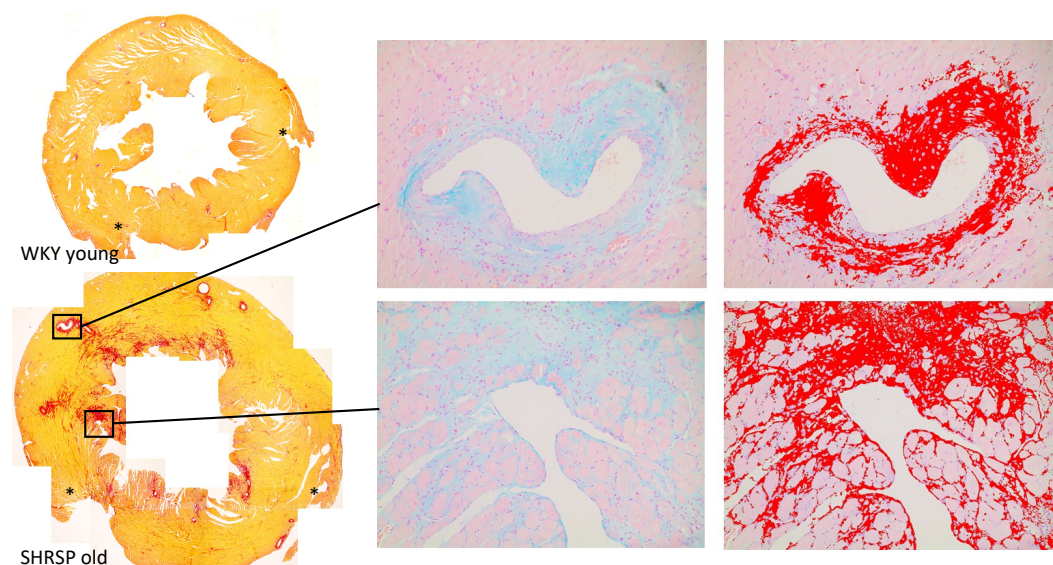


Figure 5-1. Histological sulphated glycosaminoglycans myocardial quantification

Representative subepicardial picture stained with Alcian Blue (sGAG) and Nuclear Fast red, subject to automated thresholding and quantification in inverted-colour image. Right: distribution of sGAG density (as % Alcian Blue⁺ stained area) in multiple subepidermal random, non-consecutive pictures from the same rat.

Paraffin-sections adjacent to some of those stained with Alcian Blue were stained with Picrosirius Red (1 h) after deparaffinization and rehydration as above for the purposes of (non-quantitative) macroscopic comparison of collagen with sGAG deposition in the rat myocardium.



← **Figure 5-2. Collagen and glycosaminoglycan deposition with ageing.**

Representative pictures of left ventricular remodelling in SHRSP old (52-week-old) compared to WKY young (20-week-old) male rats. Although a robust head-to-head comparison was not performed, collagen (stained with picrosirius red on the left) and sGAG (stained with Alcian Blue, pH 2.5, with nuclear fast red as counterstain, at higher magnification; Alcian Blue⁺ thresholding shown on the right) appeared to distribute similarly. * = right ventricular-left ventricular junctions.

5.2.4 Gene expression analysis

Total RNA was extracted from frozen rat tissues using QIAzol lysis reagent and RNAeasy mini-column kit (Qiagen) according to the manufacturer's instructions. For qRT-PCR, cDNA was generated from total RNA using the High-Capacity cDNA Reverse Transcription Kits (Applied Biosystems).

Taqman fast advanced master mix with specific Taqman gene expression assay probes for TonEBP (Rn01762487_m1), GAPDH (Rn01462661_g1), beta-actin (Rn00667869_m1) were used. The expression levels in tissues were normalised to either GAPDH (for myocardium) or beta actin (for other tissues; the housekeeping gene was selected upon evidence of Ct consistency across groups).

5.2.5 Ex-vivo study of arterial function on wire myography

Rationale and methodology used for the study of arterial function has already been extensively discussed in Ch2. Briefly, when rats were euthanized at the end of the experimental treatment with HS or NS, mesenteries were dissected and third-branch mesenteric arteries carefully isolated. Vascular ring segments were mounted on isometric wire myographs (Danish Myo Technology, Denmark) in physiological saline solution (PSS).

After normalization, the viability of arterial segments was assessed by contraction to KCl (62.5mmol/L), repeated after 10 minutes of washout. The contractile response to the thromboxane agonist U46619 (10^{-10} - 3×10^{-6} M). was first tested. Endothelium-dependent and -independent relaxation was assessed with acetylcholine (Ach; 10^{-10} - 3×10^{-5} M) or sodium nitroprusside (SNP; 10^{-10} - 10^{-5} M), respectively, following pre-constriction with U46619 dose that produced 75% of the maximal contractile response.

Results was compared between strains (WKY vs SHRSP) and, by strain, between NS and HS-treated animals to assess the impact of in-vivo salt-loading on vascular function.

Additional vascular segments from control (NS) WKY and SHRSP rats were incubated for 5 hours in PSS or in NaCl-supplemented-PSS (+15 mM NaCl, hypertonic, HT) after the successful viability test with KCl to assess the impact of environmental hypertonicity on vascular function. Concentration-response curves for U46619 and Ach/SNP after 5 h incubations were the same as described above.

5.2.6 Statistical analysis

Statistical analysis was performed using Prism (GraphPad Software) and SPSS (IBM).

Categorical variables are presented as absolute numbers and percentages and compared by χ^2 test. The effect of two factors (e.g. strain and salt load) on different quantitative response variables in the experimental groups was tested by two-way ANOVA. For predefined comparisons (e.g. the effect of HS vs NS), Fisher least-significant-difference test was used for normally distributed variables (presented as mean \pm SD or, graphically, as mean [95%CI]) and Mann-Whitney test for non-normally distributed variables (presented as median [interquartile range] or, graphically, as median [95%CI]). For post-hoc comparisons (e.g. between strains or sexes), labelled as such in the relative figures/tables, Holm-Sidak test was used. Data tested against a specified value were analysed by one-sample t-test.

Prior to any comparison, outliers were identified by ROUT method (Q = 1%) and excluded from analysis but reported on the relative figures.

Regression curves were derived by least-square method and compared by Extra sum-of-squares F test; for vascular function analysis, maximal contraction/relaxation and (Log)EC₅₀/IC₅₀ were independently compared. Correlations were ascertained by Pearson test, upon appropriate transformation of skewed variables to attain normal distribution.

The α level was set at 0.05 and all statistical tests were 2-tailed (*p<0.05, **p<0.01, ***p<0.001, ****p<0.0001).

5.3 Results

5.3.1 Salt-loading: experimental groups

Male and female stroke-prone spontaneously hypertensive (SHRSP) and control Wistar-Kyoto (WKY) rats (12-week-old) were treated with 1% NaCl in drinking water (high salt, HS) or normal tap water (normal salt, NS) for 3 weeks. In males, baseline blood pressure (BP) was higher, irrespective of strain differences, and salt-sensitivity of BP was confined to SHRSP (Figure 5-3).

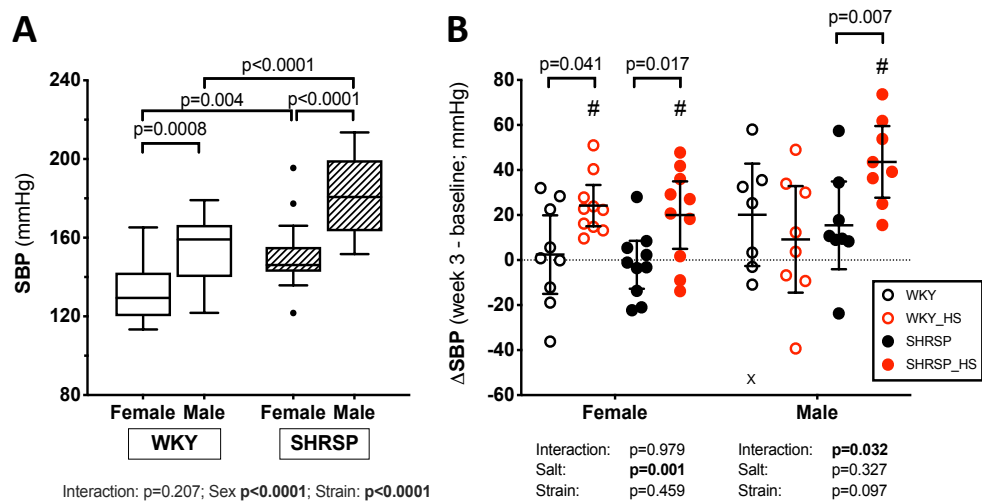


Figure 5-3. Blood pressure in the experimental groups.

Panel A: baseline systolic blood pressure (SBP) values before the experimental interventions, by sex and strain; data are presented as box-and-whisker plot (Tukey). Panel B: SBP response to experimental intervention by sex and strain. Data are presented as mean \pm 95%CI and individual dots; X = automatically excluded outlier (ROUT, Q = 1%). For all panels, 2-way ANOVA results at bottom and post-hoc tests on top; # $p < 0.05$ for two-tailed one-sample t-test vs 0 mmHg (no change vs baseline; Female WKY_HS: $p < 0.001$, Female SHRSP-HS: $p = 0.0147$; Male SHRSP-HS: $p < 0.001$).

5.3.2 Histochemical effects of salt-loading

Skin Na⁺ content (mmol/g of dry weight) was increased in SHRSP-HS (+20.7%), as expected; however, similar increases in tissue Na⁺ were observed also in liver (+10.3%), lungs (+14.8%) and skeletal muscle (+23.6%), but not in myocardium (Figure 4-4 and Tables 4-1 to 4-5). Apart from skeletal muscle, they were consistently paralleled by increases in tissue water (skin: +14.1%; liver: +4.8%; lungs: +9.0%) with similar trends observed for Na⁺ concentrations (i.e. normalized for water content, [Na⁺], mmol/L). These changes upon HS were not observed in WKY rats (Figure 5-4).

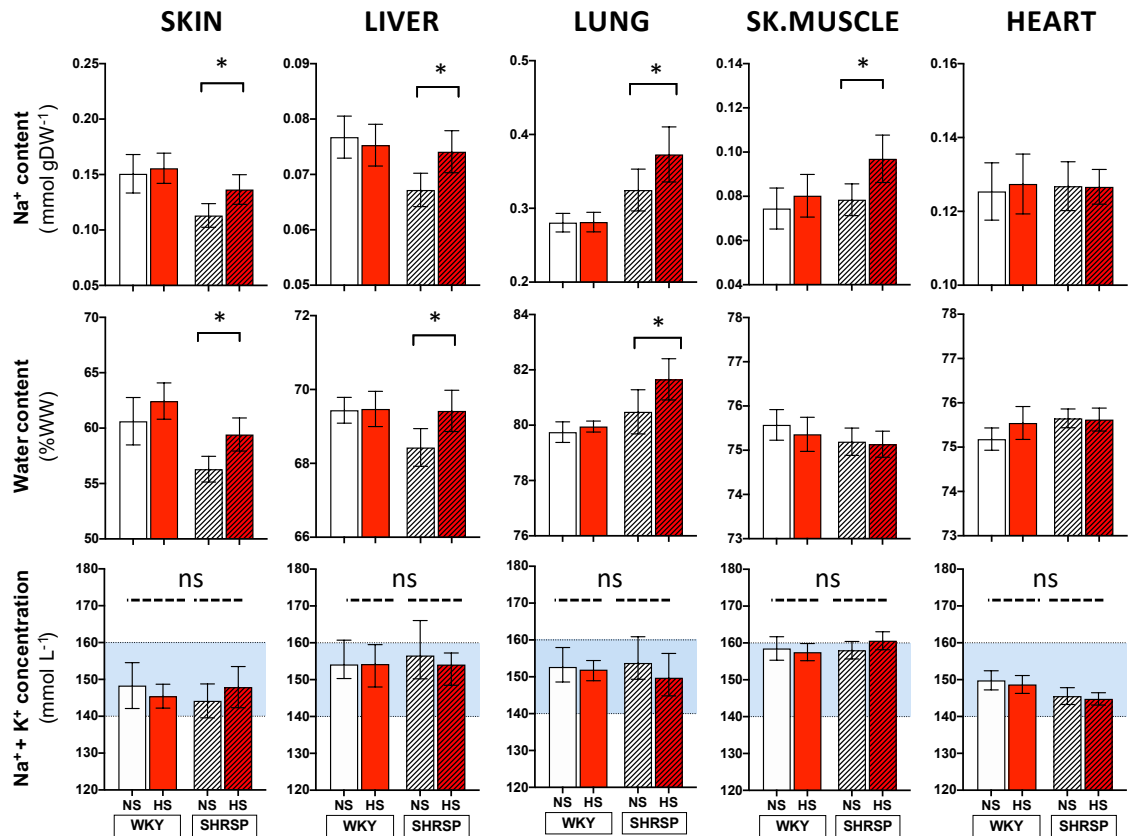


Figure 5-4. Nature and distribution of tissue Na⁺ excess upon salt loading.

Bars: empty = WKY, dashed = SHRSP, red = High Salt (HS) treatment; all bars show mean ± 95%CI; significant differences at predefined comparisons are shown by brackets, on top. Tissue Na⁺ content increased in all tissues in SHRSP-HS, but in myocardium; with the exception of skeletal muscle, it was consistently paralleled by water accrual. Total Na⁺ + K⁺ concentration in tissues fell in physiological ranges (light blue) and was unaffected by salt loading in either strain, ruling out hypertonic accumulations.

A sub-analysis for males and females showed very similar patterns (Tables 5-1 to 5-5; for all tables, data presented as mean ± SD; NS = normal salt, tap water; HS = high salt, 1% NaCl; *p<0.05, **p<0.01, ***p<0.001, ****p<0.0001).

Table 5-1. Rat SKIN histochemical analysis.

	Variables	WKY NS	WKY HS	Change %	Fisher LSD test	SHRSP NS	SHRSP HS	Change %	Fisher LSD test	2-way ANOVA		
										Interaction	HS	Strain
ALL	Water content (%WW)	60.62 ± 4.17	62.44 ± 3.29	3.00	ns 0.101	56.29 ± 2.18	59.43 ± 2.91	5.58	** 0.007	ns	**	****
	Water content (mg/mgDW)	1.565 ± 0.261	1.683 ± 0.253	7.54	ns 0.108	1.293 ± 0.116	1.476 ± 0.186	14.15	* 0.016	ns	**	****
	Na ⁺ content (mmol/gDW)	0.151 ± 0.033	0.156 ± 0.027	3.32	ns 0.588	0.113 ± 0.018	0.137 ± 0.026	20.69	* 0.021	ns	*	****
	Na ⁺ concentration (mmol/l)	95.6 ± 8.0	92.5 ± 7.2	-3.30	ns 0.262	86.7 ± 7.8	92.0 ± 9.3	6.11	0.08 0.082	*	ns	*
	K ⁺ content (mmol/gDW)	0.083 ± 0.023	0.088 ± 0.012	6.36	ns 0.346	0.075 ± 0.010	0.082 ± 0.016	10.11	ns 0.200	ns	ns	0.08
	K ⁺ concentration (mmol/l)	52.7 ± 8.7	53.0 ± 7.3	0.55	ns 0.922	57.5 ± 7.5	55.9 ± 9.8	-2.77	ns 0.612	ns	ns	0.08
	Na ⁺ + K ⁺ concentration (mmol/l)	152.9 ± 12.7	147.0 ± 7.8	-3.86	ns 0.380	146.8 ± 7.6	150.4 ± 7.8	2.45	ns 0.290	ns	ns	ns
Males	Water content (%WW)	59.42 ± 4.11	63.28 ± 3.97	6.50	* 0.033	55.88 ± 2.57	58.16 ± 2.27	4.08	ns 0.241	ns	*	**
	Water content (mg/mgDW)	1.458 ± 0.240	1.754 ± 0.329	20.30	* 0.029	1.270 ± 0.132	1.394 ± 0.123	9.76	ns 0.344	ns	*	**
	Na ⁺ content (mmol/gDW)	0.137 ± 0.027	0.161 ± 0.040	17.91	ns 0.096	0.101 ± 0.018	0.120 ± 0.018	18.43	ns 0.276	ns	ns	**
	Na ⁺ concentration (mmol/l)	91.9 ± 7.3	91.2 ± 6.4	5.26	ns 0.846	79.9 ± 6.5	85.4 ± 9.0	0.38	ns 0.221	ns	ns	**
	K ⁺ content (mmol/gDW)	0.077 ± 0.018	0.090 ± 0.012	17.56	ns 0.112	0.076 ± 0.012	0.083 ± 0.021	9.36	ns 0.443	ns	ns	ns
	K ⁺ concentration (mmol/l)	51.9 ± 9.5	52.4 ± 9.9	1.08	ns 0.919	60.00 ± 11.7	58.9 ± 12.6	-1.83	ns 0.863	ns	ns	0.09
	Na ⁺ + K ⁺ concentration (mmol/l)	143.8 ± 9.1	143.6 ± 4.3	-0.14	ns 0.971	139.9 ± 6.1	144.3 ± 14.1	3.15	ns 0.428	ns	ns	ns
Females	Water content (%WW)	61.70 ± 4.15	61.77 ± 2.65	0.11	ns 0.956	56.54 ± 2.01	60.31 ± 3.09	6.67	** 0.009	ns	ns	**
	Water content (mg/mgDW)	1.636 ± 0.272	1.626 ± 0.170	-0.61	ns 0.916	1.306 ± 0.111	1.534 ± 0.206	17.46	* 0.014	ns	ns	**
	Na ⁺ content (mmol/gDW)	0.165 ± 0.033	0.151 ± 0.011	3.32	ns 0.211	0.121 ± 0.013	0.149 ± 0.024	20.69	* 0.013	**	ns	**
	Na ⁺ concentration (mmol/l)	99.4 ± 7.1	93.5 ± 8.0	-5.89	ns 0.081	91.0 ± 5.2	96.7 ± 6.5	6.27	0.09 0.088	*	ns	ns
	K ⁺ content (mmol/gDW)	0.090 ± 0.027	0.087 ± 0.013	-2.87	ns 0.743	0.074 ± 0.009	0.082 ± 0.013	10.71	ns 0.313	ns	ns	0.07
	K ⁺ concentration (mmol/l)	53.5 ± 8.4	53.4 ± 4.9	-0.19	ns 0.973	55.9 ± 3.4	53.8 ± 7.4	-3.78	ns 0.488	ns	ns	ns
	Na ⁺ + K ⁺ concentration (mmol/l)	152.9 ± 12.7	147.0 ± 7.8	-3.86	ns 0.176	146.8 ± 7.6	150.4 ± 7.8	2.45	ns 0.409	ns	ns	ns

Table 5-2. Rat LIVER histochemical analysis.

	Variables	WKY NS	WKY HS	Change %	Fisher LSD test	SHRSP NS	SHRSP HS	Change %	Fisher LSD test	2-way ANOVA		
										Interaction	HS	Strain
ALL	Water content (%WW)	69.44 ± 0.68	69.47 ± 0.93	0.04	ns 0.911	68.43 ± 0.99	69.42 ± 1.09	1.45	** 0.003	*	*	*
	Water content (mg/mgDW)	2.274 ± 0.072	2.278 ± 0.100	0.18	ns 0.917	2.170 ± 0.097	2.275 ± 0.119	4.84	** 0.003	*	*	*
	Na ⁺ content (mmol/gDW)	0.077 ± 0.007	0.075 ± 0.007	-1.89	ns 0.553	0.067 ± 0.006	0.074 ± 0.008	10.28	** 0.006	*	ns	**
	Na ⁺ concentration (mmol/l)	33.7 ± 2.7	33.1 ± 2.8	-2.02	ns 0.437	31.0 ± 1.9	32.3 ± 2.6	4.10	ns 0.156	ns	ns	**
	K ⁺ content (mmol/gDW)	0.275 ± 0.015	0.272 ± 0.017	-0.87	ns 0.679	0.272 ± 0.018	0.275 ± 0.017	0.99	ns 0.631	ns	ns	ns
	K ⁺ concentration (mmol/l)	120.9 ± 7.3	118.8 ± 9.2	-1.74	ns 0.468	125.6 ± 8.1	120.8 ± 9.1	-3.82	ns 0.104	ns	0.10	ns
	Na ⁺ + K ⁺ concentration (mmol/l)	154.6 ± 6.8	152.7 ± 8.1	-1.23	ns 0.500	157.1 ± 9.6	153.0 ± 9.1	-2.61	ns 0.168	ns	ns	ns
Males	Water content (%WW)	68.94 ± 0.57	69.19 ± 1.06	0.36	ns 0.618	67.96 ± 1.00	69.39 ± 1.29	2.10	* 0.013	ns	*	ns
	Water content (mg/mgDW)	2.221 ± 0.058	2.249 ± 0.115	1.26	ns 0.609	2.123 ± 0.095	2.273 ± 0.144	7.07	* 0.014	ns	*	ns
	Na ⁺ content (mmol/gDW)	0.073 ± 0.006	0.072 ± 0.005	-1.55	ns 0.740	0.064 ± 0.004	0.076 ± 0.010	19.84	** 0.002	*	*	ns
	Na ⁺ concentration (mmol/l)	32.9 ± 2.8	32.1 ± 2.7	-2.64	ns 0.543	30.2 ± 2.1	32.8 ± 3.4	8.71	ns 0.104	0.10	ns	ns
	K ⁺ content (mmol/gDW)	0.272 ± 0.007	0.266 ± 0.007	-2.50	ns 0.346	0.267 ± 0.016	0.271 ± 0.015	1.76	ns 0.531	ns	ns	ns
	K ⁺ concentration (mmol/l)	122.7 ± 4.4	118.3 ± 8.6	-3.59	ns 0.251	125.6 ± 6.4	118.6 ± 10.0	-5.57	ns 0.095	ns	*	ns
	Na ⁺ + K ⁺ concentration (mmol/l)	155.7 ± 6.0	150.3 ± 9.4	-3.47	ns 0.240	157.2 ± 9.8	151.4 ± 9.9	-3.69	ns 0.231	ns	0.10	ns
Females	Water content (%WW)	69.88 ± 0.42	69.72 ± 0.77	-0.23	ns 0.683	68.76 ± 0.89	69.44 ± 0.99	0.99	0.07 0.067	ns	ns	*
	Water content (mg/mgDW)	2.321 ± 0.048	2.303 ± 0.084	-0.78	ns 0.661	2.303 ± 0.088	2.277 ± 0.108	-1.13	0.06 0.061	ns	ns	*
	Na ⁺ content (mmol/gDW)	0.080 ± 0.007	0.078 ± 0.008	-2.15	ns 0.578	0.069 ± 0.005	0.073 ± 0.005	4.45	ns 0.295	ns	ns	***
	Na ⁺ concentration (mmol/l)	34.5 ± 2.6	33.9 ± 2.7	-1.48	ns 0.632	31.5 ± 1.7	31.9 ± 1.9	1.24	ns 0.704	ns	ns	**
	K ⁺ content (mmol/gDW)	0.277 ± 0.020	0.278 ± 0.016	0.54	ns 0.860	0.276 ± 0.018	0.278 ± 0.019	0.65	ns 0.830	ns	ns	ns
	K ⁺ concentration (mmol/l)	119.3 ± 9.1	119.2 ± 9.1	-0.08	ns 0.994	125.6 ± 9.4	122.4 ± 8.7	-2.55	ns 0.447	ns	ns	ns
	Na ⁺ + K ⁺ concentration (mmol/l)	153.7 ± 7.6	154.5 ± 6.9	0.52	ns 0.828	157.0 ± 10.0	154.2 ± 8.8	-1.78	ns 0.460	ns	ns	ns

Table 5-3. Rat LUNG histochemical analysis.

	Variables	WKY NS	WKY HS	Change %	Fisher LSD test	SHRSP NS	SHRSP HS	Change %	Fisher LSD test	2-way ANOVA		
										Interaction	HS	Strain
ALL	Water content (%WW)	79.75 ± 0.72	79.95 ± 0.40	0.25	ns 0.599	80.48 ± 1.50	81.66 ± 1.50	1.47	** 0.004	0.08	*	****
	Water content (mg/mgDW)	3.944 ± 0.128	3.992 ± 0.098	-0.56	ns 0.674	4.156 ± 0.437	4.486 ± 0.462	7.94	** 0.005	0.08	*	****
	Na ⁺ content (mmol/gDW)	0.28 ± 0.024	0.281 ± 0.026	0.29	ns 0.962	0.325 ± 0.055	0.373 ± 0.072	14.84	** 0.006	*	*	****
	Na ⁺ concentration (mmol/l)	71.1 ± 4.7	70.5 ± 5.5	-0.83	ns 0.802	78.8 ± 8.1	82.1 ± 8.2	4.19	ns 0.163	ns	ns	***
	K ⁺ content (mmol/gDW)	0.32 ± 0.023	0.321 ± 0.018	0.34	ns 0.878	0.308 ± 0.022	0.304 ± 0.022	-1.20	ns 0.613	ns	ns	**
	K ⁺ concentration (mmol/l)	80.8 ± 5.3	80.6 ± 4.7	-0.19	ns 0.953	75.3 ± 8.7	69.0 ± 9.7	-8.34	* 0.017	0.10	ns	****
	Na ⁺ + K ⁺ concentration (mmol/l)	153.2 ± 9.8	151.1 ± 4.2	-1.37	ns 0.462	154.1 ± 9.9	151.1 ± 7.3	-1.95	ns 0.288	ns	ns	ns
Males	Water content (%WW)	79.43 ± 0.49	80.14 ± 0.26	0.89	ns 0.106	80.21 ± 0.90	81.25 ± 1.34	1.30	* 0.032	ns	**	**
	Water content (mg/mgDW)	3.864 ± 0.114	4.038 ± 0.066	4.50	ns 0.152	4.067 ± 0.236	4.356 ± 0.386	7.11	* 0.031	ns	*	**
	Na ⁺ content (mmol/gDW)	0.282 ± 0.017	0.292 ± 0.026	3.55	ns 0.660	0.323 ± 0.039	0.372 ± 0.073	15.09	* 0.046	ns	0.08	***
	Na ⁺ concentration (mmol/l)	73.0 ± 3.2	72.3 ± 5.7	-0.90	ns 0.832	81.6 ± 5.0	83.7 ± 8.5	2.67	ns 0.509	ns	ns	***
	K ⁺ content (mmol/gDW)	0.332 ± 0.025	0.321 ± 0.021	-3.37	ns 0.379	0.308 ± 0.026	0.312 ± 0.024	1.43	ns 0.726	ns	ns	0.06
	K ⁺ concentration (mmol/l)	83.7 ± 2.9	79.6 ± 5.8	-4.86	ns 0.284	77.0 ± 6.0	72.3 ± 10.2	-6.14	ns 0.219	ns	ns	*
	Na ⁺ + K ⁺ concentration (mmol/l)	159.1 ± 7.9	151.9 ± 2.4	-4.53	* 0.036	158.6 ± 5.4	156.0 ± 7.1	-1.64	ns 0.453	ns	0.05	ns
Females	Water content (%WW)	80.04 ± 0.80	79.80 ± 0.44	-0.30	ns 0.698	80.65 ± 1.79	81.98 ± 1.61	1.65	* 0.028	0.06	**	**
	Water content (mg/mgDW)	4.016 ± 0.208	3.955 ± 0.107	-1.52	ns 0.737	4.210 ± 0.528	4.590 ± 0.509	9.03	* 0.036	0.08	ns	**
	Na ⁺ content (mmol/gDW)	0.279 ± 0.031	0.274 ± 0.023	-1.90	ns 0.832	0.326 ± 0.066	0.374 ± 0.076	14.65	0.06 0.058	ns	ns	***
	Na ⁺ concentration (mmol/l)	69.4 ± 5.3	69.3 ± 5.2	-0.26	ns 0.957	77.1 ± 9.4	80.1 ± 8.1	4.73	ns 0.270	ns	ns	***
	K ⁺ content (mmol/gDW)	0.309 ± 0.014	0.321 ± 0.016	3.91	ns 0.153	0.308 ± 0.021	0.298 ± 0.020	-3.28	ns 0.217	0.06	ns	*
	K ⁺ concentration (mmol/l)	78.5 ± 5.8	81.3 ± 5.8	3.59	ns 0.429	74.2 ± 10.2	66.3 ± 8.9	-10.59	* 0.028	*	ns	***
	Na ⁺ + K ⁺ concentration (mmol/l)	147.9 ± 8.5	150.6 ± 5.1	1.83	ns 0.469	151.3 ± 11.2	147.1 ± 4.7	-2.78	ns 0.237	ns	ns	ns

Table 5-4. Rat SKELETAL MUSCLE histochemical analysis.

Variables	WKY NS	WKY HS	Change %	Fisher LSD test		SHRSP NS	SHRSP HS	Change %	Fisher LSD test		2-way ANOVA			
											Interaction	HS	Strain	
ALL	Water content (%WW)	75.57 ± 0.62	75.36 ± 0.77	-0.28	ns	0.349	75.19 ± 0.58	75.14 ± 0.57	-0.07	ns	0.801	ns	ns	0.06
	Water content (mg/mgDW)	3.096 ± 0.101	3.062 ± 0.124	-1.10	ns	0.355	3.033 ± 0.093	3.024 ± 0.010	-0.30	ns	0.802	ns	ns	0.06
	Na ⁺ content (mmol/gDW)	0.073 ± 0.017	0.079 ± 0.018	8.22	ns	0.365	0.078 ± 0.014	0.097 ± 0.021	23.59	**	0.004	ns	**	*
	Na ⁺ concentration (mmol/l)	24.0 ± 6.1	26.4 ± 6.5	9.92	ns	0.306	27.2 ± 5.5	32.5 ± 7.5	19.51	*	0.017	ns	*	**
	K ⁺ content (mmol/gDW)	0.411 ± 0.044	0.402 ± 0.037	-2.24	0.09	0.094	0.397 ± 0.029	0.383 ± 0.035	-3.35	ns	0.171	ns	*	***
	K ⁺ concentration (mmol/l)	134.0 ± 9.7	131.5 ± 9.2	-1.87	ns	0.421	130.8 ± 8.6	128.1 ± 8.4	-2.06	ns	0.366	ns	ns	ns
	Na ⁺ + K ⁺ concentration (mmol/l)	158.5 ± 6.0	157.5 ± 4.7	-0.63	ns	0.574	158 ± 4.8	160.6 ± 4.9	1.65	ns	0.132	ns	ns	ns
Males	Water content (%WW)	75.59 ± 0.48	75.70 ± 0.57	0.15	ns	0.684	75.31 ± 0.48	75.09 ± 0.48	-0.29	ns	0.402	ns	ns	*
	Water content (mg/mgDW)	3.099 ± 0.081	3.117 ± 0.010	0.58	ns	0.668	3.052 ± 0.077	3.016 ± 0.078	-1.18	ns	0.410	ns	ns	*
	Na ⁺ content (mmol/gDW)	0.065 ± 0.013	0.069 ± 0.007	6.23	ns	0.409	0.064 ± 0.004	0.075 ± 0.010	17.95	*	0.025	ns	*	ns
	Na ⁺ concentration (mmol/l)	20.9 ± 4.5	22.2 ± 2.1	5.98	ns	0.550	23.3 ± 5.3	25.0 ± 2.9	7.03	ns	0.414	ns	ns	0.07
	K ⁺ content (mmol/gDW)	0.433 ± 0.014	0.430 ± 0.020	-0.60	ns	0.819	0.405 ± 0.032	0.409 ± 0.017	0.96	ns	0.720	ns	ns	**
	K ⁺ concentration (mmol/l)	139.8 ± 4.4	138.8 ± 4.2	-0.72	ns	0.728	135.2 ± 7.0	135.5 ± 5.8	0.22	ns	0.918	ns	ns	0.06
	Na ⁺ + K ⁺ concentration (mmol/l)	160.7 ± 4.7	159.7 ± 4.1	-0.62	ns	0.671	158.5 ± 3.0	160.5 ± 5.0	1.26	ns	0.372	ns	ns	ns
Females	Water content (%WW)	75.55 ± 0.80	75.09 ± 0.84	-0.61	ns	0.219	75.10 ± 0.66	75.18 ± 0.67	0.11	ns	0.830	ns	ns	ns
	Water content (mg/mgDW)	3.094 ± 0.128	3.018 ± 0.131	-2.46	ns	0.213	3.019 ± 0.106	3.031 ± 0.114	0.40	ns	0.826	ns	ns	ns
	Na ⁺ content (mmol/gDW)	0.084 ± 0.016	0.088 ± 0.020	4.81	ns	0.542	0.089 ± 0.007	0.114 ± 0.008	28.85	***	0.000	*	**	**
	Na ⁺ concentration (mmol/l)	27.6 ± 6.1	29.3 ± 7.0	6.50	ns	0.479	30.3 ± 3.4	38.6 ± 3.0	27.17	***	0.001	0.06	**	**
	K ⁺ content (mmol/gDW)	0.389 ± 0.054	0.382 ± 0.032	-1.83	ns	0.689	0.390 ± 0.026	0.363 ± 0.033	-6.78	ns	0.129	ns	ns	ns
	K ⁺ concentration (mmol/l)	128.3 ± 10.3	126.4 ± 8.4	-1.48	ns	0.624	127.3 ± 8.3	122.2 ± 4.3	-4.01	ns	0.160	ns	ns	ns
	Na ⁺ + K ⁺ concentration (mmol/l)	156.3 ± 6.7	155.7 ± 4.5	-0.38	ns	0.817	157.6 ± 5.9	160.7 ± 5.1	1.97	ns	0.218	ns	ns	0.09

Table 5-5. Rat LEFT VENTRICULAR MYOCARDIUM histochemical analysis.

Variables	WKY NS	WKY HS	Change %	Fisher LSD test	SHRSP NS	SHRSP HS	Change %	Fisher LSD test	2-way ANOVA				
									Interaction	HS	Strain		
ALL													
Water content (%WW)	75.18 ± 0.49	75.55 ± 0.746	0.49	ns 0.057	75.65 ± 0.41	75.62 ± 0.50	-0.04	ns 0.888	ns	ns	*		
Water content (mg/mgDW)	3.030 ± 0.078	3.093 ± 0.125	2.08	ns 0.051	3.108 ± 0.071	3.104 ± 0.086	-0.13	ns 0.884	ns	ns	0.05		
Na ⁺ content (mmol/gDW)	0.125 ± 0.015	0.127 ± 0.016	1.59	ns 0.662	0.127 ± 0.013	0.127 ± 0.009	-0.16	ns 0.971	ns	ns	ns		
Na ⁺ concentration (mmol/l)	41.3 ± 4.4	41.1 ± 4.1	-0.56	ns 0.859	40.8 ± 3.7	40.8 ± 2.8	0.05	ns 0.988	ns	ns	ns		
K ⁺ content (mmol/gDW)	0.326 ± 0.016	0.332 ± 0.016	1.99	ns 0.173	0.326 ± 0.012	0.322 ± 0.010	-1.07	ns 0.462	ns	ns	ns		
K ⁺ concentration (mmol/l)	108.5 ± 6.5	107.6 ± 6.2	-0.83	ns 0.626	104.8 ± 4.7	104.0 ± 3.4	-0.76	ns 0.650	ns	ns	**		
Na ⁺ + K ⁺ concentration (mmol/l)	149.8 ± 5.1	148.7 ± 4.9	-0.73	ns 0.458	145.5 ± 4.3	144.8 ± 3.3	-0.48	ns 0.625	ns	ns	**		
Males													
Water content (%WW)	75.3 ± 0.39	75.61 ± 0.81	0.41	ns 0.287	75.75 ± 0.30	75.73 ± 0.57	-0.03	ns 0.959	ns	ns	ns		
Water content (mg/mgDW)	3.050 ± 0.062	3.104 ± 0.134	1.77	ns 0.262	3.126 ± 0.053	3.123 ± 0.098	-0.10	ns 0.955	ns	ns	ns		
Na ⁺ content (mmol/gDW)	0.120 ± 0.012	0.129 ± 0.020	7.24	ns 0.199	0.123 ± 0.008	0.123 ± 0.007	0.33	ns 0.960	ns	ns	ns		
Na ⁺ concentration (mmol/l)	39.4 ± 3.6	41.4 ± 5.5	5.26	ns 0.276	39.3 ± 2.2	39.4 ± 2.1	0.38	ns 0.942	ns	ns	ns		
K ⁺ content (mmol/gDW)	0.333 ± 0.011	0.331 ± 0.015	-0.21	ns 0.909	0.328 ± 0.009	0.326 ± 0.007	-0.37	ns 0.839	ns	ns	ns		
K ⁺ concentration (mmol/l)	109.1 ± 5.6	107.2 ± 8.2	-1.74	ns 0.491	104.9 ± 3.8	104.5 ± 1.6	-0.38	ns 0.900	ns	ns	0.09		
Na ⁺ + K ⁺ concentration (mmol/l)	148.5 ± 5.8	148.6 ± 5.5	0.07	ns 0.949	144.1 ± 2.7	143.9 ± 2.7	-0.14	ns 0.928	ns	ns	*		
Females													
Water content (%WW)	75.07 ± 0.56	75.50 ± 0.73	0.57	ns 0.114	75.58 ± 0.48	75.54 ± 0.47	-0.05	ns 0.891	ns	ns	ns		
Water content (mg/mgDW)	3.01 ± 0.09	3.084 ± 0.124	2.39	ns 0.112	3.096 ± 0.082	3.090 ± 0.079	-0.19	ns 0.889	ns	ns	ns		
Na ⁺ content (mmol/gDW)	0.130 ± 0.017	0.126 ± 0.013	-2.92	ns 0.555	0.130 ± 0.015	0.129 ± 0.010	-0.39	ns 0.931	ns	ns	ns		
Na ⁺ concentration (mmol/l)	43.1 ± 4.4	40.8 ± 2.7	-5.20	ns 0.190	41.9 ± 4.3	41.8 ± 2.9	-0.17	ns 0.967	ns	ns	ns		
K ⁺ content (mmol/gDW)	0.320 ± 0.019	0.333 ± 0.017	3.97	ns 0.084	0.325 ± 0.014	0.320 ± 0.010	-1.54	ns 0.479	ns	ns	ns		
K ⁺ concentration (mmol/l)	107.9 ± 7.5	107.9 ± 4.5	0.00	ns 0.997	104.8 ± 5.5	103.6 ± 4.3	-1.15	ns 0.645	ns	ns	*		
Na ⁺ + K ⁺ concentration (mmol/l)	151.0 ± 4.3	148.8 ± 4.6	-1.46	ns 0.275	146.6 ± 5.1	145.4 ± 3.6	-0.82	ns 0.544	ns	ns	*		

Lower water and Na⁺ between control (NS) strains in skin and liver reflect differences in fat content (Figure 5-5) that limit the volume of distribution (and total content, accordingly) of both.

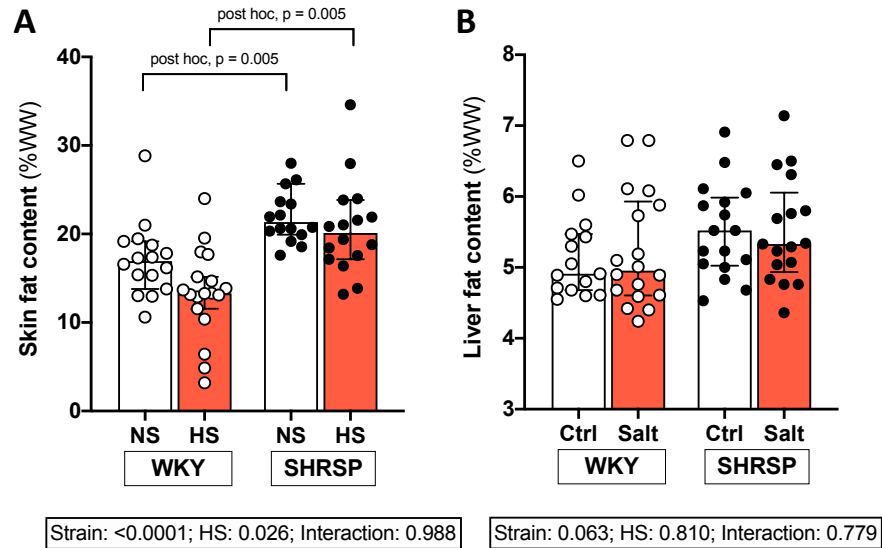


Figure 5-5. Fat content in skin and liver.

Panel A: skin fat content. Significant strain differences in skin fat content (approximately 3-5% of WW), regardless of treatment, are in keeping with the difference in water (and Na⁺ content) observed between NS WKY and SHRSP (Figure 5-3). Panel B: trends are similar for liver, although not significant; due to smaller content and relative difference (as for water content, Figure 5-3) in liver compared to skin, this likely suggests a type II statistical error, rather than a lack of strain difference. Bars: medians \pm 95%CI.

Most importantly, K⁺ concentration ([K⁺]) showed opposite trends to [Na⁺] (Tables 5-1 to 5-5). In physiological conditions, the sum of [K⁺] and [Na⁺] in both ECV and ICV is similar, although with opposite predominance of Na⁺ and K⁺, respectively (Figure 4-1); a mixture of ECV and ICV in any proportion would still result in a solution of approximately 140-160 Na⁺+K⁺ mmol/L. In all tissues, [Na⁺+K⁺] consistently fell within this range, with no differences between strains or NS/HS allocation (Figure 5-4); overall, along with the concomitant increase observed for tissue water, this points to tissue oedema.

In fact, water paralleled Na⁺ content with identical regression slopes across all groups (Figure 5-6), except for skeletal muscle where the water-independent “K⁺-to-Na⁺” (i.e. ICV-to-ECV) predominance shift is likely due to some degree of HS-induced sarcopenia, as suggested by studies extensively discussed in chapter 1 and 3 (Kitada et al., 2017).

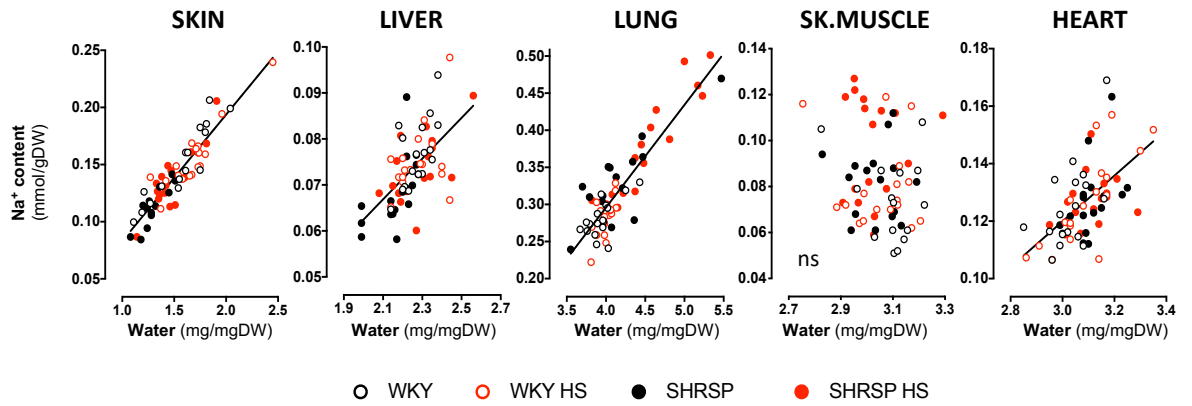


Figure 5-6. Regression lines for tissue Na⁺ and water content in different tissues.

No difference in slope or intercept was detected across experimental groups in either organ, so that one curve adequately fitted all points. For skeletal muscle, no regression line was drawn, as no significant correlation was found within either group beforehand: the dissociation between Na excess and water in skeletal muscle likely reflects an oedema-independent shift in ECV/ICV ratio due to salt-induced catabolic muscle loss (Kitada et al., 2017).

Notably, the results obtained for tissue Na⁺ across organs under experimental conditions fit extremely well with the theoretical prediction model discussed in the previous section.

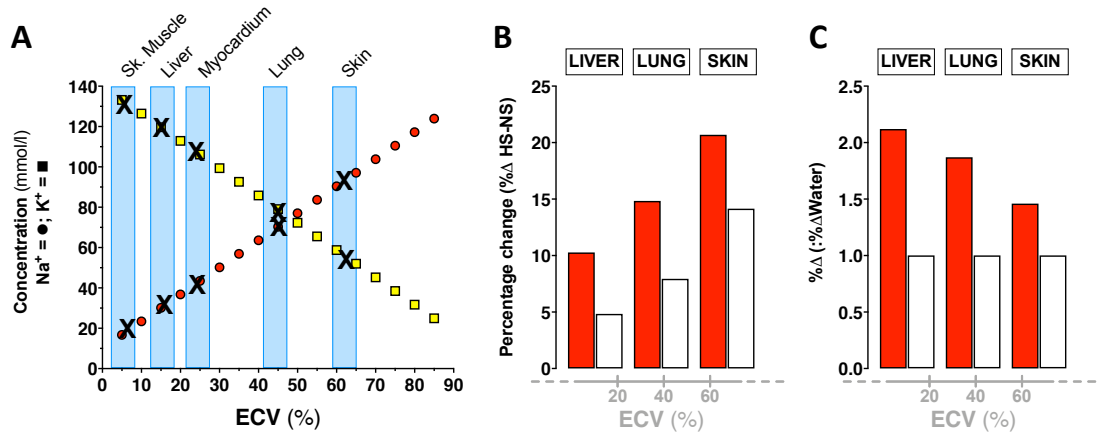


Figure 5-7. Predicted and experimental results.

Panel A: X = experimental results from control NS WKY rats in different tissues (means from Tables 5-1 to 5-5), superimposed on the general prediction model based on ECV% (Chapter 4); red circles = predicted tissue [Na⁺], yellow squares = predicted tissue [K⁺]. [Na⁺] and [K⁺] results effectively differentiate organs physiologically sitting at different points of the ECV% axis. Panel B: percentage change of Na⁺ content (red bars) and water content (white bars) in tissues showing oedema accumulation upon HS in SHRSP rats (from Tables 5-1 to 5-5); panel C: same percentage change, normalised for water change, showing a proportionally larger increase in Na⁺ compared to water content when tissue cellularity is increasingly high, as predicted.

The reported water-independent tissue Na⁺ accumulation, although not confirmed in this study as such, was previously suggested to induce VEGF-c mediated signaling via TonEBP/NFAT5 (Machnik et al., 2009, Wiig et al., 2013). TonEBP/NFAT5 is traditionally associated with the response to osmotic stress (Miyakawa et al., 1999, Choi et al., 2020), but recently reported to respond also to biomechanical stimuli in vascular smooth muscle cells (Scherer et al., 2014). Despite no evidence of hypertonicity, an increase in TonEBP/NFAT5 expression in skin, lungs and (borderline significant) liver was indeed observed in *SHRSP*-HS (Figure 5-8).

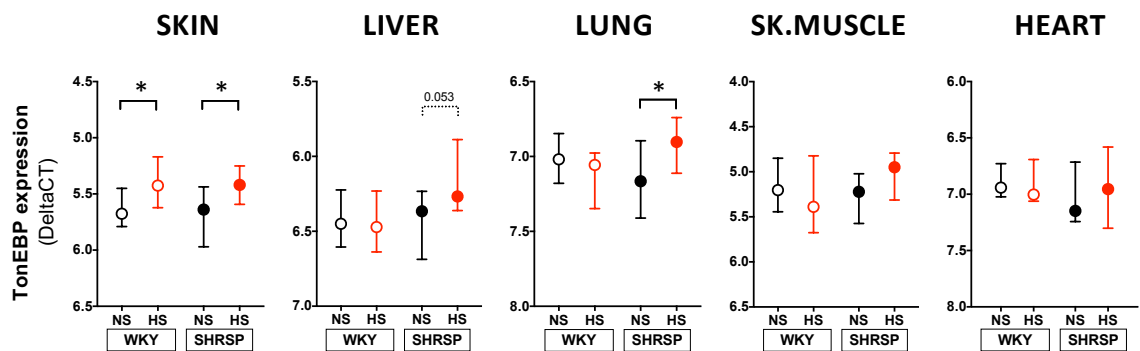


Figure 5-8. Tissue-specific TonEBP expression upon salt loading.

Increased TonEBP gene expression followed Na⁺ and water accumulation despite no hypertonicity. Data are presented as Delta Ct, median ± 95%CI for all rats; n = 16-18 animals/group

5.3.3 Ageing model

The hypertensive and target-organ damage phenotype in SHRSP is not only salt- but also age-sensitive. This is the case also for many human cardiovascular diseases and for salt-sensitivity itself, which becomes more prevalent or exacerbates with ageing.

Therefore, in a second set of experiments with normal-salt-fed rats, ageing rather than salt-loading was used as a “second-hit” and left ventricular myocardium was analysed for chemical and structural changes.

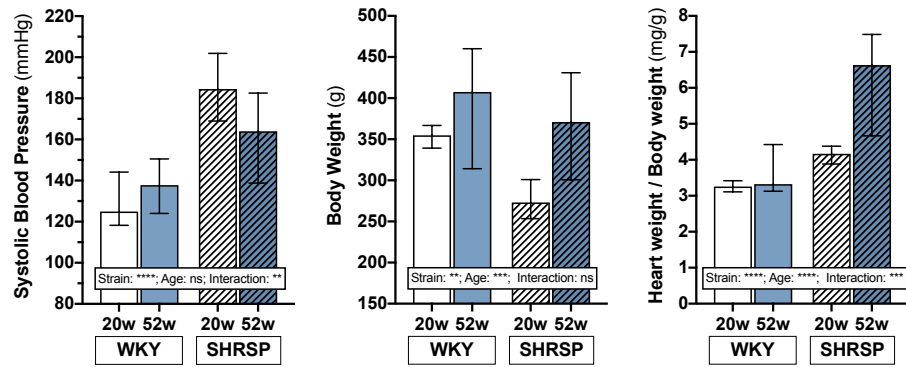


Figure 5-9. Rat phenotypes in the ageing experiment.

Differences in systolic blood pressure, body weight and myocardial remodelling (Heart weight/body weight) in the 4 groups of animals. These data, collected by Dr Adam Harvey at the time of rat culling and before the start of my PhD, were available in $n \geq 3$ /group from the experimental animals used for the herein presented myocardium chemical analysis. For all panels, 2-way ANOVA results are reported at bottom.

5.3.3.1 Chemical Analysis and TonEBP

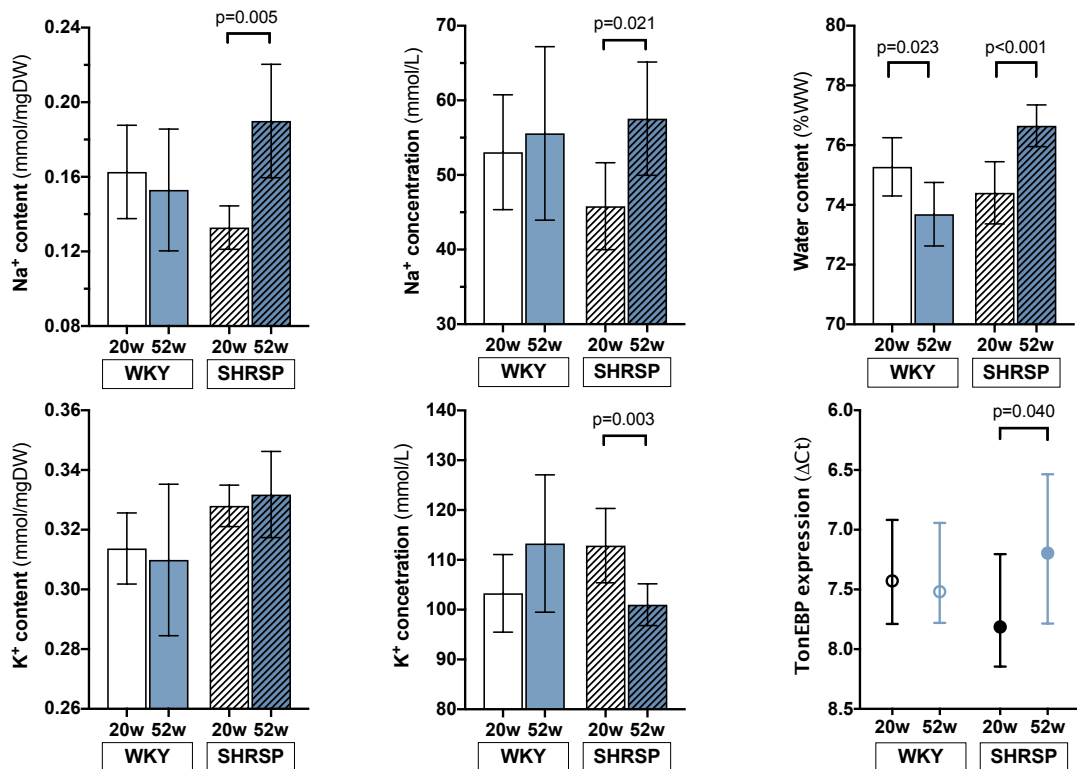


Figure 5-10. Myocardial Na⁺ excess and TonEBP expression in hypertensive ageing.

Myocardial Na⁺ content (and concentration) increased in 52 weeks vs 20 weeks old SHRSP, paralleled by water and mirrored by K⁺, so that tissue [Na⁺ + K⁺] was constant across groups (not shown); this is suggestive of myocardial oedema. Increased TonEBP gene expression followed oedema accumulation. Bars show mean \pm 95%CI, or median \pm 95%CI for TonEBP gene expression; $n=6-10$ /group.

At variance with young salt-loaded SHRSP rats, the myocardium of 52-week-old animals showed an increase in water, as well as Na⁺ content and [Na⁺], with commensurate mirror-like decrease in [K⁺] which resulted in a similar [Na⁺+K⁺] across groups. Again, TonEBP/NFAT5 myocardial gene expression was increased despite lack of hypertonicity.

5.3.3.2 Sulphated Glycosaminoglycans (sGAG) Quantification

In keeping with the observed remodelling, myocardial sGAG increased with ageing in both strains, but was higher in SHRSP animals compared to WKY. A qualitative comparison of Alcian Blue-stained and Picrosirius-stained sections suggested comparable distribution of sGAG and collagen deposition.

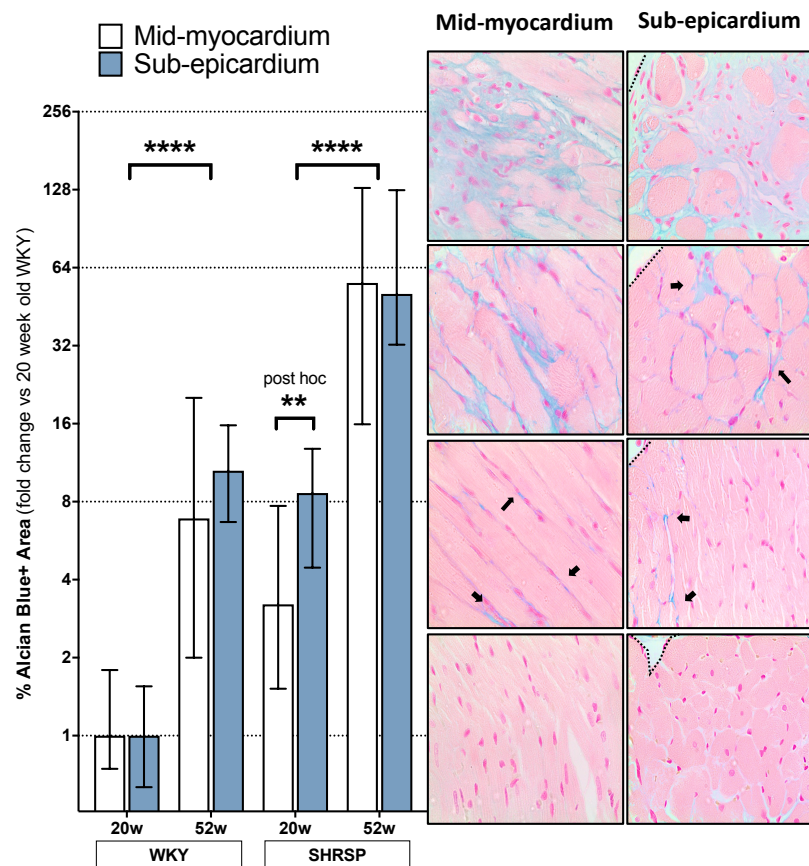


Figure 5-11. Myocardial glycosaminoglycans in hypertensive ageing.

Sulphated glycosaminoglycans (sGAG) content in mid-myocardium and sub-epicardium, estimated by Alcian Blue staining and normalised by WKY young rats; right inserts: representative Alcian Blue⁺ areas in mid-myocardium and sub-epicardium corresponding to dotted lines (i.e. 1x, 8x, 64x and 256x young WKY rats, as reference; black arrows: Alcian Blue staining; dotted lines inside inserts: epicardial border). Left ventricular sGAGs increased with ageing but was higher in SHRSP compared to WKY; whether this extracellular matrix remodelling facilitates myocardial oedema, is a consequence of it or both, in a putative vicious circle, remains unknown. Bars show median \pm 95%CI.

5.3.4 Impact of salt on arterial function

Contrarily to the expectations regarding the impact of Na⁺ excess on peripheral resistance, HS treatment in-vivo did not result in hypercontractile responses. The magnitude of response to KCl was rather reduced upon repeated stimuli (Figure 5-12).

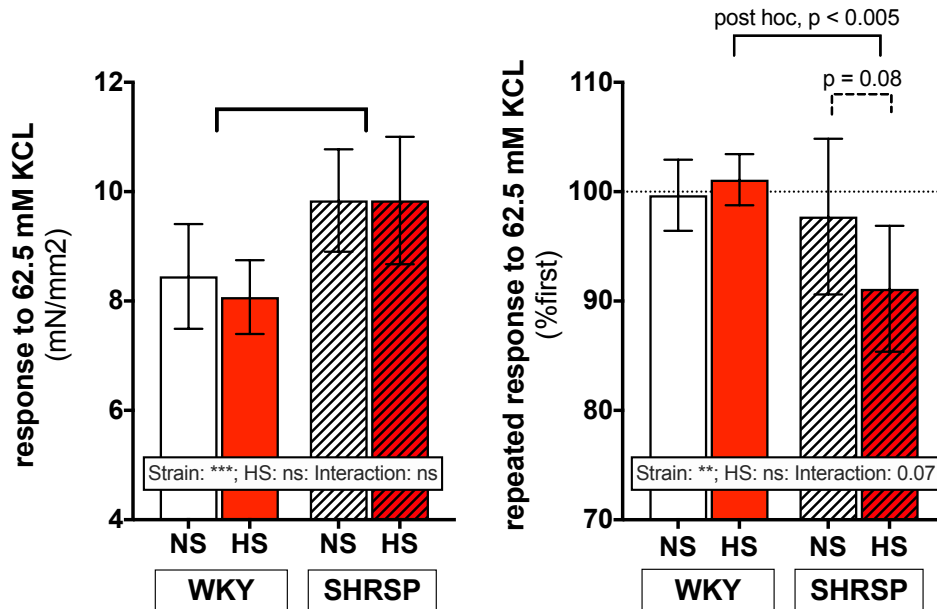


Figure 5-12. Impact of in vivo Na⁺ excess on agonist-independent contractile function.

Contractile response to KCl, by strain and experimental treatment; WKY-NS: n = 15 and HS n = 18, SHRSP-NS: n = 14 and HS n = 17; two-way ANOVA results at bottom and predefined or post hoc (inter-strain) comparisons on top. Left: the response to the first KCl stimulation was higher in SHRSP than WKY but was unaffected by in vivo HS treatment. Right: the response to a second stimulation, expressed as percentage of first peak response, was reduced in SHRSP, particularly upon HS.

Contractile responses to U46619 (a thromboxane-receptor agonist), showing higher peaks and over-sensitivity to the agonist (i.e. lower effective concentration to produce 50% of the maximal response; EC₅₀) in SHRSP compared to WKY, were unaffected by treatment of rats with salt. At variance, salt treatment reduced the vasorelaxant effect of nitric oxide (NO), directly released by the NO-donor nitroprusside (SNP), in SHRSP (Figure 5-13, top and Table 5-6). No significant differences were observed for endothelium-dependent responses (not shown).

To test whether an HT environment could induce vascular changes consistent with those observed in HS-treated rats and/or likely to sustain high blood pressure, arterioles from NS rats were also preincubated in an isotonic or hypertonic (HT; +15 mmol/L NaCl) solution. Akin to HS in vivo, HT ex vivo incubation did not affect contractile

responses; however, it induced an opposite shift toward an earlier NO-induced loss of pre-constriction tone in both WKY and SHRSP (Figure 5-13, bottom and Table 5-6). Similar effects were observed for endothelium-dependent (Ach-induced) relaxation, although with overall higher statistical p values and heterogeneity in significance (but not trends) between sexes (Table 5-6).

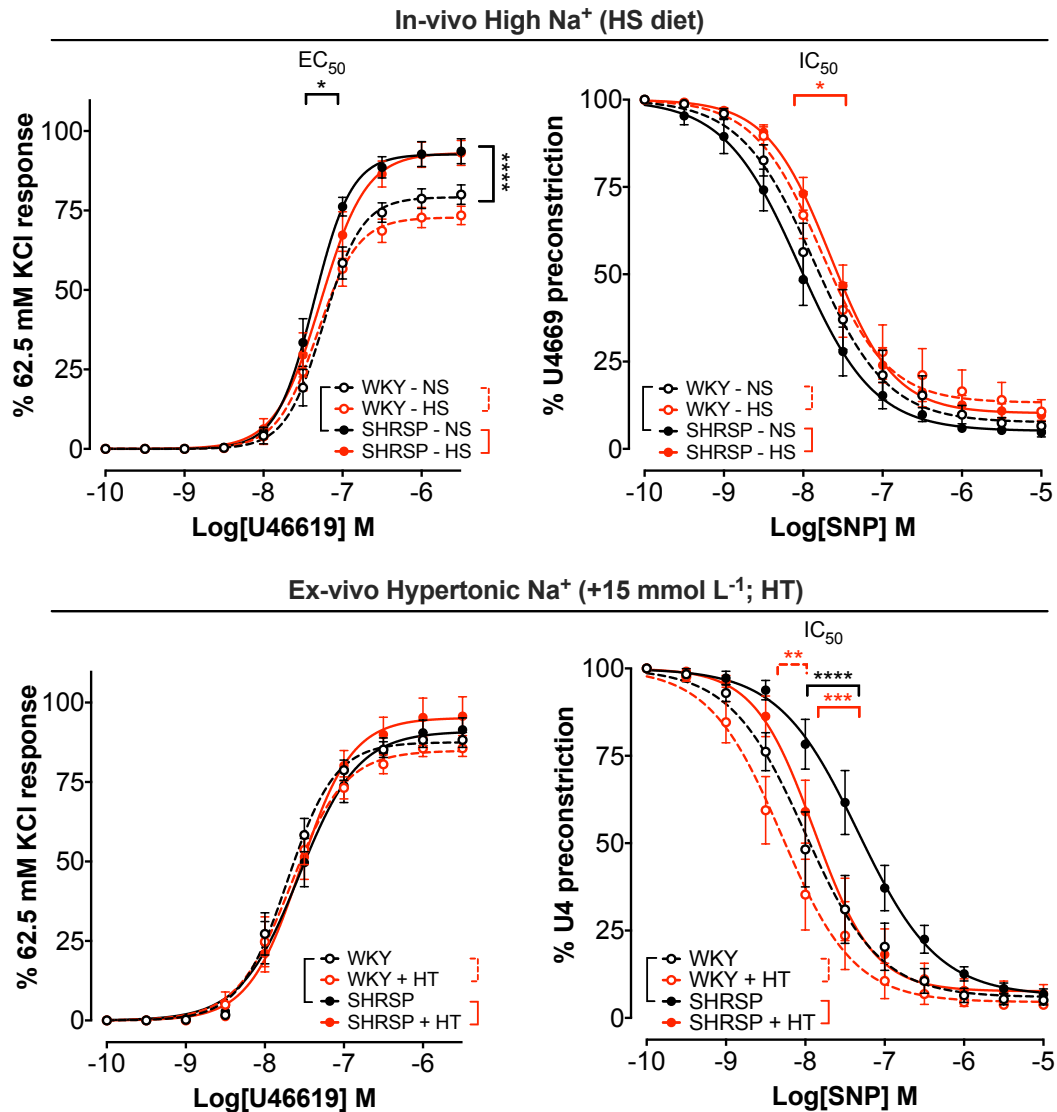


Figure 5-13. Impact of in-vivo and ex-vivo Na⁺ excess on arterial function.

Contraction and relaxation dose–response curves to U46619 (thromboxane A₂ receptor agonist; n = 11–17/group) and SNP (endothelium-independent nitric oxide donor; n = 9–16/group), respectively; mean ± SEM. Differences in maximal responses and half maximal effective/inhibitory concentrations (EC₅₀ and IC₅₀, respectively) across groups are shown by brackets; *p < 0.05, **p < 0.01, ***p < 0.001, ****p < 0.0001. Top, effect of 1% NaCl in drinking water (HS): HS did not worsen the hypercontractile phenotype observed in SHRSP rats but reduced their sensitivity to NO-mediated relaxation; no significant effect was observed in WKY rats. Bottom, effect of ex vivo 5 h incubation in a hypertonic (+15 mmol/l NaCl, HT) vs. physiological solution on vessels from NS rats: ex vivo hypertonic Na⁺ excess did not affect contractile responses, but induced oversensitivity to NO in both strains, opposite to in vivo HS; none of these ex vivo effects would justify an increase in peripheral vascular resistance. Please see Table 5-6 for all comparisons.

Table 5-6. Impact of in-vivo and ex-vivo Na⁺ excess on arterial function.

		in-vivo protocol							
		1% NaCl (HS)							
		n	WKY - NS	n	SHRSP - NS	n	WKY - HS	n	SHRSP - HS
ALL	U4 max		79.20 (75.31 to 83.35)		92.68**** (88.63 to 96.91)		72.81 (68.74 to 77.19)		93.15 (87.81 to 99.02)
	LogEC ₅₀	16	-7.238 (-7.312 to -7.163)	16	-7.361* (-7.428 to -7.292)	16	-7.317 (-7.405 to -7.226)	17	-7.274 (-7.367 to -7.178)
	Ach max rel		1.964 (-0.585 to 4.463)		4.842 (1.077 to 8.471)		4.101 (0.8967 to 7.222)		5.213 (2.342 to 8.013)
	LogIC ₅₀	16	-7.712 (-7.769 to -7.654)	14	-7.892** (-7.991 to -7.791)	17	-7.718 (-7.795 to -7.642)	17	-7.855 (-7.926 to -7.783)
	SNP max rel		7.57 (2.68 to 12.11)		5.12 (1.19 to 8.85)		13.24 (7.73 to 18.25)		10.21 [#] (6.99 to 13.29)
	LogIC ₅₀	13	-7.868 (-8.003 to -7.725)	12	-8.052* (-8.164 to -7.937)	16	-7.776 (-7.926 to -7.614)	16	-7.656#### (-7.742 to -7.568)
MALES	U4 max rel		72.23 (67.18 to 77.66)		84.93*** (80.53 to 89.55)		67.09 (62.53 to 71.92)		89.95 (80.66 to 101.30)
	LogEC ₅₀	8	-7.295 (-7.399 to -7.186)	6	-7.641**** (-7.722 to -7.562)	8	-7.258 (-7.359 to -7.159)	7	-7.283### (-7.463 to -7.082)
	Ach max rel		1.32 (-0.7834 to 3.401)		5.877 (-0.955 to 12.2)		6.207 (0.738 to 11.36)		3.469 (-0.518 to 7.347)
	LogIC ₅₀	8	-7.871 (-7.917 to -7.826)	6	-7.837 (-8.02 to -7.648)	8	-7.72* (-7.855 to -7.579)	7	-7.956 (-8.05 to -7.858)
	SNP max rel		6.88 (-0.47 to 13.37)		5.86 (-1.39 to 12.40)		18.24 (7.20 to 26.91)		8.52 (4.23 to 12.60)
	LogIC ₅₀	8	-7.861 (-8.057 to -7.646)	5	-7.894 (-8.09 to -7.686)	7	-7.709 (-7.989 to -7.366)	6	-7.550### (-7.655 to -7.443)
FEMALES	U4 max rel		86.21 (80.65 to 92.37)		96.38** (92.45 to 100.40)		77.16* (71.08 to 84.05)		95.20 (88.88 to 102.20)
	LogEC ₅₀	8	-7.190 (-7.287 to -7.090)	10	-7.212 (-7.270 to -7.156)	8	-7.370* (-7.501 to -7.228)	10	-7.269 (-7.371 to -7.163)
	Ach max rel		2.136 (-1.972 to 6.096)		4.076 (-0.3806 to 8.363)		2.124 (-1.682 to 5.843)		6.729 (2.767 to 10.54)
	LogIC ₅₀	8	-7.524 (-7.614 to -7.432)	8	-7.932*** (-8.043 to -7.816)	9	-7.71** (-7.796 to -7.625)	10	-7.788 (-7.885 to -7.69)
	SNP max rel		8.53 (2.07 to 14.47)		4.47 (3.23 to 8.68)		9.29 (3.08 to 14.95)		11.36 [#] (6.86 to 15.56)
	LogIC ₅₀	5	-7.875 (-8.051 to -7.690)	7	-8.162** (-8.290 to -8.031)	9	-7.821 (-7.982 to -7.647)	10	-7.729#### (-7.853 to -7.602)

ex-vivo incubation (5h)

		Physiological Salt Solution (PSS)		PSS + 15 NaCl mM					
		n	WKY - NS	n	SHRSP - NS	n	WKY - HS	n	SHRSP - HS
ALL	U4 max	13	82.9 (79.08 to 86.97)	11	75.06 (68.37 to 83.12)	13	77.86 (74.44 to 81.55)	12	80.64 (75.33 to 86.58)
	LogEC ₅₀		-7.727 (-7.815 to -7.636)		-7.615 (-7.792 to -7.418)		-7.701 (-7.786 to -7.611)		-7.568 (-7.691 to -7.439)
	Ach max rel	13	1.376 (-2.653 to 5.238)	12	14.93**** (9.604 to 19.94)	13	1.281 (-2.897 to 5.291)	12	7.63## (2.92 to 12.10)
	LogIC ₅₀		-7.776 (-7.877 to -7.674)		-7.529** (-7.664 to -7.390)		-7.843 (-7.946 to -7.738)		-7.621 (-7.689 to -7.554)
	SNP max rel	11	5.95 (0.67 to 10.84)	9	6.33 (0.92 to 11.19)	11	4.55 (-0.60 to 9.39)	9	7.63 (2.92 to 12.10)
	LogIC ₅₀		-8.004 (-8.152 to -7.848)		-7.334**** (-7.467 to -7.194)		-8.299** (-8.449 to -8.142)		-7.891#### (-8.014 to -7.762)
MALES	U4 max	8	83.84 (79.33 to 88.69)	6	76.69 (69.43 to 85.10)	8	78.04 (74.23 to 82.15)	6	79.26 (73.24 to 86.04)
	LogEC ₅₀		-7.741 (-7.845 to -7.633)		-7.740 (-7.925 to -7.538)		-7.859 (-7.959 to -7.755)		-7.642 (-7.787 to -7.489)
	Ach max rel	8	1.336 (-2.3 to 4.872)	6	10.74* (3.047 to 17.77)	8	1.933 (-2.738 to 6.432)	6	2.322# (-1.264 to 5.851)
	LogIC ₅₀		-7.701 (-7.785 to -7.617)		-7.665 (-7.843 to -7.472)		-7.883* (-7.997 to -7.767)		-7.627 (-7.699 to -7.558)
	SNP max rel	6	7.06 (-1.50 to 14.37)	5	5.45 (-2.75 to 12.59)	6	6.96 (-1.12 to 14.12)	5	10.86 (4.43 to 16.77)
	LogIC ₅₀		-7.883 (-8.119 to -7.623)		-7.387** (-7.580 to -7.178)		-8.520*** (-8.758 to -8.253)		-7.622 (-7.782 to -7.451)
FEMALES	U4 max	5	81.35 (74.41 to 89.28)	5	73.55 (61.71 to 94.17)	5	76.76 (72.20 to 81.86)	6	82.04 (73.18 to 93.15)
	LogEC ₅₀		-7.705 (-7.868 to -7.532)		-7.437 (-7.765 to -6.959)		-7.479 (-7.582 to -7.365)		-7.497 (-7.698 to -7.268)
	Ach max rel	5	0.4749 (-8.929 to 8.602)	6	19.59*** (12.73 to 25.98)	5	-0.1907 (-8.968 to 7.688)	6	11.24# (6.017 to 16.21)
	LogIC ₅₀		-7.957 (-8.224 to -7.672)		-7.386*** (-7.56 to -7.208)		-7.767 (-7.974 to -7.545)		-7.609# (-7.728 to -7.488)
	SNP max rel	5	3.39 (-2.83 to 9.23)	4	7.18 (0.22 to 13.10)	5	2.758 (-2.920 to 8.174)	4	3.44 (-0.19 to 6.98)
	LogIC ₅₀		-8.124 (-8.282 to -7.957)		-7.260**** (-7.425 to -7.080)		-8.101 (-8.248 to -7.947)		-8.191#### (-8.283 to -8.099)

U4 = U46619, thromboxane A2 receptor agonist; Ach = acetylcholine; SNP = sodium nitroprusside, nitric oxide (NO) donor. Max con and rel = maximal contraction (% of response to 62.5 mM KCl) and relaxation (% of pre-constriction with U46619 concentration producing 75±5% of maximal contractile response), respectively. LogEC₅₀/IC₅₀ = Log of half maximal effective/inhibitory concentrations, respectively. Data are presented as non-linear least-square regression estimates (95%CI). Numbers of viable vessels (n) available for analysis are listed in the upper left corner of each group/experimental condition.

5.4 Discussion

In keeping with the theoretical model (Chapter 4), experimental results from this new body composition study suggest that tissue Na⁺ excess upon high Na⁺ intake is a systemic, rather than skin-specific, phenomenon. This phenomenon reflects architectural changes, i.e. a shift in the extracellular-to-intracellular compartments, due to a reduction of the intracellular or accumulation of water-paralleled, isotonic Na⁺ in the extracellular space. The same changes were shown for hypertensive ageing, which could pragmatically be regarded as a condition of “cumulatively-high” Na⁺ intake. No evidence of tissue Na⁺ hypertonicity was found. Based on the vascular function experiments and consistently with the above, I also show that a hypertonic Na⁺ accumulation is unlikely to justify the observed development of experimental hypertension.

If Na⁺ were to water-independently accumulate in tissues and to exert a biologically relevant modulation of local immune cells by boosting their inflammatory potential (Kleinewietfeld et al., 2013, Jantsch et al., 2015, Zhang et al., 2015, Barbaro et al., 2017, Van Beusecum et al., 2019), one would expect that also other surrounding cells or structures would similarly be affected. Moreover, an increase in arterial resistance would be responsible for the salt-sensitive hypertension induced by blockade of the interstitial-Na⁺/TonEBP/VEGFc cascade (Machnik et al., 2009, Wiig et al., 2013), if the phenomenon were volume-independent (Laragh, 2001). Overall, these considerations indicate blood vessels as putative targets of a Na⁺-hypertonic interstitium mediated biological effects. Since supraphysiologic Na⁺ concentrations in the culture medium had already been shown to induce early changes in protein turnover and cellular hypertrophy of vascular smooth muscle cells (Gu et al., 1998), I focused on the function of intact resistance arteries, with the expectation of changes consistent with increased arterial resistance. As it is unquestionably hard to conceptually reconcile a dual osmotically-active and -inactive nature of interstitial Na⁺ excess, driving TonEBP-mediated signalling while simultaneously eluding commensurate water accrual, I also hypothesised that a hypertonic interstitium would facilitate fluid extravasation at an even more peripheral, capillary level: this specific hypothesis was investigated in vivo in humans, as discussed in Chapter 7.

The changes that I observed in rat resistance arteries upon exposure to a Na⁺-hypertonic bath solution were neither in keeping with those observed after in-vivo salt

loading, nor reminiscent of classic hypertensive vascular phenotypes. Contractile responses were unaffected and sensitivity to NO-mediated loss of tone was increased by hypertonicity: both speak against an increase in arterial resistance and are overall more reminiscent of conditions where neuromuscular tissues are exposed to Na⁺ concentrations which are “toxic” to the cell membrane electrochemical equilibrium and result in loss-of-function (e.g. lethargy or muscle weakness), like diabetes insipidus. In-vivo salt treatment similarly had no effect on the contractile response to U46619, but reduced the contraction to repeated stimuli and the relaxation to NO. Therefore, a volume-dependent nature of the induced hypertension, possibly including parallel Na⁺-and-water accumulation in the arterial wall (as for other tissues, *vide infra*), appears more plausible. Swelling of the vascular wall could well determine increased peripheral resistance and vascular stiffness (to both contraction and relaxation): this idea dates back to the 1950s (Tobian and Binion, 1952), was supported by subsequent evidence (Tobian et al., 1961, Sullivan et al., 1987, Laffer et al., 2016) extending also to heart failure (Zelis et al., 1970), but lacks firm chemical demonstration.

This sort of chemical evidence is the one I aimed for in the rat body composition study, which unfortunately could not include vessels due to the confounding chemical impact of washing blood out of the lumen to conduct tissue analysis.

Salt-loaded SHRSP rats showed an increase in skin, lung and liver Na⁺, which was paralleled by an increase also in tissue water. As previously discussed (section 4.4), their different proportional magnitude does not necessarily indicate any hypertonic or ‘uneven’ accumulation and may simply reflect different sensitivities of Na⁺ and water changes to oedema detection (Rossitto et al., 2018). In fact, the regression slope for each tissue Na⁺ and water contents was the same across the experimental groups. Similarly, the total cationic sum of [Na⁺+K⁺] never exceeded physiological ‘isotonic’ values and was identical across groups. Overall, the unaffected [Na⁺+K⁺] and the mirror trends for [Na⁺] and [K⁺] point to a shift in ECV/ICV ratio rather than any hypertonic phenomenon. Along with the concomitant increase in tissue water, this suggests the development of systemic tissue oedema in the salt-sensitive SHRSP rats upon salt-loading. Laffer et al previously concluded that also in salt-sensitive normotensive volunteers a salt-loading protocol resulted in body weight gain “*commensurate to iso-osmolar water retention*”, at variance with their salt-resistant controls (Laffer et al., 2016).

Notably, skeletal muscle and myocardium showed results at odds with the other tissues. I contend that the increase of Na⁺ without a parallel increase of water in skeletal muscle upon salt-loading can be explained by an ECV/ICV shift secondary to some degree of salt-induced sarcopenia (Kitada et al., 2017), even if no muscular oedema is in place. Of note, even NS treated SHRSPs, with their genetically-determined secondary aldosteronism and salt-retentive predisposition, were lighter than WKY, despite higher skin fat content: this may indicate a relative deficit of fat-free mass.

Myocardium showed no signs of Na⁺ or water accumulation upon salt-loading, but myocardial water-paralleled accumulation of Na⁺ (i.e. oedema) became apparent with hypertensive ageing. The increase in negatively charged sulfated glycosaminoglycan in the matrix *per se* is clearly not an argument for water-independent Na⁺ binding, in light of their equal capacity to bind also water (hygroscopic properties, crucial to the physiology and mechanics of cartilage). Previous gravimetric studies in hypertensive and normotensive dogs led to similar conclusions (Laine, 1988, Laine and Allen, 1991). Notably, even small amount of myocardial oedema were shown to induce systolic and diastolic dysfunction (Dongaonkar et al., 2010), thus highlighting the translational relevance of the finding. Resistance of skeletal or cardiac muscle to accumulation of fluids in young animals likely reflects low interstitial physical compliance (Wiig and Reed, 1985) when compared to other tissues and/or sufficient drainage provided by the lymphatic system (Chapter 7).

Even disregarding strain, age or salt loading, different organs from control animals showed marked heterogeneity in their Na⁺ and K⁺ contents, which nicely fitted the proposed theoretical model when the structural characteristics (i.e. ECV%) of each tissue were taken into account. The predictive power of the model for solid and homogeneous tissues appears confirmed not only by experimental data from my experiments, but also from others (skeletal muscle Na⁺ in Titze et al., 2005; K⁺ not provided). Reports for skin [Na⁺] are - admittedly - more heterogeneous, with values ranging from 90 to 125 mmol/l. I suggest this is due to: 1) the dual composition of skin, by epidermis and dermis, with respective ECV% close to the opposite extremes; sampling thickness and protocols have therefore a considerable impact on total Na⁺ (or K⁺) content (please see also chapter 6); 2) skin being the only site where a supraphysiological [Na⁺ + K⁺] was reported (Machnik et al., 2009, Wiig et al., 2013, Jantsch et al., 2015), thus indicating an accumulation at least in part independent of water.

However, these previous reports of hypertonicity were limited to rodents and, intriguingly, such hypertonicity (ranging between 177 and 195 mmol/l) was found also when animals were on low-salt diets (Titze et al., 2005, Machnik et al., 2009, Wiig et al., 2013). Skin interstitial fluid and lymph, at variance, were shown to have an isotonic Na⁺ content by multiple approaches even upon salt-loading (Nikpey et al., 2017).

It is certainly not straightforward to reconcile apparently diverging results, but I contend that the experimental protocols and evaporation of tissue water (or moisture, as referred to by others; Lowry and Hastings, 1942) may play a role. I personally observed the magnitude and velocity of water evaporation during my experiments whenever handling of samples on the ultraprecision scale wasn't sufficiently fast. In particular, when I plotted WW and all the consequent histochemical derived calculations as a function of the time the sample was left on the scale, I realised that just a couple of minutes of tissue handling would shift baselines from physiological isotonic values to hypertonic (Figure 5-14).

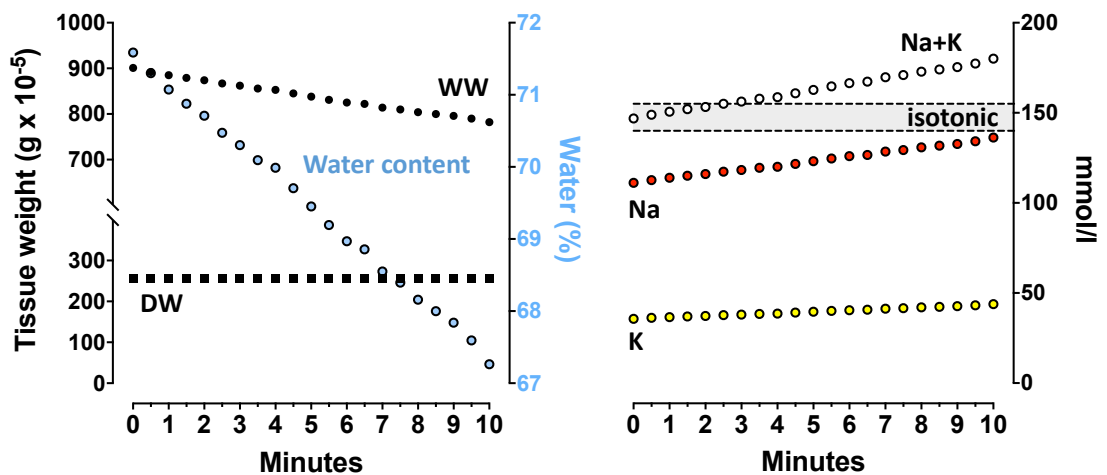


Figure 5-14. Impact of prolonged tissue handling and evaporation on histochemical analysis.

Data from a representative skin sample. Evaporation of water from tissues reduces the estimates of wet weight (WW) to a considerable extent in few minutes, while dry weight remains (by definition) stable. This dramatically and quickly impacts the estimates of water content, those of Na⁺ or K⁺ or total (Na⁺ + K⁺) concentrations and conclusions regarding iso or hypertonicity of the tissue, accordingly.

Experiments where entire mouse or rat carcasses were totally deskinning to conduct the chemical analyses (Titze et al., 2005, Machnik et al., 2009, Wiig et al., 2013) could well be affected by the time needed for the surgical procedure, compared to my approach of small, quickly collected and immediately frozen tissue samples (see methods, 5.2). This contention is obviously no firm guarantee of the validity of my

conclusions, particularly regarding human tissues. Therefore, after the rat body composition study, I designed the S₂ALT study (Chapter 6) to conduct similar histochemical analyses on the skin of patients with hypertension, one of the first clinical conditions where a hypertonic accumulation of Na⁺ had been suggested.

TISSUE SODIUM ACCUMULATION: HYPERTENSIVE PATIENTS

6.1 Background and study aims

Since the very first reports, the phenomenon of a water-independent skin Na⁺ accumulation has been linked to the pathogenesis of arterial hypertension.

Chemical analysis of skin first suggested local accumulation of Na⁺ in excess of water in rodent models of salt-sensitive hypertension, induced by infusion of the mineralocorticoid 11-deoxycorticosterone acetate (DOCA) + 1% saline to drink (Titze et al., 2005). Subsequent studies identified a complex signalling cascade which locally regulated Na⁺ via lymphatic network plasticity as the ultimate effector; whenever such regulation was impaired and the animals were salt-loaded, the resulting phenotype was salt-sensitive hypertension with skin Na⁺ excess (Machnik et al., 2009, Wiig et al., 2013). Therefore, when ²³Na-MRI of human calves revealed a much higher Na⁺ signal in hypertensive patients (particularly if old, with uncontrolled BP or with a typical salt-sensitive form as primary aldosteronism) compared to controls (Kopp et al., 2012, Kopp et al., 2013), it came as no surprise and appeared well in keeping with preclinical experimental data.

At variance with the proposed theoretical framework of a hypertonic skin-specific Na⁺ accumulation, the rat body composition study discussed in chapter 5 led to conclude that tissue Na⁺ excess was rather a systemic phenomenon, reflecting relative or absolute extracellular volume expansion. Nevertheless, some peculiar aspects of skin, the specificity of the original description and the lack of robust histochemical data from human skin samples to complement the reported ²³Na-MRI signal justified additional investigations on this specific tissue.

Skin, and particularly the relatively acellular dermis rich in negatively charged glycosaminoglycans, would be the ideal site for active storage of Na⁺ (Bhave and Neilson, 2011). Moreover, functional and structural similarities between skin and kidneys had been observed (Hofmeister et al., 2015): both serve as ‘barrier organs’ to preserve the “*milieu intérieur*” (C. Bernard) and the hairpin-like lymphatic and blood capillary sub-epidermal structures could function as the counter-current system typical of kidney physiology to maintain osmotic gradients. Therefore, at least theoretically, skin could be an exception to our isotonic findings – as kidney physiologically is! – by

virtue of these mechanisms that would maintain the originally proposed hypertonic Na⁺ gradients.

If that was the case and in light of the ‘barrier’ concept above, when approaching skin specific studies I also wondered how much of a putatively hypertonic Na⁺ excess could result from the accumulation of Na⁺ itself or, rather, to a relative deficit of water lost at the barrier. In line with this contention, the finalistic dominance of body water- over Na⁺- homeostasis had recently been reappraised (Kitada et al., 2017), as extensively discussed in chapters 1 and 3.

On these premises, the S₂ALT study was primarily designed to define the isotonic or hypertonic nature of skin Na⁺ accumulation in a hypertensive population and, secondarily, to identify clinical correlates to this phenomenon, including surface skin-specific mechanisms of Na⁺/water exchange (e.g. sweating and transepidermal water loss, TEWL). A parallel study on young healthy volunteers (SOWAS) provided histochemical insights also on the skin of human normotensive subjects.

6.2 Study-specific methods

6.2.1 Study protocols

6.2.1.1 S₂ALT: Skin Sodium Accumulation and water baLance in hyperTension

The protocol for the cross-sectional S₂ALT (Skin Sodium Accumulation and water baLance in hyperTension) study was approved by the West of Scotland Research Ethics Committee 3 (ref. 18/WS/0238) and Greater Glasgow and Clyde NHS Research and Development (ref. GN18CA634); Appendix 1. The study was conducted in compliance with the Declaration of Helsinki.

Adult, non-pregnant patients were recruited from the Blood Pressure clinic, Queen Elizabeth University Hospital, Glasgow between March and July 2019. A participant information leaflet (Appendix 2) was sent to all patients scheduled for a clinic appointment \geq 7-10 days before they attended, along with the usual reminder. On the day of their appointment (9:00 AM to 4:30 PM), non-pregnant patients willing to take part gave written, informed consent and had anthropometric (body height and weight) and routine office blood pressure (BP) measures taken as per current guidelines

(Williams et al., 2018); pulse pressure (PP) was calculated as systolic BP – diastolic BP. Relevant comorbidities and ongoing medications were recorded. On the same occasion a short dietary questionnaire was administered to estimate sodium intake, transepidermal water loss (TEWL) was measured and a pilocarpine-induced sweat sample, a skin biopsy, serum and EDTA-plasma (for Na⁺, Urea, Creatinine and s-VEGFc [measured by Quantikine ELISA assay, *R&D systems*] and for NT-proBNP, respectively) and a random spot urine sample (for microalbuminuria) were collected.

6.2.1.2 SOWAS: SOdium and WAtER Skin balance

A cross-sectional study on healthy volunteers (SOWAS: SOdium and WAtER Skin Balance) recruited among MVLS students was approved by the University of Glasgow, MVLS College Ethics Committee (ref. 200170153) and conducted between July and December 2018.

One of the study aims was to provide sex-specific skin chemical reference values from a young healthy population. The second study aim, i.e. to investigate ex-vivo the modulation of osmolytes/water-specific human skin channels by hypertonic Na⁺ conditions and aldosterone (which is a classic fluid balance regulator and its excess is known to induce skin Na⁺ accumulation; Titze et al., 2005, Kopp et al., 2012) did not undergo completion due to technical issues briefly examined below and will not be further discussed.

Student volunteers were recruited through advertisement in the University areas and media, with a 30£ voucher as a compensation for their time and potential travel expenses. Participants (50% females) attended the Research Centre for a preliminary visit (study discussion, consent and review of exclusion criteria, i.e. office BP > 140/90 mmHg, obesity, or previous diagnosis of diabetes, thyroid, renal or coagulation disease) and a main visit. This included measurement of BP, body weight and non-invasive body composition (BC-418MA, Tanita UK Ltd), and collection of blood samples, overnight-collected 24h urine, one additional spot urine sample, and 2 skin biopsies. For female participants, the main visit was arranged in the early follicular phase of their menstrual cycle, just after period termination; in 4 cases, due to personal logistics or continuous progesterone treatment (skin implants or vaginal coil) the main visit coincided with a luteal or luteal-like phase. Salinity of the 24h urine sample was checked by colorimetric strips (*Salinity View*, Health Mate®) to confirm normal salt

intake and eligibility, accordingly. Biopsies were performed on adjacent sites in the gluteal external upper quadrant, as described below.

One skin sample was cut in halves and immediately frozen for chemical (chapter 7) analyses. The second sample was used for whole-tissue culture (Maubec et al., 2015) and randomly assigned to different incubation conditions (standard culture medium, culture medium enriched in NaCl [+30 mmol/l], standard culture medium + 10⁻⁷ M aldosterone, culture medium enriched in NaCl [+30 mmol/l] + 10⁻⁷ M aldosterone). An interim analysis revealed marked histological changes in tissue architecture upon culture, e.g. epidermal layer detachments with apparent neo-epidermogenesis, independent of the specific culture condition. Because of this major confounder, this experimental arm of the study was stopped.

6.2.2 Skin punch biopsy and chemical analysis

The protocols for the skin punch biopsy and water and Na⁺/K⁺ tissue content analysis have already been described in Chapter 2 and are only briefly recollected here.

Approximately 40 minutes after application of a Na⁺-free topical anaesthetic cream, the arm (S₂ALT) or gluteal (SOWAS) surgical site was cleaned with alcohol swabs to ensure sterile conditions. The epidermis and superficial dermis were pierced by a sterile punch (3-4 mm blade diameter; Kai Medical), the biopsy removed with a sterile blade and haemostasis obtained with sterile gauze. The excised sample was immediately put into a pre-cooled Eppendorf tube, frozen in dry ice and stored at -80°C until tissue chemical analysis. The biopsy site was closed with steri-strips (3M) and wound care information sheet and plasters were provided to the participant.

At the time of the analysis, frozen skin samples were transversally cut into a superficial layer, including the epidermis and the immediately adjacent superficial dermis (ESD), and deeper dermis (DD; Figure 6-1).

Samples were weighed on a 5 decimal (0.00001 g) scale to determine Wet Weight (WW). After complete desiccation of samples to a stable dry weight (DW), water content was estimated as (WW-DW)/DW, or as percentage (WW-DW) × 100/WW. Dried samples underwent complete digestion in HNO₃ and the resulting solutions were used for Na⁺ and K⁺ quantification by flame photometry (Sherwood scientific, model

410C), with calibration standards as reference. All samples were analysed in a batch. Na⁺ and K⁺ concentrations in the analysed solutions were used to back-calculate their total content in the digested samples and were normalised by DW for Na⁺ and K⁺ tissue content (mmol/gDW), or by tissue water for Na⁺ and K⁺ tissue concentration (mmol/l).

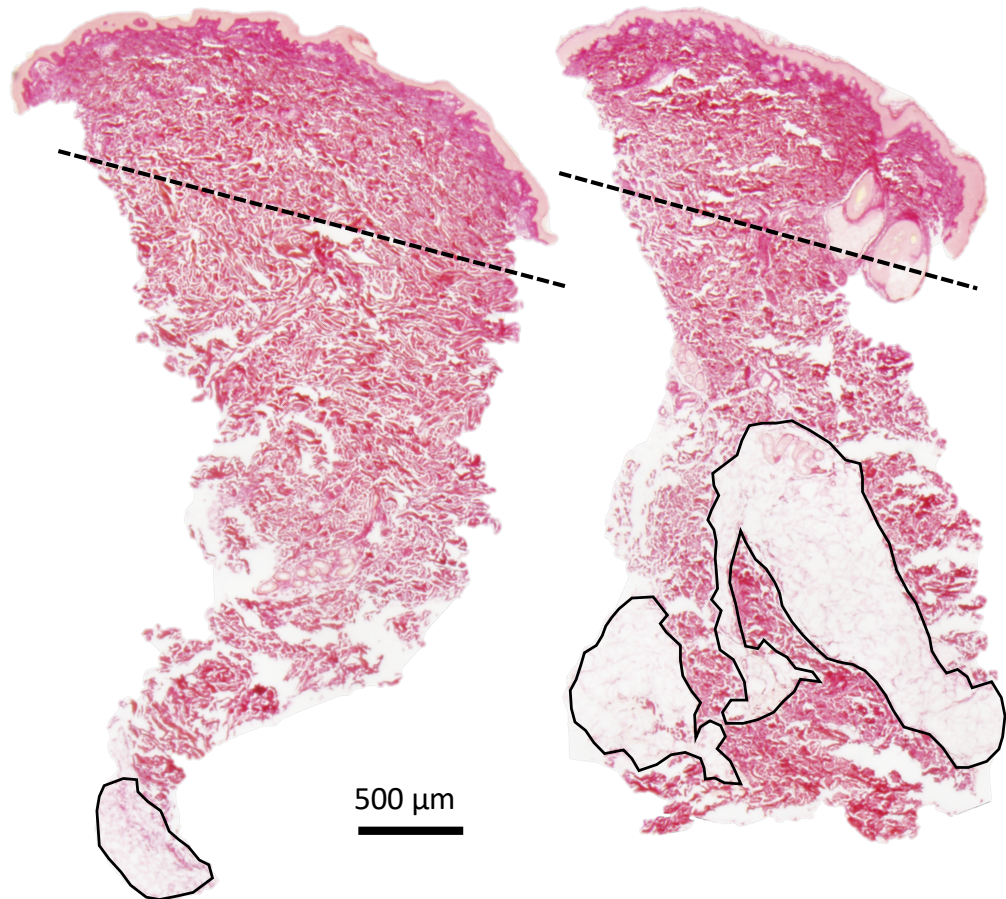


Figure 6-1. Human skin samples and anatomical strategy of analysis.

Representative skin sections from a male (left) and a female (right) subject (picrosirius-red staining); dashed line = representative of the cutting plane for separation of ESD and DD in all study samples; black-outlined areas in DD = subcutaneous fat, typically more abundant in female subjects.

6.2.3 Sodium intake questionnaire (*S₂ALT* study)

A short, validated questionnaire (Charlton et al., 2008) was administered to patients while waiting for their scheduled visit (Appendix 3). It included 42 food items with six possible consumption frequency responses: never; 1–3 times per week; 4–6 times per week; once a day; twice a day; and 3+ times a day. Predefined absolute amounts of sodium per serving size per specific item, according to *MRC Food Composition Tables* (Langenhoven et al., 1991) were multiplied by the consumption frequency factor that

each individual reported, and summed up to a total weekly Na⁺ intake for each subject, later divided by 7 to estimate daily intake. For simplicity, the absolute amounts of Na per serving for each food category were divided by 50 mg Na⁺ units and rounded to the nearest integer (Charlton et al., 2008). The frequency factor in the weekly calculation was taken as the value midway between the upper frequency value of one category and the lower of the next (i.e. 0, 2, 5, 7, 14, 21).

Missing questionnaire data were scrutinised by Little's 'missing completely at random' (MCAR) test. For subjects with more than half of the responses missing calculations of weekly scores was considered unreliable and excluded. For subjects with $\leq 10\%$ missing responses median substitution was used for imputation and calculation of weekly scores.

6.2.4 Transepidermal water loss (*S₂ALT study*)

Before blood collection and skin biopsy and following a ≥ 20 -minute period of acclimatisation in a temperature-controlled environment (20 - 21°C) and ≥ 5 minutes of quiet sitting, transepidermal water loss (TEWL; Fluhr et al., 2005) was assessed from the flexor portion of the forearm with a Tewameter® TM300 probe (Courage & Khazaka GmbH, Cologne, Germany). The probe estimates TEWL through 2 pairs of temperature and humidity sensors and Fick's diffusion law. Readings were automatically stopped and recorded by an MPA 580 system and dedicated software when a ≤ 0.1 standard deviation was reached.

6.2.5 Pilocarpine-induced sweat test (*S₂ALT study*)

Immediately before the clinic visit, upon consent and exclusion of an implanted pacemaker/cardioverter-defibrillator, a small area of skin on one arm of the study participants was cleaned with distilled water and dried. Two pilocarpine (a parasympathomimetic alkaloid) pads (Pilogel® Iontophoretic Discs, ELITech Group) were attached with straps. In order to get the pilocarpine into the skin to induce sweating, the area was stimulated by a small current (1.5 mA) for five minutes (iontophoresis; Webster Sweat Inducer Model 3700, ELITech Group). After removal of the pilocarpine pads, a dedicated plastic coil (Macroduct® no-dye collectors, ELITech Group) was attached on the stimulated arm with straps for collection of sweat over the next 30-40 minutes, including the time while the clinic visit took place.

The sweat collected in the coil was then transferred to 200 ul sterile microtubes, frozen in dry ice and stored at -80°C until chemical analysis. At the time of the analysis samples were thawed to measure the volume with a calibrated micropipette and appropriately diluted to determine Na⁺ and K⁺ concentrations (mmol/l) by flame photometry, as described in chapter 2 for HNO₃-digested tissues. Total Na⁺ or K⁺ sweat content was calculated as concentration × volume.

6.2.6 Statistics

Statistical analysis was performed using Prism (GraphPad Software) and SPSS (IBM).

Categorical variables are presented as absolute numbers and percentages and compared by χ^2 test. Student t-test for normally distributed variables (presented as mean±SD or, graphically, as mean [95%CI]) or Mann-Whitney test for non-normally distributed variables (presented as median [interquartile range] or, graphically, as median [95%CI]) were used for comparisons. Outliers were automatically identified by ROUT method (Q = 1%) and excluded from analysis but reported on the relative figures.

Correlations were ascertained by Pearson test, upon appropriate transformation of skewed variables to attain normal distribution, or Spearman if normality was not attained. Univariable and multivariable (including age, sex, BMI and estimated Na intake) linear regression models were estimated and results were presented as standardised B coefficients (95%CI).

The α level was set at 0.05 and all statistical tests were 2-tailed (*p<0.05, **p<0.01, ***p<0.001, ****p<0.0001).

6.3 Results

Out of 90 study participants, 76 agreed to undergo a skin biopsy as part of the study procedures. Their characteristics and sex-specific differences are summarised in Table 6-1.

Table 6-1. Characteristics of S₂ALT patients.

Variables	ALL (n=76)	FEMALES	p	MALES
Females	36 (47.4%)	-		-
Age (years)	58 ± 15	56 ± 16	0.359	59 ± 13
BMI (kg/m ²)	30.3 (27.5-36.3)	31.6 (26.5-38.3)	0.212	29.7 (27.8-33.9)
Office SBP (mmHg)	148 ± 21	148 ± 26	0.869	149 ± 15
Office DBP (mmHg)	89 ± 12	87 ± 13	0.278	90 ± 11
Office HR (beats per minute)	74 (65-87)	77 (66-89)	0.82	73 (64-84)
Uncontrolled HTN	56 (73.7%)	21 (60.0%)	0.006	35 (87.5%)
Number of anti-HTN medications	2 (0-4)	2 (1-3)	0.011	3 (1-3)
0	8 (10.5%)	6 (16.7%)		2 (5%)
1	17 (22.4%)	9 (25%)		8 (20%)
2	15 (19.7%)	10 (27.8%)	0.056	5 (12.5%)
3	22 (28.9%)	6 (16.7%)		16 (40%)
≥ 4	14 (18.4%)	5 (13.9%)		9 (22.5%)
ACEi/ARB	60 (78.9%)	25 (69.4%)	0.054	35 (87.5%)
CCB	41 (53.9%)	15 (41.7%)	0.042	26 (65%)
Diuretic	33 (43.4%)	12 (33.3%)	0.092	21 (52.5%)
BB	18 (23.7%)	7 (19.4%)	0.41	11 (27.5%)
MRA	9 (11.8%)	2 (5%)	0.108	7 (17.5%)
AB	12 (15.8%)	6 (5.6%)	0.842	6 (15%)
Obesity	41 (53.9%)	22 (61.1%)	0.235	19 (47.5%)
Diabetes mellitus	10 (13.3%)	3 (8.6%)	0.256	7 (17.5%)
Dyslipidaemia	43 (58.1%)	17 (50%)	0.192	26 (65%)
Chronic kidney disease	8 (10.5%)	3 (8.3%)	0.555	5 (12.5%)
Na ⁺ intake (g/d)	2.79 (2.24-3.76)	2.64 (2.39-3.44)	0.323	3.09 (2.16-4.56)
s-Na ⁺	140 (139-142)	140 (139-142)	0.565	140 (139-141)
s-Urea (mmol/l)	5.3 (4.5-6.5)	4.8 (3.9-5.9)	0.005	5.6 (4.9-7.3)
s-Creatinine (umol/l)	73 (63-86)	65 (55-73)	<0.001	84 (72-96)
u-ACR (mg/gCr)	6.7 (2.6-16.8)	6 (3.4-11.7)	0.848	6.7 (2.3-24.7)
NT-pro-BNP (pg/ml)	71.8 (43.1-184.1)	79 (46-142)	0.577	68 (34-253)

Qualitative data presented as n (%). Quantitative data presented as mean ± SD or median (interquartile range), as appropriate. BMI = Body Mass Index. SBP = systolic blood pressure. DBP = diastolic blood pressure. HR = heart rate. HTN = hypertension. Uncontrolled HTN = SBP ≥ 140 and/or DBP ≥ 90 mmHg. ACEi/ARB = ACE inhibitors or Angiotensin receptor blockers. CCB = calcium channel blockers. BB = beta blockers. MRA = mineralocorticoid antagonists. AB = alpha blockers; Na⁺ intake = estimated sodium intake (questionnaire); s- = serum. u-ACR = urinary albumin to creatinine ratio (random urine sample).

6.3.1 Histochemical analysis

As the theoretical model would predict (chapter 4), [Na⁺] and [K⁺] were lower and higher in the more cellular ESD compared to mostly acellular DD, respectively (Figure 6-2). In virtually no patients, and thereby in none of any prespecified clinical subgroups, did [Na⁺+K⁺] exceed the physiological value of 155 mmol/L in either layer (Figure 6-2), thus ruling out any hypertonic accumulation.

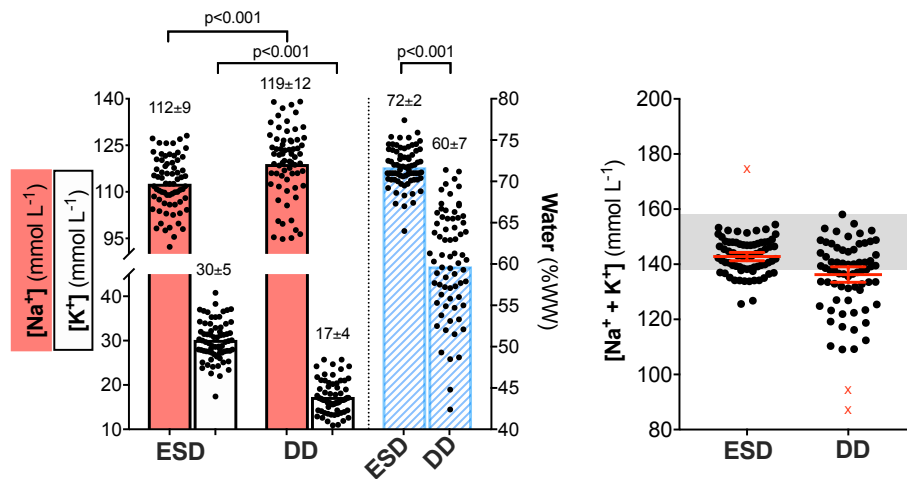
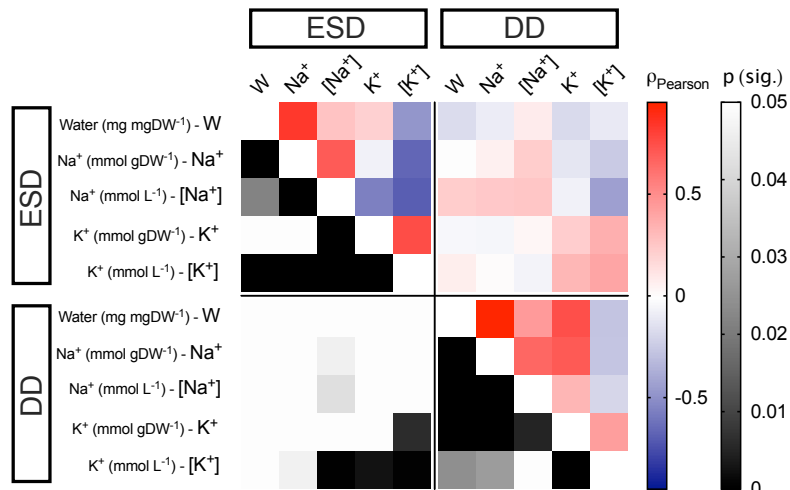


Figure 6-2 Na⁺ and K⁺ concentrations and water content by skin layer

Left: bars show mean ± 95%CI, with individual points (overlay); Na⁺ and K⁺ concentrations and water content in the Epidermis/Superficial dermis (ESD) and Deep Dermis (DD) layers, reflecting different architecture and cellularity. Right: skin Na⁺ + K⁺ concentration in ESD and DD; red X = automatically detected outliers (ROUT, Q=1%); in virtually no patient, including n = 3 cases with primary aldosteronism, did [Na⁺ + K⁺] exceed physiological values (grey).

In both ESD and DD, water content was positively and negatively correlated with [Na⁺] and [K⁺], respectively (Figure 6-3, below).



In DD, water, Na⁺ and K⁺ contents, but not concentrations, were all positively and highly correlated. This likely reflects the volume of distribution of watery fluids, either cellular or extracellular, as opposed to fat. As discussed for rat tissues (Figure 5-5), whenever a tissue volume is occupied by fat the space for cells or extracellular fluid (and water and the accompanying cations, accordingly) is reduced: therefore water content in the fat-rich DD is lower than ESD (Figure 6-2). Similarly, male DD contained more water, Na⁺ and K⁺ than female dermis, which is known to be richer in subcutaneous fat, with no such differences observed in ESD (Table 6-2).

Almost identical sex differences were observed in gluteal biopsies from young healthy volunteers (SOWAS, Table 6-3). Fluid-retentive (White et al., 2011) progestinic states were characterized by higher water and Na⁺ content, but unchanged [Na⁺+K⁺] (Figure 6-4).

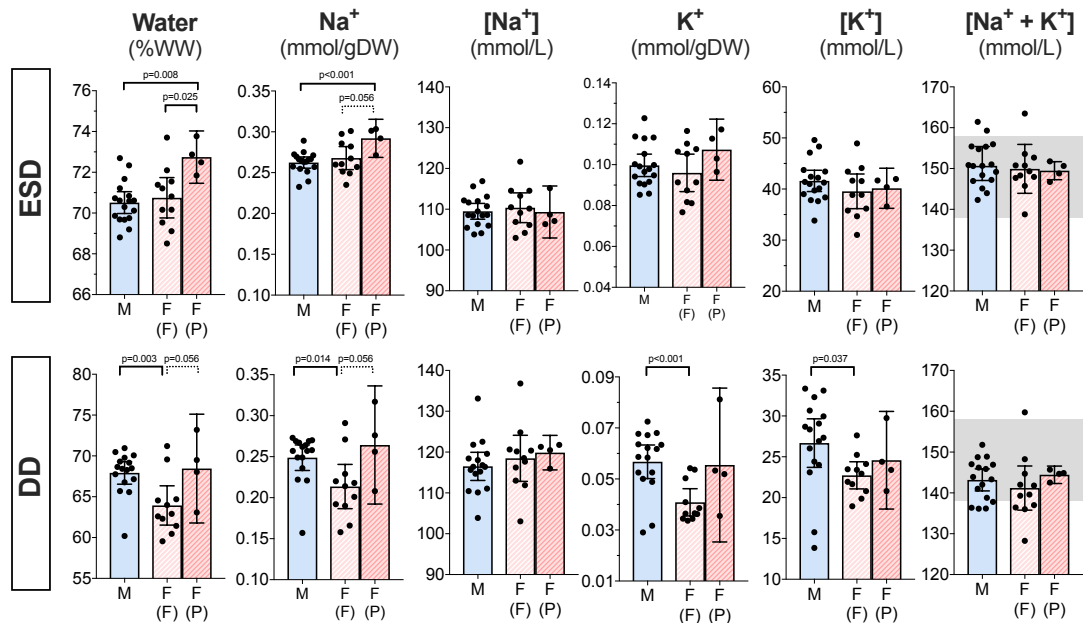


Figure 6-4. Histochemical sex-differences in the skin of young healthy volunteers and impact of fat.

Mean \pm 95%CI; blue (M) = males, light pink (F(F)) = females in follicular phase, dark pink (F(P)) = females in progestinic phase/state. No differences were observed between M and F(F) in ESD. In DD, water, Na⁺ and K⁺ content, but not concentration, were lower in F(F). F(P) overall had higher skin water and Na⁺ content than F(F).

In SOWAS, where body composition (bioimpedance) data were available, the histochemical impact of fat was further supported by the inverse correlation between gluteal dermal Na⁺ content and percentage fat mass in the leg ($\rho = -0.54$, $p = 0.005$); similar correlations were observed with directly-measured bioimpedance values (Ω ; leg: $\rho = -0.40$, $p = 0.047$; whole-body: $\rho = -0.62$, $p < 0.001$) and for dermal water content (with leg fat %: $\rho = -0.62$, $p = 0.001$; with leg Ω : $\rho = -0.42$, $p = 0.04$; with whole-body Ω : $\rho = -0.61$, $p < 0.001$).

Table 6-2. Skin histochemical differences between hypertensive males and females.

Variables		MALES (n=40)	p vs females	FEMALES (n=36)			
				ALL	pre-menop (n=14)	p	post-menop (n=22)
Epidermis/superficial dermis (ESD)	Water content (mg/mgDW)	2.57 ± 0.32	0.864	2.58 ± 0.29	2.50 ± 0.21	0.244	2.62 ± 0.33
	Water content (%WW)	71.62 ± 2.35	0.708	71.83 ± 2.36	71.32 ± 1.64	0.337	72.13 ± 2.68
	Na ⁺ content (mmol/gDW)	0.290 ± 0.049	0.821	0.290 ± 0.044	0.264 ± 0.026	0.005	0.302 ± 0.047
	Na ⁺ concentration (mmol/l)	113.5 ± 8.3	0.371	111.7 ± 8.9	105.8 ± 6.4	0.002	115.1 ± 8.4
	K ⁺ content (mmol/gDW)	0.076 ± 0.013	0.602	0.078 ± 0.009	0.082 ± 0.009	0.032	0.075 ± 0.009
	K ⁺ concentration (mmol/l)	29.9 ± 5.5	0.694	30.4 ± 4.2	32.9 ± 3.9	0.005	28.9 ± 3.7
	Na ⁺ /K ⁺ ratio	3.93 ± 0.97	0.415	3.76 ± 0.72	3.27 ± 0.50	0.001	4.06 ± 0.68
Deep dermis (DD)	Water content (mg/mgDW)	1.68 ± 0.41	0.007	1.40 ± 0.42	1.24 ± 0.26	0.159	1.46 ± 0.46
	Water content (%WW)	61.67 ± 6.82	0.009	57.26 ± 7.02	54.69 ± 5.53	0.207	58.12 ± 7.45
	Na ⁺ content (mmol/gDW)	0.208 ± 0.057	<0.001	0.158 ± 0.054	0.136 ± 0.042	0.144	0.166 ± 0.056
	Na ⁺ concentration (mmol/l)	122.7 ± 8.9	0.004	114.0 ± 13.4	111.8 ± 9.5	0.735	114.3 ± 15.1
	K ⁺ content (mmol/gDW)	0.029 ± 0.008	0.007	0.024 ± 0.006	0.022 ± 0.007	0.446	0.024 ± 0.006
	K ⁺ concentration (mmol/l)	17.2 ± 3.8	0.795	17.4 ± 3.5	17.9 ± 2.6	0.449	17.1 ± 3.9
	Na ⁺ /K ⁺ ratio	7.48 ± 1.78	0.061	6.69 ± 1.65	6.15 ± 1.24	0.226	6.95 ± 1.84

Data presented as mean ± SD and compared by Student t-test. Menop = menopause. Missing data because of technical issues or unavailable sample ≤ 8/total

Table 6-3. Characteristics of young healthy volunteers.

Variables	ALL	MALES (n= 18)	p	FEMALES (F) (n = 11)	p	FEMALES (P) (n = 4)
Females	15 (45.5%)	-		-		-
Age (years)	25 ± 4	25 ± 3	0.769	25 ± 6	0.498	28 ± 5
Office SBP (mmHg)	115 ± 11	118 ± 12	0.096	111 ± 8	0.882	115 ± 8
Office DBP (mmHg)	65 ± 9	63 ± 10	0.501	66 ± 9	0.518	69 ± 8
Office HR (beats per minute)	67 ± 8	66 ± 10	0.318	69 ± 8	0.918	69 ± 4
BMI (kg/m ²)	22.7 ± 2.8	23.0 ± 2.7	0.945	23.1 ± 3.0	0.109	20.4 ± 1.0
Body Weight (Kg)	68.3 ± 13.3	74.5 ± 13.0	0.012	62.1 ± 10.2	0.352	57.0 ± 3.9
Impedance (whole body, Ω)	630 ± 77	590 ± 68	0.0001	676 ± 33	0.891	682 ± 133
Total body water (estimated; %)	58.7 ± 6.0	62.4 ± 3.3	<0.0001	53.0 ± 5.2	0.131	58.0 ± 5.9
Total body fat (estimated; %)	19.7 ± 8.3	14.7 ± 4.5	<0.0001	27.7 ± 7.1	0.13	20.7 ± 8.1
Leg fat (estimated; %)	20.8 ± 9.9	13.2 ± 4.4	<0.0001	32.0 ± 3.9	0.098	27.2 ± 5.9
Trunk fat (estimated; %)	17.7 ± 7.1	15.3 ± 5.5	0.008	22.2 ± 6.8	0.255	16.7 ± 10.3
p-Na⁺ (mmol/l)	141 (140-141)	141 (140-142)	0.218	140 (140-141)	0.376	140 (139-142)
p-Urea (mmol/l)	4.7 ± 1.4	4.9 ± 1.7	0.336	4.5 ± 0.8	0.555	4.2 ± 1.0
p-Creatinine (umol/l)	76 ± 12	80 ± 11	0.111	72 ± 13	0.348	72 ± 13
24h-urinary volume (ml)	1875 ± 900	1800 ± 775	0.7	1950 ± 1150	0.879	2050 ± 775
24h-u Na excretion (g/d)	2.23 (1.77-3.27)	2.09 (1.47-3.52)	0.555	2.37 (1.07-3.27)	0.373	2.12 (1.89-2.48)

Qualitative data presented as n (%). Quantitative data presented as mean ± SD or median (interquartile range), as appropriate. (F) = females in follicular phase; (P) = females in progestinic phase/state. BMI = Body Mass Index. SBP = systolic blood pressure. DBP = diastolic blood pressure. HR = heart rate.

6.3.2 Clinical correlates in hypertensive patients

In the hypertensive S₂ALT population, age (range 21-86 years) was independently associated with an increase in ESD water and [Na⁺], and a decrease in [K⁺] in both layers; this likely indicates excess fluid (oedema) accumulation in the context of reduced tissue cellularity, traditionally accepted as a hallmark of skin aging (Figure 6-5).

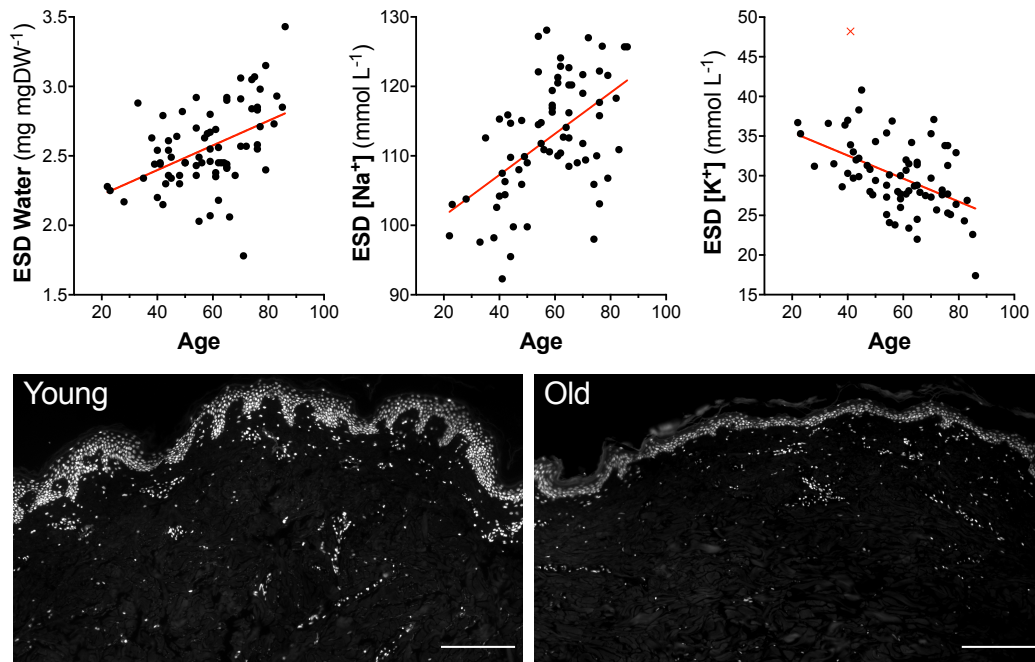


Figure 6-5 Histochemical parameters and ageing

Association of ESD water, [Na⁺] and [K⁺] with age, reflecting the shift in ECV/ICV ratio; red X = automatically detected outlier; bottom: representative pictures of age-related reduction in skin cellularity; immuno-fluorescence, DAPI-staining; scale bars = 200 µm.

Salt intake, estimated by dietary questionnaires (Little's Missing Completely At Random test, $p = 0.593$; five subjects with $> 50\%$ missing responses excluded; 22 additional subjects with $\leq 10\%$ missing responses and 10/22 only 1), predicted epidermal water content (but not Na⁺, K⁺ or their ratio), independently of age, sex and BMI.

BMI showed only a borderline-significant independent association with ESD K⁺ content.

Office diastolic BP was inversely associated with ESD water content ($\rho = -0.250$; $p = 0.03$) and a surrogate of vascular stiffness, pulse pressure (PP), was positively

correlated with Na⁺/K⁺ ratio in both layers; in ESD, the ratio was higher in patients with uncontrolled BP, independent of other covariates. No significant interaction with medications was observed.

NT-proBNP levels, positively associated with age ($\rho = 0.526$; $p < 0.001$), estimated Na⁺ intake ($\rho = 0.260$; $p = 0.03$) and systolic BP ($\rho = 0.288$; $p = 0.01$) and negatively with diastolic BP ($\rho = -0.277$; $p = 0.02$), mirrored all measures of skin oedema accumulation.

Contrarily to the predefined hypothesis that local regulatory mechanisms could make skin an exception to the isotonic nature of systemic tissue Na⁺ excess/accumulation via a relative deficit of water, transepidermal water loss showed no correlations with histochemical skin data (Figure 6-6).

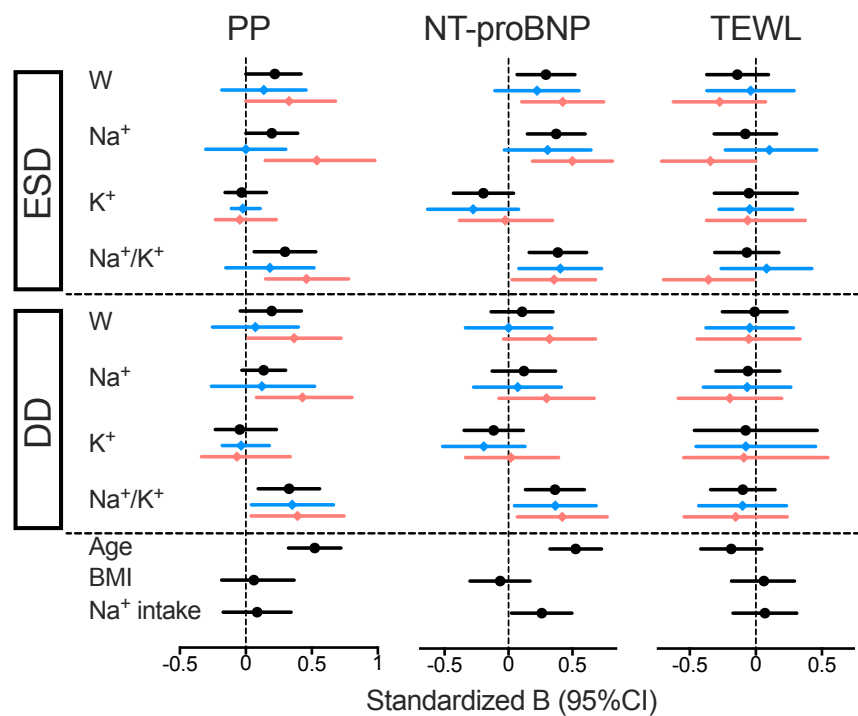


Figure 6-6 Histochemical parameters and other relevant clinical correlates

Relationships between skin histochemical parameters, age, BMI, Na intake and pulse pressure (PP), plasma NT-proBNP and transepidermal water loss (TEWL), by skin layer. Data are presented as standardised B regression coefficients (95%CI); for skin histochemical parameters, coefficients for all patients are visualised in black, for males in blue, for females in pink. PP and NT-proBNP positive associations with ESD water accumulation were mostly driven by females; the association with Na⁺/K⁺ ratio was overall generalised to both layers and sexes. No significant associations were observed with TEWL, making relative local water deficit an unlikely explanation for an even putative Na⁺ hypertonic excess.

6.3.3 Skin-specific mechanisms of Na⁺/water exchange

Both age and [Na⁺] in ESD, as a measure of skin ECV, were positively correlated with sweat [Na⁺] (Spearman $\rho = 0.367$, $p = 0.001$ and $\rho = 0.345$, $p < 0.01$, respectively; Figure 6-7). The association between ESD and sweat [Na⁺] was independent of sex, BMI and use of RAS system blockers (ACEi/ARBs; $p_{\text{adjusted}}=0.031$); the latter was the only class of antihypertensive medications showing any significant interaction with sweat [Na⁺].

In particular, patients who were on ACEi or ARBs had higher sweat [Na⁺] compared to those who were not (32.8 [26.0-45.8] vs 25.8 [18.4-39.5] mmol/l, $p = 0.038$); the same was true when the analysis was limited to those on ACEi or ARBs only ($n=13$; 39.2 [31.6-51.2] mmol/l) vs no antihypertensive medications ($n=9$; 25.7 [18.4-37.7] mmol/l; $p = 0.049$ for comparison). Sweat [Na⁺] inversely correlated with sweat [K⁺] ($\rho = -0.230$, $p = 0.041$).

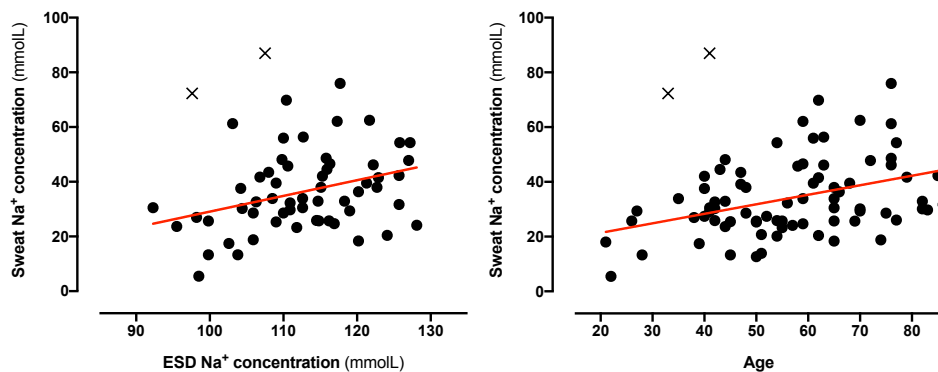


Figure 6-7. Sweat Na⁺ concentration in relation to ESD Na⁺ concentration and age.

ESD [Na⁺], as a measure of skin ECV, and age were positively correlated with sweat [Na⁺]. X = automatically identified outliers (ROUT = 1%).

Office diastolic, but not systolic, BP inversely correlated with sweat [Na⁺] (Spearman $\rho = -0.309$, $p=0.006$), independent of age and the other potential confounders ($p_{\text{adjusted}}=0.02$). Although no difference was found for sweat [Na⁺], total sweat volume and excreted Na⁺ were lower in patients with uncontrolled office BP (defined as BP > 140/90 mmHg; $p<0.01$ for both; $p_{\text{adjusted}}<0.005$).

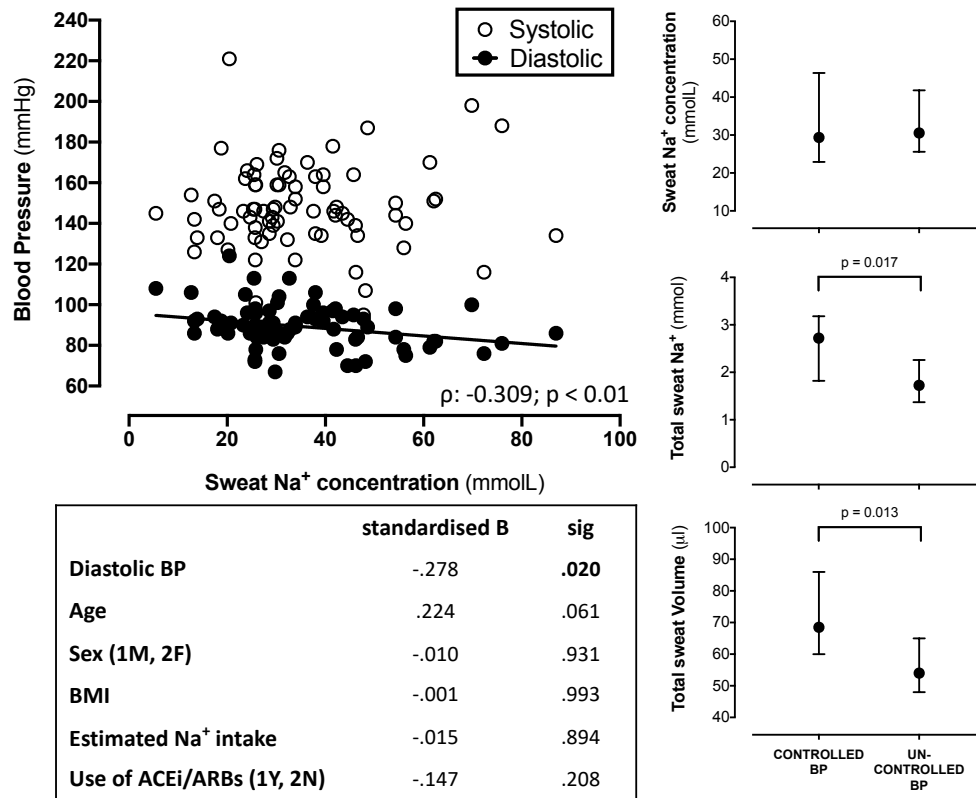


Figure 6-8. Sweat and blood pressure.

Left: Sweat [Na⁺] was inversely and independently associated with diastolic BP. BP control was associated with higher total sweat [Na⁺] and total sweat volume (data presented as median [95%CI]).

Sweat volume also positively correlated with TEWL and serum-VEGFc (p<0.05 for both).

6.4 Discussion

The S₂ALT study, designed to define the nature of skin Na⁺ excess in hypertensive patients, failed to identify any hypertonic Na⁺ accumulation. Despite some anatomical and functional aspects of the skin that could make it similar to the kidney (Hofmeister et al., 2015) and therefore support the theoretical plausibility of Na⁺ storage mechanisms different from all other organs, a direct histochemical analysis of these human skin biopsies revealed no exception to what has already been observed in the rat body composition study.

In fact, maintenance of the Na⁺ gradients in the renal medulla requires “*elaborate arrangements of renal tubules in combination with specific enrichment of active sodium transporters (Na/K-ATPase, Na-K-Cl cotransporters, Na-Cl cotransporters, etc), in addition to enormous flow in tubules and blood vessels. (...) Given the lack of conclusive evidence for structural or functional features required for the maintenance*

of local hypertonicity in the skin,” (Hyug Moo Kwon, *personal communication*) an isotonic accumulation, as suggested by Figure 6-2 and as observed also in all other organs in rats (Chapter 5), clearly appears more plausible.

There are very few other studies on direct chemical analysis of human skin to put these findings into context.

Fischereder et al. measured Na⁺ and GAG content in skin and (epigastric) arterial samples taken from renal transplant living donors and end-stage kidney recipients, free from clinically detectable oedema (Fischereder et al., 2017). Although non significantly different between groups, skin Na⁺ (mmol/gDW) and arterial tissue Na⁺ showed a positive correlation; additionally, both correlated with the respective tissue GAG content. While the simple conclusion, in keeping with Titze’s theoretical framework, was that interstitial Na⁺ storage is regulated by GAGs in humans, associations do not prove causation. Moreover, the authors did not provide data on tissue water content or total Na⁺+K⁺ concentration: based on the histochemical approach discussed in chapters 4-5, excess extracellular space (including GAGs and possibly oedema) is well in keeping with higher Na⁺ content regardless of hypertonic accumulations. What is intriguing, and supports my view of a systemic phenomenon (chapter 5), is the correlation between the systemic vasculature and skin Na⁺.

Another study, with a double-blind cross-over design, was conducted on healthy participants randomized to placebo (70 mmol sodium/d) or oral slow sodium (200 mmol/d; Selvarajah et al., 2017). Skin Na⁺, expressed as the ratio Na⁺:K⁺, was 8% higher following the slow sodium phase and positively correlated with BP and peripheral vascular resistance (PVR). The authors very carefully assessed any possible contaminations, including in the subcutaneous anaesthetic, prior to the biopsies. However, they acknowledged that “*smaller*” (which, in the context of standardised punch approaches, should read as “more superficial”) “*samples recorded greater proportional water contents*” and interpreted the phenomenon as a “*technical limitation*”. This led them to favour Na⁺:K⁺ ratios over Na⁺ concentration values; therefore, the same aforementioned limitations in the interpretation of findings apply. In fact, the reported biopsy-depth related differences do not appear a technical limitation but rather consistent with S₂ALT findings, the role of a subcutaneous fat typically more represented in deeper layers and the need for a critical histochemical interpretation of data (Figures 6-1,2).

Chachaj et al performed a cross-sectional analysis of skin biopsies from patients undergoing elective abdominal surgery, stratified according to hypertension status: while hypertensive patients did not show significantly higher skin Na⁺ content than normotensives, skin Na⁺ and water were closely correlated ($r = 0.57$; $p < 0.001$; Chachaj et al., 2018)

One last report that is worth mentioning comes from the field of human heart failure (Nijst et al., 2018). The topic of heart failure (HF), prototypic of overt - as opposed to subclinical -congestion, will be extensively discussed in the next chapter. However, some experimental aspects are briefly summarised here. A punch biopsy of the lower leg (a classic site of dependent oedema in HF patients) was obtained in patients with HF and reduced ejection fraction (HFrEF) and healthy subjects. The authors found a higher interstitial glycosaminoglycan content, which strongly associated with tissue water content and peripheral oedema, in patients with HFrEF compared to controls. The specific approach to sample handling and processing (defatting protocol) unfortunately prevented concomitant Na⁺ assessment on the biopsies, but – once again – their results appeared in keeping with the hygroscopic (and not only Na⁺-binding) properties of GAGs, with Fischereder's data and, overall, with my widely-applicable conclusions (chapter 5).

On a parallel note, S₂ALT results not only did provide direct evidence of an isotonic phenomenon, but also linked it to relevant clinical correlates.

The most robust association was with ageing, a salt-sensitive condition (Elijovich et al., 2016) with typically good response of blood pressure to diuretic therapy, accordingly. S₂ALT data suggest that this salt-sensitivity goes hand-in-hand with subclinical congestion. NTproBNP, a product of cardiac tissue in response to volume overload and a well-established predictor of cardiovascular events in people with or without baseline cardiovascular disease (Wang et al., 2004, Everett et al., 2015, Natriuretic Peptides Studies et al., 2016, Paget et al., 2011, Welsh et al., 2014), was closely associated with age, estimated salt intake and histochemical evidence of excess skin water and Na⁺.

The investigation of skin-specific mechanisms of water and Na⁺ exchange (i.e. sweat and TEWL) revealed interesting associations with measures of tissue Na⁺ status and suggests them as parts of a systemic homeostatic regulation. Similar to NTproBNP, sweat [Na⁺] was positively correlated with age and skin [Na⁺], thus reflecting a

possible attempt to eliminate excess total body Na⁺; in keeping with this contention, the higher the concentration of excreted Na⁺, the lower the diastolic BP. With all the limits of independent studies comparisons, hypertensive patients enrolled in S₂ALT had a lower sweat [Na⁺] than normotensive controls recruited in a previous study (Quintero-Atencio et al., 1966: 30.6 [25.5-42.3] mmol/l vs 34.8 [29.0-51.9] mmol/l, p = 0.038); patients with severe, uncontrolled, possibly malignant (by current definitions) hypertension in that same study had an even lower sweat Na⁺ concentration (23.3 [16.8-31.3] mmol/l). In relation to putative modulators of this response, an inverse association with [K⁺] and an interaction with the use of renin-angiotensin-aldosterone system blockers were also identified.

Although TEWL was not significantly correlated with histochemical skin data, which further excludes a barrier water loss disproportionate to Na⁺ loss in the maintenance of a putative hypertonic interstitium, it was positively associated with sweat volume and circulating VEGFc. Modulation of both sweat generation and trans-epidermal evaporation requires a rich and competent dermal microcirculation, which is regulated - among many other factors - by VEGFc via VEGFR2 and VEGFR3 (Simons et al., 2016).

The exact role of this interplay remains to be elucidated. However, with the acknowledged limitations of 1) a cross-sectional study design which prevents conclusions on causality and role of confounders, 2) the use of pilocarpine-stimulated sweating rather than a whole-body washdown or similar approaches (Lemon et al., 1986, Shirreffs and Maughan, 1997) and 3) the lack of information on sweat rate/composition or TEWL during exercise, this preliminary body of evidence suggests that neurohormonal axes and peripheral (micro)vascular function could directly modulate sweat and TEWL. These, in turn, could play an active role in the regulation of total body Na⁺ and water in hypertension. Of note, these mechanisms are potentially actionable (Laukkanen et al., 2018).

In summary, and regardless of local mechanisms of regulation, S₂ALT data call for reconsideration of excess tissue Na⁺ in light of a pragmatic histochemical approach: while it cannot - and was not designed to - unconditionally exclude an hypertonic Na⁺ accumulation in any tissue milieu or any clinical/experimental condition, it firmly supports preclinical evidence already presented in chapters 4-5 and raises due caution in the interpretation of tissue Na⁺ data. Bhavé and Neilson in their “hypothetical

framework” made the contention that “real” excess (water-independent) Na⁺ storage would occur only with very-high sodium diet (>300 mEq/d), thus concluding that “*only about 5% of essential hypertension in American patients may involve alterations in (tissue) Na⁺ storage*” (Bhave and Neilson, 2011).

Either their projection was excessively conservative, or the epidemics of high Na⁺ signal later observed by ²³Na-MRI in aging, uncontrolled and/or secondary hypertension, diabetes, CKD, heart failure and systemic sclerosis is (at least in a considerable part) a different phenomenon, i.e. subclinical oedema. Numquam est ponenda pluralitas sine necessitate (Duns, 1497).

I now interpret many of the aforementioned ‘at-risk’ patients as part of a “congestion continuum”, which can directly impact on the function of vessels and other organs and can ultimately lead to the overt syndrome currently identified as “heart failure”. The latter is the specific topic of discussion of the next chapter.

INTERSTITIUM AND MICROVASCULAR FUNCTION

7.1 Background and study aims

Heart failure (HF) is a leading cause of morbidity and mortality (Benjamin et al., 2018). Current trends of increased heart failure hospitalizations are mostly driven by heart failure with preserved ejection fraction (HFpEF), carrying a 1-year prognosis almost as poor as in patients with reduced ejection fraction (HFrEF; Chang et al., 2018, Campbell et al., 2012, Borlaug et al., 2006).

HFpEF is a clinical syndrome closely associated with multiple cardiovascular comorbidities and risk factors, such as hypertension, obesity, coronary artery disease, diabetes mellitus, atrial fibrillation and chronic kidney disease (Pfeffer et al., 2019). The notion that these comorbidities are not just associated with HFpEF but may be directly involved in its pathogenesis via comorbidity-associated inflammation and coronary microvascular dysfunction (Paulus and Tschope, 2013) has gained support from a large body of post-mortem, non-invasive and invasive evidence (Shah et al., 2018, D'Amario et al., 2019, Mohammed et al., 2015). In addition to the coronary vascular bed, peripheral vessels also appear dysfunctional (D'Amario et al., 2019). In particular, impaired systemic vasodilator reserve and low skeletal muscle capillary density, as well as low peripheral O₂ extraction paralleling microvascular rarefaction, were reported as determinants of exercise intolerance in patients with HFpEF (Borlaug et al., 2006, Haykowsky et al., 2011, Kitzman et al., 2014, Dhakal et al., 2015). Such findings challenged the paradigm of a purely cardiac disorder in favor of a more systemic phenomenon (Kitzman et al., 2015). However, whether and how a dysfunctional microcirculation could directly impact congestion, “the core of the HF syndrome” (Pfeffer et al., 2019), has not yet been investigated.

In the previous chapters, the concepts of tissue Na⁺ accumulation and Na⁺- driven lymphatic network expansion (Machnik et al., 2009) have been extensively discussed. Notably, tissue Na⁺ excess was found in most of the conditions/risk factors associated with the clinical HFpEF syndrome (i.e. older age, hypertension, diabetes, chronic kidney disease; Kopp et al., 2013, Karg et al., 2018, Schneider et al., 2017). At the time the herein presented study was conceived, results from the model (Chapter 4), rat body composition study (Chapter 5) or S₂ALT study (Chapter 6) were not available and the

putative hypertonic nature of tissue Na⁺ excess in HFpEF, as well as its functional relevance to fluid homeostasis, had not been demonstrated.

Therefore, the *Heart Failure with Preserved ejection fraction: Plethysmography for Interstitial Function and skin biopsy* (HAPPIFY) study was designed to investigate capillary-interstitium fluid exchange and to test the hypothesis that an osmotic effect secondary to high interstitial Na⁺ levels could impact microvessels and result in excess fluid extravasation and oedema in patients with HFpEF.

Secondary analyses included the assessment of arterial function in patients with HFpEF by “classic” methods, i.e. measures of arterial stiffness and flow-mediated dilatation, and by ex-vivo functional evaluation of subcutaneous resistance arteries by wire myography, in comparison to healthy subjects of similar age and sex; additionally, the subcutaneous microvasculature – including lymphatics - was anatomically and molecularly compared between groups.

7.2 Study- specific methods

7.2.1 Protocol and subjects

The HAPPIFY study conforms to the Declaration of Helsinki and the protocol (Appendix 4) was approved by the West of Scotland Research Ethics Committee 3 (ref. 17/WS/0091) and Greater Glasgow and Clyde (GG&C) NHS Research and Development (ref. GN17CA152).

Subjects with HFpEF identified from outpatient HF clinics in Glasgow, UK, and healthy volunteers with no history of cardiovascular or renal disease, hypertension or diabetes, recruited by public advertisement (Appendices 5-6), were invited to an eligibility visit where inclusion and exclusion criteria were reviewed. HFpEF diagnosis was per the 2016 European Society of Cardiology guideline definition: (i) signs and/or symptoms of HF clinically stable for > 1 month, (ii) elevated BNP > 35 pg/ml, (iii) an ejection fraction \geq 50% and (iv) evidence of structural heart disease (left atrial enlargement and/or left ventricular hypertrophy) or diastolic dysfunction.(Ponikowski et al., 2016) Patients with history of recent (<3 months) cerebrovascular event, myocardial infarction or coronary revascularisation; significant valve disease; unstable coronary artery disease; hypertrophic/infiltrative cardiomyopathy or constrictive

pericarditis; chronic kidney disease > stage 3 were not considered for participation. General exclusion criteria also entailed history of idiopathic oedema/capillary leak syndrome, myxedema, lymphatic obstruction; evidence of systemic inflammation at the time of study visit; active malignancy or any major hypercoagulable state or history of venous thrombosis/embolism on no ongoing anticoagulation; incapacity. Study procedure-specific exclusion criteria are listed below in the pertinent subsections.

The eligibility and main visits were conducted in the morning, in a temperature-controlled room, asking participants to refrain from caffeine and smoking, to fast for >8 h (eligibility) or >4h from a light breakfast if prolonged fasting for the whole night and morning was deemed unfeasible/unsafe (main) and to avoid vasoactive (ACE inhibitors/ARBs, beta blockers, calcium channel blockers, nitrates) or diuretic medications on the morning of the visit.

The study procedures included history/physical examination; full blood count, BNP, HbA1c and renal, liver and thyroid function; urinary albumin-to creatinine ratio (morning spot sample); simultaneous bilateral brachial and calf blood pressure measurement; two-dimensional echocardiography; flow-mediated dilatation; pulse wave velocity/analysis; venous occlusion strain gauge plethysmography and a gluteal skin punch biopsy.

Participants without specific contraindication (e.g. ongoing anticoagulation) were offered to participate in an optional sub-study (Appendix 4) involving surgical collection of extra skin and subcutaneous fat tissue around the site of the punch biopsy for dissection of resistance arteries and/or molecular biology.

7.2.2 Blood pressure measurement

Participants underwent 3 consecutive bilateral simultaneous measurements of brachial artery blood pressure (BP) values with a calibrated oscillometric monitor after 5 minutes of supine rest; office BP was determined as the average of the 2nd and 3rd readings. Similar measurements were later performed on the calves, up to 3 times if tolerated. Mean blood pressure (MBP) was calculated as $(0.33 \times \text{Systolic BP}) + (0.67 \times \text{Diastolic BP})$; a difference > 3 mmHg in limb MBP between sides was accounted for in the calculation of arterial resistance to flow with plethysmography (see below).

Normotension as inclusion criterion for healthy controls was defined upon evidence of office BP < 140/90 mmHg, or confirmation by 24h ambulatory blood pressure monitoring for those who showed office BP values above such threshold, without any antihypertensive medication.

7.2.3 Echocardiography

Two-dimensional echocardiography with Doppler and tissue Doppler imaging was performed by a single operator during the eligibility visit, using a Siemens ACUSON SC2000 system. Cardiac structure and function were blindly quantified off-line at the end of the study, as recommended by the American Society of Echocardiography / European Association of Cardiovascular Imaging (Lang et al., 2015, Nagueh et al., 2016).

7.2.4 Traditional non-invasive assessment of arterial function

7.2.4.1 Brachial artery Flow Mediated Dilatation (FMD)

FMD measurements were performed according to guidelines (Thijssen et al., 2011), during the eligibility visit, with a semi-automated device, as extensively detailed in Chapter 2 (2.3.2.3). Scans judged as non-diagnostic at the time of the eligibility visit (if intima-intima was not stably visible throughout the reading, in case of gross arm misplacements and/or overt failures of the probe position adjusting software) were repeated at the beginning of the main visit under the same conditions. All the images and automated outputs were manually reviewed and analysed with UNEX software off-line at the end of the study. Outputs from any scan previously judged as non-diagnostic but rescued by off-line analysis were averaged with results from the second scan, if available. The analysis was conducted blind to the group allocation of scans.

7.2.4.2 Pulse Wave Analysis (PWA) and Velocity (PWV)

Pressure waveform analysis (PWA) and pulse wave velocity (PWV) measurement were performed during the main visit with a SphygmoCor XCEL System, in a supine position after 5 minutes of rest. Rationale for and details on use of PWA and PWV for vascular phenotyping have been discussed in Chapter 2.

For PWA, multiple sequential artery pressure waveforms were acquired from a dedicated brachial cuff and averaged into an ensemble, used by the software to derive and synthesize the central aortic pressure waveform parameters.

For PWV, the carotid-femoral (cf) distance was calculated by the SphygmoCor software by subtraction method from the sternal notch to the top edge of the femoral (thigh) cuff and from the patient's carotid measurement site to the sternal notch. Once the system detected a carotid pulse signal of valid quality from the tonometer, a femoral cuff was inflated and the cfPWV measurement started automatically. All measurements were taken consecutively in duplicate, whenever possible, and averaged. Inaccurate measurements, according to the automated quality control, were discarded.

7.2.5 Plethysmography and microvascular fluid dynamics

Rationale and approach for use of strain gauge plethysmography (EC6, Hokanson) to measure forearm and calf arterial blood flow (Φ), peripheral venous pressure (P_v , as a surrogate for central venous pressure - CVP) and net fluid extravasation toward the interstitium at increasing venous occluding pressures have been extensively described in section 2.3.3 (Gamble et al., 1993, Wilkinson and Webb, 2001, Gamble, 2002, Stewart, 2003, Bauer et al., 2004).

Briefly, patients were positioned almost supine. Measurements were performed in the non-dominant arm and ipsilateral calf, unless local contraindications/exclusion criteria (e.g. previous surgery or stroke, venous varices) applied. Limbs were maintained at the height of the right atrium. Inflatable cuffs for venous occlusion were placed proximal to the strain gauges. P_v was determined by gradually increasing the occlusion pressure, sustained until any limb volume change was detected. Arterial blood flow was determined from the rate of change in limb volume after consecutive cycles of sudden venous occlusion to 45 mmHg, as described (Wilkinson and Webb, 2001). Arterial resistance to flow was calculated as $(\text{mean BP} - P_v)/\text{blood flow}$ (Stewart, 2003). To assess microvascular filtration parameters, we used cumulative 8 mmHg occluding pressure steps, lasting 3.5 minutes each and starting at the first multiple exceeding P_v , up to a maximum of 56 mmHg or less if diastolic BP was lower. The time courses (slopes) of limb volume change (in ml/100ml of tissue) at each pressure step, after exclusion of the initial curvilinear phase corresponding to venous filling, was calculated off-line (*LabChart*) as the averaged first derivative from portions of tracing

devoid of motion artifacts, and corresponds to interstitial fluid accumulation. These slopes were plotted against P_{cuff} to determine the relationship between interstitial fluid accumulation and experimental increases in hydraulic pressure.

Least-square fitting of at least 3 valid pressure points was used to identify these linear associations for each limb/participant, in order to determine the slope (microvascular filtration coefficient, K_f) and the intercept with the pressure axis (i.e. P_i ; Figure 2-6), blindly to group allocation. Limbs with less than 3 points free of motion artefacts for regression fitting (Gamble et al., 1993, Mohanakumar et al., 2019) or with predefined limb-specific exclusion criteria were excluded from analysis.

7.2.6 Surgical skin samples

All participants (except for 1 patient, due ineffective topical anesthesia) underwent a 4-mm skin punch biopsy on a gluteal external upper quadrant, after topical anesthesia with Na^+ -free lidocaine cream (LMX4, Ferndale) as described in Chapter 2.

Surgical-specific exclusion criteria were allergy to lidocaine or chlorhexidine gluconate; chronic diffuse skin condition without uninvolved areas suitable for biopsy; history of keloid scar formation; known diagnosis of hepatitis B or C or HIV or decline to undergo a skin/gluteal biopsy. The excised skin sample was cut on the bench into two hemicylinders, each including both epidermis and dermis: one was fixed in paraformaldehyde 2% for 8-10h at room temperature, washed in phosphate-buffered saline (PBS) and stored in 70% ethanol at 4°C until paraffin inclusion for subsequent histological analyses; the second was immediately put into a pre-cooled Eppendorf tube, frozen in dry ice and stored at -80°C until tissue chemical analysis.

Participants who were eligible and consenting also to an *ex vivo* sub-study, subsequently underwent a skin and subcutaneous fat biopsy (measuring approximately $2.5 \times 1 \times 1.5$ cm) on the same gluteal site, upon anaesthesia with subcutaneously-injected lidocaine 2%. Predefined additional exclusion criteria for this procedure included ongoing treatment with warfarin or other anticoagulant medication or severe obstructive iliac artery disease. A small portion of the excised dermis and epidermis was immediately frozen in dry ice and stored at -80°C for molecular biology (n = 7 HFpEF and 10 HC); the remaining available tissue was used to dissect small resistance arteries for *ex vivo* functional testing.

7.2.7 *Ex vivo assessment of vascular function*

The protocol for the functional assessment of resistance arteries has been reported in Chapter 2, section 2.3.1. Briefly, small arteries were freshly dissected from fat/dermis, stored at 4°C in physiological saline solution overnight and, on the following day, cut into 2-mm ring segments, which were mounted on isometric wire myographs. Vessels with an internal diameter $\geq 500 \mu\text{m}$ were excluded. (Mulvany and Aalkjaer, 1990, Heagerty et al., 1993) After normalization and assessment of viability by the addition of KCl (62.5mmol/L), endothelium-dependent and -independent relaxation was assessed by a dose-response to acetylcholine (Ach; 10^{-10} - 3×10^{-5} M) or the nitric oxide (NO)-donor sodium nitroprusside (SNP; 10^{-10} - 10^{-5} M), respectively, following pre-constriction with the thromboxane agonist U46619 dose that produced 75% of the maximal contractile response.

7.2.8 *Skin histochemical analysis*

The protocol for water and Na^+/K^+ tissue content analysis has already been described in Chapter 2 and is only briefly recollected here. Frozen skin samples were macroscopically transversally cut into a superficial layer (including the epidermis and the immediately adjacent superficial dermis; ESD) and a deeper dermis layer (DD) in a cold room, to prevent evaporation of moisture. Tissue water content was estimated by a gravimetric approach as wet weight (WW) – dry weight (DW), obtained after desiccation at 65°C for > 40 hours and assessed on a 5 decimal (0.00001 g) scale (Ohaus, DV214CD). Tissue Na^+ and K^+ were measured in the HNO_3 -digested samples by flame photometry (Sherwood scientific, 410C) and expressed as absolute content (mmol/gDW) or concentration (mmol/l, after normalization by tissue water). Flame photometry analysis was conducted blind to group allocation of samples.

7.2.9 *Skin microvascular immunofluorescence and image analysis*

Paraffin embedded skin sections (5- μm -thick) including both epidermis and dermis were mounted on Superfrost Plus Adhesion slides (Fisher Scientific UK Ltd), deparaffinized in xylene and rehydrated through baths of ethanol solutions (100% to 50%) to dH₂O. Sections from all participants were further processed in a single batch to maximize homogeneity of handling and staining. Antigen retrieval was performed by overnight incubation in Unitrieve (Innovex Biosciences) at 42°C; this approach was

preferred over high-temperature/pH-based approaches upon evidence of better preservation of dermal architecture in the SKILLS study (see section 2.2.3.1). After blocking in 15% donkey serum (D9663, Sigma) + Tween20 0.05% in TBS for 1h at room temperature, sections were incubated overnight at 4°C with a goat anti-human Lyve-1 antibody (AF2089, R&D systems) at a concentration of 3 µg/ml in TBS/15% serum; matched isotype goat IgGs (Vector laboratories) were used as negative controls. On the following day, sections were washed and incubated with Alexa-fluor-488-conjugated donkey anti-goat IgG secondary antibody (2 µg/ml; Invitrogen) for 1h at room temperature and counterstained with Ulex europaeus agglutinin I (UEA-I) lectin conjugated to Rhodamine (RL-1062, Vector Laboratories), specifically binding glycoproteins and glycolipids on human endothelial cells (Holthofer et al., 1982), at a final concentration of 10 µg/ml in 1xTBS for 30 mins at RT. After treatment with Sudan Black 0.1% to minimize autofluorescence, slides were stained with DAPI (100 µg/ml; Life technologies), mounted in ProLong Gold anti-fade mounting media overnight at room temperature and then stored at 4°C in the dark.

Tiled images of the entire epidermal line and the sub-papillary dermis (≥ 2 mm of minimal imaged thickness), where the blood and lymphatic network are consistently located (Figure 7-1), were acquired at 20 \times magnification using an inverted epifluorescence microscope (Axio Observer Z1, Zeiss) and a dedicated software (Zen Blue Program, Zeiss). Laser excitation and acquisition settings were maintained constant across all slides. Automated image analysis for the quantification of microvessels was performed with ImageJ, blind to group allocation of samples. The 600-µm-thick dermal area starting from the epidermis-dermis junction and spanning the entire length of the biopsy, with the exception of portions affected by gross mounting/staining artefacts, was manually identified and selected (Figure 7-1). After splitting RGB channels, a standardized threshold algorithm was used for vessel detection and measurement of total Lyve1⁺ and lectin⁺ area (as % of total selected dermal area); the stain intensity threshold was set to exclude nonspecific staining, including the faint and inconsistent lectin⁺ staining of lymphatic endothelium (Figure 7-1). On thresholded images, microvascular density (n/tissue mm²) and size (µm²) were measured with the operator-independent ‘*analyze particles*’ command, without circularity constraints due to variability in the orientation of dermal microvessels. Dermal fat quantification was performed with ImageJ, after staining of additional sections from the same samples with Picrosirius Red for 1h. Adypocytes-occupied area was manually identified and expressed as % of total area for comparisons.

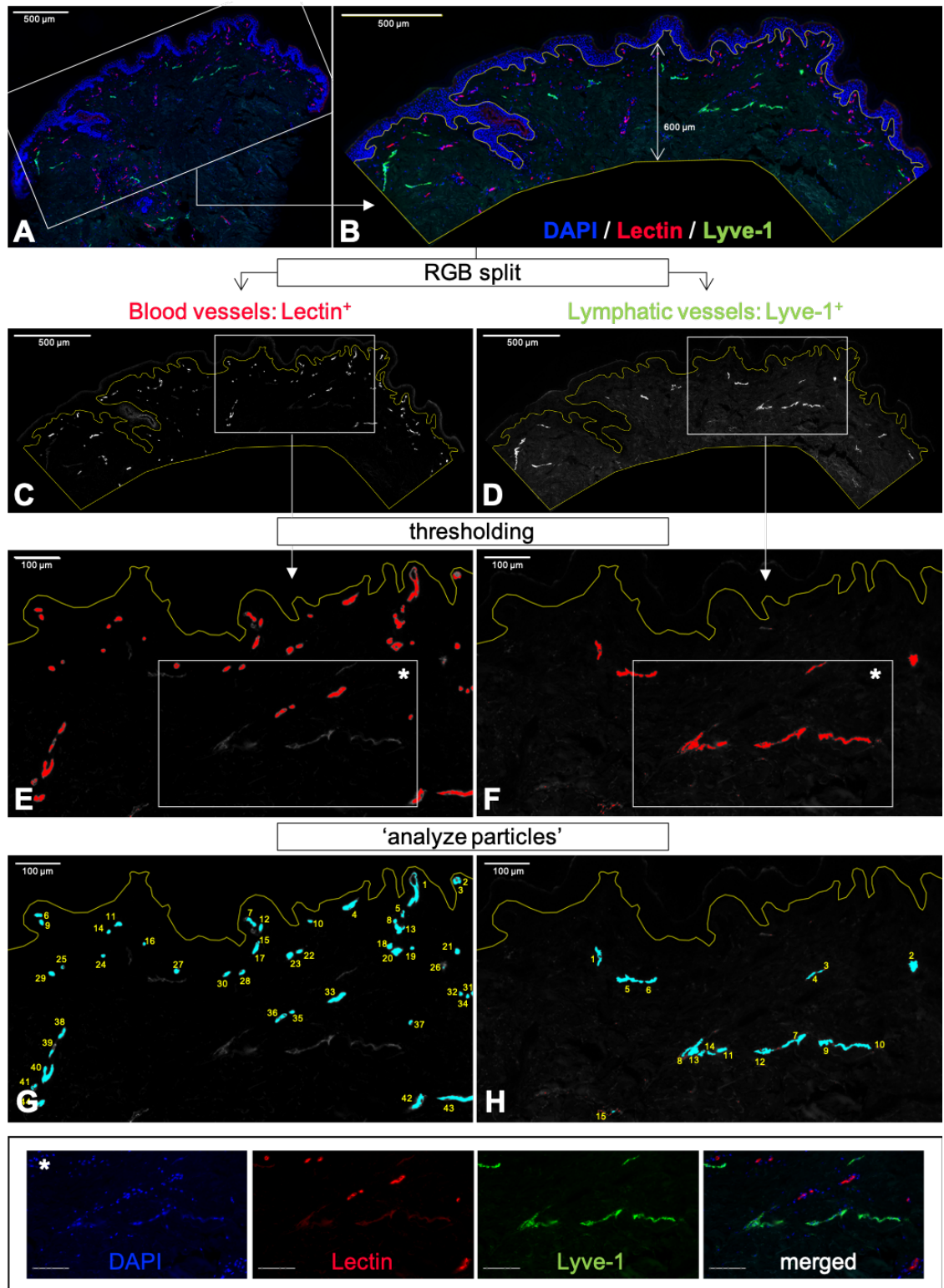


Figure 7-1. Immunofluorescence imaging analysis.

Panel A: Representative tiled image of the entire epidermal line (nuclei in blue; DAPI) and dermis. Dense blood (lectin⁺, red) and lymphatic (lyve-1⁺, green) vascular networks were located close to skin annexes and in the subpapillary dermis. Panel B: the 600-µm-thick dermal area starting from the epidermis-dermis junction was selected as the region of interest (ROI, in yellow). The red (panel C, E, G) and green (panel D, F, H) channels were split to characterize blood and lymphatic vascular network anatomy, respectively, by standardized thresholding (E and F) and ‘analyze particles’ (G and H, count and %area of total ROI). Insert (*) at bottom: the stain intensity threshold for lectin was set to exclude the low and inconsistent lectin⁺ staining of lymphatic endothelium; scale bars = 100 µm.

7.2.10 Skin gene expression analysis

Total RNA was extracted from the frozen skin samples from gluteal surgical biopsies (sub-study; n=17, 7 HFpEF and 10 HC) using QIAzol lysis reagent and RNeasy mini-column kit (Qiagen) according to the manufacturer's instructions. cDNA was generated from total RNA using the High-Capacity cDNA Reverse Transcription Kits (Applied Biosystems). After preamplification (TaqMan® PreAmp technology, Applied Biosystems) of target cDNA, a custom-made TaqMan® Array Card was used to perform quantitative gene expression of markers or growth/transcription factors specific to blood and/or lymphatic vessels, including: VEGF-A (Hs00900055_m1), VEGF-B (Hs00173634_m1), VEGFR1 (or FLT1; Hs01052961_m1), VEGFR2 (or KDR; Hs00911700_m1), VE-cadherin (Hs00901465_m1), Lyve-1 (Hs00272659_m1), Podoplanin (Hs00366766_m1), Prox-1 (Hs00896293_m1), VEGF-C (Hs01099203_m1), VEGFR3 (Hs01047677_m1). Real-time PCR was run with samples in duplicate in a QuantStudio™ 12K Flex System. Gene expression levels were compared and presented as Δ Ct values, with β -actin (Hs99999903_m1) as housekeeping gene based on evidence of CT consistency between study groups.

7.2.11 Statistical analysis

No previous data on K_f were available in HFpEF or similar aged populations for formal power calculation. Based on the heterogeneity of HFpEF and data from different diseases (type 1 diabetes, POTS) (Jaap et al., 1993, Stewart, 2003) we estimated that a sample size of n = 20/group allowed sufficient power to detect the predicted difference in the coefficient of filtration (increase) and in isovolumetric pressures (decrease) between patients with HFpEF and age/sex-matched controls, as well as differences in skin Na^+ based on pilot data in young healthy subjects (Chapter 6). After conclusion of the Ethics-approved duration of the study and recruitment of 16/20 subjects per group, an interim analysis was conducted. The results, herein presented, showed a trend for the coefficient of filtration opposite to what predicted and highly significant differences in isovolumetric pressure. Accordingly, recruitment was stopped for futility in relation to the primary hypothesis and no study extension was requested.

Statistical analysis was performed using Prism (version 8, GraphPad Software) and SPSS (version 25, IBM). Categorical variables are presented as absolute numbers and percentages and compared by χ^2 test. Continuous variables were tested for normality of

distribution by graphical plot and Kolmogorov-Smirnov test; they are presented as mean \pm SD (or SEM when stated) or median (interquartile range), as appropriate. Parametric (t-student) or non-parametric (Wilcoxon) unpaired unadjusted tests were used for comparison of primary (microvascular) and secondary endpoints between groups, accordingly. The combined effect of time and group on shear rate during FMD was tested by two-way ANOVA; time-clusters for differences between curves were defined based on ≥ 3 significant differences at consecutive timepoints based on multiple-t-test.

Least square fit was used for both non-linear regression (*ex vivo* vascular function; log(agonist) vs. response, no slope constraint) and linear regression (Na⁺/water content in skin biopsies; interstitial fluid accumulation and calculations of K_f and P_i). Comparisons of curves for vascular function and skin Na⁺/water regression slopes was performed by the extra sum-of-squares F test. Correlations were assessed by Spearman test.

The α level was set at 0.05 and all statistical tests were 2-tailed.

7.3 Results

7.3.1 Subject characteristics

Between August 2017 and December 2018, 16 eligible subjects with HFpEF and 16 healthy controls (HC) were recruited.

Clinical characteristics of the two study groups are provided in Table 7-1.

Patients with HFpEF and HC were similar for age and sex distributions. Patients with HFpEF showed typical characteristics, with high prevalence of hypertension, obesity, paroxysmal or permanent atrial fibrillation, left ventricular hypertrophy and signs of atrial remodelling and/or diastolic dysfunction (Table 7-2), diabetes and chronic kidney disease. Compared to HC, they had higher BNP, albuminuria and plasma urea, lower eGFR and haematocrit, but similar plasma albumin.

Table 7-1. HAPPIFY: group characteristics.

Variables	HC (n=16)	HFpEF (n=16)	p
Females	11 (69%)	10 (63%)	0.710
Age (years)	68 ± 5	72 ± 6	0.060
BMI (kg/m²)	25.1 ± 2.9	33.9 ± 4.4	<0.001
Overweight / Obese	8 (50%) / 1 (6%)	4 (25%) / 12 (75%)	<0.001
BSA (m²)	1.78 ± 0.21	2.00 ± 0.28	0.021
SBP (mmHg)	130 ± 14	146 ± 21	0.017
DBP (mmHg)	73 ± 8	71 ± 14	0.659
HR (beats per minute)	60 ± 7	65 ± 16	0.256
Left atrial volume index (ml/m²)	23.3 ± 6.1	46.8 ± 12.8	<0.001
Left ventricular mass index (g/m²)	84.3 ± 17.9	127.8 ± 26.6	<0.001
Left ventricular ejection fraction (%)	63.2 ± 3.5	60.8 ± 6.7	0.222
E/e'	8.0 ± 1.6	10.8 ± 2.9	0.001
Comorbidities:			
Hypertension	-	15 (94%)	<0.001
Coronary artery disease	-	3 (20%)	0.060
Atrial Fibrillation	-	11 (69%)	<0.001
Diabetes mellitus	-	7 (44%)	0.003
Chronic kidney disease	-	7 (44%)	0.003
Smoking (current/prior)	0 (0%) / 2 (13%)	3 (19%) / 7 (44%)	0.011
Medications			
ACEi/ARB	-	14 (88%)	<0.001
BB	-	14 (88%)	<0.001
CCB	-	3 (19%)	0.069
Diuretic (loop/thiazide)	-	15 (94%) / 1 (6%)	<0.001
MRA	-	1 (6%)	0.310
Long-acting nitrates	-	2 (13%)	0.144
Statin	-	8 (50%)	0.001
Digoxin	-	5 (31%)	0.015
Aspirin	-	4 (25%)	0.033
Anticoagulation	-	7 (44%)	0.003
Na⁺	140 (139-142)	140 (136-142)	0.361
K⁺	4.5 (4.2-4.7)	4.2 (4.0-4.7)	0.224
Urea (mmol/l)	5.5 (4.7-6.0)	6.4 (5.9-9.8)	0.007
Creatinine (umol/l)	71 (59-84)	79 (67-90)	0.138
eGFR (CKD-EPI; mL/min/1.73 m²)	81.7 ± 11.0	70.9 ± 17.0	0.042
Urinary ACR (mg/gCr)	4.8 (3.2-6.1)	33.9 (10.7-87.4)	0.001
Haemoglobin (g/l)	145 ± 8.8	133 ± 17	0.022
Haematocrit (%)	44.1 ± 2.5	40.5 ± 4.7	0.013
Albumin	39.3 ± 3.1	37.8 ± 2.7	0.155
BNP (pg/ml)	24 (16-32)	170 (93-320)	<0.001

Data as n (%) for qualitative variables and mean ± SD or median (interquartile range) for normally distributed or skewed quantitative variables, respectively. BMI = Body Mass Index. BSA = Body Surface Area (Mosteller). SBP and DBP = office systolic and diastolic blood pressure. E/e' = average of septal and lateral velocity ratio. HR = heart rate. Chronic kidney disease defined as eGFR <60 mL/min/1.73 m². ACEi/ARB = ACE inhibitors or Angiotensin receptor blockers. CCB = calcium channel blockers. BB = beta blockers. MRA = mineralocorticoid receptor antagonists.

Table 7-2. HAPPIFY: echocardiographic characteristics.

Variables	HC (n=16)	HFpEF (n=16)	p
Diastolic septal wall thickness (cm)	1.0 ± 0.2	1.3 ± 0.2	<0.001
Diastolic posterior wall thickness (cm)	1.0 ± 0.1	1.3 ± 0.2	<0.001
LV mass index (g/m²)	84.3 ± 17.9	127.8 ± 26.6	<0.001
LV end-diastolic volume index (ml/m²)	41.3 ± 10.0	44.2 ± 6.9	0.367
LV end-systolic volume index (ml/m²)	15.2 ± 4.1	17.0 ± 4.3	0.140
LV ejection fraction (%)	63.2 ± 3.5	60.8 ± 6.7	0.222
LA volume index (ml/m²)	23.3 ± 6.1	46.8 ± 12.8	<0.001
E velocity (cm/s)	68.1 ± 14.7	89.8 ± 25.6	0.006
A velocity (cm/s; SR only)	78.3 ± 15.1	76.8 ± 29.8	0.865
E/A ratio (SR only)	0.9 ± 0.2	1.2 ± 0.5	0.198
LV e' velocity – average (cm/s)	8.6 ± 1.9	8.7 ± 1.6	0.900
LV e' velocity – average (cm/s; SR only)	8.6 ± 1.9	7.3 ± 0.7	0.022
LV a' velocity – average (cm/s; SR only)	11.8 ± 2.0	8.7 ± 2.9	0.009
LV s' velocity – average (cm/s)	8.1 ± 1.2	7.4 ± 1.2	0.142
LV E/e' ratio – average	8.0 ± 1.6	10.8 ± 2.9	0.001
LV E/e' ratio – average (SR only)	8.0 ± 1.6	11.3 ± 3.2	0.025
TV regurgitation velocity (m/s)	2.1 ± 0.1	2.6 ± 0.5	0.005

Data presented as n (%) or mean ± SD. LV = left ventricle. LA = left atrium. SR = sinus rhythm at the time of exam (n=8). LV tissue Doppler values are avg of septal and lateral values. TV = tricuspid valve.

7.3.2 Arterial function:

7.3.2.1 Traditional in-vivo assessment

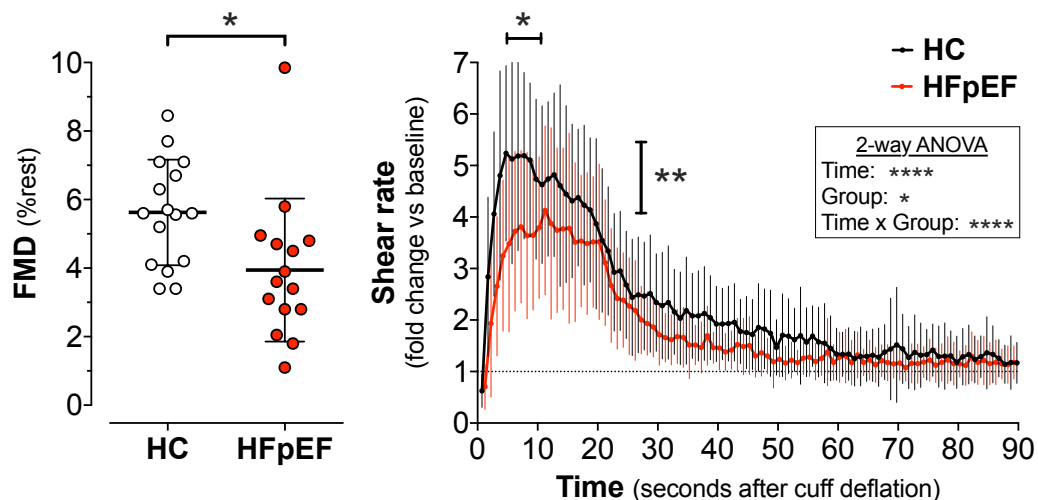
PWA revealed no difference in augmentation pressure or augmentation index between study groups, likely due to the age range investigated and the tendency of these parameters to reach a plateau above the age of 50, at variance with pulse wave velocity (McEniery et al., 2005). In fact, cfPWV was higher in HFpEF compared to HC (Table 7-3; in 3 study subjects no valid measurements could be obtained: 2 HFpEF, 1 control).

Patients with HFpEF also showed an impairment in brachial flow-mediated dilatation, a measure of endothelial dysfunction, but defective vasorelaxation was accompanied by a reduced stimulus to such response, i.e. post-ischemic shear rate (Pyke and Tschakovsky, 2005): reactive hyperaemia relative to baseline was overall lower (2-way ANOVA, $p < 0.001$) and had a different profile with early divergence and delayed time-to-peak compared to HC (Table 7-3 and Figure 7-2).

Table 7-3. HAPPIFY: macrovascular function.

Variables	HC (n=16)	HFpEF (n=16)	p
Pressure Waveform Analysis			
Brachial SBP (mmHg)	129 ± 14	151 ± 28	0.010
Brachial DBP (mmHg)	75 ± 6	78 ± 14	0.382
Central Aortic SBP (mmHg)	120 ± 12	137 ± 25	0.022
Central Aortic DBP (mmHg)	76 ± 6	80 ± 15	0.385
Central Aortic PP (mmHg)	44 ± 10	58 ± 22	0.037
HR (beats per minute)	61 ± 6	67 ± 12	0.171
Augmentation Pressure (mmHg)	16 ± 6	19 ± 9	0.258
Augmentation index @75 (%)	29.3 ± 9.5	28.2 ± 9.1	0.727
Carotid-femoral Pulse Wave Velocity (m/s)	6.8 ± 1.1	8.6 ± 1.3	0.001
Brachial artery Flow-Mediated Dilatation			
Rest internal diameter (mm)	3.78 ± 0.50	3.94 ± 0.67	0.438
Maximal internal diameter (mm)	3.99 ± 0.53	4.13 ± 0.70	0.538
FMD (mm)	0.21 ± 0.06	0.15 ± 0.08	0.033
FMD (% rest)	5.6 ± 1.5	3.9 ± 2.1	0.014
Peak shear rate (× rest)	6.7 ± 1.7	4.6 ± 1.6	0.002
Time-to-peak shear rate (sec)	7.6 ± 2.8	10.9 ± 5.4	0.041

Data presented as mean ± SD. SBP and DBP = systolic and diastolic blood pressure; PP = pulse pressure. HR = heart rate. Augmentation index @75 = HR-corrected augmentation index, assuming HR= 75 bpm.

**Figure 7-2. Peripheral arterial function assessed in vivo.**

Left panel: endothelium-dependent brachial artery flow-mediated dilatation (FMD, expressed as percentage change from baseline) was reduced in patients with HFpEF (red) compared to healthy controls (HC, B/W). Right panel: shear rate imposed on the endothelial surface of the vascular wall during the post-ischemia hyperaemic flow response (i.e. reactive hyperaemia relative to baseline) was also reduced HFpEF compared to HC. Vertical and horizontal black capped lines identify differences in magnitude of and time to peak shear rate, respectively, between groups. Inset: influence of time, group and interaction on hyperaemic response curve profile (2-way ANOVA). All figure data are presented as mean ± SD; * p<0.05, ** p<0.01, **** p<0.0001.

7.3.2.2 *Direct ex-vivo assessment*

In keeping with post-ischemic reactive hyperaemia, subcutaneous resistance arteries of patients with HFpEF showed a reduced ex-vivo endothelium-mediated response to Ach, as evident from a right-shift in the relaxation curves compared to HC (Log IC₅₀ (M) = -7.045 [95% CI: -7.072 to -7.021] vs -7.565 [-7.603 to -7.527], $p < 0.001$; sub-study, $n = 6$ subjects/group; Figure 7-3), particularly impacting the concentration range of the curve that is physiologically critical to flow autoregulation (grey area in Figure). Also maximal endothelial-independent relaxation to the NO donor SNP was reduced in HFpEF (22.0 [18.8 to 24.9]% vs 3.9 [-2.6 to 9.2]% of U46619-induced pre-constriction, $p < 0.001$), although the response was similar to HC for most of the autoregulation physiological range (Figure 7-3). Originally planned comparisons with vessels incubated in hypertonic Na⁺, as done for rats (Figure 5-13), were limited by the number of viable dissected vessels.

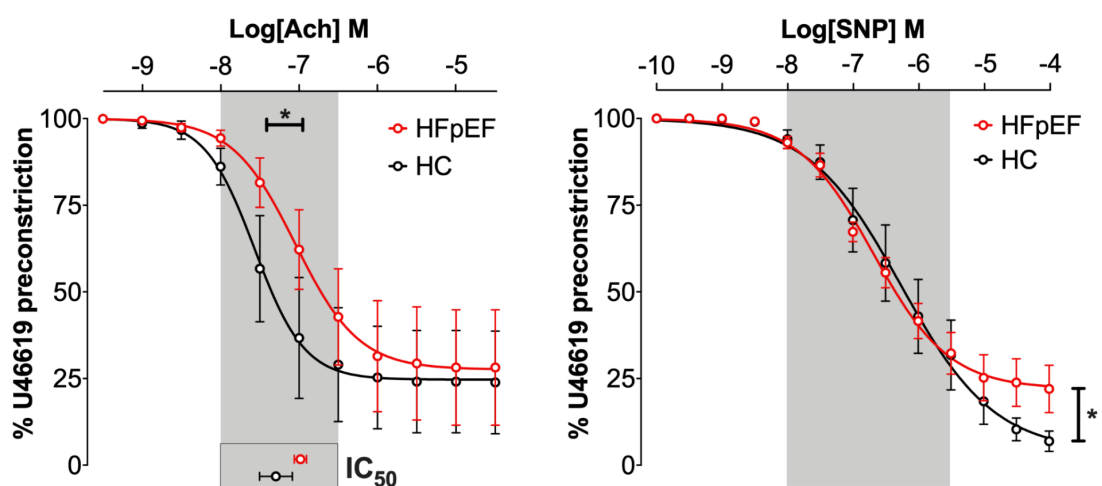


Figure 7-3. Peripheral arterial function assessed ex vivo.

Left panel: endothelium-dependent relaxation to a cumulative concentration curve of acetylcholine (Ach), expressed as percentage of U46619-induced pre-constriction. Subcutaneous resistance arteries of patients with HFpEF showed reduced vasodilation, shown by the right-shift in the HFpEF curve compared to HC: concentrations of Ach required for autoregulation of peripheral blood flow were ~5 times higher in HFpEF than controls. Right panel: endothelium-independent relaxation to a cumulative concentration curve of sodium nitroprusside (SNP), expressed as percentage of pre-constriction, revealing a lower maximal relaxation to SNP in HFpEF. Grey areas highlight the steepest portions of the curves (and relative Ach or SNP concentration ranges, accordingly), critical for fine-tuned peripheral modulation of arterial resistance and flow autoregulation. Horizontal and vertical and black capped lines identify differences in IC₅₀ and maximal relaxation, respectively, between groups. All data are shown as mean \pm SEM; $n = 6$ /group. Vessels from four additional subjects were excluded due to lack of viable vessels [$n=2$ HC], unsuitable vessel size [$n=1$ HC] or spontaneous vasomotor activity generating early loss of vascular tone after pre-constriction, at doses of Ach or SNP unable to physiologically induce relaxation in either group and automatically identified as outliers (Log EC₅₀ Ach: -9.00; ROUT method, $Q = 1\%$), possibly due to vessel damage in the mounting process [$n=1$ HFpEF]. * $p < 0.05$

7.3.3 Skin salt

Water content (%WW - or mg/mgDW, *not shown*), Na⁺ concentration (mmol/L of water) and total Na⁺ content (mmol/gDW) in the epidermis/superficial dermis (ESD) were similar between HFpEF and HC (Figure 7-4, A). In the deeper dermis (DD), water and Na⁺ content were lower in HFpEF than HC (Figure 7-4, B) in keeping with the distribution of BMI and dermal fat (Figure 7-4, C).

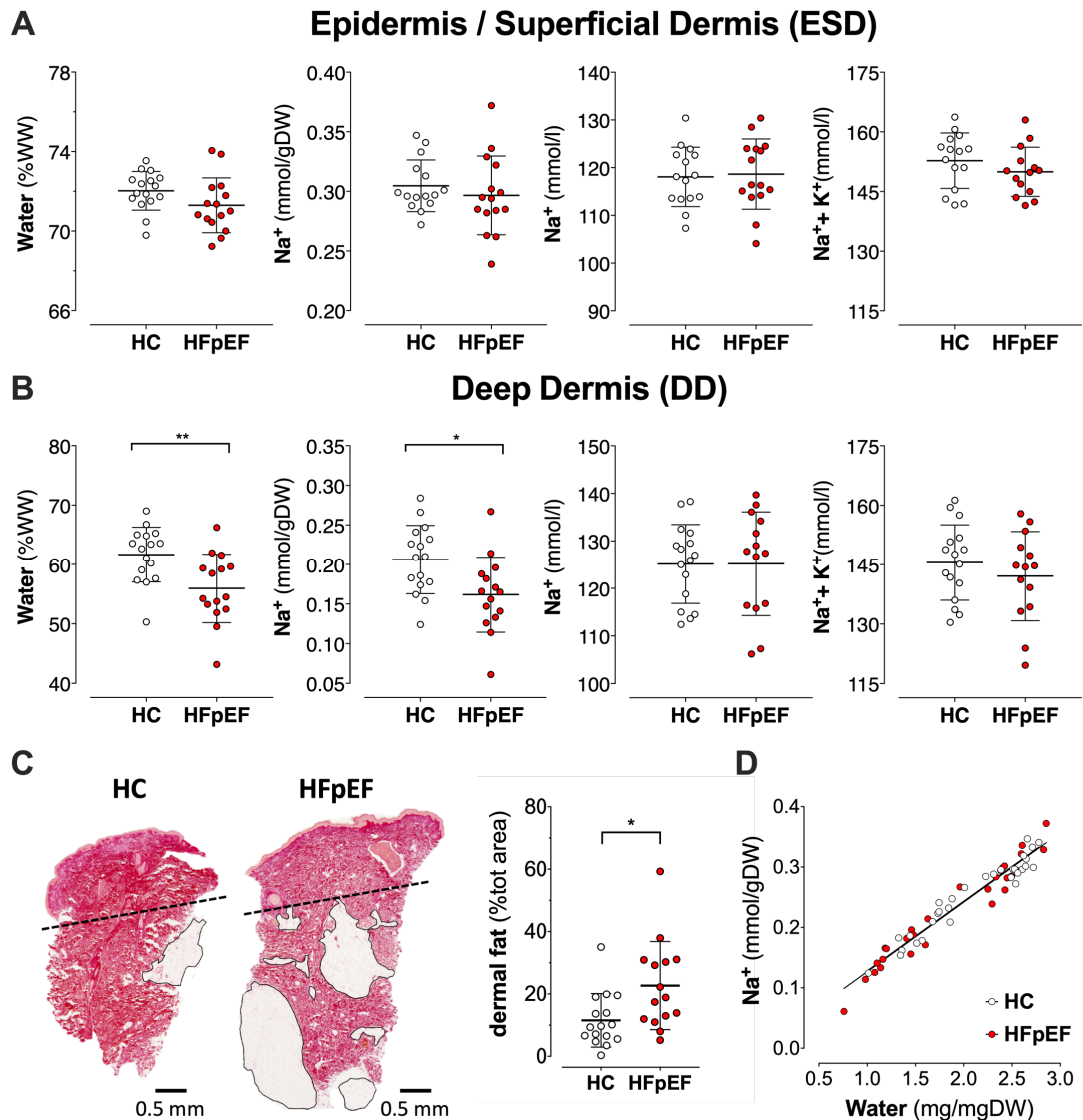


Figure 7-4. Chemical analysis of the skin.

Panels A and B: water content, Na⁺ content, Na⁺ concentration and (Na⁺ + K⁺) concentration in the outer (epidermis and superficial dermis, ESD) and the inner (deep dermis, DD) layers of the skin biopsies. Panel C: representative skin sections from a control and a HFpEF subject (picosirius red staining); dashed line: cutting plane for separation of ESD and DD; black-circled areas represent dermal fat, quantified in the sections as % of biopsy area and more abundant in patients with HFpEF than controls. All data presented as mean ± SD; * p < 0.05, ** p < 0.01. Panel D: association between Na⁺ and water content, including both ESD and DD values; the slope of the regression line was similar between study groups.

As previously discussed (chapters 5 and 6 for both rats and hypertensive subjects), fat limits the volume of distribution of both water and electrolytes in the tissue, while leaving their relative representation overall unaffected: DD Na^+ and $(\text{Na}^+ + \text{K}^+)$ concentrations, i.e. upon content normalization for water, were similar between groups, as in ESD. Both water and Na^+ content in the dermis were inversely associated with dermal fat content, semi-quantitatively assessed by fat-occupied % of biopsy area in histology sections (Spearman $\rho = -0.415$, $p = 0.020$ and $\rho = -0.431$, $p = 0.016$, respectively). No differences were found in the slope of the associations at extra sum-of-squares F test between study groups. $\text{Na}^+ + \text{K}^+$ concentration consistently fell within a physiological range (140-155 mmol/l) in both layers. Likewise, the slope of the regression line for skin water and Na^+ content did not differ by group ($p=0.810$; Figure 7-4, D) or tissue layer (ESD vs DD, $p=0.922$; *not shown*).

These histochemical data were further contrasted with those from the SOWAS study (please see section 6.2.1.2 and Table 7-4 below), where gluteal skin biopsies, sample processing and analysis were conducted with identical approach in young healthy subjects (Y-HC).

Table 7-4. Characteristics of young healthy subjects, for contrast.

Variables	SOWAS	HAPPIFY	
	Y-HC (n=17)	HC (n=16)	HFpEF (n=16)
Females	11 (64.7%)	11 (68.8%)	10 (62.5%)
Age (years)	25 ± 5	68 ± 5	72 ± 6
BMI (kg/m²)	23.8 ± 2.9	25.1 ± 2.9	33.9 ± 4.4
BSA	1.80 ± 0.25	1.78 ± 0.21	2.00 ± 0.28
SBP (mmHg)	112 ± 9	130 ± 14	146 ± 21
DBP (mmHg)	64 ± 8	73 ± 8	71 ± 14
HR (beats per minute)	67 ± 10	60 ± 7	65 ± 16
Na⁺ (mmol/l)	140 (140-141)	140 (139-142)	140 (136-142)
K⁺ (mmol/l)	4.2 (4.1-4.5)	4.5 (4.2-4.7)	4.2 (4.0-4.7)
Urea (mmol/l)	4.8 ± 1.2	5.5 (4.7-6.0)	6.4 (5.9-9.8)
Creatinine (umol/l)	75 ± 13	71 (59-84)	79 (67-90)
eGFR (CKD-EPI; mL/min/1.73 m²)	106 ± 16	81.7 ± 11.0	70.9 ± 17.0
urinary ACR (mg/gCr)	4.7 (2.2-10.5)	4.8 (3.2-6.1)	33.9 (10.7-87.4)

Data presented and abbreviations as per Table 7-1. Due to excess male participants in the original SOWAS cohort (n=18) compared to HAPPIFY, for this comparison sex-matching was achieved by random selection of 6/18 males (via randomly generated sequences). The 11 females were in the early follicular phase of their menstrual cycle, just after period termination.

While formal statistical comparison across different studies does not seem appropriate, Y-HC had a lower BMI, lower SBP and higher DBP, and higher estimated GFR compared to both HAPPIFY groups. Histochemical comparisons (Table 7-5) revealed:

1. an increase in water and Na⁺ content (in ESD) and Na⁺ concentration (in both ESD and DD), as well as the decrease in K⁺ content and concentration (in both ESD and DD), in the old compared to young subjects; this is consistent with histological changes associated with ageing already described in chapter 6 (section 6.3.2)
2. a decrease in DD water and Na⁺ content across groups, consistent with BMI distribution (Table 7-4) as a surrogate for subcutaneous fat;
3. the similar total cationic (Na⁺+K⁺) concentration across groups.

Table 7-5. Skin chemical analysis, contrasted with young healthy subjects.

Variables	SOWAS	HAPPIFY	
	Y-HC (n=17)	HC (n=16)	HFpEF (n=16)
Epidermis / Superficial Dermis (ESD)			
Water content (%WW)	70.6 ± 1.3	72.0 ± 1.0	71.3 ± 1.4
Na⁺ content (µmol/gDW)	264 ± 18	304 ± 21	296 ± 33
Na⁺ concentration (mmol/l)	109.9 ± 4.9	118.1 ± 6.2	118.6 ± 7.4
K⁺ content (µmol/gDW)	99 ± 12	90 ± 12	75 ± 10
K⁺ concentration (mmol/l)	41.0 ± 4.6	34.7 ± 4.3	30.3 ± 4.0
Na⁺ + K⁺ concentration (mmol/l)	150.9 ± 6.4	152.7 ± 7.0	150.0 ± 6.2
Deep Dermis (DD)			
Water content (%WW)	65.6 ± 3.8	61.7 ± 4.6	56.0 ± 5.8
Na⁺ content (µmol/gDW)	228 ± 39	206 ± 43	162 ± 47
Na⁺ concentration (mmol/l)	117.4 ± 7.2	125.1 ± 8.3	125.2 ± 10.9
K⁺ content (µmol/gDW)	49 ± 13	34 ± 8	22 ± 3
K⁺ concentration (mmol/l)	24.9 ± 4.2	20.4 ± 2.9	17.2 ± 2.9
Na⁺ + K⁺ concentration (mmol/l)	142.4 ± 7.3	145.5 ± 9.5	142.1 ± 11.3

Data presented as mean ± SD. WW = wet weight; DW = dry weight.

In summary, the concentration of Na⁺ in the skin of patients with HFpEF was high when contrasted to a previously reported cohort of young healthy subjects, but was accompanied also by higher water content and both were not different from skin values of healthy controls of similar age distribution. Overall, no evidence of any hypertonic, water-independent accumulation of Na⁺ was found in the skin of patients with HFpEF.

7.3.4 Rarefaction of skin microvessels and gene expression

7.3.4.1 Blood microvessels

Patients with HFpEF had dermal rarefaction of blood microvessels compared to HC ($p = 0.003$; Figure 7-5), independent of age (Spearman correlation with number of vessels: $\rho = -0.141$, $p = 0.449$).

No significant difference was observed in the size of skin vessels or in the gene expression of vascular endothelial growth factors A and B (VEGF-A, VEGF-B) and their blood-vessel specific receptors (VEGFR1 and VEGFR2); the expression of VE-cadherin, present in both blood and lymphatic vessels, was not different either (Figure 7-6).

7.3.4.2 Lymphatic microvessels

Lymphatic vessels were similarly reduced in number ($p = 0.012$) but were larger ($p = 0.007$) in HFpEF compared to HC (Figure 7-5). Neither number nor average vascular size showed significant associations with age ($\rho = -0.009$, $p = 0.963$ and $\rho = 0.307$, $p = 0.099$).

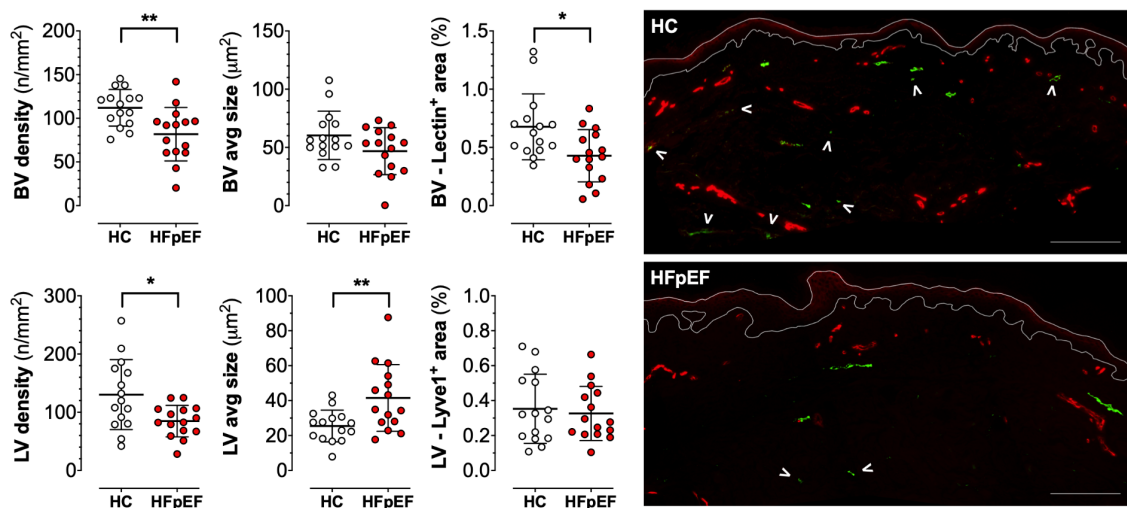


Figure 7-5. Skin microvascular anatomy.

Skin microvascular anatomy assessed as density (number of vessels/mm² tissue), average cross-sectional area of the vessels (avg size; µm²) and total stain⁺ area (expressed as percentage of the dermal area) of the vessels identified in the section. Blood vessels (BV; Panel A) showed a reduction in number and total area⁺; lymphatic vessels (LV; Panel B) were reduced in number but on average larger in size in patients with HFpEF compared to HC. Panel C: representative sections, showing blood vessels (lectin⁺, red) and lymphatic vessels (lyve-1⁺, green); arrowheads: small terminal lymphatic vessels, reduced in HFpEF compared to HC; larger vessels appeared unaffected; scale bar at bottom right = 200 µm. All data are presented as mean ± SD; * $p < 0.05$, ** $p < 0.01$.

In patients with HFpEF, skin prospero homeobox protein 1 (Prox-1, a LEC-specific transcription factor driving development and dynamic maintenance of lymphatic vessels and valves (Srinivasan and Oliver, 2011, Cha et al., 2018)) and lymphatic vessel endothelial hyaluronan receptor 1 (Lyve-1, a marker of lymphatic endothelial cells expressed since the most initial vessels), but not Podoplanin (a glycoprotein generally expressed in the endothelium of lymphatic vessels above a certain diameter (Henri et al., 2016)), were reduced compared to HC. Vascular endothelial growth factor C (VEGF-C) showed a similar trend ($p = 0.06$), but the expression of its lymphatic-specific receptor VEGFR3 did not differ between groups (Figure 7-6).

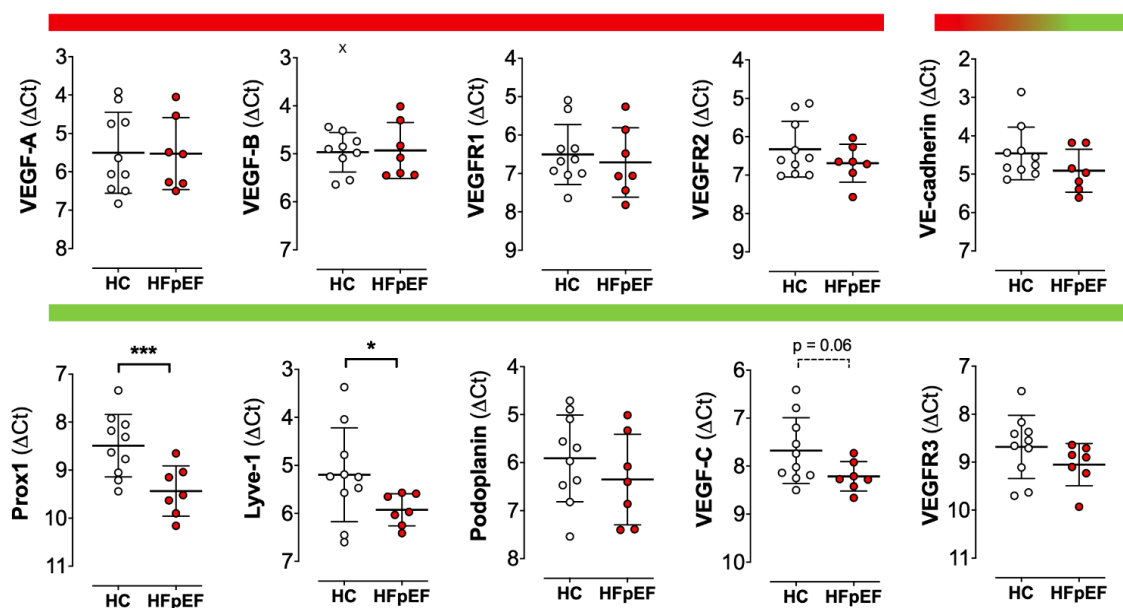


Figure 7-6. Skin microvascular gene expression.

Panel of gene expressions, presented as ΔCt (the higher the value, the lower the gene expression; β -actin as housekeeping gene); coloured bars on top to indicate blood (red), lymphatic (green) or mixed vascular specificity; x = automatically detected outlier (ROUT = 1%, GraphPad Prism). All data are presented as mean \pm SD; * $p < 0.05$, *** $p < 0.001$.

In summary, both structural and molecular skin lymphatic alterations were detected in patients with HFpEF.

7.3.5 Microvascular fluid dynamics

Patients with HFpEF had forearm and calf mean blood pressure, rest limb blood flow (normalized for ml of tissue) and arterial resistance similar to HC; at variance, their rest peripheral venous pressure (P_v) was higher, although not to values suggestive of overt decompensation (Table 7-6).

Table 7-6. Microvascular dynamics.

Variables	HC (n=16)	HFpEF (n=16)	p
FOREARM			
Mean arterial pressure (mmHg)	92 ± 7	94 ± 12	0.529
Blood flow (ml×100ml of tissue ⁻¹ ×min ⁻¹)	1.9 ± 0.8	1.9 ± 0.9	0.992
Arterial peripheral resistance (mmHg/ml×100ml tissue ⁻¹ ×min ⁻¹)	50.1 ± 14.5	56.3 ± 29.5	0.459
Venous pressure (mmHg)	5 (4-6)	8 (7-10)	<0.001
Filtration coefficient, K_f (μl×100ml of tissue ⁻¹ ×min ⁻¹ ×mmHg ⁻¹)	5.66 (4.69-8.38)	5.16 (3.86-5.43)	0.234
Isovolumetric Pressure, P_i (mmHg)	25 ± 5	17 ± 4	<0.001
CALF			
Mean arterial pressure (mmHg)	94 ± 8	96 ± 14	0.555
Blood flow (ml×100ml of tissue ⁻¹ ×min ⁻¹)	3.3 ± 1.6	3.6 ± 1.4	0.573
Arterial peripheral resistance (mmHg/ml×100ml tissue ⁻¹ ×min ⁻¹)	33.1 ± 15.4	29.3 ± 11.8	0.459
Venous pressure (mmHg)	5 (4-5)	7 (7-9)	<0.001
Filtration coefficient, K_f (μl×100ml of tissue ⁻¹ ×min ⁻¹ ×mmHg ⁻¹)	4.66 (3.70-6.15)	3.30 (2.33-3.88)	0.008
Isovolumetric Pressure, P_i (mmHg)	22 ± 4	16 ± 4	0.003

Data presented as mean ± SD or median (interquartile range) and compared with t-test or Mann-Whitney U test, as appropriate.

Because of motion artefacts, 3 forearm (n=1 HFpEF, n=2 HC) and 4 calf (n=3 HFpEF, n=1 HC) tracings were excluded from the analysis of microfiltration; one additional calf tracing from a patient with HFpEF was excluded as per procedure-specific exclusion criteria (overt bilateral venous insufficiency).

The net capillary fluid extravasation toward the interstitium (ml × 100ml of tissue⁻¹ × min⁻¹), induced with progressively higher P_v by stepped inflations of proximal cuffs, was not increased in patients with HFpEF above HC as initially predicted.

In fact, the slope of the regression line between interstitial fluid accumulation and cuff pressure was lower in HFpEF compared to HC in the calf (microvascular filtration coefficient, $K_f = 3.30$ (2.33-3.88) vs 4.66 (3.70-6.15) $\mu\text{l} \times 100\text{ml of tissue}^{-1} \times \text{min}^{-1} \times \text{mmHg}^{-1}$, $p = 0.008$); a similar non-significant trend was observed in the forearm (5.16 (3.86-5.43) vs 5.66 (4.69-8.38) $\mu\text{l} \times 100\text{ml of tissue}^{-1} \times \text{min}^{-1} \times \text{mmHg}^{-1}$; Table 7-6 and Figure 7-7). However, patients with HFpEF also showed a reduced isovolumetric pressure (P_i ; calf: 16 ± 4 vs 22 ± 4 mmHg, $p = 0.003$; forearm: 17 ± 4 vs 25 ± 5 mmHg, $p < 0.001$): in the HAPPIFY *in vivo* experimental setting, this reflects the critical pressure up to which lymphatic drainage can fully compensate for the continuous extravasation of fluid at even low P_V and no net interstitial fluid accumulation occurs (i.e. the intercepts of the lines with x axis, Figure 7-7).

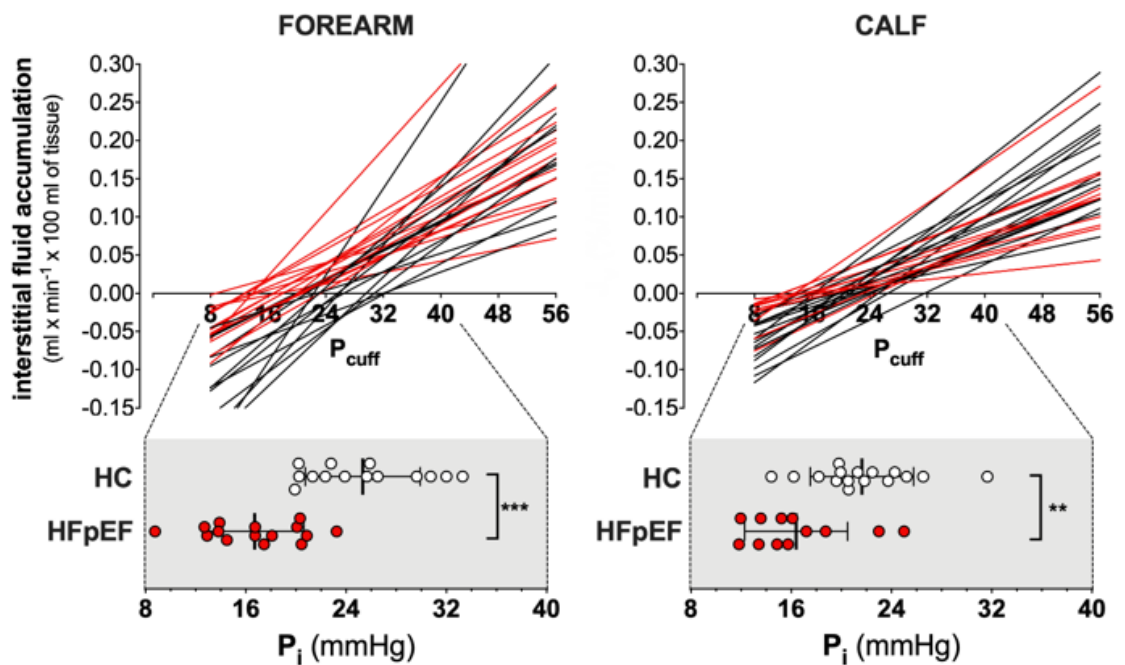


Figure 7-7. Microvascular fluid dynamics.

Net accumulation of interstitial fluid at different hydraulic pressures (P), at which cuffs were inflated to oppose venous drainage in the forearm (left panel) and the calf (right panel). Each regression line corresponds to a participant. The slope of the lines is the microvascular coefficient of filtration (K_f ; please see table 7-6). Red lines (HFpEF) intersect the x axis at lower pressures compared to black lines (HC; scale magnification below): the intersect indicates the threshold above which interstitial fluid accumulation starts to develop (isovolumetric pressure, P_i). Data presented as mean \pm SD; ** $p < 0.01$, *** $p < 0.001$.

In summary, the clearance of interstitial fluid fails early to meet demands imposed by the capillary extravasation induced by hydraulic (venous) pressure in HFpEF.

7.4 Discussion

For the first time in the understanding of HFpEF, the HAPPIFY study extended the concept of microvascular dysfunction to the lymphatic system. As predictable in retrospect, based on the results of the previous studies in rat models and hypertensive patients (chapters 5 and 6, respectively), I failed to identify any tissue Na⁺ hypertonic excess to facilitate oedema or drive peripheral arterial dysfunction. However, I showed that the lymphatic vessels of patients with HFpEF exhibit structural and molecular alterations in the skin and cannot effectively compensate for fluid extravasation and interstitial accumulation by commensurate drainage. Along with direct ex-vivo evidence of primary dysfunctional small subcutaneous resistance arteries and rarefaction of skin blood vessels, as already described in myocardium (Mohammed et al., 2015) and in skeletal muscle (Kitzman et al., 2014, Kitman et al., 2015), this functional and structural vascular impairment further supports the systemic nature of HFpEF syndrome (Kitzman et al., 2015).

7.4.1 Rarefaction of microvessels

Impaired vasodilatation is an established characteristic of patients with HFpEF and contributes to exercise disability (Borlaug et al., 2006). In the HAPPIFY study, this was confirmed not only by classical indirect approaches like brachial FMD and post-ischemic reactive hyperaemia, but also by the first *ex vivo* analysis of vascular endothelium-dependent (via Ach) and -independent (via SNP) relaxation of systemic resistance arteries (Figures 7-2 and 7-3).

In vivo, however, any hyperaemic flow response is critically affected also by the number of ultimate effectors, i.e. vessels, as demonstrated by experimental disruption of coronary microvasculature in pigs (Fearon et al., 2003). In patients with HFpEF, the reduced coronary microvascular density found in autopsy samples (Mohammed et al., 2015) is likely to cause pathological heterogeneity and mismatch in blood supply/demand (Pries and Reglin, 2017), thus impairing myocardial O₂ extraction and performance. Similarly, exercise capacity in HFpEF is further reduced by low peripheral O₂ extraction and skeletal muscle capillary density (Haykowsky et al., 2011, Dhakal et al., 2015, Kitman et al., 2014).

Here I showed that rarefaction of blood microvessels in HFpEF occurs also in the skin, by far the largest human organ and key in the regulation of body haemodynamics. On the other hand, and at variance with the above largely ‘arteriocentric’ paradigms, my findings prompt reconsideration of the role of microvasculature as a whole, to include functions other than vascular resistance homeostasis and structures other than arteries in HFpEF pathogenesis.

7.4.2 Interstitium, microvasculature and congestion in HFpEF

Congestion, i.e. oedema, is central to HF syndrome (Pfeffer et al., 2019) but to the best of my knowledge this study was the first to investigate the fine capillary-interstitium fluid homeostasis in HFpEF.

As extensively discussed in the previous chapters, over the last decade excess Na^+ has been reported in the skin and skeletal muscle of aged hypertensive patients (Kopp et al., 2013), in diabetes (Karg et al., 2018) and CKD (Schneider et al., 2017). This phenomenon had been described in rodents as water-independent (Titze et al., 2003) and capable of stimulating a lymphangiogenic signalling pathway to increase the drainage of tissue Na^+ itself (Machnik et al., 2009). Although a direct demonstration in HFpEF was missing, all the above are typical comorbidities of patients with the syndrome and I originally hypothesised that hypertonic Na^+ accumulation could drag excess fluid out of vessels and thereby favour oedema.

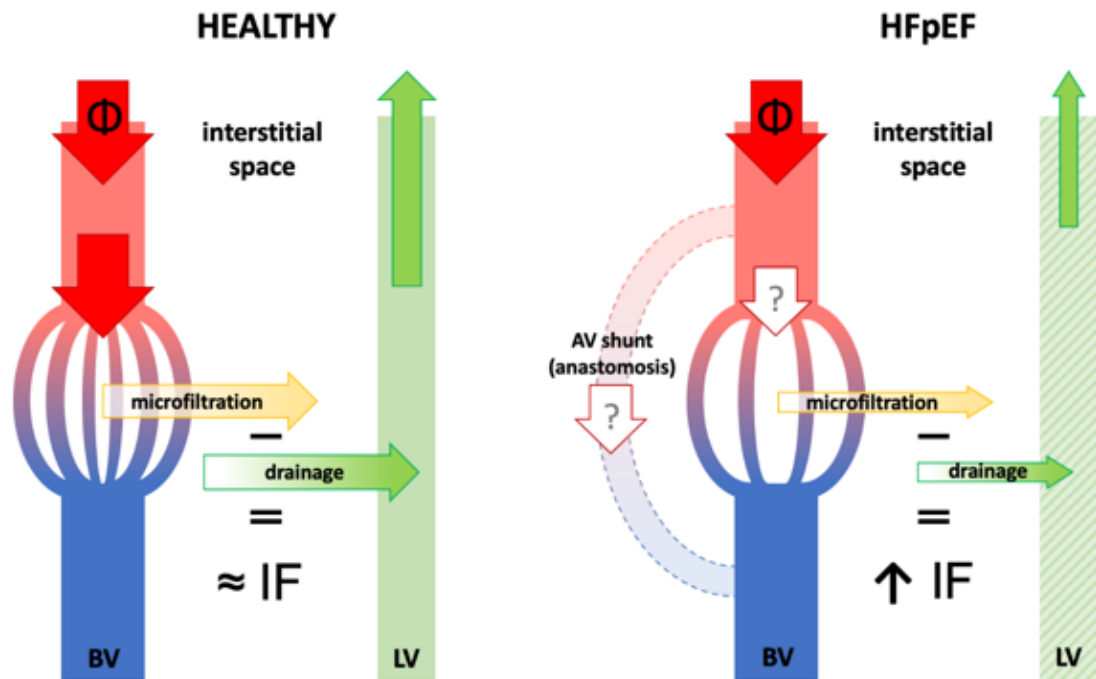
Whilst the concentration of Na^+ in the skin of patients with HFpEF was high when contrasted to a cohort of young healthy subjects (SOWAS, it was accompanied also by higher water content and was not different from controls of similar age distribution, likely reflecting the lack of overt decompensation of HF and oedema in a non-dependent site in our cohort of patients with HFpEF. The excess Na^+ and water content in the skin of our participants compared to young healthy subjects is reminiscent of the age-dependent isotonic Na^+ retention observed also in the S₂ALT study in uncomplicated hypertensive patients (Chapter 6) and reflects the expansion of the tissue extracellular volume. As in that cohort, the identical ($\text{Na}^+ + \text{K}^+$) concentration between study groups rules out any hypertonic Na^+ excess.

Accordingly, and contrarily to my initial expectations, the rate of tissue fluid accumulation induced by increasing hydraulic pressures (i.e. the microvascular

filtration coefficient, K_f) was not higher in HFpEF compared to HC. In keeping with the dependence of K_f on the vascular surface available for fluid exchange and with the rarefaction of blood vessels observed in HFpEF, it actually was lower (Figure 7-8). It is possible that blood flow in HFpEF, similar to HC when normalised by limb volume (Table 7-6), was partially diverted from exchanging capillaries to functional shunting (Pries and Reglin, 2017); in other conditions characterized by increase in local blood flow, e.g. postural tachycardia syndrome, K_f was elevated (Stewart, 2003).

At variance with *ex vivo* preparations, the *in vivo* plethysmographic approach accounted not only for the capillary fluid extravasation regulated by *Starling-Landis* balance, but also for the simultaneous fluid drainage out of the tissue. In fact, contemporary direct measurements of the hydraulic and oncotic interstitial forces revealed that under most conditions there is no sustained reabsorption of interstitial fluid at the venous end of the capillary beds, that transvascular flow is generally unidirectional (from the capillary lumen to the interstitium) and that drainage, up to 8L/day, is provided by lymphatics (Levick and Michel, 2010; please see also chapter 1). Under the assumption that the osmotic pressure of albumin ($\sigma\Pi$) was similar between study groups, based on similar plasma concentrations, the equilibrium hydraulic pressure above which net extravasation of fluids starts to overfill the interstitium (i.e. generate oedema) is mostly determined by lymphatic drainage. The results of the HAPPIFY study showed that this pressure (P_i) was lower in HFpEF compared to HC in both arms and legs. A lower P_i and a higher central venous pressure (CVP, as one can estimate by peripheral venous pressure values in Table 7-6) leaves HFpEF patients with a much lower range of pressures that can be compensated for by their lymphatics.

In other words, they appear to have reduced ‘lymphatic reserve’ (Figure 7-8).



← **Figure 7-8. Microvascular fluid dynamics and reduced lymphatic reserve in HFpEF.**

In healthy subjects, the fluid filtering out of the capillary bed of the blood vasculature (BV) is evenly balanced by commensurate fluid drainage by lymphatic vessels (LV); as a result, the physiological amount of interstitial fluid (IF) is homeostatically preserved. In HFpEF, the net fluid extravasation tends to be lower because of the reduced vascular surface available for fluid exchange (i.e. capillary rarefaction) and the possible diversion of blood flow (Φ) toward arteriovenous (AV) shunts (Pries and Reglin, 2017); however, drainage by the impaired lymphatic system is inadequate to meet demands and facilitates accumulation of interstitial fluid at lower venous pressures. Both anatomical and functional defects (dashed green) could explain the reduced lymphatic reserve.

7.4.3 The lymphatic system in HFpEF

Lymphatic vessels are organized into a series of coordinated functional units, each called *lymphangion*, separated by intraluminal one-way valves and capable of spontaneous pumping activity, as discussed in Chapter 1. Their physiology has striking similarities with heart function, namely a systole-diastole cycle and a contractility modulated by pre- and after-load, conferring remarkable plasticity in response to increased requirements (Scallan et al., 2016). The complexity of contractile machinery, valvular function and electromechanical coordination suggests that also functional impairment, rather than the sole anatomical severance traditionally implicated in most secondary lymphatic disorders, could contribute to disease whenever an imbalance develops between microvascular filtration and lymphatic drainage.

It has indeed been suggested that all “*chronic oedema could be considered as synonymous with lymphedema*” (Mortimer and Rockson, 2014), intended as relative

lymphatic failure or inadequate reserve. The functional results of the HAPPIFY study support this contention in HFpEF.

The morphological changes observed in skin lymphatics, with rarefaction of terminal capillaries and larger residual vessels, as well as the reduced gene expression of factors important for lymphangiogenesis and valve/vascular integrity maintenance (Srinivasan and Oliver, 2011, Cha et al., 2018), offer only preliminary clues as to what sustains the functional defect observed in HFpEF. In particular, I cannot conclusively identify cause and effect. Based on the study results I can only speculate as to whether a constitutive defect or a limited functional reserve of the lymphatic system is a primary predisposing factor toward an overt clinical syndrome when additional insults occur (i.e. comorbidity-driven chronic inflammation and/or elevated CVP) or, *vice-versa*, a result of their long-term, potentially additive detrimental effects (Escobedo and Oliver, 2017, Scallan et al., 2015). The latter, i.e a consequence of comorbidities and of target organ damage with diastolic dysfunction, would be in keeping with morphological changes and impaired maximal lymphatic pumping capacity reported in patients with a Fontan circulation, in whom chronically increased CVP would induce initial compensation of the afterload but long-term failure (Mohanakumar et al., 2019). Conversely, an underlying predisposing defect would remind of cases with secondary lymphedema, where systemic alterations in lymphatic drainage precede the clinical onset of lymphedema and affect also the contralateral limbs (Stanton et al., 2009, Burnand et al., 2012). Detection of lymphatic impairment also in the upper limbs, where not even trace oedema was detectable in either group compared to the calves or ankles of some of our patients with HFpEF, suggests a systemic nature of the phenomenon, although involvement of other organ-specific microvascular beds remains to be investigated.

Regardless of ‘*which-comes-first*’, reduced capacity of the lymphatic system to prevent or minimize development of oedema could mark the clinical and prognostic distinction between patients with uncomplicated comorbidity and those presenting as HFpEF (Campbell et al., 2012). Moreover, by targeting oedema and its dysfunctional/inflammatory implications, improving lymphatic function could improve quality of life, muscle performance and exercise tolerance, disrupt vicious inflammatory cycles and reduce the need or dose of diuretic treatment to maintain sustained decongestion. Of note, although routinely impractical in its surgical approach, successful external thoracic duct drainage in advanced heart failure has already shown therapeutic promise as a proof-of-concept (Witte et al., 1969).

7.4.4 Limitations

In addition to the aforementioned lack of causality demonstration, which warrants additional dedicated studies, other limitations deserve to be mentioned.

Healthy subjects were chosen as controls and comparison of HFpEF with comorbidity-matched patients is missing; similarly, a comparison between HFpEF with and without obesity (Escobedo and Oliver, 2017) would further define the specificity of the findings. Of note, none of the drug classes in use in the study, including calcium channel blockers (Telinius et al., 2014), have been reported to adversely affect lymphatic function *in vivo*.

For my conclusions I assumed similar osmotic pressures of albumin (σ_{II}), critical for isovolumetric pressure *ex vivo* (Levick and Michel, 2010), between groups; as the accurate measurement of leakiness of blood vessels to albumin, i.e. σ , is cumbersome and unfeasible in clinical settings, the assumption was based on similar plasma albumin concentrations. Notably, even if excess permeability of blood vessels in HFpEF were demonstrated, the relative compensation provided by lymphatics would still remain inadequate.

Finally, I assessed multiple physiological parameters and I cannot unconditionally exclude the presence of type I error; similar sample size reasons prevented sub-phenotyping of the HFpEF cohort.

7.5 Conclusions

In summary, this study disproves the original contention of an osmotically active interstitial Na^+ as a possible determinant of oedema in patients with HFpEF: in keeping with results in a general hypertensive population (Chapter 6), no hypertonic accumulation of Na^+ was identified.

However, it provides the first description of morphological and functional changes in the lymphatic vasculature in HFpEF, resulting in reduced clearance of extravasated fluid. Along with demonstration of a reduced blood microvascular density in the skin, such findings draw attention to a globally and systemically defective microcirculation. This definition extends beyond the traditional arterial dysfunction and calls for better

understanding of the role of arteries, veins, lymphatics and their mutual crosstalk for tissue fluid homeostasis in the pathogenesis of this multifaceted, syndromic disease.

In particular, whether the initial lymphatic anatomical and functional expansion observed in rodents under conditions of salt overload (Wiig et al., 2013, Karlsen et al., 2018) would ultimately fail when these conditions become chronic (e.g. in hypertension, diabetes and chronic kidney disease) or cumulative (in elderly comorbid patients) and result in overt HFpEF is an hypothesis deserving further investigation.

DISCUSSION

This thesis depicts a journey. It incorporates multiple studies, different in aims and methodology but underpinned by a common theme, which together advances novel concepts of sodium homeostasis in cardiovascular disease. While some of our findings dispute previous conclusions, other findings support the notion of salt-independent BP effects. The sequence of chapters does not necessarily mirror the chronological sequence of events (and results!) over the course of my PhD. However, it reasonably recapitulates how apparently independent pieces came together and shaped a comprehensive, although still largely open, story.

My interest hasn't been sparked by the current pathophysiological or population science *salt barricades*, i.e. '*primacy of renal changes vs vascular resistance in the pathogenesis of salt-sensitive hypertension*' (Titze and Luft, 2017) and '*need vs futility of lowering the thresholds for recommended salt intake*' (He et al., 2020, O'Donnell et al., 2020), respectively (please see Chapter 1), but rather by the novel reports of a water independent tissue sodium accumulation and, immediately after, of a sodium-driven shift in metabolism.

The results of my investigations synthesise the contribution of kidneys, of vessels (in the broadest meaning of the term) and of the systemic interstitium in the pathophysiological phenomenon of "salt excess", likely transverse to many cardiovascular risk factors and diseases.

8.1 The energetic implications of salt excess

This salt excess, as suggested by the *SYCAMORE* study (Chapter 3), appears to have energetic implications. I showed that kidneys could effectively dissociate Na⁺ and water handling upon high Na⁺ intake in real-life patients as in preclinical settings (Rakova et al., 2017, Kitada et al., 2017). However, they could do so in parallel with glomerular hyperfiltration, higher energy-expensive tubular workload and, ultimately, with a plasma metabolomic signature suggestive of a catabolic state. Catabolism affected mostly proteins, with either muscle mass loss or excess food consumption as putative sources. Both clearly impact body composition and the risk of cardiovascular disease (Bray et al., 2012, Lavie et al., 2012, Medina-Inojosa et al., 2018, Iliodromiti et

al., 2018, Anand et al., 2015, Brandhorst and Longo, 2019), in keeping with reports of an independent association between salt-intake and obesity (Ma et al., 2015).

As acknowledged among limitations, the retrospective cross-sectional design of the study offered no control over caloric intake. This is relevant not only to some differences observed between SYCAMORE and the original study conducted in few healthy subjects (Rakova et al., 2017; please see Chapter 3), but also to the findings of a recent secondary analysis of the DASH (Dietary Approaches to Stop Hypertension)-Sodium trial, where caloric intake was controlled but not fixed (Juraschek et al., 2020).

The DASH (Dietary Approaches to Stop Hypertension)-Sodium trial was a randomised crossover study that primarily examined the blood pressure effects of 3 levels of sodium intake (low = 0.5 mg Na⁺/kcal; medium = 1.1 mg Na⁺/kcal, or high = 1.6 mg Na⁺/kcal) in a parallel-design including a typical Western diet (control diet) or a healthy diet (DASH Diet) in adults with systolic blood pressure (SBP) of 120-159 mm Hg and diastolic blood pressure (DBP) of 80-95 mm Hg. The protocol included 24-hour urine collections at baseline and after each intervention period; urinary Na⁺, K⁺, urea and creatinine were measured in all samples (Sacks et al., 2001). Feeding was controlled and recorded, but not fixed and adjusted approximately weekly with the goal of maintaining constant weight.

By approaching the hypothesis that high salt intake could induce catabolism and weight loss from an opposite perspective, Juraschek et al tested whether low salt intake would then lead to weight gain. More precisely, based on DASH-Sodium design, they tested whether energy intake decreased upon low salt diet to maintain stable weight. At variance, they observed that estimated energy intake decreased and weight increased from low to high sodium study phases (Figure 8-1 for the control diet arm). These findings provide reassurance against a putative weight gain effect of low salt intake but also certify the failure of the trial at adjusting the energy intake of participants to maintain a stable weight, thus preventing other metabolic conclusions in the absence of calorimetry measures.

How to reconcile a decreased energy intake with weight gain upon high sodium diet? I accessed the study data from the National Heart, Lung, and Blood Institute BioLINCC repository (16th March 2020; <https://biolincc.nhlbi.nih.gov/studies/dashsodium/>) for an independent secondary analysis (University of Glasgow MVLS College Ethics

Committee approval, 6th March 2020) and I found evidence of an uneven sodium balance to justify the above (Figure 8-1). My assessment relied on reported dietary intake and urinary excretion and could not account for faecal and sweat losses, but identified excess Na^+ retention upon high sodium diet; if one accepts parallel water retention (not formally assessed in DASH-Na), this would explain weight gain.

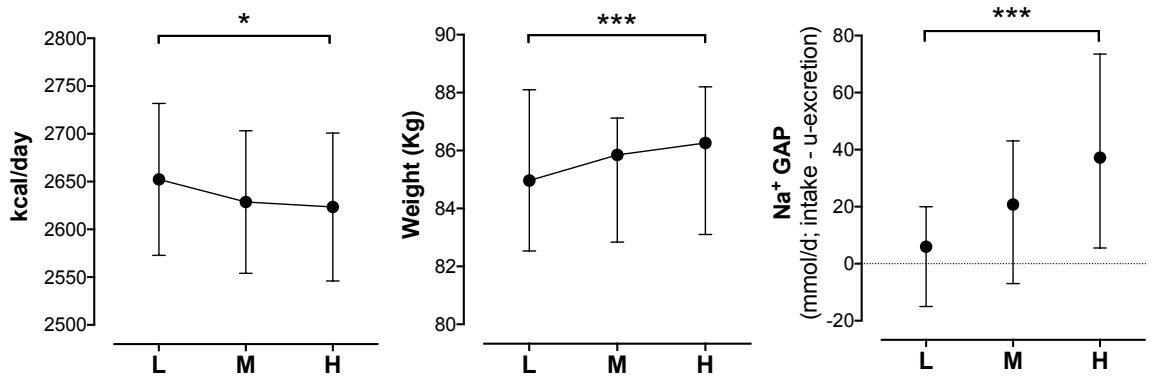


Figure 8-1. Secondary analysis of the DASH-Sodium trial

Left and middle panels: Changes in caloric intake and weight across levels of sodium intake within the control diet arm (highlighted comparisons are Holm-Sidak post-hoc tests of a mixed-model analysis, consistent with results by Juraschek et al); the study goal of maintaining stable weight failed, with weight gain upon high compared to low sodium intake despite lower caloric consumption. Panel D: net daily sodium balance (dietary intake – urinary excretion) at different levels of sodium intake (statistics as above); even balance (i.e. GAP = 0) dotted line for reference. Data presented as median (95%CI); * $p < 0.05$, *** $p < 0.001$.

The finding of uneven sodium balance also fosters additional considerations.

First: whether the underlying body mass of DASH-Na participants was left unaffected in terms of fat vs fat-free composition (and basal metabolic rate/energy requirements, accordingly) remains unknown.

Second: the magnitude and “plasticity upon intake” of the ‘insensible’ routes for water and sodium elimination (e.g. via respiration, sweat, TEWL, stools) remain similarly unknown. My contention, however, is that their contribution is not as trivial as often perceived. Preliminary evidence from the S₂ALT study (chapter 6), consistent with reports from others (Collins, 1966, Braconnier et al., 2020), suggests that sweat and TEWL are important parts of systemic homeostatic mechanisms sensitive to total body sodium and, possibly, to microcirculatory function. Rats loaded with excess sodium exhibited accumulation of water and Na^+ in the lungs (chapter 5), which are unlikely to leave respiratory dynamics entirely unaffected, and had much more watery stools than

controls (*Dr Sheon Mary, personal communication*). All in all, I believe that the suggested “*Randomized Clinical Trial in a Controlled Environment*” to “*end the salt wars*” (Jones et al., 2018) should incorporate multiple measures (i.e. faecal, respiratory, renal, sweat, body composition including calorimetry, physical activity, water and caloric intake - ideally without restrictions -, total body and local Na^+ , as a non-exhaustive list) if the aim were to shed conclusive light on a complex pathophysiology and not just to draw a convenient line for recommended population intake. In light of a foreseeably gigantic effort, should we really bother? The answer likely depends on whether our view of “salt-sensitivity” will move away from a definition based on the sole ‘blood pressure’ biomarker and embrace a broader concept of *Sensitivity* (with capital S, in the next sections), linked to whole-body Na^+ handling and tissue accumulation and possibly modulated by novel therapeutic approaches (please see sections 8.4)

Third: if *Figure 8-1 right panel* is quantitatively (rather than qualitatively) analysed, what is the amount of Na^+ -paralleled water retention? If the positive balance of Na^+ upon high sodium intake were of ~ 35 mmol per day, this would isotonicity correspond to approximately 250 ml of commensurate water, which is admittedly not plausible and not consistent with the degree of weight gain observed in DASH-Na trial (*figure 8-1, middle panel*). Increase in faecal and sweat losses upon high intake, as discussed above, could shift and/or tilt up the ‘*even balance*’ dotted line and make 35 mmol an overestimate, but to what extent? Even 1000 ml of water retention per month, simply due to dietary intake, would appear implausible in a lifespan perspective and are inconsistent with everyday clinical experience. This discrepancy actually reminds of the findings by Heer et al., which initially drove Titze’s investigations and led to the hypothesis of a water-independent hypertonic tissue Na^+ accumulation.

Was it right?

8.2 The nature of salt excess

8.2.1 An isotonic systemic phenomenon

Multiple experimental approaches in the course of my PhD studies were actually designed assuming that a water-independent Na^+ accumulation indeed occurred in tissues, certainly skin and possibly others, with still unknown implications for the

function of surrounding structures beyond what already reported for immune cells. These experiments also included the ex-vivo investigation of vascular function by wire myography in rats (chapter 6) and the in-vivo assessment of the microfiltration coefficient (Chapter 7), under the hypothesis that a hypertonic interstitium would facilitate capillary fluid extravasation.

The very first findings of the rat body composition study, however, appeared at odds with the assumptions, as no Na^+ hypertonicity was detected. Reappraisal of the methodological approach to tissue Na^+ analysis, by means of a theoretical model (chapter 4), provided the opportunity for a shift in perspective.

The simple model lacked some biophysical details (including capillary filtration dynamics and interstitial forces, interstitial matrix biophysical properties, triphasic modelling or exclusion phenomena, just to mention a few) extensively reviewed elsewhere (Aukland and Reed, 1993, Bhave and Neilson, 2011, Wiig and Swartz, 2012) but made it clear that a whole-tissue chemical analysis is substantially affected by the admixture of different and differentially represented tissue components, or by the simple addition of an extra moiety of extracellular fluid, i.e. oedema. In other words, changes in whole-tissue Na^+ concentration did not necessarily reflect hypertonicity.

All subsequent chemical analyses conducted in rat tissues, skin of healthy subjects of young or older age, of hypertensive patients and of patients with HFpEF (chapters 5-7) revealed different Na^+ concentrations but no Na^+ hypertonic accumulation whatsoever. In fact, I re-interpreted the changes in tissue Na^+ as changes in extracellular volume and, when accompanied by parallel water accumulation, as oedema.

8.2.2 A new speculative theoretical framework

How to reconcile a consistently isotonic phenomenon, as assessed by tissue chemical analysis, with the lack of total body water storage commensurate to Na^+ storage observed by Heer et al. or by the DASH-Na trial? In addition to the above discussed limitations of previous human balance studies and to the different proportional changes of Na^+ and water for the same amount of excess extracellular fluid (chapter 4), I speculate that “*sieve*” mechanisms could play a role, as herein discussed (Figure 8-2).

The SYCAMORE study confirmed that kidneys can dissociate Na^+ and water handling upon conditions of Na^+ excess. It is likely that a similar dissociation applies to the other routes of “insensible” water and sodium elimination.

I propose that, whenever the organism is challenged with a Na^+ load exceeding the excretory capacity of Na^+ and of osmotically coupled water, additional mechanisms kick in to guarantee maintenance of total body water (TBW) and tissue isotonicity. These mechanisms would entail the above routes of Na^+ -independent (free) water excretion and intracellular-to-extracellular water shifts, with the cellular membrane functionally acting as a *sieve*. As long as the intracellular space can “make room” for the extra Na^+ , the extra amount of water accompanying the unexcreted fraction of the Na^+ load (or endogenously generated to prevent dehydration) can be eliminated (Figure 8-2). This movement of the ECV/ICV sieve would induce some degree of cell shrinkage and “*osmoadaptive responses in which intracellular electrolytes are gradually replaced by uncharged small organic osmolytes including sorbitol, betaine, myo-inositol, taurine and glycerophosphocholine*” (Cheung and Ko, 2013).

Replacement of K^+ with organic osmolytes would justify the consistently physiologic values of $[\text{Na}^+ + \text{K}^+]$ found in tissues. These responses are usually typical of hyperosmotic conditions and are driven by activation of TonEBP signalling (Choi et al., 2020). In the proposed theoretical framework, TonEBP activation would not be triggered by a hyperosmotic extracellular environment; rather, by the need to maintain it isosmotic, similar to a “clamp”. Increased hydraulic pressure in the extracellular space, by eliciting analogous mechanic stress, could also contribute to the TonEBP activation (Scherer et al., 2014).

Under normal healthy conditions, cessation of the salt-load condition and upregulation of the Na^+ excretion mechanisms would slowly switch down TonEBP signalling, revert the intracellular osmotic replacement phenomenon and bring the condition back to baseline. However, in case of persistent salt-loading or under salt-Sensitive conditions with decreased Na^+ /free water excretory capacity or “stiffening of the sieve” (possibly reflected by alterations in TonEBP signalling as a molecular correlate), the increase in ECV would no longer be compensated and an increase in TBW would ensue. The putative clinical result of this maladaptive response is subclinical or clinically overt oedema.

In addition, persistent total body Na⁺ excess and relative contraction of ICV, via changes in basal metabolic rate and a possible mismatch between energy intake and fat free mass, could facilitate fat deposition and further impact ECV/ICV distribution.

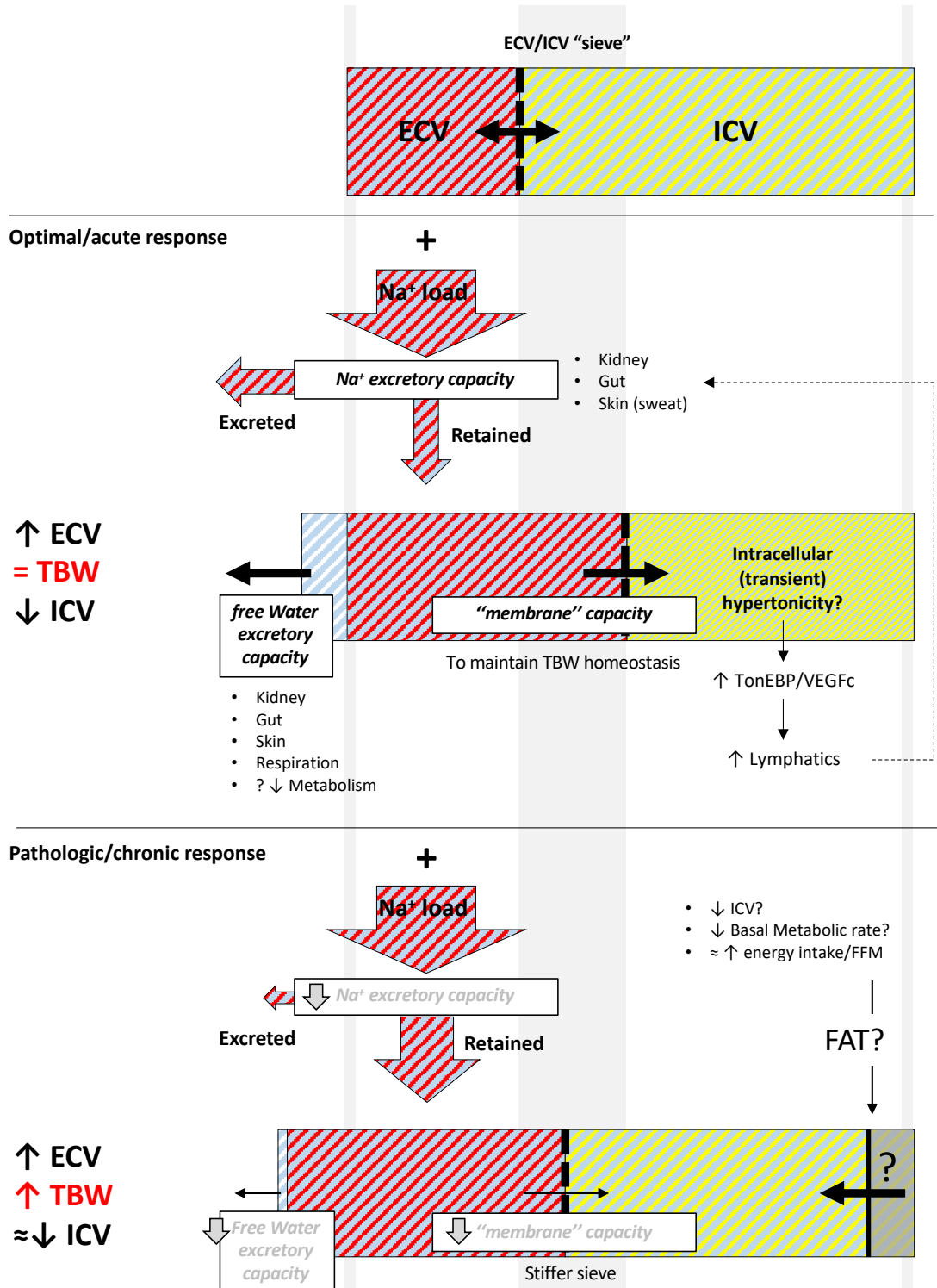


Figure 8-2. The "sieve" hypothesis.

Light blue: water; red: Na⁺; yellow: K⁺. ECV: extracellular volume, rich in Na⁺; ICV: intracellular volume, corresponding to approx. 2/3 of total body fluids, rich in K⁺. TBW: total body water. Middle and lower panels: theoretical response to a Na⁺ load under physiological and pathological conditions. Please see main text.

This complex framework is purely speculative at the time of writing. However, the concept of *fluid shifts* had been suggested also in the original report by Heer et al.: in healthy subjects high sodium intake did not induce total body water storage but induced a relative fluid shift from the interstitial into the intravascular space; notably, intravascular space is the gateway to free-water elimination, via glomerular filtration and tubular handling, as well as via *perspiratio* in the skin or lungs. In essential hypertension, abnormalities in the mechanism regulating the distribution of extracellular water are similarly not new (Tarazi et al., 1969). I herein expand on these concepts, by suggesting that also intracellular to extracellular water exchange could be impaired in hypertension and other salt-Sensitive conditions, by means of an altered *sieve* and TonEBP signalling. Surprisingly, this stress protein has been linked to autoimmune signals and inflammation, bacterial and viral infections, diabetes mellitus and diabetic nephropathy (Choi et al., 2020), but a mechanistic association with oedema (and oedema-related conditions) has never been sought.

In summary, the *sieve* hypothesis moves the attention from the idea of a hypertonic extracellular Na⁺ to those of free-water excretion capacity and intracellular cellular plasticity/response in the pathogenesis of salt-related, or Sensitive, diseases.

8.3 Neglected regulators of interstitial salt excess

Identification of pre-clinical oedema in hypertension and, by pragmatic reappraisal of the literature, in all those cardiovascular conditions with reported evidence of high ²³Na-MRI signal, suggests a '*congestion continuum*' ultimately manifesting in the overt heart failure syndrome. Patients with systolic or diastolic ventricular dysfunction are prone to congestion, i.e. heart failure, because of backward increases in hydraulic pressures. However, more and more over the last few years, the understanding and treatment of the disease has focused also on systemic, rather than purely myocardio-centric, dysfunctional mechanisms.

In the specific context of HF with preserved systolic function (or ejection fraction, HFpEF), typically accompanied by the above salt-Sensitive conditions, I identified a reduced clearance of extravasated fluid by a dysfunctional lymphatic vasculature.

Lymphatics are well-known regulators of interstitial fluid balance (Mortimer and Rockson, 2014, Herring & Paterson, 2018, Aspelund et al., 2016), but the

cardiovascular community has apparently long neglected their role in diseases other than the so called “lymphedema”. In the large majority of cases (i.e. the so-called “secondary” forms), lymphedema is diagnosed only upon severance (by surgery) or obstruction (by parasites, in low-income countries) of lymphatic vessels: if the suggested similarity between myocardium and lymphangion holds, limiting “lymphatic disease” to these conditions basically condense textbooks like Braunwald’s or Hurst’s to their chapters on cardiac tamponade. Studies like HAPPIFY are rather raising the attention to much broader functional aspects that closely parallels the topic of interstitial salt excess.

In light of all the above conclusions on tissue Na^+ nature and oedema, results by Wiig (Wiig et al., 2013) and Karlsen (Karlsen et al., 2018) on expanded lymphatic network and increased lymph flow in rodents upon salt-loading are not dissimilar from those derived in models of post-ischemic myocardial oedema (Henri et al., 2016).

Anatomical and/or functional expansion of these master-regulators of interstitial homeostasis upon insults perturbing this homeostasis makes perfect finalistic sense. And it makes similar sense that when this expansion is experimentally blocked (Wiig et al., 2013) or inadequate, as suggested by HAPPIFY, local or systemic congestion occurs. Of note, this proposition is not necessarily specific to cardiovascular disease: rheumatologists have started to appreciate that dysfunctional lymphatics may well contribute to impaired resolution of local inflammation and associated oedema in conditions like rheumatoid arthritis (Bouta et al., 2018).

If that is the case, better definition and identification of “dysfunctional lymphatics”, beyond the ‘tamponade’ conditions of classic lymphoedema, appear as a clearly unmet need. I propose this should take into account the complexity of those structures, including valvular, pace-making, systolic functions and their mutual coordination all along the entire lymphatic vascular tree.

During the course of my PhD I was fortunate to receive training in ex-vivo assessment of these multiple lymphatic aspects (Prof Michael Davis, University of Missouri, Columbia, MO): in fact, systolic and valvular function can be assessed in response to modulation of lymphatic preload and afterload by means of pressure myography (Davis et al., 2012, Scallan et al., 2012, Castorena-Gonzalez et al., 2020); a representative picture for isolated flank murine lymphatics is shown in Figure 1-3, panel C. As part of the NHS Greater Glasgow & Clyde Biorepository (REC ref. 17/WS/0207), I also had

the opportunity to access surplus surgery tissue from coronary artery bypass grafting interventions (*courtesy of Prof N. Al-Attar, Golden Jubilee National Hospital, Clydebank*) and managed to isolate small lymph nodes from the perivascular fat discarded during the skeletonization of mammary arteries. These lymph nodes proved suitable anatomic markers to identify the otherwise transparent and almost invisible pre- and post-nodal lymphatic vessels, thus providing a proof of concept for feasibility of their isolation and ex-vivo testing (Figure 8-3).

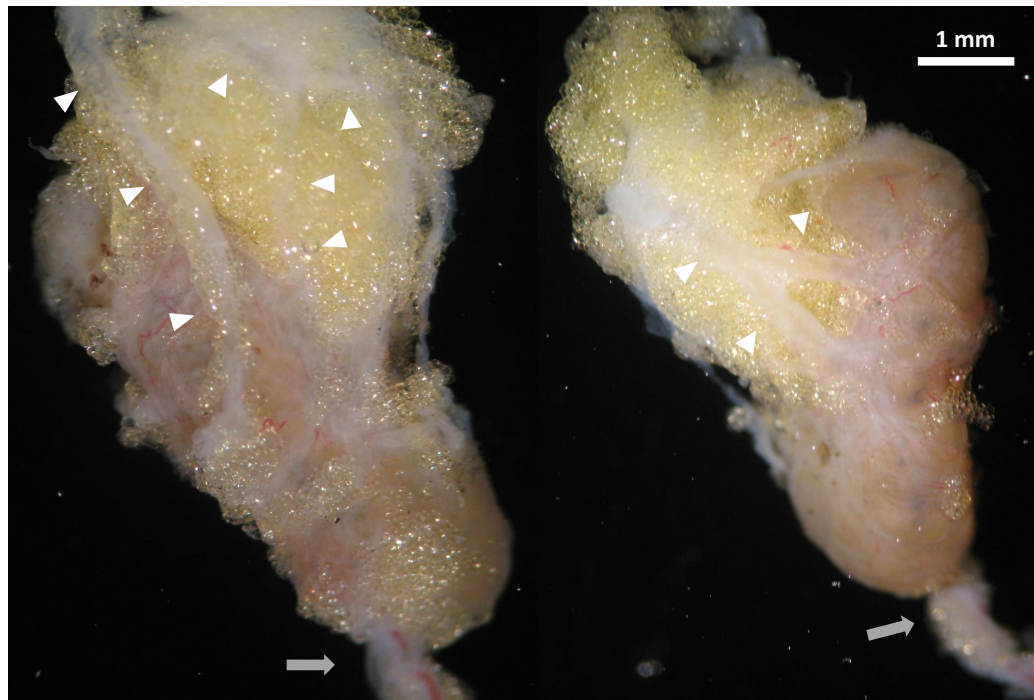


Figure 8-3. Human lymphnode with afferent and efferent lymphatic vessels.

Front and back pictures of a representative mammary lymphnode dissected from the perivascular mammary fat of a patient undergoing CABG. The transparent vascular structures marked by arrowheads are afferent (pre-nodal) lymphatics. The efferent (post-nodal) vessel, together with the accompanying vein and artery, is marked by grey arrows.

To pursue the above investigations on the role of lymphatic dysfunction in the pathogenesis of ‘traditional’ cardiovascular diseases, I plan to apply the myography methodology currently used in rodents also to human lymphatic vessels from suitable surgical groups.

Parallel optimisation and validation of non-invasive but conceptually similar and currently evolving imaging approaches (Giacalone et al., 2020) will possibly expand the opportunities for vascular phenotyping of patients and facilitate targeted treatments in the future.

8.4 Conclusions

In conclusion, my studies offered a reappraisal of the tissue Na⁺ theory, disproved its water-independence in both experimental models and human subjects and suggested systemic isotonic Na⁺ excess as an important and likely prevalent determinant in the pathogenesis of hypertension and other cardiovascular diseases.

I showed that excess Na⁺ *per se* may provide a *fil rouge* linking derangements in metabolism, renal and vascular function, even independent of blood pressure values, in the broad and often comorbid population of patients with cardiovascular disease.

I also showed that accumulation of excess Na⁺ in tissues reflects expansion of the extracellular volumes and – depending on age, tissue biophysical specificities and probably many more local or systemic variables – tissue oedema. With very few exceptions, exemplified by seminal preclinical studies in the myocardium of dogs, where even extremely small amounts of tissue oedema were shown to induce systolic and diastolic dysfunction (Dongaonkar et al., 2010), the direct functional impact of this oedema on the function of the affected organs remains unknown. There is general evidence that it may directly contribute to extracellular matrix remodelling and interstitial fibrosis via activation of profibrogenic mechanisms in fibroblasts (Brakenhielm et al., 2020), thus promoting a vicious perpetuation of structural organ dysfunction; however, additional research is clearly needed. What is known is that, once overt clinical congestion (synonymous with systemic oedema) is established, it carries ominous prognostic significance (Campbell et al., 2012). Similarly, incomplete therapeutic decongestion in HF patients is associated with higher rates of both death and clinical relapses, suggesting an adverse biological role of oedema *per se* and persistence of maladaptive underlying mechanisms to maintain the condition (Boorsma et al., 2020, Lam et al., 2018).

Treatment with diuretics is the current cornerstone of decongestive therapy in cardiovascular disease. By acting mainly via renal natriuresis and iso-osmotic urine excretion, diuretics facilitate resolution of interstitial oedema by reducing hydrostatic pressures in the capillary vessels and by shifting the local Starling equilibrium and fluids, accordingly. If the rate of urinary volume excretion exceeds the rate of fluid exchange at the capillary level, it is not uncommon clinical experience to observe intravascular fluid depletion with residual tissue congestion in diuretic-treated patients,

resulting in rebound adverse neurohormonal activation and worsening of renal function. Along with the issue of diuretic resistance, this exemplifies one of the many challenges posed by ‘traditional’ diuretics in treating congestion (Mullens et al., 2019, Wilcox et al., 2020, Boorsma et al., 2020, Felker et al., 2020).

More recently, the portfolio of therapies to target the volume status of patients expanded to include new agents, i.e. SGLT2-inhibitors, which produce a natriuretic/diuretic-like effect without many of the disadvantages of other diuretics (Griffin et al., 2020). In addition to reduce tissue Na⁺ (Karg et al., 2018), these agents were shown to reduce HF hospitalizations (i.e. the rate of transition to overt/severe clinical congestion) in patients with type 2 diabetes mellitus (Zinman et al., 2015, Neal et al., 2017) and, more recently, to improve clinical outcomes in patients with HF and reduced ejection fraction, including those without diabetes mellitus (McMurray et al., 2019). These findings come as no surprise, in light of the subclinical epidemic of Na⁺ excess discussed in this thesis. While an in-depth discussion of these new drugs is well beyond my scopes here, I wonder if a broader use of these “clever diuretics” could offer even more benefit to the CVD population at large, when guided by the identification of patients with actual tissue evidence of Na⁺ excess.

Of note, the diagnostic value of this tissue Na⁺ analysis may well extend beyond the sole cardiovascular field. Appreciation of the direct link between tissue Na⁺ signal and oedema and of its higher sensitivity to detect oedema compared with water, calls for the application of tissue Na⁺ analysis (by either ²³Na-MRI or other approaches (De Marchi et al., 2017)) to the whole range of diseases where mechanical or inflammatory localized oedema is implicated, including rheumatological, immunological, oncological and neurological conditions.

Wherever tissue Na⁺ excess is identified, a treatment directly targeting the interstitial space would clearly be the most appropriate. In this regard, the results of the HAPPIFY study, by demonstrating a reduced lymphatic function in a condition where congestion is “*the core*” (Pfeffer et al., 2019), open an entirely new line of research and potential therapeutics. Better understanding of the structural and molecular mechanisms responsible for reduced lymphatic reserve may facilitate the development of pharmacological interventions to improve interstitial fluid drainage in the whole spectrum of conditions herein identified as the ‘*congestion continuum*’.

APPENDICES

Appendix 1 - S₂ALT protocol

Skin Sodium Accumulation and water balance in hypertension: S₂ALT study

PI: Dr Giacomo Rossitto

Supervisor and Chief Investigator: Prof Christian Delles

Collaborators: Ms Jun Chen; Dr Katriona Brooksbank

Introduction and rationale

A close link between salt and cardiovascular disease, particularly high blood pressure, is well established (1, 2). Salt balance is currently believed to be largely regulated by the kidney, but recent studies have shown that the skin offers an extensive depot for tissue sodium (Na⁺) accumulation associated with ageing, hypertension, CKD and diabetes (3-6). Anatomic and functional similarities between kidneys and skin, both acting as “barrier” organs between the internal and external environment, have also been suggested (7).

It is still unclear whether it occurs as water-independent (i.e. hypertonic), or rather water-parallelled (i.e. subclinical oedema) as suggested by preliminary data from our group (8). Additionally, we speculate that even hypertonic Na⁺ excess could be due to a relative deficit of water which went lost at the skin level at some point and left its accompanying Na⁺ behind, rather than to accumulation of Na⁺ itself.

Identification and better understanding of this phenomenon may have huge implications in prevention and treatment of cardiovascular disease, in light of the tremendous benefit observed in large trials of novel treatments with natriuretic mechanism of action (e.g. SGLT2-inhibitors (9) or sacubitril-valsartan (10)).

Objectives

We aim to explore the characteristics (iso- or hyper-tonicity) and clinical correlates of skin Na⁺ accumulation in a hypertensive population, in relation to the mechanisms and degree of surface Na⁺/water exchange.

- **Primary Endpoint**
 - *To characterize the amount of skin Na⁺ and water accumulation, as assessed by a gold standard method (chemical analysis of a skin biopsy), in relation to the mechanisms of surface Na⁺/water exchange (trans-epithelial water loss and sweat)*
- **Secondary endpoints**
 - *To explore the association between Na⁺ accumulation in the skin and age, gender, anthropometric (e.g. BP, BMI, %body water) and clinical (medications, cardiovascular comorbidities) characteristics of patients*
 - *To explore the association between mechanisms of surface Na⁺/water exchange and age, gender, anthropometric (e.g. BP, BMI, %body water) and clinical (medications, cardiovascular comorbidities) characteristics of patients*

Design

This is a single-centre, secondary-care, one-off visit cross-sectional study on patients referred to the High Blood Pressure Clinic (HBPC) at the Queen Elisabeth University Hospital (Glasgow). On the day of their scheduled visit, patients who are willing to participate will be offered to undergo measurements of skin surface Na⁺/water exchange, blood and urine sampling and a 4 mm skin biopsy. We have deliberately chosen to combine the timing of the study with the usual timing of routine clinic visits to minimise the burden to study participants.

Population

We plan to recruit 150-200 participants over the course of 3 months.

Inclusion criteria

- Written informed consent
- Male or non-pregnant female ≥18 years of age attending the HBPC for a visit

Exclusion criteria

- Pregnancy
- Incapacity
- Skin conditions requiring emollients or topical steroid on both arms
- Implanted pacemaker or ICD (excluded from sweat test)
- History of allergy to lidocaine (excluded from skin biopsy)
- Concurrent dermatological or, in general, medical condition that in the opinion of the investigators would make a skin biopsy impracticable or unsafe (excluded from skin biopsy)
- Decline to undergo a skin biopsy (excluded from skin biopsy)

Identification of participants and consent

BP Clinic secretaries will send a Patient Information Leaflet (PIL) by post to all adult patients scheduled for an outpatient appointment at Glasgow HBP Clinic 7-10 days before they attend, along with the usual appointment confirmation letter, for their consideration.

On the day of the scheduled visit, the patient will undergo the usual nurse-led pre-clinic assessment, including measurement of office blood pressure values, BMI and confirmation of the current medical therapy. After BP is measured, the nurse will ask whether they have read the PIL posted and they wish to see the PI. If so, the PI will join and will discuss the study and answer any study related questions. If the patient is happy to participate, signed consent will be obtained. Interested patients will also have the opportunity to decline skin biopsy while taking part in the rest of the study.

Withdrawal

Participants may voluntarily withdraw from the study for any reason at any time. Data and stored samples of participants who withdraw will be destroyed upon request from participants or their legal representative.

Expected length of recruitment: 3 months (January-March 2019)

Study schedule and procedures

Upon consent, a small area of skin on one arm will be cleaned with water and dried, and two pilocarpine (a parasympathomimetic alkaloid) pads will be attached with straps. In order to get the pilocarpine into the skin to induce sweating, the area will be stimulated by a small current (1.5 mA) from a battery for about five minutes (iontophoresis). During these 5 minutes, lidocaine-based anaesthetic cream will be applied on the opposite arm on the site for biopsy and covered with a plaster. Pilocarpine pads will then be removed, and a plastic coil (Macroduct) will be attached on the stimulated arm with straps for collection of sweat over the next 30 minutes, including the time while the clinic visit takes place.

Participants will also be offered a brief dietary questionnaire for completion during pilocarpine stimulation and while waiting for the clinic visit.

After routine visit, a spot urine and blood samples (in addition to those requested by the consulting physician, if the case) will be taken. The sweat collection coil will be removed for analysis and transepidermal water loss will be measured with a TEWAMETER. Additionally, a skin biopsy will be performed. The surgical site where the cream had been applied will be cleaned with alcohol swabs to ensure sterile conditions and draped. The epidermis and superficial dermis will be pierced by a sterile punch, the punch removed with a sterile blade and hemostasis obtained with sterile gauze. The biopsy site will be closed with steri strips (3M). Wound care information sheet and plasters for wound care will be provided to the participant.

No further visit, tests or time will be required to the patient. However, adequate follow-up as per NHS standards will be guaranteed in the unlikely event of wound complications.

Samples will be later analysed for a) gravimetric assessment of water content, b) chemical analysis of Na⁺ and other osmolytes content [1] and c) molecular biology/omics. Plasma and urine samples will be processed and analysed for electrolyte/renal function and biomarkers of natriuresis (e.g. BNP) at the end of the study. Evidence of their elevation beyond clinically significant thresholds will be discussed with the consultants in charge of the patients; adequate follow-up as per NHS standards (including, in the first instance, repetition of the test in a clinically validated lab) will be undertaken if this evidence is considered of potential clinical relevance.

Clinical records of consenting patients will be reviewed by the PI (who is part of the HBPC team) or a medical student working towards a BSc Clinical Medicine degree for the same information usually collected during Clinics: age, gender, office BP values, BMI, current medications, final diagnosis of hypertension, history and/or imaging/biochemical evidence of ischaemic heart disease, MI, peripheral vascular disease, heart failure, left ventricular hypertrophy, airways disease, renal impairment, renovascular disease, cerebrovascular disease, diabetes, dyslipidaemia, secondary hypertension, immuno/rheumatological disorders, anaemia, smoking habit. These clinical data will be correlated with biochemical and skin results.

Study outcome measures

- **Primary outcome**
 - *Skin Na⁺ and K⁺ (mmol/g dry tissue, mmol/l) and water (mg/g dry tissue, % wet weight) and their correlation with sweat Na⁺/Cl⁻ concentration and volume and TEWL*

- **Secondary outcome**

- *Distribution of skin Na⁺, K⁺ and water by age, gender, anthropometric (BP, BMI, %body water) and clinical (medications, cardiovascular comorbidities) characteristics of patients*
- *Distribution of sweat Na⁺/Cl⁻ concentration/volume and TEWL by age, gender, anthropometric (BP, BMI, %body water) and clinical (medications, cardiovascular comorbidities) characteristics of patients*

Safety

Skin biopsies are minimally invasive procedures; for >70 biopsies performed also in patients on anticoagulation/dual antiplatelet agents, stitches were never needed. In the extremely unlikely event of stitches needed for wound closure (it never occurred in >70 biopsies performed) or wound complications (as detailed in the information provided to participants), a further appointment will be arranged for any wound care needed.

The sweat test is a safe test, generally performed in new-borns with no relevant complications (Guidelines for the Performance of the Sweat Test for the Investigation of Cystic Fibrosis in the UK 2nd Version (2014): An Evidence Based Guideline). The iontophoresis carries a theoretical risk of atrial fibrillation, for which pads are not placed on the trunk, but this has never been documented (Guidelines 2014); for similar reasons, we decided to exclude patients with implanted PM or ICD.

TEWL measurement is a non-invasive test which only requires contact of the skin surface with a device similar to a pen for few seconds.

The BCs(MedSci) student who will be involved in the performance of these tests and biopsies:

- is fully competent in 3rd year medical/surgical procedures, including venepuncture, arterial blood sampling for gas analysis surgical hand washing, correct use of personal protective equipment, safe disposal of clinical waste, needles and, other 'sharps'.
- will receive full training and supervision by the PI until he/she achieves a suitable level of independent competency in the study specific procedures, and continuous supervision throughout the study with immediate availability thereafter.
- is GCP cleared.

It is highly unlikely that any adverse experience might occur in relation to participation in the study, but prolonged stay in the BP Clinic compared to routine practice (estimated 30' more).

Benefit

There is no direct benefit to participants, apart from altruistic participation to a study on occasion of an already scheduled visit. No study data will be immediately relevant for clinical decision-making.

Statistics

This is a cross-sectional study in which descriptive and correlation statistics only will be performed.

The study size (n=150-200) is a sufficiently informative number of patients that we estimate can be recruited in the expected length of the study (3 months), according to the number of patients attending our BP Clinic (estimated \approx 30/week).

Data handling

Study data will be collected in a pseudoanonymised form, by using a case report form (CRF) developed ad hoc. Pseudoanonymised data will be accessible on the password-protected University of Glasgow personal server for the principal investigator and his supervisors. No personal patient details will be stored on University computers. Manual files including the consent forms and samples collection record will be kept in the BHF Glasgow Cardiovascular Research Centre.

To enable evaluations and/or audits from regulatory authorities, the investigator will keep records, including the identity of all participating subjects (sufficient information to link records, accessible on the password-protected University of Glasgow personal server to the research principal investigator and his supervisors only), all original signed informed consent forms, and source documents in the BHF Glasgow Cardiovascular Research Centre in accordance with ICH GCP and local regulations. Data will be retained at the Data Centre for of 10 years.

Samples storage

Biomaterials of participants, upon their consent and in anonymised form, will be stored at the University of Glasgow BHF Cardiovascular Research Centre in a -80 degrees freezer for 10 years, under the responsibility of the PI and his supervisors. The University has reviewed the BHF building tissue storage facility and is satisfied as to its suitability for storage of human tissue. The use of these materials, if needed for other purposes than S₂ALT study, will be subjected to protocol approval by the Ethics Committee and informed consent, if applicable, will be obtained by each patient.

Insurance and indemnity

This study is sponsored by NHS Greater Glasgow & Clyde. The sponsor will be liable for negligent harm caused by the design of the trial. NHS indemnity is provided under the Clinical Negligence and Other Risks Indemnity Scheme (CNORIS)

The NHS has a duty of care to patients treated, whether or not the patient is taking part in a clinical trial, and the NHS remains liable for clinical negligence and other negligent harm to patients under its duty of care.

Indemnity will also be provided for harm arising from the design of the research by the University of Glasgow Clinical Trial Insurance policy for protocol authors employed by the University of Glasgow.

Funding

British Heart Foundation Glasgow Centre of Research Excellence (grant no: RE/13/5/30177)

References

1. Global, regional, and national comparative risk assessment of 84 behavioural, environmental and occupational, and metabolic risks or clusters of risks, 1990-2016: a systematic analysis for the Global Burden of Disease Study 2016. *Lancet* (London, England). 2017;390(10100):1345-422.
2. Titze J, Luft FC. Speculations on salt and the genesis of arterial hypertension. *Kidney international*. 2017;91(6):1324-35.
3. Kopp C, Linz P, Wachsmuth L, Dahlmann A, Horbach T, Schofl C, et al. ²³Na magnetic resonance imaging of tissue sodium. *Hypertension* (Dallas, Tex : 1979). 2012;59(1):167-72.
4. Kopp C, Linz P, Dahlmann A, Hammon M, Jantsch J, Muller DN, et al. ²³Na magnetic resonance imaging-determined tissue sodium in healthy subjects and hypertensive patients. *Hypertension* (Dallas, Tex : 1979). 2013;61(3):635-40.
5. Schneider MP, Raff U, Kopp C, Scheppach JB, Toncar S, Wanner C, et al. Skin Sodium Concentration Correlates with Left Ventricular Hypertrophy in CKD. *Journal of the American Society of Nephrology : JASN*. 2017;28(6):1867-76.
6. Karg MV, Bosch A, Kannenkeril D, Striepe K, Ott C, Schneider MP, et al. SGLT-2-inhibition with dapagliflozin reduces tissue sodium content: a randomised controlled trial. *Cardiovascular diabetology*. 2018;17(1):5.
7. Hofmeister LH, Perisic S, Titze J. Tissue sodium storage: evidence for kidney-like extrarenal countercurrent systems? *Pflugers Archiv : European journal of physiology*. 2015;467(3):551-8.
8. Rossitto GT, R.M.; Petrie, M.C.; Delles, C. Much Ado About N...atrium: Modelling Tissue Sodium As A Highly Sensitive Marker Of Subclinical And Localised Oedema. *Clinical Science*. 2018 (in press).
9. Zinman B, Wanner C, Lachin JM, Fitchett D, Bluhmki E, Hantel S, et al. Empagliflozin, Cardiovascular Outcomes, and Mortality in Type 2 Diabetes. *The New England journal of medicine*. 2015;373(22):2117-28.
10. McMurray JJ, Packer M, Desai AS, Gong J, Lefkowitz MP, Rizkala AR, et al. Angiotensin-neprilysin inhibition versus enalapril in heart failure. *The New England journal of medicine*. 2014;371(11):993-1004.

Appendix 2 - S₂ALT participant information leaflet



University of Glasgow | College of Medical,
Veterinary & Life Sciences



Skin Sodium Accumulation and water balance in hyperTension:

S₂ALT study

We would like to invite you to take part in a short research study at your next Blood Pressure Clinic appointment.

Before you decide, it's important that you understand what the study is about and what will be required. Please take time to read this Participant Information Leaflet and feel free to talk to others about the study, including your GP, if you wish.

DO I HAVE TO TAKE PART?

NO. Participation is completely **VOLUNTARY**. If you decide that you do not want to participate, it will not change the standard of care that you receive from your own doctors.

WHAT IS THE PURPOSE OF THE STUDY?

This study aims to investigate how the skin is involved in the regulation of blood pressure.

We are now aware that salt accumulates in the skin with ageing and high blood pressure. However, it is not yet clear if this is in any way harmful, whether it leads to fluid build-up and whether it would need specific treatment beyond our usual blood pressure medication. Therefore we are trying to gather some more information on how this salt accumulation is regulated by sweat and skin water, from a large number of adult men and non-pregnant women with high blood pressure (and with or without other conditions like diabetes, obesity, etc. which appear to be associated with skin salt excess).

S₂ALT study will contribute towards the educational qualifications of PhD for Dr Giacomo Rossitto, and BSc Clinical Medicine degree in Cardiovascular Studies for Jun Yu Chen, medical student, under the supervision of Prof Christian Delles.

WHAT WOULD TAKING PART INVOLVE?

The study will require some extra time (approximately 30 extra minutes) during your next appointment at the Glasgow High Blood Pressure Clinic in the Queen Elizabeth University Hospital, to measure your sweat (as is done in new-born infants if some specific genetic problems are suspected) and to collect a tiny skin biopsy from your arm. The biopsy is performed with local anaesthesia (cream) and is very small [4 mm, like this blue dot: ●], so that stitches are **NOT** normally required: they were never needed in more than 80 biopsies performed thus far. The biopsy is performed by Jun Yu Chen, the medical student in training, under supervision of Dr Giacomo Rossitto and Prof Christian Delles.

We take this biopsy because it would give us information on salt and water content in the skin. However, if you prefer, you can opt to have the sweat test only.

If you agree to take part we will also inform your GP of your participation, upon your consent.

S₂ALT study, Version 1.1; 29th Dec 2018

When you attend the Blood Pressure Clinic you will be seen **first by the nurses**, who will measure your blood pressure, your height and weight and will review your current medications, as usual. If you are keen to discuss **participation**, a Research Doctor (Giacomo Rossitto) will join on that occasion and you will have the opportunity to ask any questions about the study.

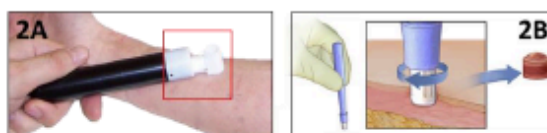
If you decide that you are happy to take part, you will sign a consent form and we will apply some anaesthetic cream on one arm (if you are happy with the biopsy) and we will start the sweat test on the other arm.

For the sweat test, skin on the arm is washed and dried. Next, two electrodes are attached with straps (Figure 1A). One of these contains a disc with pilocarpine gel, a medicine that makes the sweat glands produce sweat. A weak electric current that you will not be able to feel pushes the medicine through the skin. After this is done, the electrodes are removed and a special sweat collection device is then attached to the clean skin surface in the area where the sweat glands were stimulated (Figure 1B).



The sweat is then collected for about 30 minutes, including the time while you go through the planned visit with your doctor. While you wait to be called in by the clinic doctor we will also ask you to fill a brief questionnaire on your dietary habits. Your clinical data relevant to the high blood pressure visit (for example: age; gender; smoking/drinking habit; blood pressure values; history of diabetes, heart or kidney disease; usual medications) will be recorded by the research team including Ms Jun Chen, medical student.

After the visit, we will collect a blood sample (two tubes, i.e approximately 2-3 teaspoons of blood, in addition to any that have been requested by your clinic doctor) and a spot urine sample; we will remove the sweat collector; we will measure the evaporation of water from your forearm skin for few seconds with a device similar to a pen (Figure 2A) and will take the small skin biopsy with a round bladed punch tool (Figure 2B) from the area of your arm which is numb from the local anaesthetic.



HOW LONG DOES THE STUDY TAKE?

We expect the study to take approximately 10 extra minutes before and 20 minutes after the doctor visit. No other visits are needed.

IS THERE ANYTHING I NEED TO DO BEFORE THE STUDY VISIT?

NO: you can eat, drink, and exercise as usual, and continue to take any current medicines. Please just avoid creams and lotions on your arms for 24 hours before the visit; if you have been prescribed such treatments on both arms because of some skin conditions, please note that you will not be eligible to take part in the study.

WHAT SHOULD I DO AFTER THE STUDY VISIT?

After the skin biopsies, you should rest and avoid strenuous activity for the first 24 h. You will be provided with a wound care information sheet and all that you might need for wound care at the end of the visit.

S₂ALT study, Version 1.1; 29th Dec 2018

ARE THERE ANY RISKS/INCONVENIENCE ASSOCIATED WITH THE STUDY?

The sweat test is a safe test, generally performed in new-borns with very little risk of complications. It shouldn't be painful, though some feel a slight tingling or tickling sensation when the electrodes apply current to the skin. In rare cases, the skin may look slightly sunburned after the test.

Skin biopsies of such size are minimally invasive procedures; the cream generally provides adequate anaesthesia and the risk for allergic reactions is very low. However it is impossible to avoid some minimal discomfort after the anaesthetic wears off and you may have a very small scar like those in the picture (arrows). All biopsy sites have a small risk of bleeding (controlled in most cases with simple pressure on the site) and infection. It is relatively uncommon (1/75 in our experience), but this would require antibiotic treatment (cream or tablets).



Although unlikely, in case of any complication after the biopsy please contact Dr Giacomo Rossitto (details below and in the wound care information sheet), who supervises and is responsible for the medical student performing the biopsy.

ARE THERE ANY BENEFITS?

You will receive no direct benefit from taking part in the S₂ALT study and it will not affect your blood pressure treatment. However, you will contribute to a better understanding of blood pressure regulation.

WHAT WILL HAPPEN TO THE INFORMATION GATHERED AND TO THE SAMPLES I GIVE?

All the information collected about you during the course of the study and the results will be kept strictly confidential and anonymised and accessible only to the S₂ALT investigators and to NHS Greater Glasgow & Clyde (GGC), the sponsor for this study. We will be using information from you and/or your medical records in order to undertake this study and will act as the data controller for this study. This means that we are responsible for looking after your information and using it properly.

NHS Greater Glasgow & Clyde will use your name, NHS number and contact details to contact you about the research study, and make sure that relevant information about the study is recorded for your care, and to oversee the quality of the study. Individuals from NHS Greater Glasgow & Clyde and regulatory organisations may look at your medical and research records to check the research study has been performed safely and in accordance with international standards. The only people in NHS Greater Glasgow & Clyde who will have access to information that identifies you will be people who need to contact you to arrange visit appointments, discuss your results or audit the data collection process. The people who analyse the information will not be able to identify you and will not be able to find out your name, NHS number or contact details. NHS Greater Glasgow & Clyde will keep identifiable information about you for 10 years after the study has finished.

Your rights to access, change or move your information are limited, as we need to manage your information in specific ways in order for the research to be reliable and accurate. If you withdraw from the study, we will keep the information about you that we have already obtained. To safeguard your rights, we will use the minimum personally-identifiable information possible. You can find out more about how we use your information from Dr Giacomo Rossitto, the doctor leading the S₂ALT study (contact details below).

All samples (skin, sweat, blood and urine) will be analysed anonymously in the BHF Glasgow Cardiovascular Research Centre to evaluate the make-up of skin in relation to water and sodium balance and to the clinical information recorded. We will discuss unexpected abnormal blood tests results with the consultant in charge of you; if clinically relevant, they would need to be repeated in an NHS, rather than a research, lab. No samples or identifiable information about you will be accessible outside the research team or NHS Greater Glasgow & Clyde.

Finally, in the consent form you will have the option to decide whether your samples and the information collected about you CAN OR CANNOT be used for other research in the future, upon ethical approval, and whether you would like to be contacted for future relevant research OR NOT.

WHAT HAPPENS TO THE RESULTS OF THE STUDY?

The results of the study will be included in a student dissertation, presented in internal, national and international scientific meetings, will be published in scientific journal(s) and on University of Glasgow Institute of Cardiovascular and Medical Sciences website: in all these cases no identifiable personal data will be used. A summary sheet with the results of the study and/or a copy of any publication will be available to you upon request.

WHAT IF SOMETHING GOES WRONG?

In the unlikely event of anything going wrong or if you have any problems with the study you should contact Dr Giacomo Rossitto (contact details below).

This study is sponsored by NHS Greater Glasgow & Clyde (NHS GGC). NHS indemnity is provided under the Clinical Negligence and Other Risks Indemnity Scheme (CNORIS). NHS has no legal liability for non-negligent harm. However, if you are harmed and this is due to someone's negligence, you may have grounds for a legal action against NHS Greater Glasgow and Clyde but you may have to pay your legal costs. Harm relating to the design of the study will be covered by the University of Glasgow insurance.

If you believe that you have been harmed in any way by taking part in this study, you have the right to pursue a complaint and seek any resulting compensation through the NHS GGC or the University of Glasgow. Details about this are available from the research team. Also, as a patient of the NHS, you have the right to pursue a complaint through the usual NHS process. To do so, you can submit a written complaint to the Patient Liaison Manager, Complaints Office by telephoning 01412014500 or email complaints@ggc.scot.nhs.uk.

WHO HAS REVIEWED THE STUDY?

Prof Christian Delles, as PhD supervisor, the West of Scotland Research Ethics Committee 3 and the NHS Greater Glasgow and Clyde Research and Development Department.

FUNDING British Heart Foundation (BHF) Glasgow Centre of Research Excellence.

IF ANYTHING IS NOT CLEAR OR YOU WOULD LIKE OTHER INFORMATION BEFORE TO CONSENT, PLEASE ASK:
Dr Giacomo Rossitto (GMC No 7555833) E-mail: giacomo.rossitto@glasgow.ac.uk; Mobile: 07833916704

IF YOU WOULD LIKE TO HAVE AN INDEPENDENT CONTACT FOR HELP OR ADVICE, PLEASE FEEL FREE TO ASK:
Dr Gemma Currie, MBCHB, MRCP (UK), PhD; E-mail: gemma.currie@glasgow.ac.uk; Phone: 0141-330-5189

WE WOULD LIKE TO THANK YOU FOR TAKING THE TIME TO READ THIS LEAFLET AND FOR YOUR CONSIDERATION ABOUT TAKING PART IN THIS STUDY.

Appendix 3 - S₂ALT salt intake questionnaire



S₂ALT study

NUTRITIONAL AND LIFESTYLE HABITS

The following questions are about your dietary and life-style habits. All your answers will be strictly confidential.

Study ID:

--	--	--	--

During the PAST 7 days (1 week) did you eat any of the following? IF YES, HOW OFTEN?

FOOD ITEM	NO, NEVER	YES				
		NOT EVERY DAY		EVERY DAY		
		1-3 times a week	4-6 times a week	1 time a day	2 times a day	3+ times a day
White bread / white bread rolls	<input type="radio"/>	<input type="radio"/>	<input type="radio"/>	<input type="radio"/>	<input type="radio"/>	<input type="radio"/>
Brown /wholewheat bread / Rolls	<input type="radio"/>	<input type="radio"/>	<input type="radio"/>	<input type="radio"/>	<input type="radio"/>	<input type="radio"/>
Breakfast Cereal (processed)	<input type="radio"/>	<input type="radio"/>	<input type="radio"/>	<input type="radio"/>	<input type="radio"/>	<input type="radio"/>
Breakfast Cereal (minimally processed - weetabix, muesli, etc.)	<input type="radio"/>	<input type="radio"/>	<input type="radio"/>	<input type="radio"/>	<input type="radio"/>	<input type="radio"/>
Crackers	<input type="radio"/>	<input type="radio"/>	<input type="radio"/>	<input type="radio"/>	<input type="radio"/>	<input type="radio"/>
Cookies, biscuits, rusks	<input type="radio"/>	<input type="radio"/>	<input type="radio"/>	<input type="radio"/>	<input type="radio"/>	<input type="radio"/>
Cake / scone / muffin / puddings / pancake / fruit pie	<input type="radio"/>	<input type="radio"/>	<input type="radio"/>	<input type="radio"/>	<input type="radio"/>	<input type="radio"/>
Roti / samosa / spring roll / doughnut	<input type="radio"/>	<input type="radio"/>	<input type="radio"/>	<input type="radio"/>	<input type="radio"/>	<input type="radio"/>
Pizza	<input type="radio"/>	<input type="radio"/>	<input type="radio"/>	<input type="radio"/>	<input type="radio"/>	<input type="radio"/>
Pasta/noodle dishes with cheese sauces (macaroni cheese, lasagne, noodle salad etc.)	<input type="radio"/>	<input type="radio"/>	<input type="radio"/>	<input type="radio"/>	<input type="radio"/>	<input type="radio"/>
Popcorn	<input type="radio"/>	<input type="radio"/>	<input type="radio"/>	<input type="radio"/>	<input type="radio"/>	<input type="radio"/>
Crisps	<input type="radio"/>	<input type="radio"/>	<input type="radio"/>	<input type="radio"/>	<input type="radio"/>	<input type="radio"/>
Beef sausage	<input type="radio"/>	<input type="radio"/>	<input type="radio"/>	<input type="radio"/>	<input type="radio"/>	<input type="radio"/>
Bacon / salami / pork sausages (processed meat, cooked, smoked and canned)	<input type="radio"/>	<input type="radio"/>	<input type="radio"/>	<input type="radio"/>	<input type="radio"/>	<input type="radio"/>
Meat or chicken pies/sausage rolls	<input type="radio"/>	<input type="radio"/>	<input type="radio"/>	<input type="radio"/>	<input type="radio"/>	<input type="radio"/>
Chicken - battered and chicken burger only	<input type="radio"/>	<input type="radio"/>	<input type="radio"/>	<input type="radio"/>	<input type="radio"/>	<input type="radio"/>
Meat and meat dishes (steaks, minced meat, cottage pie, mince, meatballs, stew, bobotie, etc.)	<input type="radio"/>	<input type="radio"/>	<input type="radio"/>	<input type="radio"/>	<input type="radio"/>	<input type="radio"/>
Gravy, made with stock or gravy powder	<input type="radio"/>	<input type="radio"/>	<input type="radio"/>	<input type="radio"/>	<input type="radio"/>	<input type="radio"/>
Dried, cured meat	<input type="radio"/>	<input type="radio"/>	<input type="radio"/>	<input type="radio"/>	<input type="radio"/>	<input type="radio"/>

S₂ALT study, Version 1.1; 29th Dec 2018

FOOD ITEM	NO, NEVER	YES					
		NOT EVERY DAY		EVERY DAY			
		1-3 times a week	4-6 times a week	1 time a day	2 times a day	3+ times a day	
Milk (all types, also dairy fruit juice, malted milk, milk shakes)	<input type="radio"/>	<input type="radio"/>	<input type="radio"/>	<input type="radio"/>	<input type="radio"/>	<input type="radio"/>	
Fermented milk	<input type="radio"/>	<input type="radio"/>	<input type="radio"/>	<input type="radio"/>	<input type="radio"/>	<input type="radio"/>	
Cheese	<input type="radio"/>	<input type="radio"/>	<input type="radio"/>	<input type="radio"/>	<input type="radio"/>	<input type="radio"/>	
Yoghurt	<input type="radio"/>	<input type="radio"/>	<input type="radio"/>	<input type="radio"/>	<input type="radio"/>	<input type="radio"/>	
Eggs	<input type="radio"/>	<input type="radio"/>	<input type="radio"/>	<input type="radio"/>	<input type="radio"/>	<input type="radio"/>	
Tinned fish (tuna, etc.)	<input type="radio"/>	<input type="radio"/>	<input type="radio"/>	<input type="radio"/>	<input type="radio"/>	<input type="radio"/>	
Other fish and seafood	<input type="radio"/>	<input type="radio"/>	<input type="radio"/>	<input type="radio"/>	<input type="radio"/>	<input type="radio"/>	
Potato chips / French fries and potato salad	<input type="radio"/>	<input type="radio"/>	<input type="radio"/>	<input type="radio"/>	<input type="radio"/>	<input type="radio"/>	
Canned vegetables, incl. baked beans, tomato paste, sweetcorn, etc.	<input type="radio"/>	<input type="radio"/>	<input type="radio"/>	<input type="radio"/>	<input type="radio"/>	<input type="radio"/>	
Soup (all types)	<input type="radio"/>	<input type="radio"/>	<input type="radio"/>	<input type="radio"/>	<input type="radio"/>	<input type="radio"/>	
Salad dressing/mayonnaise	<input type="radio"/>	<input type="radio"/>	<input type="radio"/>	<input type="radio"/>	<input type="radio"/>	<input type="radio"/>	
Ice cream (all types)	<input type="radio"/>	<input type="radio"/>	<input type="radio"/>	<input type="radio"/>	<input type="radio"/>	<input type="radio"/>	
Margarines, all types, also butter	<input type="radio"/>	<input type="radio"/>	<input type="radio"/>	<input type="radio"/>	<input type="radio"/>	<input type="radio"/>	
Chutney / Worcester sauce	<input type="radio"/>	<input type="radio"/>	<input type="radio"/>	<input type="radio"/>	<input type="radio"/>	<input type="radio"/>	
Savoury sauces (mushroom, monkey gland, white, cheese)	<input type="radio"/>	<input type="radio"/>	<input type="radio"/>	<input type="radio"/>	<input type="radio"/>	<input type="radio"/>	
Tomato sauce	<input type="radio"/>	<input type="radio"/>	<input type="radio"/>	<input type="radio"/>	<input type="radio"/>	<input type="radio"/>	
Salt	<input type="radio"/>	<input type="radio"/>	<input type="radio"/>	<input type="radio"/>	<input type="radio"/>	<input type="radio"/>	
Aromat / mustard	<input type="radio"/>	<input type="radio"/>	<input type="radio"/>	<input type="radio"/>	<input type="radio"/>	<input type="radio"/>	
Peanuts	<input type="radio"/>	<input type="radio"/>	<input type="radio"/>	<input type="radio"/>	<input type="radio"/>	<input type="radio"/>	
Peanut butter	<input type="radio"/>	<input type="radio"/>	<input type="radio"/>	<input type="radio"/>	<input type="radio"/>	<input type="radio"/>	
Marmite spread	<input type="radio"/>	<input type="radio"/>	<input type="radio"/>	<input type="radio"/>	<input type="radio"/>	<input type="radio"/>	
Chocolate sweets and sauce	<input type="radio"/>	<input type="radio"/>	<input type="radio"/>	<input type="radio"/>	<input type="radio"/>	<input type="radio"/>	
Beer and cider	<input type="radio"/>	<input type="radio"/>	<input type="radio"/>	<input type="radio"/>	<input type="radio"/>	<input type="radio"/>	

**THANK YOU FOR TAKING THE TIME
TO COMPLETE THIS QUESTIONNAIRE!**

Reference: Charlton KE et al, Public Health Nutrition 2008, 11(1), 83-94

S₂ALT study, Version 1.1; 29th Dec 2018

Appendix 4 - HAPPIFY protocol

HAPPIFY

Heart failure with Preserved ejection fraction: Plethysmography for Interstitial Function and skin biopsY (HAPPIFY Study)

PI: Dr Giacomo Rossitto (giacomo.rossitto@glasgow.ac.uk)

Supervisors: Prof C. Delles, Prof M. Petrie, Prof R.T. Touyz

Co-investigators: Dr N. Lang, Dr P. Rocchiccioli, Dr Clare L. Murphy

INTRODUCTION/RATIONALE

Heart failure with preserved ejection fraction (HFpEF) currently accounts for approximately half of cases of heart failure (HF). In contrast with HF with reduced ejection fraction (HFrEF), HFpEF incidence has increased rapidly during the past decades and no effective treatment has yet been found [1]. This is partially due to a complex and heterogeneous pathophysiology, in which comorbidities play a key role. Hypertension is the most prevalent comorbidity (76-96% of cases) and, through development of hypertensive heart disease, is a precursor to overt HFpEF[2].

Notably, "peripheral" mechanisms, including impaired ventricular–arterial coupling (both at rest and during stress), vascular stiffness and endothelial dysfunction leading to impaired vasodilation, have been suggested to be contributors to HFpEF pathophysiology [2, 3].

Once HFpEF occurs, it is characterized by signs and symptoms mostly related to impaired management of fluids and extracellular volume, often regarded as secondary to myocardial dysfunction and consequent imbalance in the Starling forces at capillary level [1].

However, recent evidence pointed to primary changes in peripheral (skin) interstitium as a possible factor in the development of hypertension [4, 5]. In particular, dynamic and hypertonic tissue salt accumulation has been demonstrated in both animal models and humans [6, 7]. Blockade or downregulation of interstitial salt regulators (immune cells and lymphatic network) resulted in an excessive interstitial salt accumulation and a salt-sensitive hypertensive phenotype in a rodent model [4, 5]. In humans, tissue salt accumulation has been associated with refractory hypertension and aging, which is a key contributor in the development of HFpEF [7]. However, demonstration of a functional and clinical relevance for these interstitial changes is currently lacking.

We speculate that primary changes in the interstitial milieu might directly result in "interstitial dysfunction" and change in its permeability (as per Starling forces) or "buffering" capacity, as well as in secondary vascular and cardiac function impairment. This would mark the progression of hypertension to HFpEF, through overt fluid tolerance impairment.

HYPOTHESES

Interstitial function is impaired in HFpEF patients as compared to age-matched healthy controls.

Secondarily, this impairment in interstitial function might reflect tissue salt accumulation and parallel impairment in vascular and cardiac function.

OBJECTIVES

Primary objective:

- To compare microvascular filtration [8, 9] (as an index of “interstitial function”) between HFpEF patients and age-matched healthy controls.

Secondary objectives:

- To compare skin Na⁺ content and its determinants (e.g. lymphatic vessels, GAGs network, immune cells) and to assess their association with interstitial function
- To compare other components of extracellular matrix and to assess their association with interstitial/vascular function
- To compare resistance artery function, as assessed ex vivo (HAPPIFY-G sub-study).

Tertiary objectives:

- To compare non-invasively assessed arterial function (Pulse wave analysis/pulse wave velocity; PWA/PWV), endothelial function (EndoPAT[®]/Flow Mediated Dilation) and venous function (strain gauge plethysmography); circulating and urinary biomarkers (CV risk, natriuretic axis) between groups.

DESIGN

HAPPIFY is a cross-sectional, physiological, proof-of-concept study, investigating the interstitial function of HFpEF patients compared to age-matched healthy controls.

To this aim, participants will undergo a non-invasive assessment of microvascular filtration, as measured by strain gauge plethysmography (SGP) [10], and a skin biopsy for ex vivo evaluation of determinants of interstitial function. A non-invasive evaluation of their vascular function will also be performed to inform on secondary outcomes.

Participants also consenting to the HAPPIFY-G sub-study will undergo an additional gluteal subcutaneous fat biopsy on the same study visit, aimed at evaluating ex vivo resistance vessels function and the structure/composition of the associated interstitium.

POPULATION

We will recruit 20 HFpEF patients, identified from outpatient Heart Failure Clinic list, and 20 age-matched controls, identified through advertisements/SHARE. We will enrol controls in a 2:1 female-to-male ratio, to match the anticipated gender split of the HFpEF population.

Inclusion Criteria

General

- Written informed consent
- Age between 55 and 80

Cases:

- Diagnosis of HFpEF, as per ESC HF guidelines criteria, namely:
 - Heart failure (HF) symptoms \pm signs, generally unchanged for ≥ 1 month
 - AND Ejection fraction (EF) $\geq 50\%$
 - AND relevant structural heart disease (LA enlargement and/or LVH) or diastolic dysfunction [mean e' septal and lateral wall < 8 cm/s + (average $E/e' > 15$ OR lateral $E/e' > 13$)]
 - AND Elevated NT-proBNP ≥ 125 pg/ml or BNP ≥ 35 pg/ml.

Age-matched controls:

- No symptoms or signs of HF
- Normotensive

Exclusion criteria**General**

- Ejection fraction (EF) $< 50\%$
- Stroke, myocardial infarction, coronary artery bypass graft or percutaneous coronary angioplasty within the last 3 months
- Significant valve disease ($>$ moderate severity)
- Known hypertrophic/infiltrative cardiomyopathy or constrictive pericarditis
- Unstable coronary artery disease
- Known stage 4-5 CKD
- Illicit drug use
- History of idiopathic oedema/capillary leak syndrome, myxedema, lymphatic obstruction
- Evidence of systemic inflammation at the time of study visit
- Active malignancy
- Any major hypercoagulable state or history of venous thrombosis/embolism
- Severe concurrent medical condition that in the opinion of the investigators would prevent participation in study procedures or with life expectancy < 1 year
- Incapacity

Specific (skin/gluteal biopsy):

- Allergy to lidocaine hydrochloride, chlorhexidine gluconate or to isopropyl alcohol
- Chronic diffuse skin condition without uninvolved areas suitable for biopsy.
- History of keloid scar formation.
- Known diagnosis of hepatitis B or C or HIV.
- Current treatment with warfarin or other anticoagulant medication and/or P2Y receptors inhibitors.
- Severe obstructive iliac artery disease
- Any other medical condition that in the opinion of the investigators would make a biopsy unsafe
- Decline to undergo a skin/gluteal biopsy

Relative (exclusion from segmental limb assessment):

- Chronic venous insufficiency - post-thrombotic syndrome
- Lymph-node dissection

STUDY SCHEDULE

Participant identification

Potential study participants will be identified by the clinical consultant cardiologists (Prof M. Petrie, Dr. N. Lang, Dr Clare Murphy) during their Heart Failure Clinic appointments. The clinicians will ask the patient if he/she is happy to discuss potential participation in research with the research team (Dr Rossitto). If so, Dr Rossitto will subsequently provide the patients with a patient information leaflet (PIL). If they then decide to take part a study visit will then be arranged, where informed consent will be taken by the research team (Dr Rossitto).

Healthy volunteers will be recruited through SHARE and advertisements in both public and healthcare domains within the NHSGGC catchment area. The posters will include contact details for the Happify research team and for those healthy volunteers who are considering participating the investigator will send them a copy of the PIL with a checklist for initial self-assessment of eligibility.

After appropriate time for consideration (≥ 24 h), any subject interested in participation will be able to contact the PI as per the contact details in the PIL to have their self-assessment of eligibility reviewed. If eligible, an appointment for a study visit will be booked, upon patient's verbal consent.

Eligibility visit [est. time ~ 60 -70 mins]: Queen Elizabeth University Hospital (QEUEH) CRF

Subjects interested in participation will be invited to an eligibility visit discuss in person the details of the study and of the sub-study and to review inclusion/exclusion criteria.

The voluntary nature of participation will be stressed to potential participants, with no impact on routine clinical care.

1. Consent

All participants will have to provide written consent to take part in the study. The consent will be taken by the investigator before any of the study procedures can commence.

HAPPIFY-G sub-study will also be discussed in this occasion and HAPPIFY participants will be provided the HAPPIFY-G sub-study PIL. However, consent for undergoing gluteal biopsies will be taken separately, during the main study visit, after appropriate time for consideration (≥ 24 h).

2. Eligibility assessment

All consenting participants will undergo: review of medical history and drug therapy; physical examination (focused on HF signs), including weight; assessment of symptoms burden (Modified KCCQ questionnaire [11], to be completed at patient's convenience in the research facility or at home); measurement of blood pressure, heart rate and O₂ saturation; blood tests for exclusion of renal/metabolic/thyroid comorbidities + BNP; performance of transthoracic echo-Doppler/tissue Doppler; performance of spirometry (FEV₁, FVC, PEF; MicroLab Spirometer). Participants will be provided a container for 24h-urine collection.

Main Study visit [est. time ~ 2.5 h]: Queen Elizabeth University Hospital (QEUEH) CRF

Eligible participants will be invited to attend this visit in the early morning at Queen Elizabeth University Hospital (QEUEH) CRF. They will be asked to withhold their cardiovascular medicine on that morning and to bring with them a 24h-urine collection with the last sample collected as the first morning urine of that day (i.e upon getting up from bed).

HAPPIFY

The participants will have their Happify study procedures carried out in a 2h-fasting state, in a quiet, temperature-controlled room.

Initial assessment will include blood and urine samples.

Study measurements will then include

- Strain Gauge Plethysmography est. time 40'
Measurements with Strain Gauge Plethysmography will consist of an inflation-deflation protocol, with no need for drug use or vascular puncture, to evaluate interstitial filtration. This will assess changes in limb volume when a sub-diastolic pressure is opposed to venous drainage [10].
- PWA/PWV analysis est. time 15'
- Endothelial function (Endo-PAT[®]/FMD) est. time 20-30'
- Skin biopsy est. time 10'

After the skin biopsy, the wound will be appropriately closed and all participants will be provided with a wound care information sheet.

Because of its small size (3-4 mm diameter, 4-5 mm depth), we don't anticipate the routine need to use stitches or to have the participants to come back for additional visits to have it checked.

However, if stitches are needed for wound closure or in case of wound complications (as detailed in the information provided to participants), a further appointment will be promptly arranged for stitches removal or for any wound care needed.

HAPPIFY-G sub-study

Participants will be informed about the optional HAPPIFY Gluteal subcutaneous fat biopsy (HAPPIFY-G) sub-study during their first face to face meeting with the research team (either routine clinic visit or screening visit).

To minimise the related time burden and biopsy sites, the gluteal biopsy will be performed at the end of the main visit, at the same site as the skin biopsy, after additional numbing of the surrounding area with a subcutaneous injection of local anaesthetic. The sample will be approximately 1.5-2 cm in length and 1cm deep.

The wound will be closed with dissolvable or non-dissolvable stitches, as appropriate. Similarly to skin biopsies, a wound care information sheet will be provided.

All participants in HAPPIFY-G will be invited back to the CRF or BHF GCRC for a wound check +/- removal of sutures 1 week following their gluteal biopsies. Alternatively, participants will be able to go to their local GP for a wound check +/- removal of sutures. A letter will be posted to the participants GP, upon consent. This letter will inform them that their patient has had a gluteal biopsy and has chosen to attend their practice for removal of their sutures.

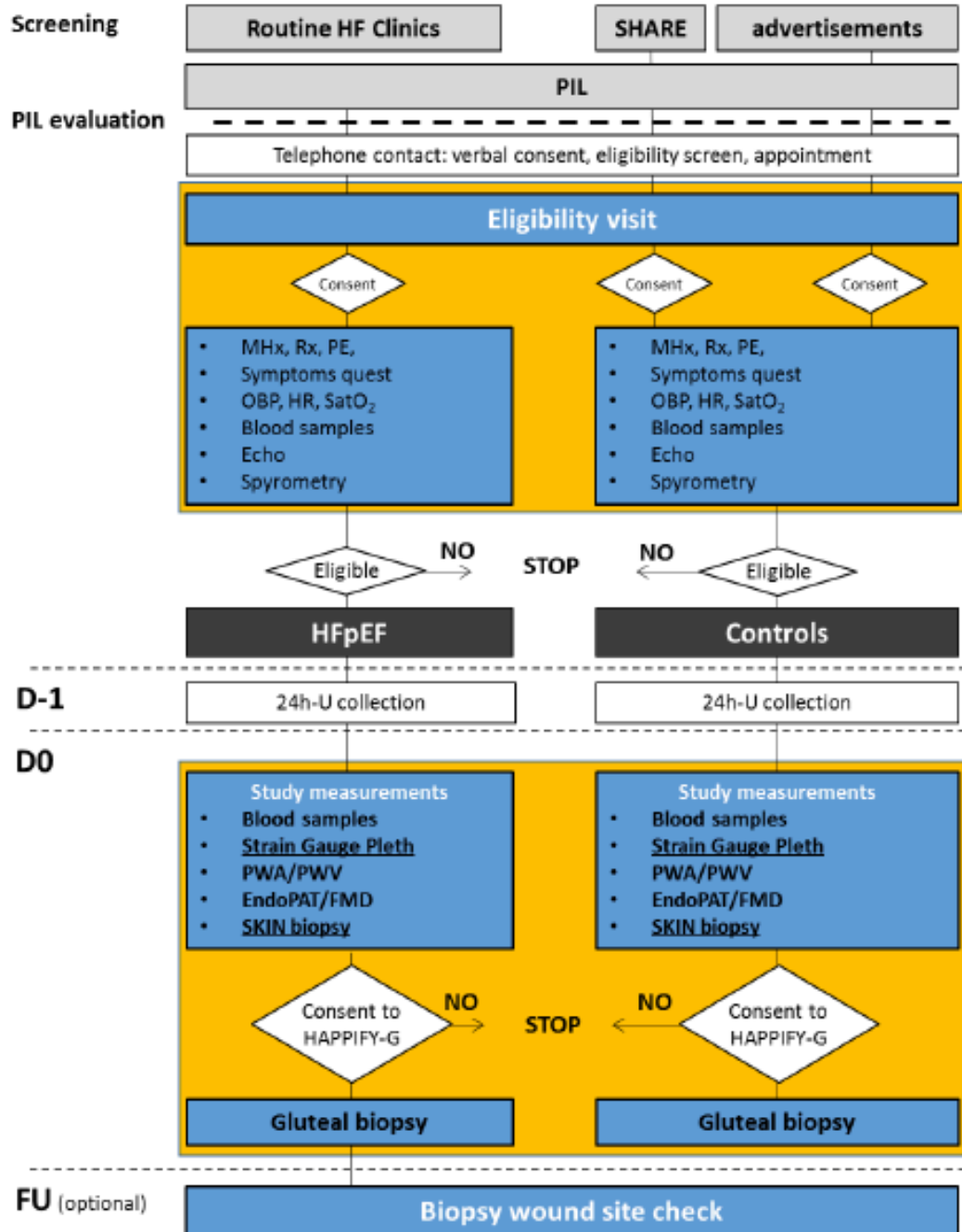
Withdrawal

Participants have the right to withdraw from the study or sub-study at any point for any reason. The investigator can withdraw participants from the study in the event of inter-current illness between contact and study visit. Data and stored samples of participants who withdraw will be destroyed upon request of participants or their legal representative.

Participants who withdraw from the study will be replaced with additional participants until reach of the expected number of participants.

Expected length of recruitment: 8 months.

Flow Chart of the study



* Performed after study measurements, if upper limb is used

Legend: yellow boxes = research visits; HF = heart failure; HFpEF = HF with preserved ejection fraction; 24h-U = 24 hours urine; MHx = medical history; Rx = review of therapy; PE = physical examination; OBP = office BP; HR = heart rate; SatO₂ = O₂ saturation; pleth = plethysmography; PWA/PWV = pulse wave velocity/analysis; PAT = Peripheral Arterial Tone; FMD = flow mediated dilation; FU = follow-up.

OUTCOMES MEASURES (primary and secondary)

Primary:

- Values of K_f (filtration coefficient) and P_{vi} (microvascular equilibrium pressure, as an estimate of lymphatic function), as determined by SGP during a stepped inflation protocol [9, 10].

Secondary:

- skin Na^+ concentration, as assessed ex vivo by skin biopsies.
- lymphatic vessels network, as assessed on skin biopsies by immunohistochemistry
- Skin glycosaminoglycans content and composition, as assessed ex vivo by skin biopsies.
- Morphological description of inflammatory/fibrotic changes in the extracellular matrix, as assessed ex vivo by skin biopsies.
- Resistance artery endothelium-dependent and -independent dilatation and contraction to stimuli, as assessed by myography on vessels isolated from gluteal biopsies.

STATISTICS

Sample size calculation

This is a pilot study and no specific data on interstitial function as assessed by SGP are available in this specific population for a formal size calculation. Moreover, we had to take into account the heterogeneity of HFpEF population when comparing our expected results with those available in the literature on different disease conditions (e.g. postural orthostatic tachycardia syndrome, nephrotic syndrome, type 1 diabetes mellitus) [12-14].

According to available data on these other patient populations and assuming we will see an effect similar to what is already published, we estimate that the proposed sample size ($n = 20$ per group) would allow us to detect a significant difference in the interstitial function (K_f , P_{vi}) and structure/composition (ex vivo analysis of skin biopsies) between two "extremes" of a continuum (HFpEF patients vs healthy age-matched controls).

Moreover, we estimate that at least 50% of participants will consent to both the main protocol AND the sub-study involving gluteal biopsies, thus allowing sufficient power also for investigations of ex vivo assessed function of small resistance arteries [15].

The epidemiological evidence that HFpEF patients are predominantly old and female justifies the recruitment strategy for controls [2].

Data Analysis

Continuous variables will be expressed as mean \pm SD or median (interquartile range), as appropriate, after testing for normality of distribution with Kolmogorov-Smirnov test.

Parametric (t-student) or non-parametric (Wilcoxon) unpaired test will be used for comparisons between groups, accordingly.

Pearson's χ^2 test or Mann-Whitney U test will be used for categorical variables, as appropriate.

Differences will be considered significant at $p < 0.05$.

SAFETY

Because of the prolonged venous stasis associated with strain gauge measurement, subjects with any major hypercoagulable state or history of venous thrombosis/embolism are excluded from participation. Pressures used for cuff inflation during the SGP protocol are always sub-diastolic (with BP assessed before initiation of the exam), thus excluding any potential limitation to arterial circulation related to the procedure. Apart from the foreseeable discomfort associated with lying for the time of SGP measurements and/or with venous stasis in the limbs, the non-invasive part of the study, does not pose other relevant safety issues on participants.

Skin and gluteal biopsies, at variance, are invasive procedures, carrying a minimal risk of bleeding, infection, abnormal scarring and, potentially allergic reaction to the local anaesthetic.

For skin biopsies, all these risks are anticipated to be minimal, because of the small size and the use of non-injectable anaesthetics.

Gluteal biopsies inherently carry some more risk, related to a larger and deeper procedure and the need for s.c. lidocaine. They will be performed only upon specific additional consent to HAPPIFY-G sub-study.

All procedures will be performed only by a trained doctor. Patients with specific risk factors for excessive bleeding, for inadequate wound healing or for infection are excluded, as per protocol. Uttermost care will be paid to guarantee absolute sterility to minimize the risk of infections.

Participants will be asked to inform investigators of all adverse events (AE) occurring after the study visits. All serious adverse events will be reported to the sponsor within 24h. All AE will be recorded and appropriately managed by investigators, as per normal good clinical practice.

BENEFIT

No incentives will be offered to participants; however, we would be happy to reimburse reasonable travel expenses to and from the hospital.

Participants will have the general benefit of taking part in a clinical research project. Healthy volunteers will have the peculiar benefit of blood pressure and echo assessment. Participants, and, upon their consent, their GPs, will be informed of any relevant data emerging during the study.

DATA MANAGEMENT

Study data will be collected in a pseudoanonymised form, by using a case report form (CRF) developed ad hoc. Pseudoanonymised data will be accessible on the password-protected University of Glasgow personal server for the principal investigator and his supervisors. No personal patient details will be stored on University computers. Manual files including the consent forms and samples collection record will be kept in the BHF Glasgow Cardiovascular Research Centre.

To enable evaluations and/or audits from regulatory authorities, the investigator will keep records, including the identity of all participating subjects (sufficient information to link records, accessible on the password-protected University of Glasgow personal server to the research principal investigator and his supervisors only), all original signed informed consent forms, and source documents in the BHF Glasgow Cardiovascular Research Centre in accordance with ICH GCP, local regulations, or as

HAPPIFY

specified in the Clinical Study Agreement, whichever is longer. Data will be retained at the Data Centre for of 5 years.

SAMPLES STORAGE

Biomaterials of participants, upon their consent and in anonymised form, will be stored at the University of Glasgow BHF Cardiovascular Research Centre in a -80 degrees freezer, under the responsibility of the PI and his supervisors. The use of these materials, if needed for other purposes than HAPPIFY study, will be subjected to protocol approval by the Ethics Committee and informed consent, if applicable, will be obtained by each patient.

ETHICAL CONSIDERATIONS

The study will be carried out in accordance with the World Medical Association Declaration of Helsinki (1964) and its revisions (Tokyo [1975], Venice [1983], Hong Kong [1989], South Africa [1996] and Edinburgh [2000]).

Favourable ethical opinion will be sought from an appropriate REC before participants are entered into this clinical study. Subjects will only be allowed to enter the study once either they have provided written informed consent.

The PI will be responsible for updating the Ethics Committee of any new information related to the study.

INSURANCE AND INDEMNITY

This study is sponsored by NHS Greater Glasgow & Clyde. The sponsor will be liable for negligent harm caused by the design of the trial. NHS indemnity is provided under the Clinical Negligence and Other Risks Indemnity Scheme (CNORIS)

The NHS has a duty of care to patients treated, whether or not the patient is taking part in a clinical trial, and the NHS remains liable for clinical negligence and other negligent harm to patients under its duty of care.

Indemnity will also be provided for harm arising from the design of the research by the University of Glasgow Clinical Trial Insurance policy for protocol authors employed by the University of Glasgow.

FUNDING

British Heart Foundation Glasgow Centre of Research Excellence (grant no: RE/13/5/30177)

REFERENCES

1. Ponikowski, P., et al., *2016 ESC Guidelines for the diagnosis and treatment of acute and chronic heart failure: The Task Force for the diagnosis and treatment of acute and chronic heart failure of the European Society of Cardiology (ESC) Developed with the special contribution of the Heart Failure Association (HFA) of the ESC*. Eur Heart J, 2016. **37**(27): p. 2129-200.
2. Borlaug, B.A., *The pathophysiology of heart failure with preserved ejection fraction*. Nat Rev Cardiol, 2014. **11**(9): p. 507-15.
3. Franssen, C., et al., *From comorbidities to heart failure with preserved ejection fraction: a story of oxidative stress*. Heart, 2016. **102**(4): p. 320-30.
4. Wiig, H., et al., *Immune cells control skin lymphatic electrolyte homeostasis and blood pressure*. J Clin Invest, 2013. **123**(7): p. 2803-15.
5. Machnik, A., et al., *Macrophages regulate salt-dependent volume and blood pressure by a vascular endothelial growth factor-C-dependent buffering mechanism*. Nat Med, 2009. **15**(5): p. 545-52.
6. Kopp, C., et al., *(23)Na magnetic resonance imaging of tissue sodium*. Hypertension, 2012. **59**(1): p. 167-72.
7. Kopp, C., et al., *23Na magnetic resonance imaging-determined tissue sodium in healthy subjects and hypertensive patients*. Hypertension, 2013. **61**(3): p. 635-40.
8. Gamble, J., I.B. Gartside, and F. Christ, *A reassessment of mercury in silastic strain gauge plethysmography for microvascular permeability assessment in man*. J Physiol, 1993. **464**: p. 407-22.
9. Bauer, A., F. Christ, and J. Gamble, *Can lymphatic drainage be measured non-invasively in human limbs, using plethysmography?* Clin Sci (Lond), 2004. **106**(6): p. 627-33.
10. Gamble, J., *Realisation of a technique for the non-invasive, clinical assessment of microvascular parameters in man; the KM factor*. Eur Surg Res, 2002. **34**(1-2): p. 114-23.
11. Mishra, R.K., et al., *Kansas City Cardiomyopathy Questionnaire Score Is Associated With Incident Heart Failure Hospitalization in Patients With Chronic Kidney Disease Without Previously Diagnosed Heart Failure: Chronic Renal Insufficiency Cohort Study*. Circ Heart Fail, 2015. **8**(4): p. 702-8.
12. Stewart, J.M., *Microvascular filtration is increased in postural tachycardia syndrome*. Circulation, 2003. **107**(22): p. 2816-22.
13. Lewis, D.M., et al., *Peripheral microvascular parameters in the nephrotic syndrome*. Kidney Int, 1998. **54**(4): p. 1261-6.
14. Jaap, A.J., et al., *Increased microvascular fluid permeability in young type 1 (insulin-dependent) diabetic patients*. Diabetologia, 1993. **36**(7): p. 648-52.
15. Petrie, M.C., et al., *Angiotensin converting enzyme (ACE) and non-ACE dependent angiotensin II generation in resistance arteries from patients with heart failure and coronary heart disease*. J Am Coll Cardiol, 2001. **37**(4): p. 1056-61.

CONTACTS

Principal Investigator

Dr Giacomo Rossitto¹
Clinical Research Fellow
Institute of Cardiovascular and Medical Sciences
BHF Glasgow Cardiovascular Research Centre
126 University Place
Glasgow G12 8TA
Tel: 0141 330 2627
E-mail: Giacomo.Rossitto@glasgow.ac.uk

Supervisors

Prof Christian Delles¹
Professor of Cardiovascular prevention, Honorary Consultant Physician
Tel: 0141 330 2749
E-mail: Christian.Delles@glasgow.ac.uk

Prof Mark Petrie^{1,2}
Professor of Cardiology
Tel: 0141 330 4558
E-mail: Mark.Petrie@glasgow.ac.uk

Prof Rhian Touyz¹
Director of Research Institute/Professor (Institute of Cardiovascular and Medical Sciences)
Tel: 0141 330 7775
E-mail: Rhian.Touyz@glasgow.ac.uk

Co-investigators

Dr Ninian Lang^{1,2}
Clinical Senior Lecturer
Tel: 0141 330 6937
E-mail: Ninian.Lang@glasgow.ac.uk

Dr Paul Rocchiccioli²
Consultant Cardiologist
E-mail: p.rocchiccioli@nhs.net

Dr Clare L. Murphy³
Consultant Physician and Cardiologist
Tel: 0141 314 7214
E-mail: claremurphy4@nhs.net

HAPPIFY

¹Institute of Cardiovascular and Medical Sciences
BHF Glasgow Cardiovascular Research Centre
126 University Place
Glasgow G12 8TA

²Golden Jubilee National Hospital
Agamemnon Street
Clydebank G81 4DY

³Royal Alexandra Hospital
Corsebar Road
Paisley PA2 9PN
Renfrewshire

Clinical Trial Manager

Dr Katriona Brooksbank

Institute of Cardiovascular and Medical Sciences
BHF Glasgow Cardiovascular Research Centre
126 University Place
Glasgow G12 8TA
Tel: 0141 330 2627
E-mail: katriona.brooksbank@glasgow.ac.uk

Sponsor

NHS Greater Glasgow & Clyde

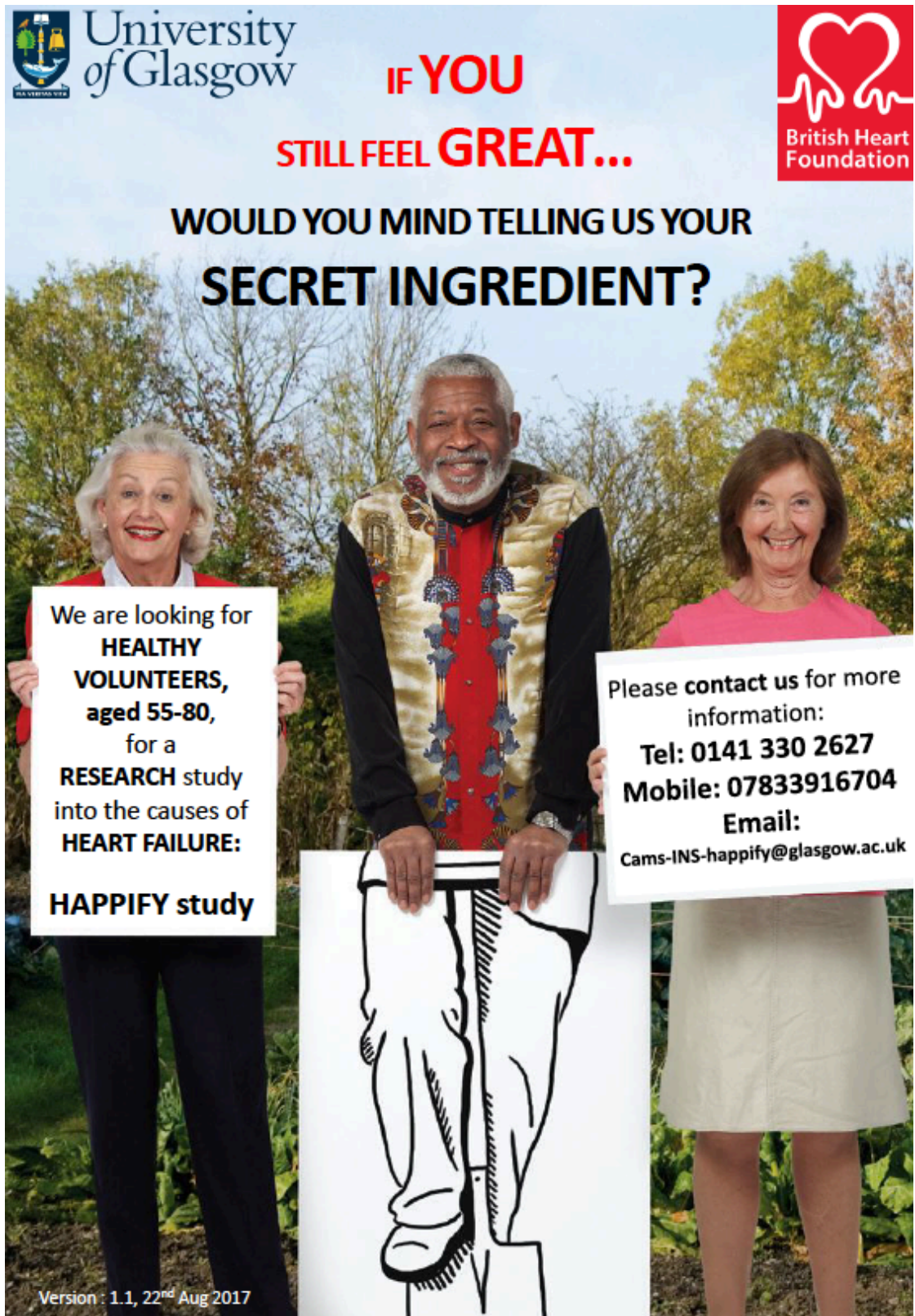
Sponsor's representative

Dr Maureen Travers
Research Co-ordinator
NHS Greater Glasgow & Clyde
Research and Development Management Office
West Glasgow Ambulatory Care Hospital
Dalnair Street
Glasgow
G3 8SW
Tel: 01412321813
E-mail: Maureen.Travers@ggc.scot.nhs.uk

Funding Body

British Heart Foundation
Glasgow Centre of Research Excellence - grant no: RE/13/5/30177

Appendix 5 - HAPPIFY advertisement for healthy volunteers



The advertisement features three individuals standing in a garden. On the left, an older woman with white hair holds a sign. In the center, a man with a grey beard and a gold and red patterned vest holds a large white sign with a black line drawing of a human torso. On the right, a woman with brown hair holds a sign. The background shows green foliage and a clear sky.

 University of Glasgow

IF YOU

STILL FEEL GREAT...

 British Heart Foundation

WOULD YOU MIND TELLING US YOUR SECRET INGREDIENT?

We are looking for **HEALTHY VOLUNTEERS, aged 55-80,** for a **RESEARCH** study into the causes of **HEART FAILURE:**

HAPPIFY study

Please contact us for more information:
Tel: 0141 330 2627
Mobile: 07833916704
Email:
Cams-INS-happify@glasgow.ac.uk

Version : 1.1, 22nd Aug 2017

Appendix 6 - HAPPIFY participant information leaflet

A very similar leaflet, with only slightly different wording in relation to NOT having heart failure, was provided to healthy volunteers.

Version number: 1.3, date: 30th Aug 2018



Heart failure with Preserved ejection fraction: Plethysmography for Interstitial Function and skin biopsy **[HAPPIFY Study]**

Participant Information Leaflet - PATIENTS

INVITATION TO PARTICIPATE

My name is **Giacomo Rossitto**, I'm a medical doctor undertaking a PhD course under the supervision of Prof Christian Delles, Prof Mark Petrie and Prof Rhian Touyz. We are carrying out this **research study** and we would like to invite you to take part.

However, before you decide, it's important that you understand what the study is about and what will be required, as described in this Participant Information Leaflet. Please take time to **read it carefully and feel free to talk to others about the study**, including your GP, if you wish.

Participation is completely VOLUNTARY. If you decide that you do not want to participate, it will not change the standard of care that you receive from your own doctors.

WHAT IS THE STUDY ABOUT?

This study is about **heart failure**.

Having heart failure means that for some reason the heart does not have enough strength and/or elasticity to pump blood all the way round the body efficiently.

Unfortunately, we do not yet fully understand why and how heart failure develops, particularly when there is no clear history of previous heart muscle damage (Preserved Ejection Fraction).

One of the possible reasons is that the "mortar" (interstitium) which supports and keeps the cardiac and vascular cells together, as for bricks in a wall, becomes weaker. This is what the HAPPIFY study is about.

Therefore, we are comparing the interstitial function and structure between **heart failure patients** and participants who do **NOT** have heart failure.

WHY AM I ASKED TO PARTICIPATE?

We have identified you as a potential participant among patients attending Heart Failure Clinics. If you are willing to participate in our research study, please get in touch and we will be happy to meet with you to discuss any further question you might have.

DO I HAVE TO TAKE PART?

No, you do not have to take part in the study if you do not want to.

You can come out of the study at any time and withdraw your consent even after you have given it. You don't have to give a reason why and if you withdraw your treatment will not be affected. In this case, any personal samples/data will be destroyed upon your request.

WHAT WOULD TAKING PART INVOLVE?

1. Eligibility visit

If you are happy to be part of this study, we will ask you to meet for a **first visit to screen for eligibility**.

The HAPPIFY investigator will go through all the information ~~again~~ with you and will answer any of your questions on the study. If you are eligible and wish to take part in the study, you will be asked to **sign a consent form**.

Upon consent, we will collect some **medical information** from you and from your medical records, as well as some **clinical data**, such as blood pressure, heart rate and weight.

We will also take some **blood samples** (approximately 6 teaspoons of blood), perform an **ultrasound exam of your heart** (echo; taking approximately 30 minutes) to take some measurements of the cardiac structure and function and a **breath test** (spirometry; taking 5 minutes) to measure the amount and the rate of air that you breathe in and out.

All this is to double-check that all the criteria for entering the study are met.

You will also receive a **container for collecting all the urine in the 24 hours** just before the MAIN study visit (i.e. last sample collected upon arising from bed on that day), for which an appointment will be made and will be confirmed to you upon the results of the blood tests.

During this first eligibility visit, the HAPPIFY investigator will also **inform** you about the **optional HAPPIFY Gluteal subcutaneous fat biopsy (HAPPIFY-G) sub-study**. This involves a small additional fat biopsy being taken at the end of the main study visit. A separate participant information sheet will be provided. **It is important to understand that you do not have to take part in this sub-study if you do not want to:** we only ask in advance so that we can minimize the time burden for those willing to take part in both studies.

2. **Main visit**

The main study visit will last **one single morning**. We will ask you to collect a **24h urine sample** since the day before, which you can then bring with you to the main study visit.

The most important part of the study will require you to **lie face upward as still as possible for 30-40 minutes, while we inflate and deflate cuffs on your arms and/or thighs**. This is to measure any small changes in your forearms and/or calf diameter, by a very sensitive and small gauge (about half the size of earphones wires): the instrument used is called **Plethysmograph**. The cuff pressure that we will use is much lower than your blood pressure and therefore won't block the blood going into the arm.

Please note that **if you are unable to lie supine for very long, we can slightly change the position or offer you an additional pillow to make you more comfortable** throughout the whole measurement.

After completion of the plethysmography, we will take some more **blood samples** (approximately 3 teaspoons of blood), one further **spot urine sample** (approximately half a glass of water) and we will measure how stiff your arteries are using an instrument that works in the same way as an ordinary **blood pressure monitor**. This will take approximately 20-30 minutes.

At the end of the visit we will take a **skin biopsy** from the buttock area. A small round bladed instrument will be used to remove a round core of tissue ranging from 3 to 4 millimetre in diameter for lab analysis of the "mortar". Local anaesthetic (a topic cream or a "cooling spray") will be administered to make the area numb. 1 or 2 stitches may be used to close the wound, but most of the time they are not needed because of its **small size [like this dot: ●]**.

2b. Optional procedure (to be carried out at the end of the main study visit)

If you also consent to the HAPPIFY-G sub-study involving a gluteal biopsy, it will be performed at the same time and site as the skin biopsy, after additional numbing of the area with a subcutaneous injection of local anaesthetic. Further details are in the additional separate participant information sheet provided during the eligibility visit. **Please note once again that you can ignore this section if you do not want to take part also in this sub-study.**

HOW LONG DOES EACH STUDY VISIT TAKE?

The **eligibility visit** will take approximately **60-70 minutes** and the main study will take approximately **2.5 hours** and will be arranged at the **Clinical Research Facility** of the **Queen Elizabeth University Hospital**.

IS THERE ANYTHING I NEED TO DO BEFORE EACH STUDY VISIT?

We ask you to prepare a **list** of any tablets or **medicine** you are taking (including painkillers or other “as needed” medications). During the eligibility visit the research team may ask you to **withhold** some “cardiovascular” **medicine** on the morning of the main visit, in particular **your water pills**. You will be able to take them later in the morning, at the end of the visit.

We also ask that **12 hours before the main study** visit you refrain from drinking alcohol, drinking caffeinated products and smoking. We suggest you wear loose, comfortable **clothing**. Instructions for 24h-urine collection will be provided at the eligibility visit.

WHAT SHOULD I DO AFTER THE MAIN STUDY AND THE SKIN BIOPSY?

After the skin biopsy, you should **rest for 12 h** and avoid any strenuous activity for the first 48 h. You will be provided with a **wound care information sheet** and all that you might need to care for the site at the end of the main study visit.

Because of the small size of the wounds, we **don't expect you will need to come for additional visits** to have it checked. However, if stitches are needed for wound closure or in case of signs of any complication (as per instructions you will receive), a further appointment will be promptly arranged for stitches removal or for any wound care needed.

ARE THERE ANY RISKS/INCONVENIENCE ASSOCIATED WITH THE STUDY?

Most of the **study procedures**, with the **exception of the skin biopsy and blood sampling**, are **non-invasive** and there are no major foreseeable risks associated, apart from the time burden to you for participation.

The **plethysmography** measurements require us to block the venous flow of blood going out of your veins in your limb for 20-30 minutes: it doesn't affect the inflow, but you might experience some **tingling sensation** which will disappear quickly as soon as the cuff is deflated.

With regard to the **skin biopsy**, it is obviously impossible to cut the skin without leaving a mark, so after you may have a **small scar** which appears as a 3 to 4 **millimetre** fine line, which sometimes heals as a circular indentation or puckering. There are certain individuals who may have an abnormal response to skin healing with larger raised scar than usual (keloids), but you may have noticed this in the past if you have ever cut yourself. All biopsy sites have a **small risk of bleeding** (controlled in most cases with simple pressure on the site) and **infection**. Though relatively uncommon, this would require antibiotic treatment (topic or systemic).

The small risk of an allergic reaction to the local anaesthetic is further minimized by the use of a cream instead of injections or of a cooling spray.

ARE THERE ANY BENEFITS?

You will not receive any compensation for taking part in the HAPPIFY research study. However, we will be **happy to reimburse reasonable travel expenses** to and from the hospital.

Most of the measurements we take during the study visits are not used in routine clinical care; however, if we do find evidence of clinical relevance (for example from blood samples or blood pressure measurements) we will notify you, the consultant in charge of you and your GP, if you consent.

Moreover, thanks to your **altruistic participation**, the HAPPIFY study will help us to better understand the characteristics of the patients with heart failure like you and to design further studies to improve their treatment.

WHAT HAPPENS TO THE INFORMATION GATHERED AND TO THE SAMPLES I GIVE?

All the information collected about you during the course of the study and the results will be kept **strictly confidential and anonymised** and **accessible only to the HAPPIFY investigators and to NHS Greater Glasgow & Clyde**, the sponsor for this study based in the United Kingdom.

We will be using **information from you and/or your medical records in order to undertake this study and will act as the data controller for this study**. This means that we are responsible for looking after your information and using it properly.

NHS Greater Glasgow & Clyde will use your name, NHS number and contact details to contact you about the research study, and make sure that relevant information about the study is recorded for your care, and to oversee the quality of the study. Individuals from NHS Greater Glasgow & Clyde and regulatory organisations may look at your medical and research records to check the accuracy of the research study. The only people in NHS Greater Glasgow & Clyde who will have access to information that identifies you will be people who need to contact you to arrange visit appointments, discuss with you results or audit the data collection process. The people who analyse the information will not be able to identify you and will not be able to find out your name, NHS number or contact details.

NHS Greater Glasgow & Clyde will keep identifiable information about you for 5 years after the study has finished.

Your rights to access, change or move your information are limited, as we need to manage your information in specific ways in order for the research to be reliable and accurate. If you withdraw from the study, we will keep the information about you that we have already

obtained. To safeguard your rights, we will use the minimum personally-identifiable information possible.

You can find out more about how we use your information **Dr Giacomo Rossitto, the HAPPIFY investigator** (contact details below).

All samples (skin and/or gluteal fat, blood and urine) will be analysed **anonymously in the BHF Glasgow Cardiovascular Research Centre** to evaluate the make-up of skin interstitium in relation to sodium balance and renal function (as per urine and blood samples) and the function of very tiny vessels residing in the fat. Remaining samples will be stored in the BHF Research Centre, according to UK and EU legislation.

Results of your blood or urine tests will be **available to you upon request at any time.**

No samples or identifiable information about you will be accessible outside the research team or NHS Greater Glasgow & Clyde.

WHAT HAPPENS TO THE RESULTS OF THE STUDY?

The results of the study will be **presented** in internal, national and international scientific meetings, will be **published** in scientific journal(s) and on University of Glasgow Institute of Cardiovascular and Medical Sciences website: **in all these cases no identifiable personal data will be used.**

A summary sheet with the results of the study and/or a copy of any publication will be available to you upon request.

WHAT IF SOMETHING GOES WRONG?

In the **unlikely event of anything going wrong** or if you have **any problems with the study** you should **contact Dr Giacomo Rossitto, the HAPPIFY investigator** (contact details below).

This study is sponsored by NHS Greater Glasgow & Clyde (NHS GGC). NHS indemnity is provided under the Clinical Negligence and Other Risks Indemnity Scheme (CNORIS). NHS has no legal liability for non-negligent harm. However, if you are harmed and this is due to someone's negligence, you may have grounds for a legal action against NHS Greater Glasgow and Clyde but you may have to pay your legal costs. Harm relating to the design of the study will be covered by the University of Glasgow insurance.

If you believe that you have been harmed in any way by taking part in this study, you have the **right to pursue a complaint** and seek any resulting compensation **through the NHS GGC or the University of Glasgow**. **Details about this are available from the research team**. Also, as a patient of the NHS, you have the right to pursue a complaint through the **usual NHS process**. To do so, you can submit a written complaint to the Patient Liaison Manager, Complaints Office by telephoning 0141 201 4500 or email complaints@ggc.scot.nhs.uk.

WHO HAS REVIEWED THE STUDY?

Prof Christian Delles and Prof Mark Petrie, as PhD supervisors, the **West of Scotland Research Ethics Committee 3** and the **NHS Greater Glasgow and Clyde Research and Development Department**.

FUNDING British Heart Foundation (BHF) Glasgow Centre of Research Excellence.

PLEASE FEEL FREE TO ASK Dr GIACOMO ROSSITTO IF ANYTHING IS NOT CLEAR OR YOU WOULD LIKE OTHER INFORMATION BEFORE TO CONSENT.

Dr Giacomo Rossitto (GMC No 7555833)

E-mail: cams-ins-happify@glasgow.ac.uk; Phone: 0141-330-2627; Mobile: 07833916704

IF YOU WOULD LIKE TO HAVE AN INDEPENDENT CONTACT FOR HELP OR ADVICE OF ANY KIND, PLEASE FEEL FREE TO ASK Dr GEMMA CURRIE.

Dr Gemma Currie, MBCHB, MRCP (UK), PhD

E-mail: gemma.currie@glasgow.ac.uk; Phone: 0141-330-5189

WE WOULD LIKE TO THANK YOU FOR TAKING THE TIME TO READ THIS LEAFLET AND FOR YOUR CONSIDERATION ABOUT TAKING PART IN THIS STUDY.

Appendix 7 – SYCAMORE: metabolomic peaks, higher in high-Na⁺ vs low-Na⁺.

	FC	p	pcorrected	Ion	Evidence	Metabolite	Notes
intermediates or end products of the urea cycle / protein catabolism	1.39	0.0001	0.016	-	Identified +F	proline	Conditionally-essential aminoacid; critical for muscle and connective tissues
	1.52	0.0002	0.023	-	Annotated	n-ac-l-glutamate 5-semialdehyde	Intermediate in urea cycle
	1.48	0.0002	0.023	-	Identified +F	Leucine	Essential, branched-chain aminoacid
	1.38	0.0004	0.024	+	Identified +F	proline	Conditionally-essential aminoacid; critical for muscle and connective tissues
	1.69	0.0004	0.024	+	Annotated	hydroxyprolyl-valine	an incomplete breakdown product of protein digestion or protein catabolism.
	1.77	0.0004	0.024	+	Annotated	n6,n6,n6-trimethyl-l-lysine	methylated derivative of the amino acid lysine; component of histone proteins, a precursor of carnitine and a coenzyme of fatty acid oxidation
	1.45	0.0005	0.024	+	Identified +F	l-tryptophan	Essential aminoacid
	1.44	0.0006	0.029	-	Identified	l-valine	Essential, branched-chain aminoacid
	1.48	0.0009	0.037	+	Identified +F	Leucine	Essential, branched-chain aminoacid
	1.88	0.0013	0.043	+	Annotated	pyrrolidonecarboxylic acid	cyclic derivative of glutamic acid
	1.40	0.0017	0.048	-	Identified +F	tyrosine	Conditionally-essential aminoacid
	1.57	0.0017	0.048	+	Annotated	homoarginine	L-alpha-amino acid
	1.45	0.0018	0.050	+	Identified	isoleucine	Essential, branched-chain aminoacid
	1.54	0.0048	0.096	+	Identified	hydroxyproline	major component of the protein collagen; marker of collagen catabolism, tissue degradation or for the consumption of processed meat.
	1.30	0.0054	0.106	+	Annotated	methionyl-cysteine	incomplete breakdown product of protein digestion or protein catabolism.
	1.33	0.006	0.108	-	Annotated	hydroxyproline	major component of the protein collagen; marker of collagen catabolism, tissue degradation or for the consumption of processed meat.
	1.29	0.0062	0.108	+	Annotated	Histidinyl-Cysteine	incomplete breakdown product of protein digestion or protein catabolism.
	1.39	0.0063	0.108	+	Identified +F	l-tyrosine	Conditionally-essential aminoacid
	1.48	0.0068	0.109	+	Annotated	proline	Conditionally-essential aminoacid; critical for muscle and connective tissues
	1.25	0.0069	0.109	-	Identified +F	lysine	Essential aminoacid
1.38	0.0069	0.109	+	Identified	Lysine	Essential aminoacid	
1.31	0.0072	0.110	+	Annotated	indoleacetic acid	breakdown product of tryptophan metabolism	

	FC	p	p _{corrected}	Ion	Evidence	Metabolite	Notes
urea cycle / protein catabolism	1.34	0.0095	0.125	-	Annotated	l-phenylalanine	Essential aminoacid
	1.29	0.0126	0.149	+	Identified +F	Threonine	Essential aminoacid
	1.32	0.019	0.168	+	Annotated	citrulline	Intermediate in urea cycle
	1.18	0.02	0.170	-	Annotated	threonine	Essential aminoacid
	1.26	0.0212	0.173	+	Annotated +F	guanidinoacetic acid	metabolite in the Urea cycle and metabolism of amino groups, and in the metabolic pathways of several amino acids.
	1.53	0.0212	0.173	+	Annotated	hydroxypropyl-histidine	incomplete breakdown product of protein digestion or protein catabolism.
	1.33	0.0238	0.186	-	Annotated	pyroglutamylglycine	alpha amino acid
	1.21	0.0315	0.2	+	Annotated	3-methylhistidine	product of peptide bond synthesis and methylation of actin and myosin; marker of muscle protein breakdown.
	1.21	0.0374	0.231	+	Annotated	hydantoin-5-propionic acid	metabolite of histidine
	1.27	0.0377	0.231	-	Annotated +F	histidine	Essential aminoacid
	1.26	0.042	0.248	+	Annotated +F	histidine	Essential aminoacid
	1.24	0.0452	0.255	+	Annotated	leucyl-proline	incomplete breakdown product of protein digestion or protein catabolism
	1.26	0.0464	0.255	-	Identified	Ornithine	Intermediate in urea cycle
1.18	0.0468	0.255	-	Identified	Alanine	Non-essential aminoacid	
triglycerides / fatty acid metabolism	2.01	0.0001	0.016	-	Annotated	DG	diacylglycerol
	2.25	0.0001	0.016	+	Annotated	DG	diacylglycerol
	1.39	0.0003	0.024	-	Annotated	Tiglylglycine	an acyl glycine (minor metabolite of fatty acids).
	1.21	0.0014	0.045	-	Annotated	undecanoic acid	medium chain length monocarboxylic acid
	1.49	0.0019	0.052	-	Annotated	7z,10z-hexadecadienoic acid	fatty acid metabolite
	1.37	0.0043	0.09	-	Annotated	n-undecanoylglycine	acylglycine, with C-11 fatty acid group as the acyl moiety
	1.39	0.01	0.128	+	Annotated	pc(20:4(5z,8z,11z,14z)/0:0)	phosphatidylcholine
	1.21	0.0147	0.157	+	Annotated	pc(18:0/0:0)	glycerophospholipid
	1.43	0.0149	0.157	-	Annotated	9-keto stearic acid	also called octadecanoic acid; it is one of the useful types of saturated fatty acid that comes from many animal and vegTable S fats and oils
	1.35	0.0158	0.159	+	Annotated	pe(20:4(5z,8z,11z,14z)/0:0)	glycerophospholipid
	1.35	0.0191	0.168	-	Annotated	pe(20:4(5z,8z,11z,14z)/0:0)	glycerophospholipid
1.42	0.0247	0.189	+	Identified	choline	methyl donor in various metabolic processes, and in lipid metabolism. Choline is now considered to be an essential vitamin.	

	FC	p	p _{corrected}	Ion	Evidence	Metabolite	Notes
TG/FA	1.22	0.0263	0.195	+	Annotated	pc(o-8:0/o-8:0)	phosphatidylcholine
	1.37	0.0314	0.212	-	Annotated	pe(o-18:1(9z)/0:0)	glycerophospholipid
	1.21	0.034	0.222	+	Annotated	lysopc(18:2(9z,12z))	lyso-phosphatidylcholine
	1.68	0.0385	0.25	-	Annotated	n-butyrylglycine	an acyl glycine (minor metabolite of fatty acids).
	1.29	0.0465	0.255	-	Annotated	pe(18:1(9z)/0:0)	glycerophospholipid
acyl-carnitines	1.68	0.0003	0.024	+	Annotated	valerylcarnitine	acyl carnitines: organic compounds containing a fatty acid attached to carnitine. They facilitate the transfer of long-chain fatty acids from cytoplasm into mitochondria to undergo beta-oxidation
	1.78	0.0004	0.024	+	Annotated	isovalerylcarnitine	
	1.84	0.0004	0.024	+	Annotated	isovalerylcarnitine	
	1.47	0.0038	0.081	+	Annotated	hydroxyisovaleroyl carnitine	
	1.30	0.0178	0.165	+	Annotated	palmitoylcarnitine	
	1.32	0.0419	0.248	+	Annotated	stearoylcarnitine	
	1.45	0.0463	0.255	+	Annotated	butyrylcarnitine	
food-related compounds	1.40	0.0001	0.016	+	Annotated	pyrrolidine	in alcoholic beverages and tobacco
	1.52	0.0011	0.04	+	Annotated	tetramethoxyflavone	found in herbs and spices
	1.30	0.0024	0.062	+	Annotated	isocrotonic acid	food preservative
	1.32	0.0044	0.091	+	Annotated	2-napthyloxyacetic acid	food component
	1.32	0.0047	0.096	+	Annotated	tricyclazole	Rice fungicide
	1.31	0.0069	0.109	+	Annotated	dimethylbenzyl carbonyl hexanoate	food additive
	1.43	0.0069	0.109	-	Annotated	4-methoxybenzyl formate	food flavouring
	1.24	0.0078	0.111	-	Annotated	4-methylnonanoic acid	flavouring in cooked meats
	1.31	0.0078	0.111	+	Annotated	dihydrochalcone	in mushrooms
	1.38	0.008	0.111	+	Annotated	isocrotonic acid	food preservative
	1.47	0.0087	0.119	+	Annotated	3,6,8,4',5'-pentamethoxyflavone	found in citrus
	1.15	0.0138	0.157	-	Annotated	phytanic acid	fatty acid (from dairy products, ruminant animal fats, and certain fish)
	1.33	0.0141	0.157	+	Annotated	acetophenone	food flavouring
	1.31	0.0149	0.157	+	Annotated	benzene	used in pesticides and rubbers
1.41	0.0183	0.165	+	Annotated	(1s,2s,4r,8r)-p-menthane-1,2,8,9-tetrol	found in fats and oils	

	FC	p	p _{corrected}	Ion	Evidence	Metabolite	Notes
food	1.32	0.0198	0.17	-	Annotated	cyclohexyl 3-methylbutanoate	food flavouring
	1.17	0.0211	0.173	+	Annotated	peperinic acid	in aged peppermint oil.
	1.52	0.0212	0.173	+	Annotated	geniposidic acid	in beverages
	1.43	0.022	0.173	-	Annotated	1-OH-1-phenyl-3-hexadecanone	found in fats and oils.
	1.35	0.0257	0.193	+	Annotated	3-(2-furanyl)-2-phenyl-2-propenal	flavouring for tobacco and food product
	1.22	0.0266	0.195	-	Annotated	ethyl (±)-3-methylpentanoate	flavouring ingredient
	1.38	0.0424	0.248	-	Annotated	1-phenyl-1,3-hexadecanedione	in fats and oils
Others	2.38	0.0002	0.023	-	Annotated	DHEAs	Sex hormone
	1.55	0.0258	0.193	-	Annotated	Androsterone sulfate	Sex hormone
	1.72	0.0005	0.024	-	Annotated	1alpha,25-dihydroxy (...) vit d3	Vit D derivative
	1.46	0.0006	0.029	-	Annotated	3r-hydroxy-hexanoic acid	component of urine
	1.52	0.0026	0.064	-	Identified	rhamnose	6-deoxy-hexose
	1.64	0.0036	0.078	+	Annotated	dihydrothymine	intermediate breakdown product of thymine; toxic at high levels
	1.39	0.0061	0.108	-	Annotated	3-hydroxy-2-methylpyridine-4,5-dicarboxylate	last step in the synthesis of succinate semialdehyde, an intermediate in butanoate metabolism.
	1.32	0.0077	0.111	+	Annotated	1alpha,25-dihydroxy (...) vit d3	Vit D derivative
	1.30	0.0093	0.124	-	Annotated	5-hydroxyindoleacetic acid	breakdown product of serotonin that is excreted in the urine.
	1.24	0.0162	0.159	+	Annotated	xanthylic acid	metabolic intermediate in the Purine Metabolism
	1.40	0.0163	0.159	-	Annotated	cholesterol sulfate	associated with hypercholesterolemia
	1.21	0.0273	0.198	+	Identified +F	creatinine	-
	1.33	0.0277	0.198	-	Annotated	(r)-3-hydroxydecanoic acid	intermediate in fatty acid biosynthesis.
	1.42	0.0318	0.212	+	Annotated	Noradrenaline	-
	1.21	0.0321	0.215	-	Annotated	glucosamine	aminosugar
	1.30	0.0455	0.255	-	Annotated	n1-met-2-pyridone-5-carboxamide	uremic toxin.
1.34	0.0463	0.255	+	Annotated	n1-met-2-pyridone-5-carboxamide	uremic toxin.	
1.33	0.0469	0.255	+	Annotated	Lipoic acid	Enzymatic cofactor (e.g. citric acid cycle)	

FC = fold change; p and p_{corrected} High-Na⁺ vs Low-Na⁺, p_{corrected} < 0.05 in bold and dark grey shaded. Ion: positive or negative mode peak acquisition. Evidence for LC/MS peaks: identified (matched by retention time and mass to a standard) or annotated (assigned putatively on the basis of mass) compounds □ fragmentation (F), based on the Metabolite Standards Initiative guidelines

Appendix 8 – SYCAMORE: metabolomic peaks, higher in low-Na⁺ vs high-Na⁺.

	FC	p	p _{corrected}	Ion	Evidence	Metabolite	Notes
uc/pc	0,74	0,0124	0,149	+	Annotated	alanyl-aspartate	incomplete breakdown product of protein digestion/catabolism.
	0,75	0,0161	0,159	-	Annotated	alanyl-aspartate	incomplete breakdown product of protein digestion/catabolism.
	0,60	0,0247	0,189	-	Annotated	glycyl-arginine	incomplete breakdown product of protein digestion/catabolism.
	0,76	0,0360	0,227	+	Annotated	prolyl-glutamate	incomplete breakdown product of protein digestion/catabolism.
food	0,65	0,0034	0,076	-	Annotated	3-hydroxyphenylacetic acid	Antioxidant. It has a protective biological activity in human.
	0,71	0,0056	0,106	-	Annotated	cyclohexyl 3-methylbutanoate	food flavouring (blackcurrant)
	0,80	0,0113	0,141	-	Annotated	beta-d-3-[5-deoxy-5-(dimethylarsinyl)ribofuranosyloxy]-2-hydroxy-1-propanesulfonic acid	found in green vegTable Ss
	0,82	0,0153	0,159	+	Annotated	(2alpha,3alpha,5alpha,22r,23r)-2,3,22,23-tetrahydroxy-25-methylergost-24(28)en-6-one	found in common bean
	0,76	0,0427	0,249	-	Annotated	wharangin	found in green vegTable Ss
Others	0,78	0,0154	0,159	+	Annotated	4-Amino-3-hydroxybutyrate	hydroxy fatty acid
	0,76	0,0197	0,170	-	Annotated	l-aspartate 4-semialdehyde	involved in lysine / homoserine biosynthesis
	0,84	0,0359	0,228	+	Annotated	n-acetyl-l-aspartate	source of acetate for lipid, myelin and CNS neurotransmitters.

Uc/pc = urea cycle/protein catabolism. FC = fold change; p and p_{corrected} High-Na⁺ vs Low-Na⁺, p_{corrected} < 0.05 in bold and dark grey shaded. Ion: positive or negative mode peak acquisition. Evidence for LC/MS peaks: identified (matched by retention time and mass to a standard) or annotated (assigned putatively on the basis of mass) compounds □ fragmentation (F), based on the Metabolite Standards Initiative guidelines

Appendix 9 – ImageJ MACRO for Alcian Blue⁺ area quantification.

```
run("Image Sequence...", "open=E:\\mic\\XXX\\untitled000.tif sort");
run("Invert", "stack");
run("Color Threshold...");
// Color Thresholder 1.50i
// Autogenerated macro, single images only!
min=newArray(3);
max=newArray(3);
filter=newArray(3);
a=getTitle();
run("HSB Stack");
run("Convert Stack to Images");
selectWindow("Hue");
rename("0");
selectWindow("Saturation");
rename("1");
selectWindow("Brightness");
rename("2");
min[0]=70;
max[0]=255;
filter[0]="stop";
min[1]=0;
max[1]=255;
filter[1]="pass";
min[2]=30;
max[2]=255;
filter[2]="pass";
for (i=0;i<3;i++){
  selectWindow(""+i);
  setThreshold(min[i], max[i]);
  run("Convert to Mask");
  if (filter[i]=="stop") run("Invert");
}
imageCalculator("AND create", "0","1");
imageCalculator("AND create", "Result of 0","2");
for (i=0;i<3;i++){
  selectWindow(""+i);
  close();
}
selectWindow("Result of 0");
close();
selectWindow("Result of Result of 0");
rename(a);
// Colour Thresholding-----
run("Close");
run("Make Binary", "method=Default background=Light calculate list");
run("Image Sequence... ", "format=TIFF name=ANALISI
save=E:\\mic\\analisi\\ANALISI0000.tif");
run("Measure...", "choose=E:\\mic\\analisi\\");
saveAs("Results", "E:\\mic\\analisi\\Results.xls");
close();
```

REFERENCES

- ADLER, A. J., TAYLOR, F., MARTIN, N., GOTTLIEB, S., TAYLOR, R. S. & EBRAHIM, S.** 2014. Reduced dietary salt for the prevention of cardiovascular disease. *Cochrane Database Syst Rev*, 2014, Cd009217.
- ALLHAT COLLABORATIVE RESEARCH GROUP**, 2002. Major outcomes in high-risk hypertensive patients randomized to angiotensin-converting enzyme inhibitor or calcium channel blocker vs diuretic: The Antihypertensive and Lipid-Lowering Treatment to Prevent Heart Attack Trial (ALLHAT). *Jama*, 288, 2981-97.
- ANAND, S. S., HAWKES, C., DE SOUZA, R. J., MENTE, A., DEGHAN, M., NUGENT, R., ZULYNYAK, M. A., WEIS, T., BERNSTEIN, A. M., KRAUSS, R. M., KROMHOUT, D., JENKINS, D. J. A., MALIK, V., MARTINEZ-GONZALEZ, M. A., MOZAFFARIAN, D., YUSUF, S., WILLETT, W. C. & POPKIN, B. M.** 2015. Food Consumption and its Impact on Cardiovascular Disease: Importance of Solutions Focused on the Globalized Food System: A Report From the Workshop Convened by the World Heart Federation. *J Am Coll Cardiol*, 66, 1590-1614.
- ANTONELLI, G., ARTUSI, C., MARINOVA, M., BRUGNOLO, L., ZANINOTTO, M., SCARONI, C., GATTI, R., MANTERO, F. & PLEBANI, M.** 2014. Cortisol and cortisone ratio in urine: LC-MS/MS method validation and preliminary clinical application. *Clin Chem Lab Med*, 52, 213-20.
- ASPELUND, A., ROBCIUC, M. R., KARAMAN, S., MAKINEN, T. & ALITALO, K.** 2016. Lymphatic System in Cardiovascular Medicine. *Circ Res*, 118, 515-30.
- ATHER, S., BANGALORE, S., VEMURI, S., CAO, L. B., BOZKURT, B. & MESSERLI, F. H.** 2011. Trials on the effect of cardiac resynchronization on arterial blood pressure in patients with heart failure. *Am J Cardiol*, 107, 561-8.
- AUKLAND, K. & REED, R. K.** 1993. Interstitial-lymphatic mechanisms in the control of extracellular fluid volume. *Physiol Rev*, 73, 1-78.
- BARBARO, N. R., FOSS, J. D., KRYSHAL, D. O., TSYBA, N., KUMARESAN, S., XIAO, L., MERNAUGH, R. L., ITANI, H. A., LOPERENA, R., CHEN, W., DIKALOV, S., TITZE, J. M., KNOLLMANN, B. C., HARRISON, D. G. & KIRABO, A.** 2017. Dendritic Cell Amiloride-Sensitive Channels Mediate Sodium-Induced Inflammation and Hypertension. *Cell Rep*, 21, 1009-1020.
- BAUER, A., CHRIST, F. & GAMBLE, J.** 2004. Can lymphatic drainage be measured non-invasively in human limbs, using plethysmography? *Clin Sci (Lond)*, 106, 627-33.
- BECKETT, N. S., PETERS, R., FLETCHER, A. E., STAESSEN, J. A., LIU, L., DUMITRASCU, D., STOYANOVSKY, V., ANTIKAINEN, R. L., NIKITIN, Y., ANDERSON, C., BELHANI, A., FORETTE, F., RAJKUMAR, C., THIJIS, L., BANYA, W. & BULPITT, C. J.** 2008. Treatment of hypertension in patients 80 years of age or older. *N Engl J Med*, 358, 1887-98.
- BELGRADO, J. P., VANDERMEEREN, L., VANKERCKHOVE, S., VALSAMIS, J. B., MALLOIZEL-DELAUNAY, J., MORAINÉ, J. J. & LIEBENS, F.** 2016. Near-Infrared Fluorescence Lymphatic Imaging to Reconsider Occlusion Pressure of

Superficial Lymphatic Collectors in Upper Extremities of Healthy Volunteers. *Lymphat Res Biol*, 14, 70-7.

BENJAMIN, E. J., VIRANI, S. S., CALLAWAY, C. W., CHAMBERLAIN, A. M., CHANG, A. R., CHENG, S., CHIUVE, S. E., CUSHMAN, M., DELLING, F. N., DEO, R., DE FERRANTI, S. D., FERGUSON, J. F., FORNAGE, M., GILLESPIE, C., **ISASI, C. R.**, JIMENEZ, M. C., JORDAN, L. C., JUDD, S. E., LACKLAND, D., LICHTMAN, J. H., LISABETH, L., LIU, S., LONGENECKER, C. T., LUTSEY, P. L., MACKKEY, J. S., MATCHAR, D. B., MATSUSHITA, K., MUSSOLINO, M. E., NASIR, K., O'FLAHERTY, M., PALANIAPPAN, L. P., PANDEY, A., PANDEY, D. K., REEVES, M. J., RITCHEY, M. D., RODRIGUEZ, C. J., ROTH, G. A., ROSAMOND, W. D., SAMPSON, U. K. A., SATOU, G. M., SHAH, S. H., SPARTANO, N. L., TIRSCHWELL, D. L., TSAO, C. W., VOEKS, J. H., WILLEY, J. Z., WILKINS, J. T., WU, J. H., ALGER, H. M., WONG, S. S. & MUNTNER, P. 2018. Heart Disease and Stroke Statistics-2018 Update: A Report From the American Heart Association. *Circulation*, 137, e67-e492.

BENJAMINI, Y., KRIEGER, A. M. & D., Y. 2006. Adaptive linear step-up procedures that control the false discovery rate. *Biometrika*, 93, 491-507.

BHAVE, G. & NEILSON, E. G. 2011. Body fluid dynamics: back to the future. *J Am Soc Nephrol*, 22, 2166-81.

BLAUSTEIN, M. P., LEENEN, F. H., CHEN, L., GOLOVINA, V. A., HAMLYN, J. M., PALLONE, T. L., VAN HUYSSSE, J. W., ZHANG, J. & WIER, W. G. 2012. How NaCl raises blood pressure: a new paradigm for the pathogenesis of salt-dependent hypertension. *Am J Physiol Heart Circ Physiol*, 302, H1031-49.

BOORSMA, E. M., TER MAATEN, J. M., DAMMAN, K., DINH, W., GUSTAFSSON, F., GOLDSMITH, S., BURKHOF, D., ZANNAD, F., UDELSON, J. E. & VOORS, A. A. 2020. Congestion in heart failure: a contemporary look at physiology, diagnosis and treatment. *Nat Rev Cardiol*, 17, 641-655.

BORLAUG, B. A. 2014. The pathophysiology of heart failure with preserved ejection fraction. *Nat Rev Cardiol*, 11, 507-15.

BORLAUG, B. A., MELENOVSKY, V., RUSSELL, S. D., KESSLER, K., PACAK, K., BECKER, L. C. & KASS, D. A. 2006. Impaired chronotropic and vasodilator reserves limit exercise capacity in patients with heart failure and a preserved ejection fraction. *Circulation*, 114, 2138-47.

BOUTA, E. M., BELL, R. D., RAHIMI, H., XING, L., WOOD, R. W., BINGHAM, C. O., 3RD, RITCHLIN, C. T. & SCHWARZ, E. M. 2018. Targeting lymphatic function as a novel therapeutic intervention for rheumatoid arthritis. *Nat Rev Rheumatol*, 14, 94-106.

BRACONNIER, P., MILANI, B., LONCLE, N., LOURENCO, J. M., BRITO, W., DELACOSTE, J., MAILLARD, M., STUBER, M., BURNIER, M. & PRUIJM, M. 2020. Short-term changes in dietary sodium intake influence sweat sodium concentration and muscle sodium content in healthy individuals. *J Hypertens*, 38, 159-166.

- BRAKENHIELM, E., GONZÁLEZ, A. & DÍEZ, J.** 2020. Role of Cardiac Lymphatics in Myocardial Edema and Fibrosis: JACC Review Topic of the Week. *J Am Coll Cardiol*, 76, 735-744.
- BRANDHORST, S. & LONGO, V. D.** 2019. Dietary Restrictions and Nutrition in the Prevention and Treatment of Cardiovascular Disease. *Circ Res*, 124, 952-965.
- BRAY, G. A., SMITH, S. R., DE JONGE, L., XIE, H., ROOD, J., MARTIN, C. K., MOST, M., BROCK, C., MANCUSO, S. & REDMAN, L. M.** 2012. Effect of dietary protein content on weight gain, energy expenditure, and body composition during overeating: a randomized controlled trial. *Jama*, 307, 47-55.
- BURNAND, K. M., GLASS, D. M., MORTIMER, P. S. & PETERS, A. M.** 2012. Lymphatic dysfunction in the apparently clinically normal contralateral limbs of patients with unilateral lower limb swelling. *Clin Nucl Med*, 37, 9-13.
- CAMPBELL, R. T., JHUND, P. S., CASTAGNO, D., HAWKINS, N. M., PETRIE, M. C. & MCMURRAY, J. J.** 2012. What have we learned about patients with heart failure and preserved ejection fraction from DIG-PEF, CHARM-preserved, and I-PRESERVE? *J Am Coll Cardiol*, 60, 2349-56.
- CANNON, W. B.** 1929. Organization for physiological homeostasis. *Physiological reviews*, 9, 399-431.
- CASTORENA-GONZALEZ, J. A., SRINIVASAN, R. S., KING, P. D., SIMON, A. M. & DAVIS, M. J.** 2020. Simplified method to quantify valve back-leak uncovers severe mesenteric lymphatic valve dysfunction in mice deficient in connexins 43 and 37. *J Physiol*, 598, 2297-2310.
- CECCATO, F., ANTONELLI, G., BARBOT, M., ZILIO, M., MAZZAI, L., GATTI, R., ZANINOTTO, M., MANTERO, F., BOSCARO, M., PLEBANI, M. & SCARONI, C.** 2014. The diagnostic performance of urinary free cortisol is better than the cortisol:cortisone ratio in detecting de novo Cushing's syndrome: the use of a LC-MS/MS method in routine clinical practice. *Eur J Endocrinol*, 171, 1-7.
- CHA, B., GENG, X., MAHAMUD, M. R., ZHANG, J. Y., CHEN, L., KIM, W., JHO, E. H., KIM, Y., CHOI, D., DIXON, J. B., CHEN, H., HONG, Y. K., OLSON, L., KIM, T. H., MERRILL, B. J., DAVIS, M. J. & SRINIVASAN, R. S.** 2018. Complementary Wnt Sources Regulate Lymphatic Vascular Development via PROX1-Dependent Wnt/beta-Catenin Signaling. *Cell Rep*, 25, 571-584.e5.
- CHACHAJ, A., PUŁA, B., CHABOWSKI, M., GRZEGRZÓŁKA, J., SZAHIDEWICZ-KRUPSKA, E., KARCZEWSKI, M., JANCZAK, D., DZIĘGIEL, P., PODHORSKA-OKOŁÓW, M., MAZUR, G., GAMIAN, A. & SZUBA, A.** 2018. Role of the Lymphatic System in the Pathogenesis of Hypertension in Humans. *Lymphat Res Biol*, 16, 140-146.
- CHANG, P. P., WRUCK, L. M., SHAHAR, E., ROSSI, J. S., LOEHR, L. R., RUSSELL, S. D., AGARWAL, S. K., KONETY, S. H., RODRIGUEZ, C. J. & ROSAMOND, W. D.** 2018. Trends in Hospitalizations and Survival of Acute Decompensated Heart Failure in Four US Communities (2005-2014): ARIC Study Community Surveillance. *Circulation*, 138, 12-24.

CHARLTON, K. E., STEYN, K., LEVITT, N. S., JONATHAN, D., ZULU, J. V. & NEL, J. H. 2008. Development and validation of a short questionnaire to assess sodium intake. *Public Health Nutr*, 11, 83-94.

CHEUNG, C. Y. & KO, B. C. 2013. NFAT5 in cellular adaptation to hypertonic stress - regulations and functional significance. *J Mol Signal*, 8, 5.

CHOI, S. Y., LEE-KWON, W. & KWON, H. M. 2020. The evolving role of TonEBP as an immunometabolic stress protein. *Nat Rev Nephrol*, 16, 352-364.

CHOW, C. K., TEO, K. K., RANGARAJAN, S., ISLAM, S., GUPTA, R., AVEZUM, A., BAHONAR, A., CHIFAMBA, J., DAGENAIS, G., DIAZ, R., KAZMI, K., LANAS, F., WEI, L., LOPEZ-JARAMILLO, P., FANGHONG, L., ISMAIL, N. H., PUOANE, T., ROSENGREN, A., SZUBA, A., TEMIZHAN, A., WIELGOSZ, A., YUSUF, R., YUSUFALI, A., MCKEE, M., LIU, L., MONY, P. & YUSUF, S. 2013. Prevalence, awareness, treatment, and control of hypertension in rural and urban communities in high-, middle-, and low-income countries. *Jama*, 310, 959-68.

CHRIST, F., GAMBLE, J., BASCHNEGGER, H. & GARTSIDE, I. B. 1997. Relationship between venous pressure and tissue volume during venous congestion plethysmography in man. *J Physiol*, 503 (Pt 2), 463-7.

CHRISTA, M., WENG, A. M., GEIER, B., WÖRMANN, C., SCHEFFLER, A., LEHMANN, L., OBERBERGER, J., KRAUS, B. J., HAHNER, S., STÖRK, S., KLINK, T., BAUER, W. R., HAMMER, F. & KÖSTLER, H. 2019. Increased myocardial sodium signal intensity in Conn's syndrome detected by ²³Na magnetic resonance imaging. *Eur Heart J Cardiovasc Imaging*, 20, 263-270.

COFFMAN, T. M. 2014. The inextricable role of the kidney in hypertension. *J Clin Invest*, 124, 2341-7.

COGSWELL, M. E., LORIA, C. M., TERRY, A. L., ZHAO, L., WANG, C. Y., CHEN, T. C., WRIGHT, J. D., PFEIFFER, C. M., MERRITT, R., MOY, C. S. & APPEL, L. J. 2018. Estimated 24-Hour Urinary Sodium and Potassium Excretion in US Adults. *Jama*, 319, 1209-1220.

COGSWELL, M. E., MUGAVERO, K., BOWMAN, B. A. & FRIEDEN, T. R. 2016. Dietary Sodium and Cardiovascular Disease Risk--Measurement Matters. *N Engl J Med*, 375, 580-6.

COLLINS, K. J. 1966. The action of exogenous aldosterone on the secretion and composition of drug-induced sweat. *Clin Sci*, 30, 207-21.

CURRIE, G. & DELLES, C. 2016. Use of Biomarkers in the Evaluation and Treatment of Hypertensive Patients. *Curr Hypertens Rep*, 18, 54.

CURRIE, G. & NILSSON, P. M. 2019. Healthy vascular ageing and early vascular ageing. In: TOUYZ, R. M. & DELLES, C. (eds.) *Textbook of Vascular Medicine*. Springer: Cham.

CURTIS, L. H., WHELLAN, D. J., HAMMILL, B. G., HERNANDEZ, A. F., ANSTROM, K. J., SHEA, A. M. & SCHULMAN, K. A. 2008. Incidence and prevalence of heart failure in elderly persons, 1994-2003. *Arch Intern Med*, 168, 418-24.

D'AMARIO, D., MIGLIARO, S., BOROVIAC, J. A., RESTIVO, A., VERGALLO, R., GALLI, M., LEONE, A. M., MONTONE, R. A., NICCOLI, G., ASPROMONTE, N. & CREA, F. 2019. Microvascular Dysfunction in Heart Failure With Preserved Ejection Fraction. *Front Physiol*, 10, 1347.

DAHL, L. K., HEINE, M. & TASSINARI, L. 1962. Role of genetic factors in susceptibility to experimental hypertension due to chronic excess salt ingestion. *Nature*, 194, 480-2.

DAVIS, M. J., SCALLAN, J. P., WOLPERS, J. H., MUTHUCHAMY, M., GASHEV, A. A. & ZAWIEJA, D. C. 2012. Intrinsic increase in lymphangion muscle contractility in response to elevated afterload. *Am J Physiol Heart Circ Physiol*, 303, H795-808.

DE MARCHI, M., MANUELIAN, C. L., TON, S., MANFRIN, D., MENEGHESSO, M., CASSANDRO, M. & PENASA, M. 2017. Prediction of sodium content in commercial processed meat products using near infrared spectroscopy. *Meat Sci*, 125, 61-65.

DHAKAL, B. P., MALHOTRA, R., MURPHY, R. M., PAPPAGIANOPOULOS, P. P., BAGGISH, A. L., WEINER, R. B., HOUSTIS, N. E., EISMAN, A. S., HOUGH, S. S. & LEWIS, G. D. 2015. Mechanisms of exercise intolerance in heart failure with preserved ejection fraction: the role of abnormal peripheral oxygen extraction. *Circ Heart Fail*, 8, 286-94.

DOBBIE, L. J., MACKIN, S. T., HOGARTH, K., LONERGAN, F., KANNENKERIL, D., BROOKSBANK, K. & DELLES, C. 2020. Validation of semi-automated flow-mediated dilation measurement in healthy volunteers. *Blood Press Monit*, 25, 216-223.

DONGAONKAR, R. M., STEWART, R. H., GEISLER, H. J. & LAINE, G. A. 2010. Myocardial microvascular permeability, interstitial oedema, and compromised cardiac function. *Cardiovasc Res*, 87, 331-9.

DUNS, J. 1497. *Questiones subtilissime Scoti in metaphysicam Aristotelis ; Ejusdem de primo rerum principio tractatus; Atque theoremata. (ed. Hibernicus, M.; de Venetiis: per Bonetum Locatellum, 1497).*

EHRlich, E. N. 1966. Reciprocal variations in urinary cortisol and aldosterone in response to increased salt intake in humans. *J Clin Endocrinol Metab*, 26, 1160-9.

EISENHOFER, G., GOLDSTEIN, D. S., WALTHER, M. M., FRIBERG, P., LENDERS, J. W., KEISER, H. R. & PACAK, K. 2003. Biochemical diagnosis of pheochromocytoma: how to distinguish true- from false-positive test results. *J Clin Endocrinol Metab*, 88, 2656-66.

ELIJOVICH, F., WEINBERGER, M. H., ANDERSON, C. A., APPEL, L. J., BURSZTYN, M., COOK, N. R., DART, R. A., NEWTON-CHEH, C. H., SACKS, F. M. & LAFFER, C. L. 2016. Salt Sensitivity of Blood Pressure: A Scientific Statement From the American Heart Association. *Hypertension*, 68, e7-e46.

ESCOBEDO, N. & OLIVER, G. 2017. The Lymphatic Vasculature: Its Role in Adipose Metabolism and Obesity. *Cell Metab*, 26, 598-609.

ETTEHAD, D., EMDIN, C. A., KIRAN, A., ANDERSON, S. G., CALLENDER, T., EMBERSON, J., CHALMERS, J., RODGERS, A. & RAHIMI, K. 2016. Blood

pressure lowering for prevention of cardiovascular disease and death: a systematic review and meta-analysis. *Lancet*, 387, 957-967.

EVERETT, B. M., ZELLER, T., GLYNN, R. J., RIDKER, P. M. & BLANKENBERG, S. 2015. High-sensitivity cardiac troponin I and B-type natriuretic Peptide as predictors of vascular events in primary prevention: impact of statin therapy. *Circulation*, 131, 1851-60.

FEARON, W. F., BALSAM, L. B., FAROUQUE, H. M., CAFFARELLI, A. D., ROBBINS, R. C., FITZGERALD, P. J., YOCK, P. G. & YEUNG, A. C. 2003. Novel index for invasively assessing the coronary microcirculation. *Circulation*, 107, 3129-32.

FELKER, G. M., ELLISON, D. H., MULLENS, W., COX, Z. L. & TESTANI, J. M. 2020. Diuretic Therapy for Patients With Heart Failure: JACC State-of-the-Art Review. *J Am Coll Cardiol*, 75, 1178-1195.

FENSKE, M. 2006. Urinary free cortisol and cortisone excretion in healthy individuals: influence of water loading. *Steroids*, 71, 1014-8.

FISCHEREDER, M., MICHALKE, B., SCHMÖCKEL, E., HABICHT, A., KUNISCH, R., PAVELIC, I., SZABADOS, B., SCHÖNERMARCK, U., NELSON, P. J. & STANGL, M. 2017. Sodium storage in human tissues is mediated by glycosaminoglycan expression. *Am J Physiol Renal Physiol*, 313, F319-f325.

FLUHR, J. W., ELSNER, P., BERARDESCA, E. & MAILBACH, H. I. 2005. *Bioengineering of the Skin. Water and the Stratum Corneum.*, Boca Raton, FL, CRC Press.

FOLCH, J., LEES, M. & SLOANE STANLEY, G. H. 1957. A simple method for the isolation and purification of total lipides from animal tissues. *J Biol Chem*, 226, 497-509.

FOROUZANFAR, M. H., LIU, P., ROTH, G. A., NG, M., BIRYUKOV, S., MARCZAK, L., ALEXANDER, L., ESTEP, K., HASSEN ABATE, K., AKINYEMIJU, T. F., ALI, R., ALVIS-GUZMAN, N., AZZOPARDI, P., BANERJEE, A., BÄRNIGHAUSEN, T., BASU, A., BEKELE, T., BENNETT, D. A., BIADGILIGN, S., CATALÁ-LÓPEZ, F., FEIGIN, V. L., FERNANDES, J. C., FISCHER, F., GEBRU, A. A., GONA, P., GUPTA, R., HANKEY, G. J., JONAS, J. B., JUDD, S. E., KHANG, Y. H., KHOSRAVI, A., KIM, Y. J., KIMOKOTI, R. W., KOKUBO, Y., KOLTE, D., LOPEZ, A., LOTUFO, P. A., MALEKZADEH, R., MELAKU, Y. A., MENSAH, G. A., MISGANAW, A., MOKDAD, A. H., MORAN, A. E., NAWAZ, H., NEAL, B., NGALESONI, F. N., OHKUBO, T., POURMALEK, F., RAFAY, A., RAI, R. K., ROJAS-RUEDA, D., SAMPSON, U. K., SANTOS, I. S., SAWHNEY, M., SCHUTTE, A. E., SEPANLOU, S. G., SHIFA, G. T., SHIUE, I., TEDLA, B. A., THRIFT, A. G., TONELLI, M., TRUELSEN, T., TSILIMPARIS, N., UKWAJA, K. N., UTHMAN, O. A., VASANKARI, T., VENKETASUBRAMANIAN, N., VLASSOV, V. V., VOS, T., WESTERMAN, R., YAN, L. L., YANO, Y., YONEMOTO, N., ZAKI, M. E. & MURRAY, C. J. 2017. Global Burden of Hypertension and Systolic Blood Pressure of at Least 110 to 115 mm Hg, 1990-2015. *Jama*, 317, 165-182.

FOY, B. D. & BURSTEIN, D. 1990. Interstitial sodium nuclear magnetic resonance relaxation times in perfused hearts. *Biophys J*, 58, 127-34.

- FUNDER, J. W., CAREY, R. M., MANTERO, F., MURAD, M. H., REINCKE, M., SHIBATA, H., STOWASSER, M. & YOUNG, W. F., JR.** 2016. The Management of Primary Aldosteronism: Case Detection, Diagnosis, and Treatment: An Endocrine Society Clinical Practice Guideline. *J Clin Endocrinol Metab*, 101, 1889-916.
- GAMBLE, J.** 2002. Realisation of a technique for the non-invasive, clinical assessment of microvascular parameters in man; the KM factor. *Eur Surg Res*, 34, 114-23.
- GAMBLE, J., CHRIST, F. & GARTSIDE, I. B.** 1998. Human calf precapillary resistance decreases in response to small cumulative increases in venous congestion pressure. *J Physiol*, 507 (Pt 2), 611-7.
- GAMBLE, J., GARTSIDE, I. B. & CHRIST, F.** 1993. A reassessment of mercury in silastic strain gauge plethysmography for microvascular permeability assessment in man. *J Physiol*, 464, 407-22.
- GBD 2017 DIET COLLABORATORS**, 2019. Health effects of dietary risks in 195 countries, 1990-2017: a systematic analysis for the Global Burden of Disease Study 2017. *Lancet*, 393, 1958-1972.
- GENSALT** 2007. GenSalt: rationale, design, methods and baseline characteristics of study participants. *J Hum Hypertens*, 21, 639-46.
- GERHALTER, T., CARLIER, P. G. & MARTY, B.** 2017. Acute changes in extracellular volume fraction in skeletal muscle monitored by ²³Na NMR spectroscopy. *Physiol Rep*, 5.
- GIACALONE, G., YAMAMOTO, T., BELVA, F. & HAYASHI, A.** 2020. Bedside 3D Visualization of Lymphatic Vessels with a Handheld Multispectral Optoacoustic Tomography Device. *J Clin Med*, 9.
- GLOAGUEN, Y., MORTON, F., DALY, R., GURDEN, R., ROGERS, S., WANDY, J., WILSON, D., BARRETT, M. & BURGESS, K.** 2017. PiMP my metabolome: an integrated, web-based tool for LC-MS metabolomics data. *Bioinformatics*, 33, 4007-4009.
- GRIFFIN, K. A., CHURCHILL, P. C., PICKEN, M., WEBB, R. C., KURTZ, T. W. & BIDANI, A. K.** 2001. Differential salt-sensitivity in the pathogenesis of renal damage in SHR and stroke prone SHR. *Am J Hypertens*, 14, 311-20.
- GRIFFIN, M., RAO, V. S., IVEY-MIRANDA, J., FLEMING, J., MAHONEY, D., MAULION, C., SUDA, N., SIWAKOTI, K., AHMAD, T., JACOBY, D., RIELLO, R., BELLUMKONDA, L., COX, Z., COLLINS, S., JEON, S., TURNER, J. M., WILSON, F. P., BUTLER, J., INZUCCHI, S. E. & TESTANI, J. M.** 2020. Empagliflozin in Heart Failure: Diuretic and Cardiorenal Effects. *Circulation*, 142, 1028-1039.
- GU, J. W., ANAND, V., SHEK, E. W., MOORE, M. C., BRADY, A. L., KELLY, W. C. & ADAIR, T. H.** 1998. Sodium induces hypertrophy of cultured myocardial myoblasts and vascular smooth muscle cells. *Hypertension*, 31, 1083-7.
- GUYTON, A. C., COLEMAN, T. G. & GRANGER, H. J.** 1972. Circulation: overall regulation. *Annu Rev Physiol*, 34, 13-46.

- GUYTON, A. C., COLEMAN, T. G., YOUNG, D. B., LOHMEIER, T. E. & DECLUE, J. W.** 1980. Salt balance and long-term blood pressure control. *Annu Rev Med*, 31, 15-27.
- GUYTON, A. C. & HALL, J. E.** 2011. *Textbook of Medical Physiology* Philadelphia, PA, Elsevier.
- HALL, J. E.** 2016. Renal Dysfunction, Rather Than Nonrenal Vascular Dysfunction, Mediates Salt-Induced Hypertension. *Circulation*, 133, 894-906.
- HALL, J. E., GUYTON, A. C., SMITH, M. J., JR. & COLEMAN, T. G.** 1980. Blood pressure and renal function during chronic changes in sodium intake: role of angiotensin. *Am J Physiol*, 239, F271-80.
- HAMMON, M., GROSSMANN, S., LINZ, P., KOPP, C., DAHLMANN, A., GARLICH, C., JANKA, R., CAVALLARO, A., LUFT, F. C., UDER, M. & TITZE, J.** 2015. ²³Na Magnetic Resonance Imaging of the Lower Leg of Acute Heart Failure Patients during Diuretic Treatment. *PLoS One*, 10, e0141336.
- HANSELL, P., WELCH, W. J., BLANTZ, R. C. & PALM, F.** 2013. Determinants of kidney oxygen consumption and their relationship to tissue oxygen tension in diabetes and hypertension. *Clin Exp Pharmacol Physiol*, 40, 123-37.
- HAYKOWSKY, M. J., BRUBAKER, P. H., JOHN, J. M., STEWART, K. P., MORGAN, T. M. & KITZMAN, D. W.** 2011. Determinants of exercise intolerance in elderly heart failure patients with preserved ejection fraction. *J Am Coll Cardiol*, 58, 265-74.
- HE, F. J., TAN, M., MA, Y. & MACGREGOR, G. A.** 2020. Salt Reduction to Prevent Hypertension and Cardiovascular Disease: JACC State-of-the-Art Review. *J Am Coll Cardiol*, 75, 632-647.
- HE, F. J., TAN, M. & MACGREGOR, G. A.** 2019. Urinary sodium excretion measures and health outcomes. *Lancet*, 393, 1293.
- HEAGERTY, A. M., AALKJAER, C., BUND, S. J., KORSGAARD, N. & MULVANY, M. J.** 1993. Small artery structure in hypertension. Dual processes of remodeling and growth. *Hypertension*, 21, 391-7.
- HEER, M., BAISCH, F., KROPP, J., GERZER, R. & DRUMMER, C.** 2000. High dietary sodium chloride consumption may not induce body fluid retention in humans. *Am J Physiol Renal Physiol*, 278, F585-95.
- HENRI, O., POUHE, C., HOUSSARI, M., GALAS, L., NICOL, L., EDWARDS-LEVY, F., HENRY, J. P., DUMESNIL, A., BOUKHALFA, I., BANQUET, S., SCHAPMAN, D., THUILLEZ, C., RICHARD, V., MULDER, P. & BRAKENHIELM, E.** 2016. Selective Stimulation of Cardiac Lymphangiogenesis Reduces Myocardial Edema and Fibrosis Leading to Improved Cardiac Function Following Myocardial Infarction. *Circulation*, 133, 1484-97; discussion 1497.
- HENRIKSEN, O.** 1977. Local sympathetic reflex mechanism in regulation of blood flow in human subcutaneous adipose tissue. *Acta Physiol Scand Suppl*, 450, 1-48.
- HERRING, N. & PATERSON, D. J.** 2018. *Levick's Introduction to Cardiovascular Physiology*, CRC Press Book.

HOFMEISTER, L. H., PERISIC, S. & TITZE, J. 2015. Tissue sodium storage: evidence for kidney-like extrarenal countercurrent systems? *Pflugers Arch*, 467, 551-8.

HOLTHOFER, H., VIRTANEN, I., KARINIEMI, A. L., HORMIA, M., LINDER, E. & MIETTINEN, A. 1982. Ulex europaeus I lectin as a marker for vascular endothelium in human tissues. *Lab Invest*, 47, 60-6.

ILIODROMITI, S., CELIS-MORALES, C. A., LYALL, D. M., ANDERSON, J., GRAY, S. R., MACKAY, D. F., NELSON, S. M., WELSH, P., PELL, J. P., GILL, J. M. R. & SATTAR, N. 2018. The impact of confounding on the associations of different adiposity measures with the incidence of cardiovascular disease: a cohort study of 296 535 adults of white European descent. *Eur Heart J*, 39, 1514-1520.

INSTITUTE OF MEDICINE COMMITTEE ON STRATEGIES TO REDUCE SODIUM, I. 2010. The National Academies Collection: Reports funded by National Institutes of Health. In: HENNEY, J. E., TAYLOR, C. L. & BOON, C. S. (eds.) *Strategies to Reduce Sodium Intake in the United States*. Washington (DC): National Academies Press (US)

INSTITUTE OF MEDICINE 2005. *Dietary reference intakes for water, potassium, sodium, chloride, and sulfate*, Washington, D.C., The National Academy Press.

INTERSALT COLLABORATIVE RESEARCH GROUP, 1988. Intersalt: an international study of electrolyte excretion and blood pressure. Results for 24 hour urinary sodium and potassium excretion. *Bmj*, 297, 319-28.

JAAP, A. J., SHORE, A. C., GARTSIDE, I. B., GAMBLE, J. & TOOKE, J. E. 1993. Increased microvascular fluid permeability in young type 1 (insulin-dependent) diabetic patients. *Diabetologia*, 36, 648-52.

JANTSCH, J., SCHATZ, V., FRIEDRICH, D., SCHRODER, A., KOPP, C., SIEGERT, I., MARONNA, A., WENDELBORN, D., LINZ, P., BINGER, K. J., GEBHARDT, M., HEINIG, M., NEUBERT, P., FISCHER, F., TEUFEL, S., DAVID, J. P., NEUFERT, C., CAVALLARO, A., RAKOVA, N., KUPER, C., BECK, F. X., NEUHOFER, W., MULLER, D. N., SCHULER, G., UDER, M., BOGDAN, C., LUFT, F. C. & TITZE, J. 2015. Cutaneous Na⁺ storage strengthens the antimicrobial barrier function of the skin and boosts macrophage-driven host defense. *Cell Metab*, 21, 493-501.

JONES, D. W., LUFT, F. C., WHELTON, P. K., ALDERMAN, M. H., HALL, J. E., PETERSON, E. D., CALIFF, R. M. & MCCARRON, D. A. 2018. Can We End the Salt Wars With a Randomized Clinical Trial in a Controlled Environment? *Hypertension*, 72, 10-11.

JURASCHEK, S. P., MILLER, E. R., 3RD, CHANG, A. R., ANDERSON, C. A. M., HALL, J. E. & APPEL, L. J. 2020. Effects of Sodium Reduction on Energy, Metabolism, Weight, Thirst, and Urine Volume: Results From the DASH (Dietary Approaches to Stop Hypertension)-Sodium Trial. *Hypertension*, 75, 723-729.

KARG, M. V., BOSCH, A., KANNENKERIL, D., STRIEPE, K., OTT, C., SCHNEIDER, M. P., BOEMKE-ZELCH, F., LINZ, P., NAGEL, A. M., TITZE, J., UDER, M. & SCHMIEDER, R. E. 2018. SGLT-2-inhibition with dapagliflozin reduces tissue sodium content: a randomised controlled trial. *Cardiovasc Diabetol*, 17, 5.

- KARLSEN, T. V., NIKPEY, E., HAN, J., REIKVAM, T., RAKOVA, N., CASTORENA-GONZALEZ, J. A., DAVIS, M. J., TITZE, J. M., TENSTAD, O. & WIIG, H.** 2018. High-Salt Diet Causes Expansion of the Lymphatic Network and Increased Lymph Flow in Skin and Muscle of Rats. *Arterioscler Thromb Vasc Biol*, 38, 2054-2064.
- KIM, S., TOKUYAMA, M., HOSOI, M. & YAMAMOTO, K.** 1992. Adrenal and circulating renin-angiotensin system in stroke-prone hypertensive rats. *Hypertension*, 20, 280-91.
- KITADA, K., DAUB, S., ZHANG, Y., KLEIN, J. D., NAKANO, D., PEDCHENKO, T., LANTIER, L., LAROCQUE, L. M., MARTON, A., NEUBERT, P., SCHRODER, A., RAKOVA, N., JANTSCH, J., DIKALOVA, A. E., DIKALOV, S. I., HARRISON, D. G., MULLER, D. N., NISHIYAMA, A., RAUH, M., HARRIS, R. C., LUFT, F. C., WASSERMANN, D. H., SANDS, J. M. & TITZE, J.** 2017. High salt intake reprioritizes osmolyte and energy metabolism for body fluid conservation. *J Clin Invest*, 127, 1944-1959.
- KITZMAN, D. W., NICKLAS, B., KRAUS, W. E., LYLES, M. F., EGGEBEEN, J., MORGAN, T. M. & HAYKOWSKY, M.** 2014. Skeletal muscle abnormalities and exercise intolerance in older patients with heart failure and preserved ejection fraction. *Am J Physiol Heart Circ Physiol*, 306, H1364-70.
- KITZMAN, D. W., UPADHYA, B. & VASU, S.** 2015. What the dead can teach the living: systemic nature of heart failure with preserved ejection fraction. *Circulation*, 131, 522-4.
- KLAHR, S., HAMM, L. L., HAMMERMAN, M. R. & MANDEL, L. J.** 2011. Renal Metabolism: Integrated Responses. *Comprehensive Physiology*.
- KLEINewietfeld, M., MANZEL, A., TITZE, J., KVAKAN, H., YOSEF, N., LINKER, R. A., MULLER, D. N. & HAFLER, D. A.** 2013. Sodium chloride drives autoimmune disease by the induction of pathogenic TH17 cells. *Nature*, 496, 518-22.
- KOPP, C., BEYER, C., LINZ, P., DAHLMANN, A., HAMMON, M., JANTSCH, J., NEUBERT, P., ROSENHAUER, D., MULLER, D. N., CAVALLARO, A., ECKARDT, K. U., SCHETT, G., LUFT, F. C., UDER, M., DISTLER, J. H. W. & TITZE, J.** 2017. Na⁺ deposition in the fibrotic skin of systemic sclerosis patients detected by ²³Na-magnetic resonance imaging. *Rheumatology (Oxford)*, 56, 556-560.
- KOPP, C., LINZ, P., DAHLMANN, A., HAMMON, M., JANTSCH, J., MULLER, D. N., SCHMIEDER, R. E., CAVALLARO, A., ECKARDT, K. U., UDER, M., LUFT, F. C. & TITZE, J.** 2013. ²³Na magnetic resonance imaging-determined tissue sodium in healthy subjects and hypertensive patients. *Hypertension*, 61, 635-40.
- KOPP, C., LINZ, P., WACHSMUTH, L., DAHLMANN, A., HORBACH, T., SCHOFL, C., RENZ, W., SANTORO, D., NIENDORF, T., MULLER, D. N., NEININGER, M., CAVALLARO, A., ECKARDT, K. U., SCHMIEDER, R. E., LUFT, F. C., UDER, M. & TITZE, J.** 2012. (²³)Na magnetic resonance imaging of tissue sodium. *Hypertension*, 59, 167-72.
- KOPP, U. C.** 2011. *Neural Control of Renal Function*, San Rafael (CA), Morgan & Claypool Life Sciences.

- KOTCHEN, T. A., COWLEY, A. W., JR. & FROHLICH, E. D.** 2013. Salt in health and disease--a delicate balance. *N Engl J Med*, 368, 1229-37.
- KROGH, A., LANDIS, E. M. & TURNER, A. H.** 1932. THE MOVEMENT OF FLUID THROUGH THE HUMAN CAPILLARY WALL IN RELATION TO VENOUS PRESSURE AND TO THE COLLOID OSMOTIC PRESSURE OF THE BLOOD. *J Clin Invest*, 11, 63-95.
- KURTZ, T. W., DICARLO, S. E., PRAVENEK, M., JEŽEK, F., ŠILAR, J., KOFRÁNEK, J. & MORRIS, R. C., JR.** 2018. Testing Computer Models Predicting Human Responses to a High-Salt Diet. *Hypertension*, 72, 1407-1416.
- KURTZ, T. W., DICARLO, S. E., PRAVENEK, M., SCHMIDLIN, O., TANAKA, M. & MORRIS, R. C., JR.** 2016. An alternative hypothesis to the widely held view that renal excretion of sodium accounts for resistance to salt-induced hypertension. *Kidney Int*, 90, 965-973.
- LAFFER, C. L., SCOTT, R. C., 3RD, TITZE, J. M., LUFT, F. C. & ELIJOVICH, F.** 2016. Hemodynamics and Salt-and-Water Balance Link Sodium Storage and Vascular Dysfunction in Salt-Sensitive Subjects. *Hypertension*, 68, 195-203.
- LAINE, G. A.** 1988. Microvascular changes in the heart during chronic arterial hypertension. *Circ Res*, 62, 953-60.
- LAINE, G. A. & ALLEN, S. J.** 1991. Left ventricular myocardial edema. Lymph flow, interstitial fibrosis, and cardiac function. *Circ Res*, 68, 1713-21.
- LAM, C. S. P., VOORS, A. A., DE BOER, R. A., SOLOMON, S. D. & VAN VELDHUISEN, D. J.** 2018. Heart failure with preserved ejection fraction: from mechanisms to therapies. *Eur Heart J*, 39, 2780-2792.
- LANG, R. M., BADANO, L. P., MOR-AVI, V., AFILALO, J., ARMSTRONG, A., ERNANDE, L., FLACHSKAMPF, F. A., FOSTER, E., GOLDSTEIN, S. A., KUZNETSOVA, T., LANCELLOTTI, P., MURARU, D., PICARD, M. H., RIETZSCHEL, E. R., RUDSKI, L., SPENCER, K. T., TSANG, W. & VOIGT, J. U.** 2015. Recommendations for cardiac chamber quantification by echocardiography in adults: an update from the American Society of Echocardiography and the European Association of Cardiovascular Imaging. *J Am Soc Echocardiogr*, 28, 1-39.e14.
- LANGENHOVEN, M., KRUGER, M., GOUWS, E. & FABER, M.** 1991. *MRC Food Composition Tables*, South Africa, Parow: Medical Research Council.
- LARAGH, J.** 2001. Laragh's lessons in pathophysiology and clinical pearls for treating hypertension. *Am J Hypertens*, 14, 491-503.
- LAUKKANEN, T., KUNUTSOR, S. K., KHAN, H., WILLEIT, P., ZACCARDI, F. & LAUKKANEN, J. A.** 2018. Sauna bathing is associated with reduced cardiovascular mortality and improves risk prediction in men and women: a prospective cohort study. *BMC Med*, 16, 219.
- LAURENT, S., COCKCROFT, J., VAN BORTEL, L., BOUTOUYRIE, P., GIANNATTASIO, C., HAYOZ, D., PANNIER, B., VLACHOPOULOS, C., WILKINSON, I. & STRUIJKER-BOUDIER, H.** 2006. Expert consensus document on arterial stiffness: methodological issues and clinical applications. *Eur Heart J*, 27, 2588-605.

- LAVIE, C. J., DE SCHUTTER, A., PATEL, D. A., ROMERO-CORRAL, A., ARTHAM, S. M. & MILANI, R. V.** 2012. Body composition and survival in stable coronary heart disease: impact of lean mass index and body fat in the "obesity paradox". *J Am Coll Cardiol*, 60, 1374-80.
- LEMON, P. W., YARASHESKI, K. E. & DOLNY, D. G.** 1986. Validity/reliability of sweat analysis by whole-body washdown vs. regional collections. *J Appl Physiol* (1985), 61, 1967-71.
- LENDERS, J. W., DUH, Q. Y., EISENHOFER, G., GIMENEZ-ROQUEPLO, A. P., GREBE, S. K., MURAD, M. H., NARUSE, M., PACAK, K. & YOUNG, W. F., JR.** 2014. Pheochromocytoma and paraganglioma: an endocrine society clinical practice guideline. *J Clin Endocrinol Metab*, 99, 1915-42.
- LERCHL, K., RAKOVA, N., DAHLMANN, A., RAUH, M., GOLLER, U., BASNER, M., DINGES, D. F., BECK, L., AGUREEV, A., LARINA, I., BARANOV, V., MORUKOV, B., ECKARDT, K. U., VASSILIEVA, G., WABEL, P., VIENKEN, J., KIRSCH, K., JOHANNES, B., KRANNICH, A., LUFT, F. C. & TITZE, J.** 2015. Agreement between 24-hour salt ingestion and sodium excretion in a controlled environment. *Hypertension*, 66, 850-7.
- LEVEY, A. S., STEVENS, L. A., SCHMID, C. H., ZHANG, Y. L., CASTRO, A. F., 3RD, FELDMAN, H. I., KUSEK, J. W., EGGERS, P., VAN LENTE, F., GREENE, T. & CORESH, J.** 2009. A new equation to estimate glomerular filtration rate. *Ann Intern Med*, 150, 604-12.
- LEVICK, J. R. & MICHEL, C. C.** 2010. Microvascular fluid exchange and the revised Starling principle. *Cardiovasc Res*, 87, 198-210.
- LEVY, D., LARSON, M. G., VASAN, R. S., KANNEL, W. B. & HO, K. K.** 1996. The progression from hypertension to congestive heart failure. *Jama*, 275, 1557-62.
- LOPEZ GELSTON, C. A., BALASUBBRAMANIAN, D., ABOUELKHEIR, G. R., LOPEZ, A. H., HUDSON, K. R., JOHNSON, E. R., MUTHUCHAMY, M., MITCHELL, B. M. & RUTKOWSKI, J. M.** 2018. Enhancing Renal Lymphatic Expansion Prevents Hypertension in Mice. *Circ Res*, 122, 1094-1101.
- LOWRY, O. H. & HASTINGS, A. B.** 1942. Histochemical changes associated with aging: I methods and calculations. *J Biol Chem*, 143.
- LOWRY, O. H., HASTINGS, A. B. et al.** 1946. Histochemical changes associated with aging; liver, brain, and kidney in the rat. *J Gerontol*, 1, 345-57.
- LOWRY, O. H., HASTINGS, A. B., HULL, T. Z. & BROWN, A. N.** 1942. Histochemical changes associated with aging: II. Skeletal and cardiac muscle in rats. 143.
- MA, Y., HE, F. J. & MACGREGOR, G. A.** 2015. High salt intake: independent risk factor for obesity? *Hypertension*, 66, 843-9.
- MACHNIK, A., NEUHOFER, W., JANTSCH, J., DAHLMANN, A., TAMMELA, T., MACHURA, K., PARK, J. K., BECK, F. X., MULLER, D. N., DERER, W., GOSS, J., ZIOMBER, A., DIETSCH, P., WAGNER, H., VAN ROOIJEN, N., KURTZ, A., HILGERS, K. F., ALITALO, K., ECKARDT, K. U., LUFT, F. C., KERJASCHKI, D. & TITZE, J.** 2009. Macrophages regulate salt-dependent volume and blood pressure by

a vascular endothelial growth factor-C-dependent buffering mechanism. *Nat Med*, 15, 545-52.

MADÉLIN, G., KLINE, R., WALVICK, R. & REGATTE, R. R. 2014. A method for estimating intracellular sodium concentration and extracellular volume fraction in brain in vivo using sodium magnetic resonance imaging. *Sci Rep*, 4, 4763.

MAIOLINO, G., ROSSITTO, G., BISOGNI, V., CESARI, M., SECCIA, T. M., PLEBANI, M. & ROSSI, G. P. 2017. Quantitative Value of Aldosterone-Renin Ratio for Detection of Aldosterone-Producing Adenoma: The Aldosterone-Renin Ratio for Primary Aldosteronism (AQUARR) Study. *J Am Heart Assoc*, 6.

MALLAMACI, F., LEONARDIS, D., BELLIZZI, V. & ZOCCALI, C. 1996. Does high salt intake cause hyperfiltration in patients with essential hypertension? *J Hum Hypertens*, 10, 157-61.

MANCIA, G., FAGARD, R., NARKIEWICZ, K., REDON, J., ZANCHETTI, A., BOHM, M., CHRISTIAENS, T., CIFKOVA, R., DE BACKER, G., DOMINICZAK, A., GALDERISI, M., GROBBEE, D. E., JAARSMA, T., KIRCHHOF, P., KJELDSEN, S. E., LAURENT, S., MANOLIS, A. J., NILSSON, P. M., RUILOPE, L. M., SCHMIEDER, R. E., SIRNES, P. A., SLEIGHT, P., VIIGIMAA, M., WAEBER, B., ZANNAD, F., REDON, J., DOMINICZAK, A., NARKIEWICZ, K., NILSSON, P. M., BURNIER, M., VIIGIMAA, M., AMBROSIONI, E., CAUFIELD, M., COCA, A., OLSEN, M. H., SCHMIEDER, R. E., TSIOUFIS, C., VAN DE BORNE, P., ZAMORANO, J. L., ACHENBACH, S., BAUMGARTNER, H., BAX, J. J., BUENO, H., DEAN, V., DEATON, C., EROL, C., FAGARD, R., FERRARI, R., HASDAI, D., HOES, A. W., KIRCHHOF, P., KNUUTI, J., KOLH, P., LANCELLOTTI, P., LINHART, A., NIHOYANNOPOULOS, P., PIEPOLI, M. F., PONIKOWSKI, P., SIRNES, P. A., TAMARGO, J. L., TENDERA, M., TORBICKI, A., WIJNS, W., WINDECKER, S., CLEMENT, D. L., COCA, A., GILLEBERT, T. C., TENDERA, M., ROSEI, E. A., AMBROSIONI, E., ANKER, S. D., BAUERSACHS, J., HITIJ, J. B., CAULFIELD, M., DE BUYZERE, M., DE GEEST, S., DERUMEAUX, G. A., ERDINE, S., FARSANG, C., FUNCK-BRENTANO, C., GERC, V., GERMANO, G., GIELEN, S., HALLER, H., HOES, A. W., JORDAN, J., KAHAN, T., KOMAJDA, M., LOVIC, D., MAHRHOLDT, H., OLSEN, M. H., OSTERGREN, J., PARATI, G., PERK, J., POLONIA, J., POPESCU, B. A., REINER, Z., RYDEN, L., SIRENKO, Y., STANTON, A., et al. 2013. 2013 ESH/ESC guidelines for the management of arterial hypertension: the Task Force for the Management of Arterial Hypertension of the European Society of Hypertension (ESH) and of the European Society of Cardiology (ESC). *Eur Heart J*, 34, 2159-219.

MANCIA, G., OPARIL, S., WHELTON, P. K., MCKEE, M., DOMINICZAK, A., LUFT, F. C., ALHABIB, K., LANAS, F., DAMASCENO, A., PRABHAKARAN, D., LA TORRE, G., WEBER, M., O'DONNELL, M., SMITH, S. C. & NARULA, J. 2017. The technical report on sodium intake and cardiovascular disease in low- and middle-income countries by the joint working group of the World Heart Federation, the European Society of Hypertension and the European Public Health Association. *Eur Heart J*, 38, 712-719.

MAUBEC, E., LAOUÉAN, C., DESCHAMPS, L., NGUYEN, V. T., SCHEERSEN-YARICH, I., WACKENHEIM-JACOBS, A. C., STEFF, M., DUHAMEL, S., TUBIANA, S., BRAHIMI, N., LECLERC-MERCIER, S., CRICKX, B., PERRET, C., ARACTINGI, S., ESCOUBET, B., DUVAL, X., ARNAUD, P., JAISSER, F., MENTRÉ, F. & FARMAN, N. 2015. Topical Mineralocorticoid Receptor Blockade

Limits Glucocorticoid-Induced Epidermal Atrophy in Human Skin. *J Invest Dermatol*, 135, 1781-1789.

MCENIERY, C. M., YASMIN, HALL, I. R., QASEM, A., WILKINSON, I. B. & COCKCROFT, J. R. 2005. Normal vascular aging: differential effects on wave reflection and aortic pulse wave velocity: the Anglo-Cardiff Collaborative Trial (ACCT). *J Am Coll Cardiol*, 46, 1753-60.

MCMURRAY, J. J. V., SOLOMON, S. D., INZUCCHI, S. E., KOBER, L., KOSIBOROD, M. N., MARTINEZ, F. A., PONIKOWSKI, P., SABATINE, M. S., ANAND, I. S., BELOHLAVEK, J., BOHM, M., CHIANG, C. E., CHOPRA, V. K., DE BOER, R. A., DESAI, A. S., DIEZ, M., DROZDZ, J., DUKAT, A., GE, J., HOWLETT, J. G., KATOVA, T., KITAKAZE, M., LJUNGMAN, C. E. A., MERKELY, B., NICOLAU, J. C., O'MEARA, E., PETRIE, M. C., VINH, P. N., SCHOU, M., TERESHCHENKO, S., VERMA, S., HELD, C., DEMETS, D. L., DOCHERTY, K. F., JHUND, P. S., BENGTSSON, O., SJOSTRAND, M. & LANGKILDE, A. M. 2019. Dapagliflozin in Patients with Heart Failure and Reduced Ejection Fraction. *N Engl J Med*, 381, 1995-2008.

MEDINA-INOJOSA, J. R., SOMERS, V. K., THOMAS, R. J., JEAN, N., JENKINS, S. M., GOMEZ-IBARRA, M. A., SUPERVIA, M. & LOPEZ-JIMENEZ, F. 2018. Association Between Adiposity and Lean Mass With Long-Term Cardiovascular Events in Patients With Coronary Artery Disease: No Paradox. *J Am Heart Assoc*, 7.

MENTE, A., O'DONNELL, M., RANGARAJAN, S., MCQUEEN, M., DAGENAIS, G., WIELGOSZ, A., LEAR, S., AH, S. T. L., WEI, L., DIAZ, R., AVEZUM, A., LOPEZ-JARAMILLO, P., LANAS, F., MONY, P., SZUBA, A., IQBAL, R., YUSUF, R., MOHAMMADIFARD, N., KHATIB, R., YUSOFF, K., ISMAIL, N., GULEC, S., ROSENGREN, A., YUSUFALI, A., KRUGER, L., TSOLEKILE, L. P., CHIFAMBA, J., DANS, A., ALHABIB, K. F., YEATES, K., TEO, K. & YUSUF, S. 2018. Urinary sodium excretion, blood pressure, cardiovascular disease, and mortality: a community-level prospective epidemiological cohort study. *Lancet*, 392, 496-506.

MENTE, A., O'DONNELL, M. J., RANGARAJAN, S., MCQUEEN, M. J., POIRIER, P., WIELGOSZ, A., MORRISON, H., LI, W., WANG, X., DI, C., MONY, P., DEVANATH, A., ROSENGREN, A., OGUZ, A., ZATONSKA, K., YUSUFALI, A. H., LOPEZ-JARAMILLO, P., AVEZUM, A., ISMAIL, N., LANAS, F., PUOANE, T., DIAZ, R., KELISHADI, R., IQBAL, R., YUSUF, R., CHIFAMBA, J., KHATIB, R., TEO, K. & YUSUF, S. 2014. Association of urinary sodium and potassium excretion with blood pressure. *N Engl J Med*, 371, 601-11.

MENTE, A., O'DONNELL, M. J. & YUSUF, S. 2019. Urinary sodium excretion measures and health outcomes - Authors' reply. *Lancet*, 393, 1295-1296.

MESSERLI, F. H., HOFSTETTER, L. & BANGALORE, S. 2018. Salt and heart disease: a second round of "bad science"? *Lancet*, 392, 456-458.

MESSERLI, F. H., RIMOLDI, S. F. & BANGALORE, S. 2017. The Transition From Hypertension to Heart Failure: Contemporary Update. *JACC Heart Fail*, 5, 543-551.

MICHEL, C. C. 1980. Filtration coefficients and osmotic reflexion coefficients of the walls of single frog mesenteric capillaries. *J Physiol*, 309, 341-55.

- MICHEL, C. C.** 1989. Microvascular permeability, venous stasis and oedema. *Int Angiol*, 8, 9-13.
- MIYAKAWA, H., WOO, S. K., DAHL, S. C., HANDLER, J. S. & KWON, H. M.** 1999. Tonicity-responsive enhancer binding protein, a rel-like protein that stimulates transcription in response to hypertonicity. *Proc Natl Acad Sci U S A*, 96, 2538-42.
- MOHAMMED, S. F., HUSSAIN, S., MIRZOYEV, S. A., EDWARDS, W. D., MALESZEWSKI, J. J. & REDFIELD, M. M.** 2015. Coronary microvascular rarefaction and myocardial fibrosis in heart failure with preserved ejection fraction. *Circulation*, 131, 550-9.
- MOHANAKUMAR, S., TELINIUS, N., KELLY, B., LAURIDSEN, H., BOEDTKJER, D., PEDERSEN, M., DE LEVAL, M. & HJORTDAL, V.** 2019. Morphology and Function of the Lymphatic Vasculature in Patients With a Fontan Circulation. *Circ Cardiovasc Imaging*, 12, e008074.
- MORIMOTO, A., UZU, T., FUJII, T., NISHIMURA, M., KURODA, S., NAKAMURA, S., INENAGA, T. & KIMURA, G.** 1997. Sodium sensitivity and cardiovascular events in patients with essential hypertension. *Lancet*, 350, 1734-7.
- MORISAWA, N., KITADA, K., FUJISAWA, Y., NAKANO, D., YAMAZAKI, D., KOBUCHI, S., LI, L., ZHANG, Y., MORIKAWA, T., KONISHI, Y., YOKOO, T., LUFT, F. C., TITZE, J. & NISHIYAMA, A.** 2020. Renal sympathetic nerve activity regulates cardiovascular energy expenditure in rats fed high salt. *Hypertens Res*, 43, 482-491.
- MORRIS, R. C., JR., SCHMIDLIN, O., SEBASTIAN, A., TANAKA, M. & KURTZ, T. W.** 2016. Vasodysfunction That Involves Renal Vasodysfunction, Not Abnormally Increased Renal Retention of Sodium, Accounts for the Initiation of Salt-Induced Hypertension. *Circulation*, 133, 881-93.
- MORTIMER, P. S. & ROCKSON, S. G.** 2014. New developments in clinical aspects of lymphatic disease. *J Clin Invest*, 124, 915-21.
- MULLENS, W., DAMMAN, K., HARJOLA, V. P., MEBAZAA, A., BRUNNER-LA ROCCA, H. P., MARTENS, P., TESTANI, J. M., TANG, W. H. W., ORSO, F., ROSSIGNOL, P., METRA, M., FILIPPATOS, G., SEFEROVIC, P. M., RUSCHITZKA, F. & COATS, A. J.** 2019. The use of diuretics in heart failure with congestion - a position statement from the Heart Failure Association of the European Society of Cardiology. *Eur J Heart Fail*, 21, 137-155.
- MULVANY, M. J. & AALKJAER, C.** 1990. Structure and function of small arteries. *Physiol Rev*, 70, 921-61.
- MURRAY, C. J. & LOPEZ, A. D.** 2013. Measuring the global burden of disease. *N Engl J Med*, 369, 448-57.
- NAGUEH, S. F., SMISETH, O. A., APPLETON, C. P., BYRD, B. F., 3RD, DOKAINISH, H., EDVARDBSEN, T., FLACHSKAMPF, F. A., GILLEBERT, T. C., KLEIN, A. L., LANCELLOTTI, P., MARINO, P., OH, J. K., POPESCU, B. A. & WAGGONER, A. D.** 2016. Recommendations for the Evaluation of Left Ventricular Diastolic Function by Echocardiography: An Update from the American Society of

Echocardiography and the European Association of Cardiovascular Imaging. *J Am Soc Echocardiogr*, 29, 277-314.

NATRIURETIC PEPTIDES STUDIES, WILLEIT, P., KAPTOGE, S., WELSH, P., BUTTERWORTH, A. S., CHOWDHURY, R., SPACKMAN, S. A., PENNELLS, L., GAO, P., BURGESS, S., FREITAG, D. F., SWEETING, M., WOOD, A. M., COOK, N. R., JUDD, S., TROMPET, S., NAMBI, V., OLSEN, M. H., EVERETT, B. M., KEE, F., ÄRNLÖV, J., SALOMAA, V., LEVY, D., KAUKANEN, J., LAUKKANEN, J. A., KAVOUSHI, M., NINOMIYA, T., CASAS, J. P., DANIELS, L. B., LIND, L., KISTORP, C. N., ROSENBERG, J., MUELLER, T., RUBATTU, S., PANAGIOTAKOS, D. B., FRANCO, O. H., DE LEMOS, J. A., LUCHNER, A., KIZER, J. R., KIECHL, S., SALONEN, J. T., GOYA WANNAMETHEE, S., DE BOER, R. A., NORDESTGAARD, B. G., ANDERSSON, J., JØRGENSEN, T., MELANDER, O., BALLANTYNE CH, M., DEFILIPPI, C., RIDKER, P. M., CUSHMAN, M., ROSAMOND, W. D., THOMPSON, S. G., GUDNASON, V., SATTAR, N., DANESH, J. & DI ANGELANTONIO, E. 2016. Natriuretic peptides and integrated risk assessment for cardiovascular disease: an individual-participant-data meta-analysis. *Lancet Diabetes Endocrinol*, 4, 840-9.

NEAL, B., PERKOVIC, V., MAHAFFEY, K. W., DE ZEEUW, D., FULCHER, G., ERONDU, N., SHAW, W., LAW, G., DESAI, M. & MATTHEWS, D. R. 2017. Canagliflozin and Cardiovascular and Renal Events in Type 2 Diabetes. *N Engl J Med*, 377, 644-657.

NICHOLS, W. W. & O'ROURKE, M. F. 2011. *In: CHARALAMBOS VLACHOPOULOS, M. O. R., WILMER W. NICHOLS (ed.) McDonald's Blood Flow in Arteries*. 6 ed. London: CRC Press.

NIEMAN, L. K., BILLER, B. M., FINDLING, J. W., NEWELL-PRICE, J., SAVAGE, M. O., STEWART, P. M. & MONTORI, V. M. 2008. The diagnosis of Cushing's syndrome: an Endocrine Society Clinical Practice Guideline. *J Clin Endocrinol Metab*, 93, 1526-40.

NIJST, P., OLINEVICH, M., HILKENS, P., MARTENS, P., DUPONT, M., TANG, W. H. W., LAMBRICHTS, I., NOBEN, J. P. & MULLENS, W. 2018. Dermal Interstitial Alterations in Patients With Heart Failure and Reduced Ejection Fraction: A Potential Contributor to Fluid Accumulation? *Circ Heart Fail*, 11, e004763.

NIKPEY, E., KARLSEN, T. V., RAKOVA, N., TITZE, J. M., TENSTAD, O. & WIIG, H. 2017. High-Salt Diet Causes Osmotic Gradients and Hyperosmolality in Skin Without Affecting Interstitial Fluid and Lymph. *Hypertension*, 69, 660-668.

NOMURA, K., ASAYAMA, K., JACOBS, L., THIJS, L. & STAESSEN, J. A. 2017. Renal function in relation to sodium intake: a quantitative review of the literature. *Kidney Int*, 92, 67-78.

O'DONNELL, M., MENTE, A., ALDERMAN, M. H., BRADY, A. J. B., DIAZ, R., GUPTA, R., LÓPEZ-JARAMILLO, P., LUFT, F. C., LÜSCHER, T. F., MANCIA, G., MANN, J. F. E., MCCARRON, D., MCKEE, M., MESSERLI, F. H., MOORE, L. L., NARULA, J., OPARIL, S., PACKER, M., PRABHAKARAN, D., SCHUTTE, A., SLIWA, K., STAESSEN, J. A., YANCY, C. & YUSUF, S. 2020. Salt and cardiovascular disease: insufficient evidence to recommend low sodium intake. *Eur Heart J*, 41, 3363-3373.

O'DONNELL, M., MENTE, A., RANGARAJAN, S., MCQUEEN, M. J., WANG, X., LIU, L., YAN, H., LEE, S. F., MONY, P., DEVANATH, A., ROSENGREN, A., LOPEZ-JARAMILLO, P., DIAZ, R., AVEZUM, A., LANAS, F., YUSOFF, K., IQBAL, R., ILOW, R., MOHAMMADIFARD, N., GULEC, S., YUSUFALI, A. H., KRUGER, L., YUSUF, R., CHIFAMBA, J., KABALI, C., DAGENAIS, G., LEAR, S. A., TEO, K. & YUSUF, S. 2014. Urinary sodium and potassium excretion, mortality, and cardiovascular events. *N Engl J Med*, 371, 612-23.

OKAMOTO, K., YAMORI, Y. & NAGAOKA, A. 1974. Establishment of the stroke-prone spontaneously hypertensive rats (SHR). *Circulation Research*, 34, 143–153.

OLSEN, M. H., ANGELL, S. Y., ASMA, S., BOUTOUYRIE, P., BURGER, D., CHIRINOS, J. A., DAMASCENO, A., DELLES, C., GIMENEZ-ROQUEPLO, A. P., HERING, D., LÓPEZ-JARAMILLO, P., MARTINEZ, F., PERKOVIC, V., RIETZSCHEL, E. R., SCHILLACI, G., SCHUTTE, A. E., SCUTERI, A., SHARMAN, J. E., WACHTELL, K. & WANG, J. G. 2016. A call to action and a lifecourse strategy to address the global burden of raised blood pressure on current and future generations: the Lancet Commission on hypertension. *Lancet*, 388, 2665-2712.

WORLD HEALTH ORGANIZATION, 2012. Guideline: sodium intake for adults and children.

PAGET, V., LEGEDZ, L., GAUDEBOUT, N., GIRERD, N., BRICCA, G., MILON, H., VINCENT, M. & LANTELME, P. 2011. N-terminal pro-brain natriuretic peptide: a powerful predictor of mortality in hypertension. *Hypertension*, 57, 702-9.

PASSING, H. & BABLOK 1983. A new biometrical procedure for testing the equality of measurements from two different analytical methods. Application of linear regression procedures for method comparison studies in clinical chemistry, Part I. *J Clin Chem Clin Biochem*, 21, 709-20.

PAULUS, W. J. & TSCHOPE, C. 2013. A novel paradigm for heart failure with preserved ejection fraction: comorbidities drive myocardial dysfunction and remodeling through coronary microvascular endothelial inflammation. *J Am Coll Cardiol*, 62, 263-71.

PETRACCA, M., VANCEA, R. O., FLEYSHER, L., JONKMAN, L. E., OESINGMANN, N. & INGLESE, M. 2016. Brain intra- and extracellular sodium concentration in multiple sclerosis: a 7 T MRI study. *Brain*, 139, 795-806.

PFEFFER, M. A., SHAH, A. M. & BORLAUG, B. A. 2019. Heart Failure With Preserved Ejection Fraction In Perspective. *Circ Res*, 124, 1598-1617.

PONIKOWSKI, P., VOORS, A. A., ANKER, S. D., BUENO, H., CLELAND, J. G., COATS, A. J., FALK, V., GONZALEZ-JUANATEY, J. R., HARJOLA, V. P., JANKOWSKA, E. A., JESSUP, M., LINDE, C., NIHOYANNOPOULOS, P., PARISSIS, J. T., PIESKE, B., RILEY, J. P., ROSANO, G. M., RUILOPE, L. M., RUSCHITZKA, F., RUTTEN, F. H. & VAN DER MEER, P. 2016. 2016 ESC Guidelines for the diagnosis and treatment of acute and chronic heart failure: The Task Force for the diagnosis and treatment of acute and chronic heart failure of the European Society of Cardiology (ESC) Developed with the special contribution of the Heart Failure Association (HFA) of the ESC. *Eur Heart J*, 37, 2129-200.

PRIES, A. R. & REGLIN, B. 2017. Coronary microcirculatory pathophysiology: can we afford it to remain a black box? *Eur Heart J*, 38, 478-488.

PRIOR, I. A., EVANS, J. G., HARVEY, H. P., DAVIDSON, F. & LINDSEY, M. 1968. Sodium intake and blood pressure in two Polynesian populations. *N Engl J Med*, 279, 515-20.

PRUIJM, M., HOFMANN, L., MAILLARD, M., TREMBLAY, S., GLATZ, N., WUERZNER, G., BURNIER, M. & VOGT, B. 2010. Effect of sodium loading/depletion on renal oxygenation in young normotensive and hypertensive men. *Hypertension*, 55, 1116-22.

PYKE, K. E. & TSCHAKOVSKY, M. E. 2005. The relationship between shear stress and flow-mediated dilatation: implications for the assessment of endothelial function. *J Physiol*, 568, 357-69.

QUINTERO-ATENCIO, J., VÁSQUEZ-LEÓN, H. & PINO-QUINTERO, L. M. 1966. Association of sweat sodium with arterial-blood pressure. *N Engl J Med*, 274, 1224-8.

RAKOVA, N., JUTTNER, K., DAHLMANN, A., SCHRODER, A., LINZ, P., KOPP, C., RAUH, M., GOLLER, U., BECK, L., AGUREEV, A., VASSILIEVA, G., LENKOVA, L., JOHANNES, B., WABEL, P., MOISSL, U., VIENKEN, J., GERZER, R., ECKARDT, K. U., MULLER, D. N., KIRSCH, K., MORUKOV, B., LUFT, F. C. & TITZE, J. 2013. Long-term space flight simulation reveals infradian rhythmicity in human Na(+) balance. *Cell Metab*, 17, 125-31.

RAKOVA, N., KITADA, K., LERCHL, K., DAHLMANN, A., BIRUKOV, A., DAUB, S., KOPP, C., PEDCHENKO, T., ZHANG, Y., BECK, L., JOHANNES, B., MARTON, A., MULLER, D. N., RAUH, M., LUFT, F. C. & TITZE, J. 2017. Increased salt consumption induces body water conservation and decreases fluid intake. *J Clin Invest*, 127, 1932-1943.

RASK, E., OLSSON, T., SODERBERG, S., ANDREW, R., LIVINGSTONE, D. E., JOHNSON, O. & WALKER, B. R. 2001. Tissue-specific dysregulation of cortisol metabolism in human obesity. *J Clin Endocrinol Metab*, 86, 1418-21.

REBOLDI, G., VERDECCHIA, P., FIORUCCI, G., BEILIN, L. J., EGUCHI, K., IMAI, Y., KARIO, K., OHKUBO, T., PIERDOMENICO, S. D., SCHWARTZ, J. E., WING, L., SALADINI, F. & PALATINI, P. 2018. Glomerular hyperfiltration is a predictor of adverse cardiovascular outcomes. *Kidney Int*, 93, 195-203.

RODEHEFFER, R. J. 2011. Hypertension and heart failure: the ALLHAT imperative. *Circulation*, 124, 1803-5.

ROSSI, G. P., CELOOTTO, G., ROSSITTO, G., SECCIA, T. M., MAIOLINO, G., BERTON, C., BASSO, D. & PLEBANI, M. 2016. Prospective validation of an automated chemiluminescence-based assay of renin and aldosterone for the work-up of arterial hypertension. *Clin Chem Lab Med*, 54, 1441-50.

ROSSITTO, G., MAIOLINO, G., LERCO, S., CELOOTTO, G., BLACKBURN, G., MARY, S., ANTONELLI, G., BERTON, C., BISOGNI, V., CESARI, M., SECCIA, T. M., LENZINI, L., PINATO, A., MONTEZANO, A., TOUYZ, R. M., PETRIE, M. C., DALY, R., WELSH, P., PLEBANI, M., ROSSI, G. P. & DELLES, C. 2020. High

Sodium Intake, Glomerular Hyperfiltration and Protein Catabolism in Patients with Essential Hypertension. *Cardiovasc Res*.

ROSSITTO, G., TOUYZ, R. M., PETRIE, M. C. & DELLES, C. 2018. Much Ado about N...atrium: modelling tissue sodium as a highly sensitive marker of subclinical and localized oedema. *Clin Sci (Lond)*, 132, 2609-2613.

SACKS, F. M., SVETKEY, L. P., VOLLMER, W. M., APPEL, L. J., BRAY, G. A., HARSHA, D., OBARZANEK, E., CONLIN, P. R., MILLER, E. R., 3RD, SIMONS-MORTON, D. G., KARANJA, N. & LIN, P. H. 2001. Effects on blood pressure of reduced dietary sodium and the Dietary Approaches to Stop Hypertension (DASH) diet. DASH-Sodium Collaborative Research Group. *N Engl J Med*, 344, 3-10.

SAFAR, M. E., THUILLIEZ, C., RICHARD, V. & BENETOS, A. 2000. Pressure-independent contribution of sodium to large artery structure and function in hypertension. *Cardiovasc Res*, 46, 269-76.

SCALLAN, J. P., HILL, M. A. & DAVIS, M. J. 2015. Lymphatic vascular integrity is disrupted in type 2 diabetes due to impaired nitric oxide signalling. *Cardiovasc Res*, 107, 89-97.

SCALLAN, J. P., WOLPERS, J. H., MUTHUCHAMY, M., ZAWIEJA, D. C., GASHEV, A. A. & DAVIS, M. J. 2012. Independent and interactive effects of preload and afterload on the pump function of the isolated lymphangion. *Am J Physiol Heart Circ Physiol*, 303, H809-24.

SCALLAN, J. P., ZAWIEJA, S. D., CASTORENA-GONZALEZ, J. A. & DAVIS, M. J. 2016. Lymphatic pumping: mechanics, mechanisms and malfunction. *J Physiol*, 594, 5749-5768.

SCHEDL, H. P., CHEN, P. S., JR., GREENE, G. & REDD, D. 1959. The renal clearance of plasma cortisol. *J Clin Endocrinol Metab*, 19, 1223-9.

SCHERER, C., PFISTERER, L., WAGNER, A. H., HODEBECK, M., CATTARUZZA, M., HECKER, M. & KORFF, T. 2014. Arterial wall stress controls NFAT5 activity in vascular smooth muscle cells. *J Am Heart Assoc*, 3, e000626.

SCHNEIDER, M. P., RAFF, U., KOPP, C., SCHEPPACH, J. B., TONCAR, S., WANNER, C., SCHLIEPER, G., SARITAS, T., FLOEGE, J., SCHMID, M., BIRUKOV, A., DAHLMANN, A., LINZ, P., JANKA, R., UDER, M., SCHMIEDER, R. E., TITZE, J. M. & ECKARDT, K. U. 2017. Skin Sodium Concentration Correlates with Left Ventricular Hypertrophy in CKD. *J Am Soc Nephrol*, 28, 1867-1876.

SELVARAJAH, V., MAKI-PETAJA, K. M., PEDRO, L., BRUGGRABER, S. F. A., BURLING, K., GOODHART, A. K., BROWN, M. J., MCENIERY, C. M. & WILKINSON, I. B. 2017. Novel Mechanism for Buffering Dietary Salt in Humans: Effects of Salt Loading on Skin Sodium, Vascular Endothelial Growth Factor C, and Blood Pressure. *Hypertension*, 70, 930-937.

SHAH, S. J., LAM, C. S. P., SVEDLUND, S., SARASTE, A., HAGE, C., TAN, R. S., BEUSSINK-NELSON, L., LJUNG FAXEN, U., FERMER, M. L., BROBERG, M. A., GAN, L. M. & LUND, L. H. 2018. Prevalence and correlates of coronary microvascular dysfunction in heart failure with preserved ejection fraction: PROMIS-HFpEF. *Eur Heart J*, 39, 3439-3450.

- SHIRREFFS, S. M. & MAUGHAN, R. J.** 1997. Whole body sweat collection in humans: an improved method with preliminary data on electrolyte content. *J Appl Physiol* (1985), 82, 336-41.
- SIMONS, M., GORDON, E. & CLAESSEON-WELSH, L.** 2016. Mechanisms and regulation of endothelial VEGF receptor signalling. *Nat Rev Mol Cell Biol*, 17, 611-25.
- SRINIVASAN, R. S. & OLIVER, G.** 2011. Prox1 dosage controls the number of lymphatic endothelial cell progenitors and the formation of the lymphovenous valves. *Genes Dev*, 25, 2187-97.
- STANTON, A. W., MODI, S., BENNETT BRITTON, T. M., PURUSHOTHAM, A. D., PETERS, A. M., LEVICK, J. R. & MORTIMER, P. S.** 2009. Lymphatic drainage in the muscle and subcutis of the arm after breast cancer treatment. *Breast Cancer Res Treat*, 117, 549-57.
- STEWART, J. M.** 2003. Microvascular filtration is increased in postural tachycardia syndrome. *Circulation*, 107, 2816-22.
- STOREY, J. D., BASS, A. J., DABNEY, A., ROBINSON, D.** 2019. *qvalue: Q-value estimation for false discovery rate control. R package version 2.16.0* [Online]. Available: <http://github.com/jdstorey/qvalue>.
- SULLIVAN, J. M., PREWITT, R. L., RATTS, T. E., JOSEPHS, J. A. & CONNOR, M. J.** 1987. Hemodynamic characteristics of sodium-sensitive human subjects. *Hypertension*, 9, 398-406.
- TANOUE, A., ITO, S., HONDA, K., OSHIKAWA, S., KITAGAWA, Y., KOSHIMIZU, T. A., MORI, T. & TSUJIMOTO, G.** 2004. The vasopressin V1b receptor critically regulates hypothalamic-pituitary-adrenal axis activity under both stress and resting conditions. *J Clin Invest*, 113, 302-9.
- TARAZI, R. C., DUSTAN, H. P. & FROHLICH, E. D.** 1969. Relation of plasma to interstitial fluid volume in essential hypertension. *Circulation*, 40, 357-66.
- TELINIUS, N., MOHANAKUMAR, S., MAJGAARD, J., KIM, S., PILEGAARD, H., PAHLE, E., NIELSEN, J., DE LEVAL, M., AALKJAER, C., HJORTDAL, V. & BOEDTKJER, D. B.** 2014. Human lymphatic vessel contractile activity is inhibited in vitro but not in vivo by the calcium channel blocker nifedipine. *J Physiol*, 592, 4697-714.
- THE REFERENCE VALUES FOR ARTERIAL STIFFNESS' COLLABORATION** 2010. Determinants of pulse wave velocity in healthy people and in the presence of cardiovascular risk factors: 'establishing normal and reference values'. *Eur Heart J*, 31, 2338-50.
- THIJSSSEN, D. H., BLACK, M. A., PYKE, K. E., PADILLA, J., ATKINSON, G., HARRIS, R. A., PARKER, B., WIDLANSKY, M. E., TSCHAKOVSKY, M. E. & GREEN, D. J.** 2011. Assessment of flow-mediated dilation in humans: a methodological and physiological guideline. *Am J Physiol Heart Circ Physiol*, 300, H2-12.
- THIJSSSEN, D. H. J., BRUNO, R. M., VAN MIL, A., HOLDER, S. M., FAITA, F., GREYLING, A., ZOCK, P. L., TADDEI, S., DEANFIELD, J. E., LUSCHER, T., GREEN, D. J. & GHIADONI, L.** 2019. Expert consensus and evidence-based

recommendations for the assessment of flow-mediated dilation in humans. *Eur Heart J*, 40, 2534-2547.

TITZE, J., BAUER, K., SCHAFFLHUBER, M., DIETSCH, P., LANG, R., SCHWIND, K. H., LUFT, F. C., ECKARDT, K. U. & HILGERS, K. F. 2005. Internal sodium balance in DOCA-salt rats: a body composition study. *Am J Physiol Renal Physiol*, 289, F793-802.

TITZE, J., KRAUSE, H., HECHT, H., DIETSCH, P., RITTWEGER, J., LANG, R., KIRSCH, K. A. & HILGERS, K. F. 2002. Reduced osmotically inactive Na storage capacity and hypertension in the Dahl model. *Am J Physiol Renal Physiol*, 283, F134-41.

TITZE, J., LANG, R., ILIES, C., SCHWIND, K. H., KIRSCH, K. A., DIETSCH, P., LUFT, F. C. & HILGERS, K. F. 2003. Osmotically inactive skin Na⁺ storage in rats. *Am J Physiol Renal Physiol*, 285, F1108-17.

TITZE, J. & LUFT, F. C. 2017. Speculations on salt and the genesis of arterial hypertension. *Kidney Int*, 91, 1324-1335.

TITZE, J., MAILLET, A., LANG, R., GUNGA, H. C., JOHANNES, B., GAUQUELIN-KOCH, G., KIHM, E., LARINA, I., GHARIB, C. & KIRSCH, K. A. 2002. Long-term sodium balance in humans in a terrestrial space station simulation study. *Am J Kidney Dis*, 40, 508-16.

TITZE, J., SHAKIBAEI, M., SCHAFFLHUBER, M., SCHULZE-TANZIL, G., PORST, M., SCHWIND, K. H., DIETSCH, P. & HILGERS, K. F. 2004. Glycosaminoglycan polymerization may enable osmotically inactive Na⁺ storage in the skin. *Am J Physiol Heart Circ Physiol*, 287, H203-8.

TOBIAN, L., JANECEK, J., TOMBOULIAN, A. & FERREIRA, D. 1961. Sodium and potassium in the walls of arterioles in experimental renal hypertension. *J Clin Invest*, 40, 1922-5.

TOBIAN, L., JR. & BINION, J. T. 1952. Tissue cations and water in arterial hypertension. *Circulation*, 5, 754-8.

TONNEIJCK, L., MUSKIET, M. H., SMITS, M. M., VAN BOMMEL, E. J., HEERSPINK, H. J., VAN RAALTE, D. H. & JOLES, J. A. 2017. Glomerular Hyperfiltration in Diabetes: Mechanisms, Clinical Significance, and Treatment. *J Am Soc Nephrol*, 28, 1023-1039.

TOWNSEND, R. R., WILKINSON, I. B., SCHIFFRIN, E. L., AVOLIO, A. P., CHIRINOS, J. A., COCKCROFT, J. R., HEFFERNAN, K. S., LAKATTA, E. G., MCENIERY, C. M., MITCHELL, G. F., NAJJAR, S. S., NICHOLS, W. W., URBINA, E. M. & WEBER, T. 2015. Recommendations for Improving and Standardizing Vascular Research on Arterial Stiffness: A Scientific Statement From the American Heart Association. *Hypertension*, 66, 698-722.

VAN BEUSECUM, J. P., BARBARO, N. R., MCDOWELL, Z., ADEN, L. A., XIAO, L., PANDEY, A. K., ITANI, H. A., HIMMEL, L. E., HARRISON, D. G. & KIRABO, A. 2019. High Salt Activates CD11c(+) Antigen-Presenting Cells via SGK (Serum Glucocorticoid Kinase) 1 to Promote Renal Inflammation and Salt-Sensitive Hypertension. *Hypertension*, 74, 555-563.

- VAN BORTEL, L. M., LAURENT, S., BOUTOUYRIE, P., CHOWIENCZYK, P., CRUICKSHANK, J. K., DE BACKER, T., FILIPOVSKY, J., HUYBRECHTS, S., MATTACE-RASO, F. U., PROTOGEROU, A. D., SCHILLACI, G., SEGERS, P., VERMEERSCH, S. & WEBER, T.** 2012. Expert consensus document on the measurement of aortic stiffness in daily practice using carotid-femoral pulse wave velocity. *J Hypertens*, 30, 445-8.
- WADDINGHAM, M. T. & PAULUS, W. J.** 2017. Microvascular Paradigm in Heart Failure With Preserved Ejection Fraction: A Quest for Proof of Concept. *Circ Heart Fail*, 10.
- WANG, T. J., LARSON, M. G., LEVY, D., BENJAMIN, E. J., LEIP, E. P., OMLAND, T., WOLF, P. A. & VASAN, R. S.** 2004. Plasma natriuretic peptide levels and the risk of cardiovascular events and death. *N Engl J Med*, 350, 655-63.
- WARNOCK, D. G.** 1999. Low-renin and nonmodulating essential hypertension. *Hypertension*, 34, 395-7.
- WEINBERGER, M. H., FINEBERG, N. S., FINEBERG, S. E. & WEINBERGER, M.** 2001. Salt sensitivity, pulse pressure, and death in normal and hypertensive humans. *Hypertension*, 37, 429-32.
- WEINBERGER, M. H., MILLER, J. Z., LUFT, F. C., GRIM, C. E. & FINEBERG, N. S.** 1986. Definitions and characteristics of sodium sensitivity and blood pressure resistance. *Hypertension*, 8, 1127-34.
- WEINBERGER, M. H., STEGNER, J. E. & FINEBERG, N. S.** 1993. A comparison of two tests for the assessment of blood pressure responses to sodium. *Am J Hypertens*, 6, 179-84.
- WELSH, P., POULTER, N. R., CHANG, C. L., SEVER, P. S. & SATTAR, N.** 2014. The value of N-terminal pro-B-type natriuretic peptide in determining antihypertensive benefit: observations from the Anglo-Scandinavian Cardiac Outcomes Trial (ASCOT). *Hypertension*, 63, 507-13.
- WHITE, C. P., HITCHCOCK, C. L., VIGNA, Y. M. & PRIOR, J. C.** 2011. Fluid Retention over the Menstrual Cycle: 1-Year Data from the Prospective Ovulation Cohort. *Obstet Gynecol Int*, 2011, 138451.
- WIIG, H. & REED, R. K.** 1985. Interstitial compliance and transcapillary Starling pressures in cat skin and skeletal muscle. *Am J Physiol*, 248, H666-73.
- WIIG, H., SCHRODER, A., NEUHOFER, W., JANTSCH, J., KOPP, C., KARLSEN, T. V., BOSCHMANN, M., GOSS, J., BRY, M., RAKOVA, N., DAHLMANN, A., BRENNER, S., TENSTAD, O., NURMI, H., MERVAALA, E., WAGNER, H., BECK, F. X., MULLER, D. N., KERJASCHKI, D., LUFT, F. C., HARRISON, D. G., ALITALO, K. & TITZE, J.** 2013. Immune cells control skin lymphatic electrolyte homeostasis and blood pressure. *J Clin Invest*, 123, 2803-15.
- WIIG, H. & SWARTZ, M. A.** 2012. Interstitial fluid and lymph formation and transport: physiological regulation and roles in inflammation and cancer. *Physiol Rev*, 92, 1005-60.

- WILCOX, C. S., TESTANI, J. M. & PITT, B.** 2020. Pathophysiology of Diuretic Resistance and Its Implications for the Management of Chronic Heart Failure. *Hypertension*, 76, 1045-1054.
- WILKINSON, I. B. & WEBB, D. J.** 2001. Venous occlusion plethysmography in cardiovascular research: methodology and clinical applications. *Br J Clin Pharmacol*, 52, 631-46.
- WILLIAMS, B., MANCIA, G., SPIERING, W., AGABITI ROSEI, E., AZIZI, M., BURNIER, M., CLEMENT, D. L., COCA, A., DE SIMONE, G., DOMINICZAK, A., KAHAN, T., MAHFOUD, F., REDON, J., RUILOPE, L., ZANCHETTI, A., KERINS, M., KJELDSSEN, S. E., KREUTZ, R., LAURENT, S., LIP, G. Y. H., MCMANUS, R., NARKIEWICZ, K., RUSCHITZKA, F., SCHMIEDER, R. E., SHLYAKHTO, E., TSIOUFIS, C., ABOYANS, V. & DESORMAIS, I.** 2018. 2018 ESC/ESH Guidelines for the management of arterial hypertension. *Eur Heart J*, 39, 3021-3104.
- WIMPERIS, S.** 2011. Relaxation of quadrupolar nuclei measured via multiple-quantum filtration. In: HARRIS, R. K. & WASYLISHEN, R. E. (eds.) *Encyclopedia of Magnetic Resonance*. John Wiley & Sons.
- WISHART, D. S., FEUNANG, Y. D., MARCU, A., GUO, A. C., LIANG, K., VAZQUEZ-FRESNO, R., SAJED, T., JOHNSON, D., LI, C., KARU, N., SAYEEDA, Z., LO, E., ASSEMPOUR, N., BERJANSKII, M., SINGHAL, S., ARNDT, D., LIANG, Y., BADRAN, H., GRANT, J., SERRA-CAYUELA, A., LIU, Y., MANDAL, R., NEVEU, V., PON, A., KNOX, C., WILSON, M., MANACH, C. & SCALBERT, A.** 2018. HMDB 4.0: the human metabolome database for 2018. *Nucleic Acids Res*, 46, D608-d617.
- WITTE, M. H., DUMONT, A. E., CLAUSS, R. H., RADER, B., LEVINE, N. & BREED, E. S.** 1969. Lymph circulation in congestive heart failure: effect of external thoracic duct drainage. *Circulation*, 39, 723-33.
- WRIGHT, J. T., JR., WILLIAMSON, J. D., WHELTON, P. K., SNYDER, J. K., SINK, K. M., ROCCO, M. V., REBOUSSIN, D. M., RAHMAN, M., OPARIL, S., LEWIS, C. E., KIMMEL, P. L., JOHNSON, K. C., GOFF, D. C., JR., FINE, L. J., CUTLER, J. A., CUSHMAN, W. C., CHEUNG, A. K. & AMBROSIUS, W. T.** 2015. A Randomized Trial of Intensive versus Standard Blood-Pressure Control. *N Engl J Med*, 373, 2103-16.
- YANG, G. H., ZHOU, X., JI, W. J., ZENG, S., DONG, Y., TIAN, L., BI, Y., GUO, Z. Z., GAO, F., CHEN, H., JIANG, T. M. & LI, Y. M.** 2014. Overexpression of VEGF-C attenuates chronic high salt intake-induced left ventricular maladaptive remodeling in spontaneously hypertensive rats. *Am J Physiol Heart Circ Physiol*, 306, H598-609.
- ZELIS, R., DELEA, C. S., COLEMAN, H. N. & MASON, D. T.** 1970. Arterial sodium content in experimental congestive heart failure. *Circulation*, 41, 213-6.
- ZHANG, W. C., ZHENG, X. J., DU, L. J., SUN, J. Y., SHEN, Z. X., SHI, C., SUN, S., ZHANG, Z., CHEN, X. Q., QIN, M., LIU, X., TAO, J., JIA, L., FAN, H. Y., ZHOU, B., YU, Y., YING, H., HUI, L., LIU, X., YI, X., LIU, X., ZHANG, L. & DUAN, S. Z.** 2015. High salt primes a specific activation state of macrophages, M(Na). *Cell Res*, 25, 893-910.

ZINMAN, B., WANNER, C., LACHIN, J. M., FITCHETT, D., BLUHMKI, E., HANTEL, S., MATTHEUS, M., DEVINS, T., JOHANSEN, O. E., WOERLE, H. J., BROEDL, U. C. & INZUCCHI, S. E. 2015. Empagliflozin, Cardiovascular Outcomes, and Mortality in Type 2 Diabetes. *N Engl J Med*, 373, 2117-28.